FUZZY LOGIC SYSTEM FOR INTERMIXED BIOGAS AND PHOTOVOLTAICS MEASUREMENT AND CONTROL

by

LISTON MATINDIFE

submitted in accordance with the requirements for
the degree of

MAGISTER TECHNOLOGIAE

In the subject

ELECTRICAL ENGINEERING

at the

University of South Africa

Supervisor: PROF Z WANG

DECEMBER 2016

DECLARATION

Name: LISTON MATINDIFE

Student number: 57478295

Degree: MAGISTER TECHNOLOGIAE IN ELECTRICAL ENGINEERING

Exact wording of the title of the dissertation or thesis as appearing on the copies submitted for examination:

FUZZY LOGIC SYSTEM FOR INTERMIXED BIOGAS AND PHOTOVOLTAICS MEASUREMENT AND CONTROL

I declare that the above dissertation/thesis is my own work and that all the sources that I have used or quoted have been indicated and acknowledged by means of complete references.

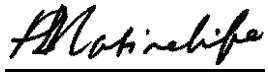

SIGNATURE

07 – 12 – 2016
DATE

ABSTRACT

The major contribution of this dissertation is the development of a new integrated measurement and control system for intermixed biogas and photovoltaic systems to achieve safe and optimal energy usage. Literature and field studies show that existing control methods fall short of comprehensive system optimization and fault diagnosis, hence the need to re-look these control methods. The control strategy developed in this dissertation is a considerable enhancement on existing strategies as it incorporates intelligent fuzzy logic algorithms based on C source codes developed on the MPLABX programming environment. Measurements centered on the PIC18F4550 microcontroller were carried out on existing biogas and photovoltaic installations. The designed system was able to accurately predict digester stability, quantify biogas output and carry out biogas fault detection and control. Optimized battery charging and photovoltaic fault detection and control was also successfully implemented. The system optimizes the operation and performance of biogas and photovoltaic energy generation.

Key terms: Fuzzy logic system; Fuzzy logic algorithms; Biogas fault detection; Photovoltaic fault detection; Intermixed biogas and photovoltaics; Renewable energy on-line monitoring; Biogas measurement and control; Photovoltaic measurement and control; Biogas and photovoltaic sensors; MPLABX C source codes.

ACKNOWLEDGEMENTS

To **GOD** is all the glory.

I would like to thank my supervisor **Professor Zenghui Wang** for his invaluable guidance throughout this study, without which I would not have progressed much.

Thanks also to the management and personnel of the rural electrification fund (REF) for availing the facilities to implement the research project designed measurement and control unit and for taking time out of their busy schedule to respond to the interview sessions.

A special thanks to my wife, son and daughter for allowing me to attend to my studies without disturbance when instead I was supposed to spend time with them.

Last but not least I would like to thank my fellow work colleagues and management at Kwekwe Polytechnic for their unwavering support during my studies.

TABLE OF CONTENTS

LIST OF APPENDICES

LIST OF TABLES

LIST OF FIGURES

LIST OF ACRONYMS AND ABBREVIATIONS

CAD	COMPUTER AIDED DESIGN
CH_4	METHANE
CO_2	CARBON DIOXIDE
COD	CHEMICAL OXYGEN DEMAND
COG	CENTRE OF GRAVITY
DS	DRY SOLIDS
H_2	HYDROGEN
HRT	HYDRAULIC RETENTION TIME
ICD3	IN-CIRCUIT DEBUGGER
IDE	INTEGRATED DEVELOPMENT ENVIRONMENT
LED	LIGHT EMITTING DIODE
LDR	LIGHT DEPENDENT RESISTOR (PHOTOCELL)
MPLABX	SOFTWARE APPLICATION FOR PROGRAMMINING MICROCONTROLLERS
MPP	MAXIMUM POWER POINT
NH_3	AMMONIA
PCB	PRINTED CIRCUIT BOARD
pH	POTENTIAL FOR HYDROGEN
PIC	PERIPHERAL INTERFACE CONTROLLER/PROGRAMMABLE INTERFACE CONTROLLER
PICKIT3	IN-CIRCUIT DEBUGGING PROGRAMMER
PPM	PARTS PER MILLION
PV	PHOTOVOLTAIC
PWM	PULSE –WIDTH-MODULATION
REA	RURAL ELECTRIFICATION AGENCY
REF	RURAL ELECTRIFICATION FUND
SCADA	SUPERVISORY CONTROL AND DATA ACQUISITION
SOC	STATE OF CHARGE
SDD	SOLID STATE DIGESTER

TDS	TOTAL DRY SOLIDS
TS	TOTAL SOLIDS
UNISA	UNIVERSITY OF SOUTH AFRICA
UoD	UNIVERSE OF DISCOURSE
VFA	VOLATILE FATTY ACIDS
VLA	VENTILATED LEAD ACID
VLRA	VALVE-REGULATED-LEAD-ACID
VS	VOLATILE SOLIDS

CHAPTER 1

INTRODUCTION

1.1 INTRODUCTION

This dissertation looks at developing and applying fuzzy logic algorithms (Zadeh, 1965; Singh et al., 2013), to the measurement and control of intermixed[1] biogas and photovoltaic systems. However the fuzzy logic algorithms are often incorporated into a broader software framework to address each measurement and control aspect of the intermixed system at hand. The system that incorporates fuzzy logic algorithms and integrates independent biogas and photovoltaic on-line monitoring[2] into a single unit is a unique design of this dissertation. Prior to this dissertation no on-line monitoring system existed for the small to medium scale intermixed biogas and photovoltaic systems. Based on the biogas generation, photovoltaic generation and embedded system application it is established that this study falls within the field of renewable energy measurement and control.

Rural households have since time immemorial been obtaining most of their energy from firewood. These same households have now been introduced to biogas and photovoltaic energy. The main challenge is that of very limited appreciation of the extent these energy systems can actually provide all the energy requirements of the rural households. Biogas is mainly used for heating and cooking, whilst the photovoltaic system is mainly used for electricity for electrical gadgets. Hence a measurement and control system to maximize on these biogas and photovoltaic systems needs to be developed. The system should be low cost, reliable and user friendly.

Any renewable energy generation system is designed to operate within certain limits and to produce maximum output based on certain system conditions. Hence, by setting performance criteria[3] of the intermixed biogas and photovoltaic system, as is in this dissertation a monitoring system is designed to compel the renewable energy system set up under consideration to meet these performance criteria and to operate within the required limits. The expected system performance criteria is arrived at based on literature from existing biogas and photovoltaic systems of the same design specifications, system design data and feedback from field measurements and observations of the intermixed biogas and photovoltaic system being monitored in this study.

This dissertation also addresses the selection of the critical components and the design of some circuits of the hardware. The hardware is made up of various sensors, sensor circuits, various output devices and a microcontroller which is the heart of the hardware. The algorithms are implemented using in-house developed C source codes. The development of the whole embedded system is centered on MPLABX (Microchip, 2015a), which is an Integrated Development Environment (*IDE*).

[1] Intermixed in this situation simply refers to a situation where both biogas and photovoltaic installations exist at a single site.
[2] On-line monitoring means automatic measurement and control.
[3] Performance criteria are the inputs, outputs, stability requirements, fault levels and normal operation parameters.

The use of fuzzy logic algorithms in the formulation of a measurement and control strategy for intermixed biogas and photovoltaic systems will provide improved process operation, increased system output capability, simplified system fault detection and increased confidence/ ease of use by non skilled rural people.

1.2 BACKGROUND TO THE STUDY

Fixed dome biogas digesters as shown in Figs. 1.1 & 1.2 are the common type installed in Zimbabwean rural establishments (Hivos & Snv, 2012; Southern, 2015). For establishments such as rural clinics, schools and indeed very small villages the medium scale bio digesters that range between fifty and eighty cubic metres are the norm. On the other hand small scale bio digesters that range between four and twenty cubic metres suffice for the single household. For even bigger establishments the large scale bio digesters that range from one hundred cubic metres and above are used. However this research focuses on the medium scale bio digesters which are normally installed by the Rural Electrification Fund (REF), formerly the Rural Electrification Agency (REA) as depicted in Fig. 1.1. These biogas digesters are basic installed, and normally without any form of instrumentation as shown in Fig. 1.2.

The electrical demands for the rural establishments mentioned above and not connected to the national grid are met by photovoltaic systems that are normally installed by REF and by a limited number of non-governmental organizations. The REF photovoltaic systems such as the ones shown in Fig. 1.3 (solar panels with an adjacent control room housing the inverter, charge controller, circuit breakers, measuring and indication instruments), come with a minimum power rating of one thousand watts comprising twelve solar arrays, a twenty four volt twelve battery set, an inverter and a simple charge controller. It is observed that the battery charging method is simple and the equipment protection strategy used is based on a simple fuse.

Fig. 1.1: Biogas digester of size 50 m^3 under construction
(Rural Electrification Fund, 2015)

Fig. 1.2: Installed household dome digester showing the manhole and gas outlet
(Hivos & Snv, 2012)

a. Lower Gweru Administrative Office b. Lower Gweru Clinic

Fig. 1.3: Typical installations in rural institutions for the solar mini grid
(Rural Electrification Fund, 2015)

1.3 STATEMENT OF THE PROBLEM

In Zimbabwe biogas digesters have been installed since 1979 with an intended output of 7400 domestic units by the year 2017 (Hivos & Snv, 2012). However some of the bio digesters are no longer functioning or have totally collapsed. On existing structures sometimes gas is being produced in very little quantities or is not available at all when needed. The reasons for low or no output capability are not normally apparent or will not be determined at all. Bio digester installations that use cow dung as primary feed are sometimes connected to sewer lines exhausting hospital or industrial waste with the intention of seeding, that is increasing population

of fermentation and methanogenesis (Teodorita et al., 2008) bacteria but it is observed that the output instead continues to decrease.

To mitigate the low output capability it is required to evolve an approach to aggrandize the output capability of the biogas digester. The average rural household lacks the expertise to use or maintain digester systems relying on external expensive and sometimes unavailable technical experts. This approach when implemented will also act in addition to giving constant high output supply as an affordable intermediary expert to globally aid the user in various digester aspects including enabling known gas leaks, safe pressure levels, raw material feeding interval, feedstock quality and quantity which is not the case at present. According to Business (2013):

'*One of the major challenges facing the country is that of lack of capacity in designing, construction and management of large biogas installations in both the private and public sectors*.'

Some of the 300 REA photovoltaic installations exhibit low power output even when there is abundant sun shine. There is no immediate way to tell if the problem is due to solar cells (dirt or black spots due to trees), battery, power module, connected loads, charging system or the principle of battery charging. The average rural householder lacks the technical expertise in photovoltaic systems. It is required to evolve an approach to aggrandize the output capability and aid in the use of rural household photovoltaic arrangement. Operability and system performance issues are then clearly articulated.

The increased adoption of renewable energy systems at rural household level has put more scrutiny on process operation and adoption of better technologies (Karimov, 2012) to evolve an affordable monitoring approach to aggrandize the output capability and aid in the ability to use the arrangements (Bernhard, 2013; Kanokwan, 2006). The aspects addressed in the preceding paragraphs form a gap in the use and operation of small to medium scale intermixed biogas and photovoltaic systems.

1.4 RESEARCH QUESTIONS AND OBJECTIVES

The main research question for this study is:

How can fuzzy logic algorithms be developed and implemented in the design of a measurement and control system for intermixed biogas and photovoltaic systems?

To be able to answer the main research question the following six sub-questions need to be answered:

1) What are the parameters and mechanisms that define the energy generation processes for each of the biogas and photovoltaic systems?

2) What are the established aspects required to optimize system[4] output?
3) What is/are the shortfalls in the current method/s, if any, used to optimize system output?
4) Can fuzzy logic algorithms be developed and implemented in the measurement and control strategy for intermixed biogas and photovoltaic systems?
5) What hardware is to be specified, both for sensing and control?
6) Can microcontroller based embedded technique be suitably applied to the measurement and control of intermixed biogas and photovoltaic systems?

The aim of this research is to achieve the following objectives by addressing the sub-questions above:

1) To identify from literature and design specifications the parameters and mechanisms that define the energy generation processes.
2) To identify from literature and design specifications the established aspects required to optimize system output.
3) To identify the gap in the current method/s used to optimize system output.
4) To develop, code in C source codes and implement suitable fuzzy logic algorithms in the measurement and control of intermixed biogas and photovoltaic systems.
5) To design sensor and control circuits based on suitably selected sensors and output devices.
6) To design an embedded measurement and control system complete with inputs, outputs and in-house developed C source codes software based on MPLABX Microchip's Integrated Development Environment *(IDE).*

1.5 SCOPE (DELIMITATIONS) AND LIMITATIONS

Field implementation of the photovoltaic system will not be done, but will be restricted to a laboratory[5] setup, however fully addressing the aspects of fuzzy logic algorithms measurement and control of battery charging/discharging and fault detection (including shading of solar panels). This is because the terms of agreement with REF do not allow tampering with already existing photovoltaic circuitry such that the researchers cannot (not allowed to) modify the system charge controller circuit to incorporate pulse width modulation (PWM), nor induce over loading and under loading on the inverter that is supplying critical equipment, to make measurements. However REF has agreed to incorporate the photovoltaic monitoring strategy into their subsequent new installations. On the other hand the biogas fuzzy logic algorithms measurement and control system is fully implementable on site and will be restricted to system imbalance early warning notification (from buffering capacity which will be validated by making manual titration measurements), biogas output level, fault detection and control.

For the conventional fixed dome small to medium scale biogas digesters that are naturally stirred and heated, expensive online monitoring instruments/analyzers, automatic stirring, automatic

[4] System is either the biogas or photovoltaic energy generation.
[5] Laboratory is not strictly 'laboratory' in the sense since the specifications that will be used are 24V dc supply, 0 to 6A variable load current, REF single panel specification, simple constructed inverter and charge controller.

loading of feedstock and acid neutralizing agents will be excluded from the study. Whilst for photovoltaic systems motorized and maximum power point (MPP) tracking systems will not be treated either in this study.

The choice of sensors and output devices will be restricted to simple inexpensive types with all relevant circuits developed in-house. Subsystem and complete system simulation will be restricted to the use of MPLABX and Labcenter Electronics Proteus. Cabling is exclusively used to connect the various units of the embedded system.

1.6 RESEARCH DESIGN AND METHODOLOGY

This research is based on the mixed qualitative and quantitative research methods. The bias however is towards the quantitative positivistic research paradigm (Jerry, 2007; O'Leary, 2007a) that involves the collection and interpretation of data.

The qualitative research method which is the beginning stage involves a literature study on the mechanisms of energy generation process with a view of determining the methods that have been developed or need to be developed to optimize system output and the conducting of field based consultations/interviews to establish the user's (experts and non-experts) perceptions on existing biogas and photovoltaic systems.

The second stage involves the design of the fuzzy logic algorithms, module[6] flowcharting, software and hardware structure comprising the data acquisition plus control. This second stage with elevated, quantitative data collection (measurement) by using the designed measuring circuits, software simulation and experimentation indicates a high degree of empirical positivistic approach (O'Leary, 2007c).

The final stage involves the analysis of the data which is a two-fold process. The first case is the processing and interpretation of the data by the designed algorithms to give the desired control outputs. In the second case the data is analyzed using descriptive statistics which allows presentation of the research findings in the form of calculations, graphs or tables. A detailed report of the aspects mentioned in this section will be given in Chapter 3.

1.7 RESEARCH ETHICS

The requirements for research ethics guided by the UNISA revised policy on research ethics (2013) were duly met, and are tabulated below:

1) Ethical clearance (Appendix A) was obtained from the College of Science, Engineering and Technology's (CSET) Research and Ethics Committee at the University of South Africa (UNISA).
2) Permission was sought and obtained from the administrators of the biogas and photovoltaic installations to conduct interviews where the interviewees were free to accept or decline to

[6] Module refers to sub parts of the complete software program.

participate. To this end, a sample of a signed informed consent form is provided in Appendix B.

3) The research was implemented without interfering neither with the constructional designs nor the operation status of the existing biogas and photovoltaic systems.
4) Permission was sought and obtained from REF to implement the monitoring system on their installations provided the conditions in 3) above are observed.
5) Information from any other consultations done was treated in the strictest confidence and the anonymity of the participants maintained.

1.8 SIGNIFICANCE OF THE STUDY

The increased use of renewable energy systems in rural establishments has put more scrutiny on process operation and the need to develop an affordable monitoring system to increase the output capability and assist in the ability to use these energy systems. In the current biogas and photovoltaic installations very basic independent monitoring is done and in some cases is not done at all.

In this research a comprehensive integrated intelligent monitoring system for intermixed biogas and photovoltaic systems is developed. This is new to approach altogether for renewable energy monitoring and control that has not been done before at the mentioned user level. The application of this approach to large scale national renewable energy installations has not been investigated, nor is it known to exist.

The successful implementation of fuzzy logic algorithms in the measurement and control of intermixed biogas and photovoltaic systems addresses part of the knowledge gap in renewable energy monitoring and control. Whilst a self contained online-monitoring and control system easily used and understood by the layman has been developed.

1.9 LAYOUT OF THE CHAPTERS

The dissertation is made-up of nine chapters as shown in Fig. 1.4. Chapter 1 is the introduction which gives the background to the study, scope (delimitations) and limitations, significance of the study and a brief description of the research design and methodology. Chapter 2 gives a review of the related literature to cover the mechanisms of energy generation process, established aspects to optimize system output, fuzzy logic algorithms and a review of this research with emphasis on addressing the shortfall in the currently used method/s to improve system performance. Chapter 3 details the research design and methodology. Chapters 4 and 5 address the initial system development stages pertaining to fuzzy logic algorithms, module flowcharting, the measuring and control circuits design. Chapter 6 details the software development process that is made up of C source programming and simulation in Microchips' MPLABX and Labcenters' Proteus software packages. In Chapter 7 the coherent hardware structure (embedded system design) which represents the result of all the circuits, supporting software and PIC18F4550 microcontroller is elaborated on. The research findings are given in Chapter 8 and appropriately presented. Chapter 9 gives the conclusion pertaining to the research objectives and findings. Future work and recommendations are also given in Chapter 9.

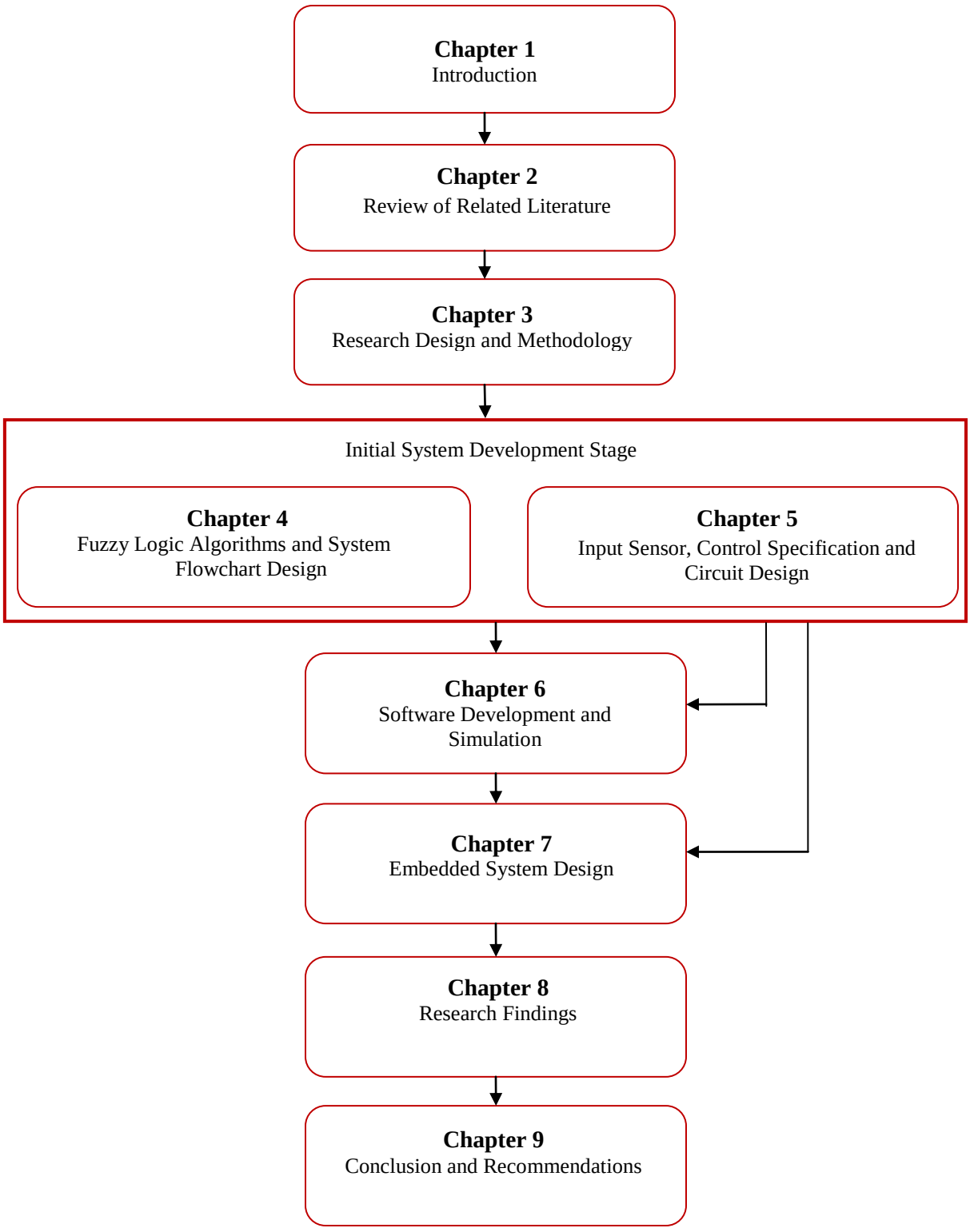

Fig. 1.4: Layout of the Dissertation chapters

CHAPTER 2

REVIEW OF RELATED LITERATURE

2.1 INTRODUCTION

As a basis for the argument for this research there is need to consider what other researchers have done in the area of measurement and control of biogas and photovoltaic systems. Situations where the monitoring strategy is independently done or is in integrated form if any will be researched on. It is necessary to consider the mechanism of energy generation as a starting point and to determine the methods that have been developed to improve system performance. These aspects are considered in this chapter together with a detailed review of fuzzy logic algorithms and comprehensive review of this research itself.

2.2 MECHANISM OF ENERGY GENERATION PROCESS

2.2.1 BIOGAS GENERATION

The by-products of anaerobic (oxygen free) digestion process shown in Fig. 2.1 are mainly carbon dioxide (CO_2) and methane (CH_4) gases. However to a lesser extent hydrogen sulphide (NH_3) and hydrogen (H_2) are also produced. A brief explanation of the mechanisms involved in biogas generation is done in the following sections.

2.2.1.1 Hydrolysis

According to Bharathiraja et al. (2016), carbohydrates, proteins and lipids[7] which are polymers are degraded into smaller units called monomers and oligomers. These constitute the amino acids, sugars and long chain fatty acids (LFAC). The breakdown process is achieved through exoenzymes[8] produced by the microorganisms present in the material. The next fermentation[9] stage in the process is only possible pending successful hydrolysis since fermentation bacteria cannot directly take in carbohydrates, proteins or lipids into their cells. Hydrolysis is a multi-valued dependent process where the independent values are defined by the shape of the organic material, effective surface area of organic material, concentration of the feedstock and enzyme manufacture process.

[7] Lipids are molecules that include fat, waxes, sterols etc and they occur naturally.
[8] Exoenzyme, also called extracellular defines an enzyme that operates outside the cell that produces it.
[9] Fermentation is bacteria or yeast based chemical breaking down of sugar to alcohol, gasses and acids.

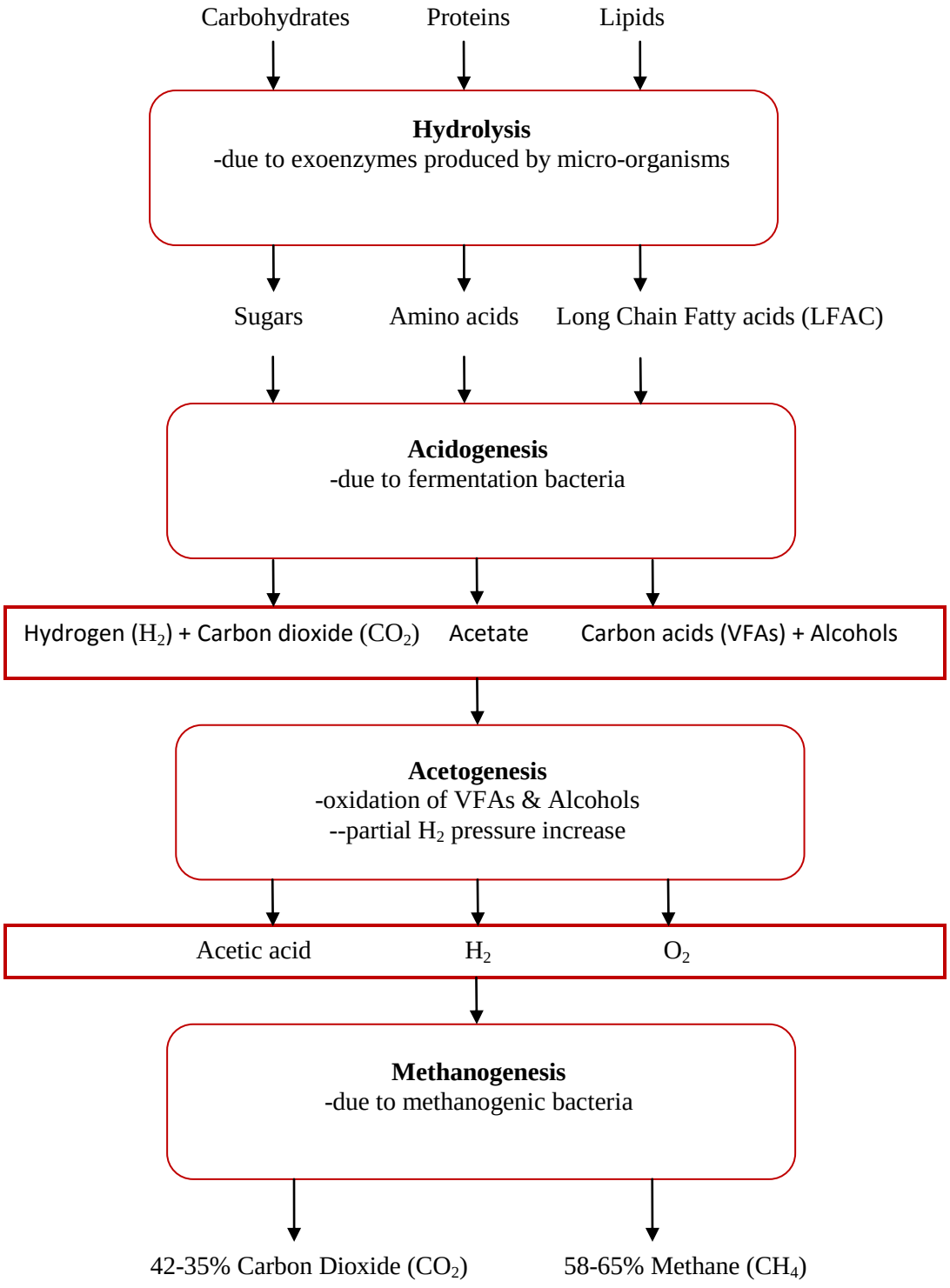

Fig. 2.1: A Brief description of the anaerobic digestion process

(Falk, 2011; Kanokwan, 2006; Labatut & Gooch, 2015; Teodorita et al., 2008)

2.2.1.2 Acidogenesis

Acidogenesis which is the fermentation stage involves the chemical breakdown of the products of hydrolysis by fermentation bacteria. The result of the fermentation process is composed of acetate, carbon dioxide (CO_2), hydrogen (H_2), alcohols and volatile fatty acids (VFAs). This process which depends on pH, dissolved feedstock and hydrogen concentrations, produces the following relative amounts of the products, fifty one percent acetate, nineteen percent hydrogen and thirty percent higher VFAs and alcohols. According to Labatut & Gooch (2015), the VFAs are made up of the following components:

'*acetic acid/acetate, propionic acid/propionate, butyric acid/butyrate, valeric acid/valerate, caproic acid/caproate, and enanthic acid/enanthate, from which acetate is predominant*'.

The results of fermentation are shown in Table 2.1, where the expression $C_6H_{12}O_6$ represents the chemical symbol for glucose. To prevent 'killing' the anaerobic process due to too much acidity the concentration of VFAs acetic acid by volume should be low and this should typically be less than five hundred milligrams of acetic acid per litre of feedstock solution (500mg/L) (Labatut & Gooch, 2015]).

Table 2.1: The results of fermentation process (Kanokwan, 2006)

Products	**Reaction**
Acetate	$C_6H_{12}O_6 + 2H_2O \rightarrow 2CH_3COOH + 2CO_2 + 4H_2$
Propionate + Acetate	$3C_6H_{12}O_6 \rightarrow 4CH_3CH_2COOH + 2CH_3COOH + 2CO_2 + 2H_20$
Butyrate	$C_6H_{12}O_6 \rightarrow CH_3CH_2CH_2COOH + 2CO_2 + 2H_2$
Lactate	$C_6H_{12}O_6 \rightarrow 2CH_3CHOHCOOH$
Ethanol	$C_6H_{12}O_6 \rightarrow 2CH_3CH_2OH + 2CO_2$

2.2.1.3 Acetogenesis

VFAs and alcohols cannot be directly acted upon by methanogenesis bacteria. The VFAs and alcohols are made compatible to methanogenesis through the acetogenesis stage which converts these to acetate , hydrogen and carbon dioxide. The VFAs and alcohols that are made up of carbon chains longer than two units (atoms) and longer than one unit (atom) (Teodorita et al., 2008), respectively, are oxidized into acetate and hydrogen. This has the overall effect of increasing the hydrogen partial pressure which can have a negative effect on acetogenesis. However an increase in temperature favors the mechanisms in this stage.

2.2.1.4 Methanogenesis

This is the final but slowest stage in the biogas generation process. Methanogenesis bacteria acting on acetic acid, hydrogen and carbon dioxide will produce methane as detailed in the Table 2.2, Methanogenesis breakdown process.

Table 2.2: Methanogenesis breakdown process (Deublein & Steinhauser, 2008)

Substrate type	**Chemical reaction**	**ΔG_f '[10] (kJ mol^{-1})**	**Methanogic species**
CO_2 – Type	$4H_2 + HCO_3^- + H^+ \rightarrow CH_4 + 3H_2O$	-135.4	All species
	$CO_2 + 4H_2 \rightarrow CH_4 + 2H_2O$	-131.0	
CO_2 – Type	$4HCOO^- + H_2O + H^+ \rightarrow CH_4 + 3HCO_3^-$	-130.4	Many species
Acetate	$CH_3COO^- + H_2O \rightarrow CH_4 + HCO_3$	-30.9	Some species
Methyl type	$4CH_3OH \rightarrow 3CH_4 + HCO_3^- + H^+ + H_2O$	-314.3	One species
Methyl type	$CH_3OH + H_2 \rightarrow CH_4 + H_2O$	-13.0	
e.g. Methyl type: ethanol	$2CH_3CH_2OH + CO_2 \rightarrow CH_4 + 2CH_3COOH$	-116.3	

In this stage the bacteria is very sensitive to pH and temperature changes. The methanogenesis mechanism which normally runs parallel to the acetogenesis process is also severely affected by the feeding rate and composition of the feedstock.

2.2.2 OPTIMISATION OF BIOGAS DIGESTERS OUTPUT

As described in section 2.2.1, the biogas generation process is inherently complex and sensitive, hence justifying the need for intelligent control and optimization. There are many published techniques and many commercially available ways to generate and monitor biogas. Previuos work from other researchers and designers has identified the following issues that need to be considered for process and perfomance evaluation of biogas generation:

[10] This is the Gibbs free energy that signifies how readily a reaction will take place. This shows that methanogenesis reaction on hydrogen and carbon dioxide takes place more easily than on acetate.

2.2.2.1 First level anaerobic digester parameters

We would like to term the parameters described in this section as first level type. This term has come about since these are the parameters required to define a comprehensive monitoring system as a starting point. The type of parameter and the prescribed limits of operation according to literature review are described hence forth.

It has been established that a pH value of between 5 and 6.5 will facilitate the hydrolysis stage in the anaerobic digester, whilst in methanogenesis the pH is required to be neutral and in the ranges of 6.8 to 8 (Eu-agrobiogas, 2009). With regards to temperature, the requirements are such that existing industrial anaerobic digesters operate at 43 to 55^{o}C (Thermophilic) to give a minimum time for biogas production of fifteen to twenty days. Domestic anaerobic digesters would normally operate at 30 to 42^{o}C (Mesophilic) with retention[11] times between thirty to forty days (Teodarita et al., 2008).

The concentration of volatile fatty acids should not exceed 1,500-2,000 mg/L as acetic acid since this would imply a definite stoppage of the process in the anaerobic digester process and hence it is paramount to monitor this parameter (Labatut & Gooch, 2015). The other parameters that can be used to monitor the stability of the anaerobir digester process are total ammonia nitrogen and alkalinity or buffer capacity. Total ammonia nitrogen levels greater than 1,500 mg/L of ammonia at pH values greater than neutral will destroy the anaerobic process however biodigesters can operate at moderate ammonium nitrogen concentrations without completely destroying anaerobic digetion process (Bernhard,2013; Labatut & Gooch, 2015). Buffer capacity is a measure of the tendency of the substrate to avoid change in pH which is a requirement in digesters. Typical alkalinity values in biodigesters range from 2000 – 5500mgl^{-1} bicarbonate and normally values above 4000mgL^{-1} bicarbonate means a good buffering capacity (Eu-agrobiogas ,2009; Labatut & Gooch, 2015; Wisconsin, 1992).

Anaerobic digester process is not fully defined if the intended biogas output is not quantified. For methane gas, which is the required product it is recommended to monitor the gas production on a daily basis *"(L–CH_4/day)*" as an "*online*" indicator of bio digester performance (Kanokwan, 2006, p.19). Carbon dioxide level monitoring is very important as it complements methane level monitoring since a rise in carbon dioxide level implies less methane is being produced, and therefore there must be a problem in the digester process.

With regards to digester system protection and safe operating status the following observations are made:

1) Composite gas pressure needs to be measured so that it does not reach abnormal levels. In fixed dome type digesters too much un checked pressure would push active feedstock out through the exhaust affecting the balance of materials.
2) Level measurement is also important as it gives indication of the digester fill level both during feedstock inputting and during operation over the retention time.

[11] Retention is the time taken before a usable amount of biogas is produced.

3) It is important to monitor oxygen levels as this would indicate a leak in the system structure. Presence of oxygen would effectively stop the anaerobic process.
4) The output gas should be monitored of hydrogen sulphide and moisture concentrations as an increase in these would form sulphuric acid which can be corrosive to internal sensors, metal regulators and pipe work.

2.2.2.2 Second level anaerobic digester parameters

This section describes second level type parameters. The parameters described here are only considered when designing an advanced monitoring system. The observations made by considering incorporating these parameters in monitoring are:

1) Electrical conductivity (EC) gives a measure of the effective decomposition of the effective feed in abiodigester (Eu-agrobiogas, 2009).
2) A negative redox potential for the raw material solution/slurry (less than -300mV) is a much required and necessary condition for any anaerobic digestion to occur (Bernhard, 2013, p.20).
3) Hydrogen and carbon monoxide measurements are more complex but can also be considered for bio digester process monitoring (Giovannini et al., 2016).

2.2.2.3 First level operational parameters

One important operational parameter is the hydraulic retention rate (HRT) which is defined as the time period that the feedstock remains inside the digester. An elevated organic loading rate will reduce the HRT as space needs to be created for the incoming feedstock. The HRT is expressed as the effective digester volume (m^3) divided by organic loading per day (m^3/day). The organic loading can be on hourly or daily basis whilst the HRT takes a number of days. Too low a HRT will result in low gas output whilst too high a HRT will result result temporily in good gas output. However, if the HRT remains too high the gas output will eventually decrease since fresh input feedstock takes a longer time to come into the digester. Hence a balance has to be struck between gas yeild and HRT.

In the operation of the digester, process monitoring is best done at a point in the earlier stages of the digetser whilst the overall measurement of the by products constituents and gas composition is best done at the output stage of the digester (Labatut & Gooch, 2015). The measurement of feedstock composition is to be made at the input of the digester and this involves input feedstock amount, pH and volatile solids (VS)[12] weight. It has also been established that liquid feedstocks (waste water) require a chemical oxygen demand (COD) measurement instead of VS or TS as these contain undefined volatile substances such as acetic acid and ethanol (Bernhard, 2013).

2.2.2.4 Second level operational parameters

What we term second level operational parameters are described below. This is because basic digester operation can take place without taking into consideration these parameters. However, fine tuning and system enhancement can occur if we do implement these.

[12] Volatile solids is the organic matter in the solution used to produce methane, and this is approximately equal to the total solids (TS).

The first observation is that toxic materials that take the form of soluble salts of zinc, nickel, chromium, mercury and copper in the feedstock can reduce biogas production and these have to be removed or reduced. Enhancement of biogas generation and dilution of toxic substances to mention but a few can be achieved by having a combined (Co-digestion) feedstock of cow dung and vegetable or agricultural waste (Bharathiraja et al., 2016; Corro et al., 2013; Kanokwan, 2006; Shah et al., 2015).
The other oberservations are:

1) Normal operational intervention parameters are the increase or decrease of temperature, stir and acid dosage (Biró et al., 2012).
2) Too much ‘’mixing’’ in the digester as a contributary factor to anaerobic process interruption or complete destruction (Kanokwan, 2006 p.15).

2.2.3 PHOTOVOLTAIC GENERATION

Fig. 2.2 gives a typical photovoltaic layout incorporating solar panel, charge controller, battery/bank inverter and alternating current based load.

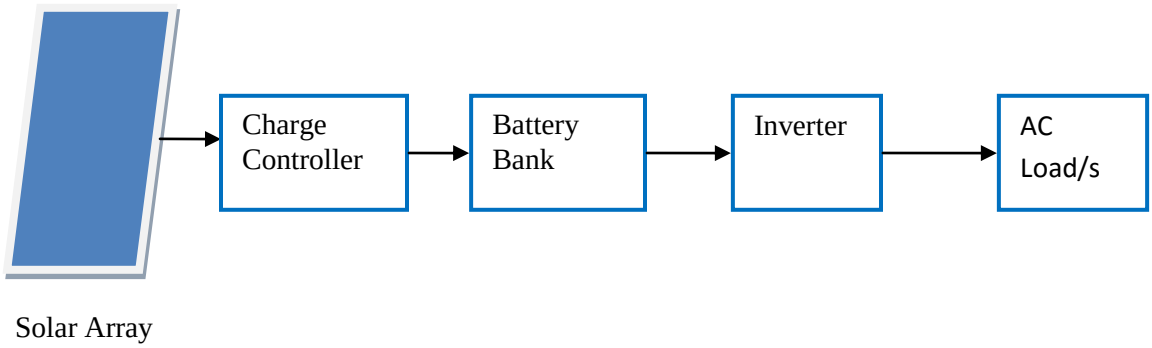

Fig. 2.2: A typical layout of photovoltaic system

The battery whether it is the ventilated-lead-acid (VLA) or the valve-regulated-lead-acid (VRLA) commonly known as the wet and sealed batteries respectively is the most important component of a photovoltaic system for constant load current. A depleted lead-acid battery will initially accommodate a relatively large charging current. However, further up the charging ladder the battery chemical makeup changes requiring a different charging strategy altogether since at seventy to eighty percent (Daoud & Midoun, 2005) level of charging the battery water breaks down to hydrogen and oxygen if the large charging current is maintained. This decomposition process is unwelcome in battery charging as it causes *“dryout”* (Byrne, 2010).

Parameters such as the charging rate, upper limit of charging current, battery internal resistance, terminal voltage, temperature and moisture vary continuously during the charging and discharging process (Cinar & Akarslan; 2012) resulting in a non-linear (Yong et al., 2008) battery charging and discharging control mechanism. For lead acid batteries both overcharging and under charging are undesirable (Byrne, 2010; Reddy, 2011). To this end it is required to design a charging strategy that effectively addresses all of these issues. These issues coupled with the inability of formulating an exact mathematical model of the battery (Daoud & Midoun,

2005) renders traditional control methods ineffective and the adoption of a fuzzy logic control strategy for the battery charging and discharging (Rekha & Kavitha 2014) would be more appropriate.

2.2.4 OPTIMISATION OF PHOTOVOLTAICS OUTPUT

The power (Watts) and voltage (Volts) output of a typical photovoltaic cell at constant temperature varies as the solar radiation level (W/m^2) as shown in Fig. 2.3. Clearly to obtain maximum power as the day progresses a maximum power point tracking strategy would be appropriate. Advanced charge control modules incorporate this control strategy as one way of optimizing system output.

On the other hand, the battery needs to be kept at an acceptable output voltage level under load and the state-of-charge (SOC) monitored. The SOC (Achaibou, Haddadi & Malek, 2012; Burgos et al., 2015) gives a representation of the usable capacity of a battery as a function of time. At manufacture a battery is capable of providing ideally one hundred percent of its capacity but over time the maximum capacity it can give decreases. The photovoltaic batteries' SOC which is given as the ratio of present capacity ($Q(t)$) to the theoretical capacity (Q_n) (Achaibou et al., 2012; Chang, 2013) will affect the overall charging mechanism. Hence it is very necessary for photovoltaic system to incorporate SOC measurement. Depending on the level of estimation required, different methods of obtaining the SOC are available and originally these included the specific gravity, open circuit voltage and coulomb counting methods. While more advanced methods include adaptive and hybrid systems (Chang, 2013; Tseng & Lin, 2005).

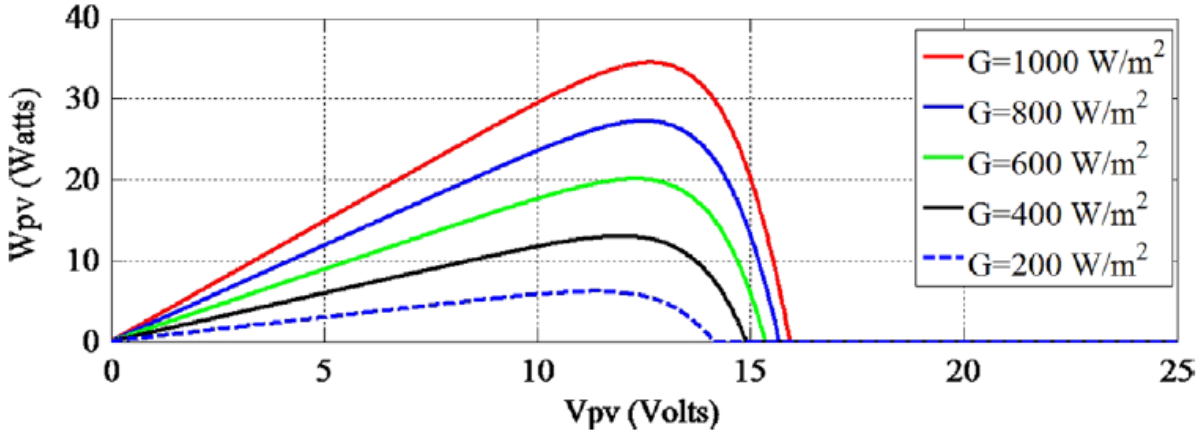

Fig. 2.3: P-V curves of a solar cell at different irradiance
(Hasan & Parida, 2016)

Different charging methods exist and these include the constant-current (one-current rate), constant-current (multiple decreasing-current steps), modified constant current, constant potential, modified constant potential with constant initial current, modified constant potential

with a constant finish rate, modified constant potential with a constant start and finish rate, taper charge, pulse charging, trickle charging, float charging and rapid charging (Reddy, 2011) .

2.3 FUZZY LOGIC ALGORITHMS

2.3.1 Membership Functions and Fuzzification

Fuzzy logic (Zadeh, 1965), is a linguistic based computing system that possess non-linear dynamics problem solving capabilities. In biogas and photovoltaic systems the energy generation processes involved are complex and the measurement information generated is imprecise and fragmented. The use of fuzzy logic algorithms has the overall effect of reducing the complexity (Singh et al., 2013) and cost of measurement and control equipment used.

The first step in developing a fuzzy logic based monitoring system is to specify the required input and output values (crisp data) and their ranges. Secondly to convert the crisp data to membership values (fuzzification), thirdly to synthesize output membership values based on developed fuzzy rules (fuzzy inference) and finally to convert the output membership values to crisp output values (defuzzification). The block diagram of the whole process is as shown in Fig. 2.4.

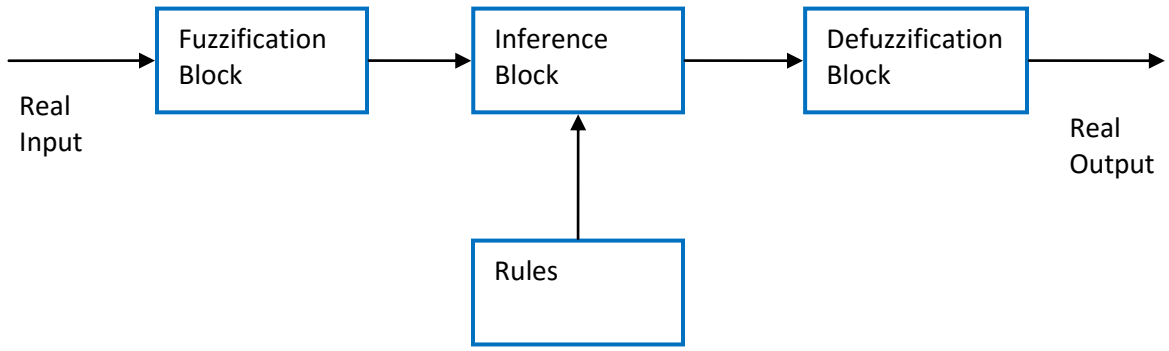

Fig. 2.4: Block diagram of fuzzy logic implementation process

As opposed to classical set theory where an entity either belongs or does not belong to a set, fuzzy set theory accommodates partial membership of the entity in the set. Indeed the fuzzy set is described by Zadeh (1965) as a '*class with a continuum of grades of membership*'. This is interpreted to mean that an entities' degree of belonging in a set can be on a sliding scale from zero(0) to unity(1). Furthermore the rules that govern operation on classical set theory are extended and adapted to fuzzy set theory.

A fuzzy set *A* according to Klir (2003) is related to a membership function μ_A by μ_A : $\longrightarrow$ *U [0,1]* where *U* is a classical set such that when $x \epsilon U$, $\mu_A(x)$ gives degree of membership of *x* in *A* and the case where $\mu_A(x) = 0$ *or* $\mu_A(x) = 1$ for all $x \epsilon U$ is known as a crisp

set. A single membership function whose different characteristics are shown in Fig. 2.5 is related to a single fuzzy set. The membership functions in Fig. 2.5 are defined as a. Monotonically increasing linear-function, b. Monotonically increasing sigmoidal-function, c. Monotonically decreasing linear- function, d. Triangular function, e. Gaussian function, and f. Trapezoidal function. However, the most extensively used membership functions are the monotonically increasing linear, monotonically decreasing linear and triangular functions (Cirstea et al., 2002).

In the case were the bio digester process has to be evaluated such that pH and alkalinity (buffering capacity) are input parameters and digester status is the output, the membership

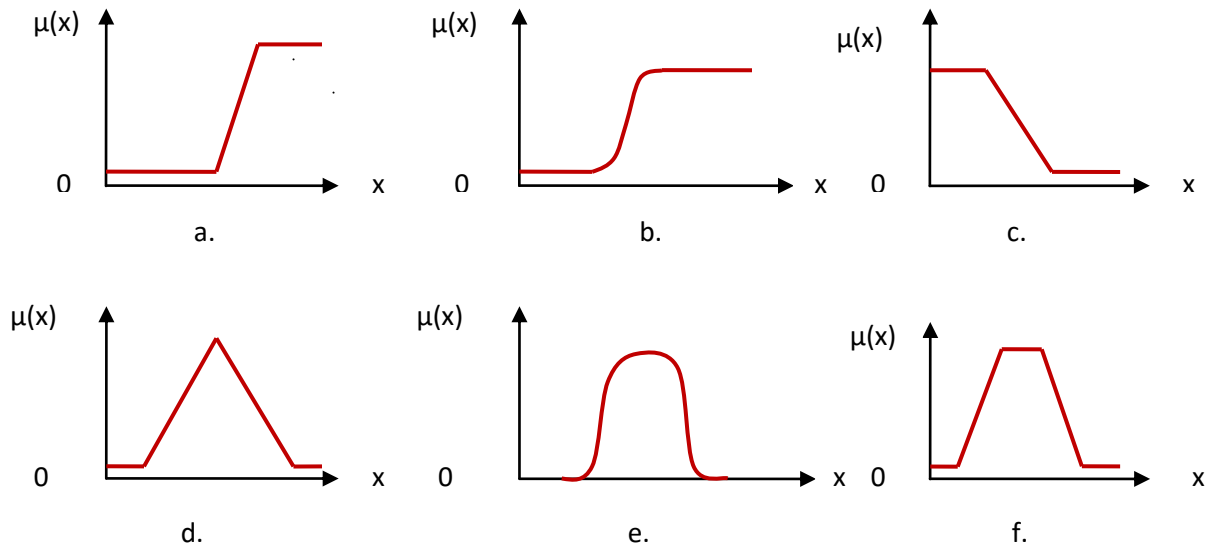

Fig. 2.5: Types of membership functions:
(Cirstea et al., 2002; Pappis & Siettos, 2005)

functions showing the Universe of Discourse (UoD)[13] are formulated as shown in Fig. 2.6. These membership functions incorporate a variable (word based term) to describe the respective membership function. As an example the pH can either be quite acidic (Q.acd), moderate acidic (M.acid), neutral (Neutral), moderate alkalinity (M.alkaline) or high alkaline (H.akaline). The Alkalinity value can be low (L), medium (M) or high (H). Whilst the digester operation status (Stability) could either have failed (F), be failing (FL) or is operating at Optimum (O).

2.3.2 Rules

Fuzzy rules can be implemented on decision trees. Predictive models that are tree-like describe decision trees. Observations are mapped onto several levels of a tree until final result is obtained. Hence fuzzy rules are not necessarily decision trees.

[13] Universe of Discourse (UoD) is the total range of influence of that parameter.

IF-THEN rules that relate the input to output linguistic variables and can include the following fuzzy logic operators AND, OR and NOT are structured as follows:
IF *condition (premise or antecedent)* **THEN** *conclusion (consequent)* (Carr & Shearer, 2007). It should also be noted that the IF-THEN rules can also be realized in the form of a fuzzy rule base or rule matrix).

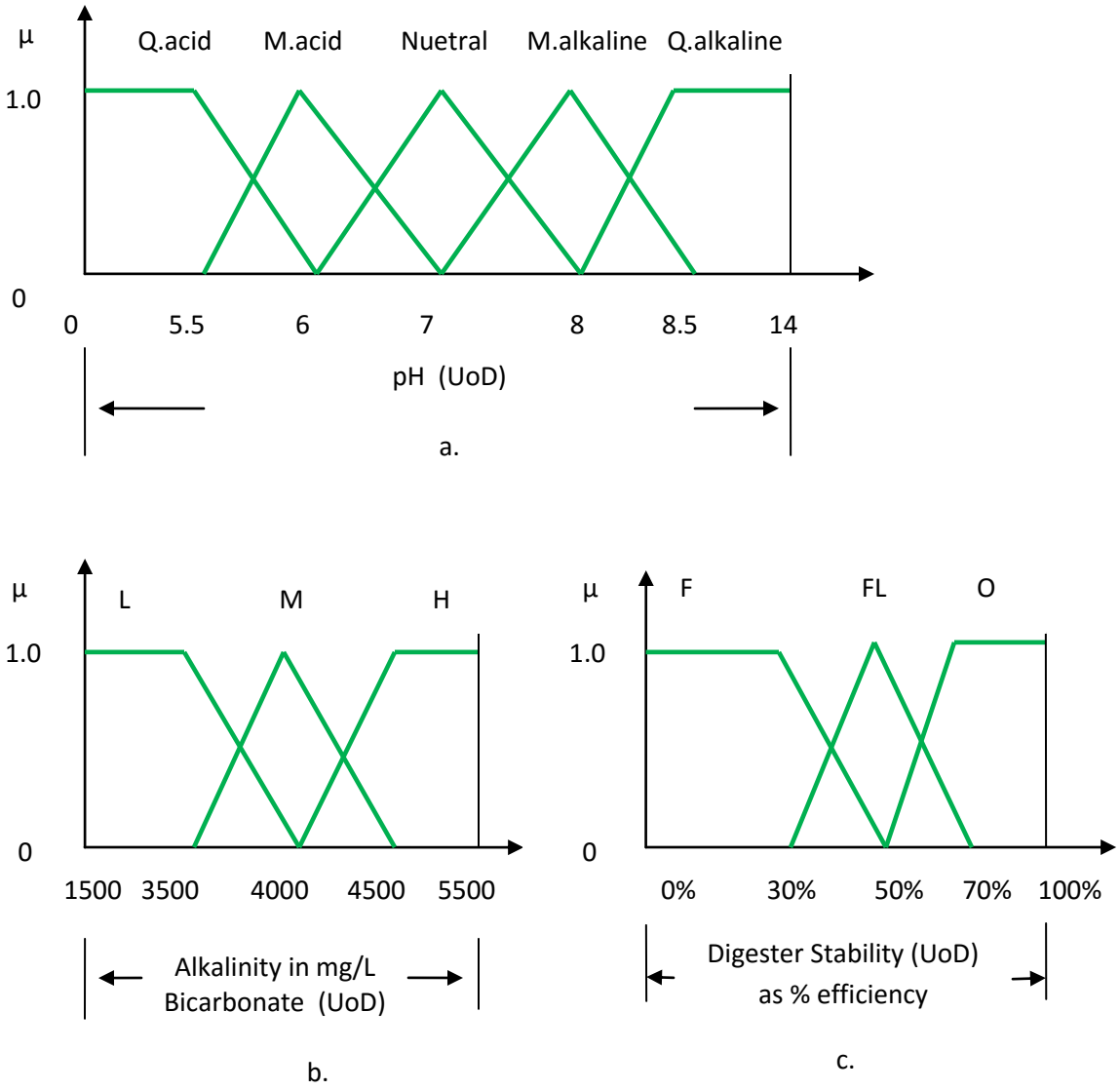

Fig. 2.6: Membership functions UoD of pH, Alkalinity and Digester operation status incorporating the linguistic terms

An example of a fuzzy rule is given below as:
IF *pH is Quite Acidic* **AND** *Alkalinity is Low* **THEN** *Digester Operation is Failed.*
From which *pH*, *Alkalinity* and *Digester Operation* are defined as fuzzy variables and *Quite Acidic*, *Low* and *Failed* as linguistic terms (values or states) (Salmoladas & Petrou, 1994). A rule base or rule matrix for the fuzzy control showing all the possible combinations of input and out is formulated as shown in Table 2.3.

Table 2.3: Rule Matrix for the digester operation

pH	Alkalinity		
	H	M	L
Q.acid	F	F	F
M.acid	O	O	FL
N	O	O	FL
M.alkaline	O	O	FL
Q.alkaline	F	F	F

From Table 2.3, it is realized that the number of possible rules is given by the number of first inputs (inputs1) multiplied by the number of second inputs (inputs2), that is 5 x 3 =15 in this case. A few rules are shown below.

1) Rule 1: **IF** *pH is Q.acid* **AND** *Alkalinity is H* **THEN** *Digester Operation is Failed.*

2) Rule 2: **IF** *pH is Q.acid* **AND** *Alkalinity is M* **THEN** *Digester Operation is Failed.*

3) Rule 3: **IF** *pH is Q.acid* **AND** *Alkalinity is L* **THEN** *Digester Operation is Failed.*

4) Rule 4: **IF** *pH is M.acid* **AND** *Alkalinity is H* **THEN** *Digester Operation is Optimum.*

5) Rule 5: **IF** *pH is M.acid* **AND** *Alkalinity is M* **THEN** *Digester Operation is Optimum.*

6) Rule 6: **IF** *pH is M.acid* **AND** *Alkalinity is L* **THEN** *Digester Operation is Failing,*

Etc.

2.3.3 Inference

2.3.3.1 Purpose for inference

This is the part that performs fuzzy reasoning or decision making and is made up of the Mamdani inference (Iancu, 2012; Iancu & Gabroveanu, 2010) method to evaluate:

1) Each rule's firing level based on the input
2) Output of each rule and
3) Summation of the results of each rule to realize the fuzzy output.

Taking the sample rules given above for our system, the actual degree of membership of each rule can be evaluated say for the two inputs where pH =5.7 and Alkalinty = 3900 mgl^{-1} bicarbonate as shown in Fig. 2.7.

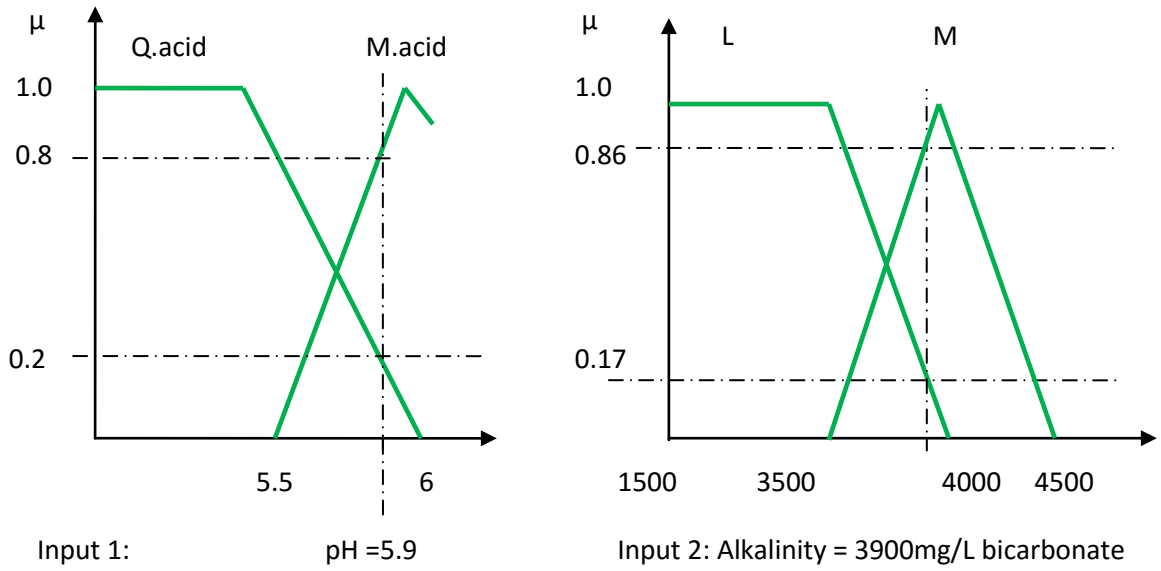

Fig. 2.7: Degree of membership of real (crisp) inputs represented by pH = 5.7 and Alkalinity = 3900 mg/L into the fuzzy logic controller

In this example the following degrees of membership for the UoD of pH and Alkalinity are given in Table 2.4.

Table 2.4: Degree of memberships for example given in Figure 2.7

	Degree of membership							
Membership function	Q.acid	M.acid	Nuetral	M.alkaline	Q.alkaline	L	M	H
Input 1	0.2	0.8	0.0	0.0	0.0	N/A	N/A	N/A
Input 2	N/A	N/A	N/A	N/A	N/A	0.17	0.86	0.0

2.3.3.2 Rule firing strength

The inference process, mainly revolves around either the Max-Min or the Max-Product (Dot) methods (Pappis & Siettos, 2005). For degree of membership values $\mu_A(x)$ and $\mu_B(x)$ of sets A and B, typically these processes are given as:

$\mu_A(x)$ *AND* $\mu_B(x) = min[\mu_A(x), \mu_B(x)]$ for the Max-Min where the minimum value of the premise is considered, and
$\mu_A(x)$ *AND* $\mu_B(x) = \mu_A(x)\mu_B(x)$ for the Max–Product where the product of the premise is considered.

To elaborate further consider the case where $\mu_A(x) = 0.5$ and $\mu_B(x) = 0.8$ for two triangular membership functions. Then for the Max-Min method the resultant degree of membership is $\min[0.5,0.8] = 0.5$ giving a truncated triangular function that forms a trapezium. Whilst for the Max- Product method the resultant degree of membership is $0.5x0.8 = 0.4$ giving a scaled down version of an un-truncated triangular function whose peak is 0.4.

The firing strengths for the complete rule matrix in Table 2.3, considering the degree of membership values in Table 2.4 are given below:

1) **IF** *pH is Q.acid* (0.2) **AND** *Alkalinity is H(0.0)* **THEN** *Digester Operation is Failed(0.0)*

2) **IF** *pH is Q.acid* (0.2) **AND** *Alkalinity is M (0.86*) **THEN** *Digester Operation is Failed(0.2)*

3) **IF** *pH is Q.acid(0.2)* **AND** *Alkalinity is L(0.17)* **THEN** *Digester Operation is Failed(0.17)*

4) **IF** *pH is M.acid(0.8)* **AND** *Alkalinity is H(0.0)* **THEN** *Digester Operation is Optimum(0.0)*

5) **IF** *pH is M.acid(0.8)* **AND** *Alkalinity is M(0.86)* **THEN** *Digester Operation is Optimum(0.8)*

6) **IF** *pH is M.acid(0.8)* **AND** *Alkalinity is L(0.17)* **THEN** *Digester Operation is Failing(0.17)*

7) **IF** *pH is Neutral(0.0)* **AND** *Alkalinity is H(0.0)* **THEN** *Digester Operation is Optimum(0.0)*

8) **IF** *pH is Neutral(0.0)* **AND** *Alkalinity is M(0.86)* **THEN** *Digester Operation is Optimum(0.0)*

9) **IF** *pH is Neutral(0.0)* **AND** *Alkalinity is L(0.17)* **THEN** *Digester Operation is Failing(0.0)*

10) **IF** *pH is M.alkaline(0.0)* **AND** *Alkalinity is H(0.0)* **THEN** *Digester Operation is Optimum(0.0)*

11) **IF** *pH is M.alkaline(0.0)* **AND** *Alkalinity is M(0.86)* **THEN** *Digester Operation is Optimum(0.0)*

12) **IF** *pH is M.alkaline(0.0)* **AND** *Alkalinity is L(0.17)* **THEN** *Digester Operation is Failing(0.0)*

13) **IF** *pH is Q.alkaline(0.0)* **AND** *Alkalinity is H(0.0)* **THEN** *Digester Operation is Failed(0.0)*

14) **IF** *pH is Q.alkaline(0.0)* **AND** *Alkalinity is M(0.86)* **THEN** *Digester Operation is Failed(0.0)*

15) **IF** *pH is Q.alkaline(0.0)* **AND** *Alkalinity is L(0.17)* **THEN** *Digester Operation is Failed(0.0)*

2.3.3.3 Output combination of the rules

Preceding the defuzzification process it is required to combine same like (conclusion) rule outputs whose single firing strengths has been obtained, so as to find their effective combined firing strength. The combination of the rule outputs can be achieved by adopting the Max-Min, Max-Dot (Max-Product),Averaging or Root-Sum-Square methods (Gopal & Raol, 2012).

According to Gopal & Raol (2012) each of the methods used for combining rule outputs as stated above can be briefly described as:

1) Max-Min method: Measure relative magnitudes of the respective rules and take note of the most significant one. Then evaluate the centre of mass (centroid) whose horizontal coordinate will give you the output, of the area under this most significant function. However this method seemingly uninvolved mathematically excludes all the other smaller rule magnitudes in deciding the output.
2) Max-Dot method: From the product process the membership function peak is effectively reduced (as illustrated in 2.3.3.2 above) from its previous height while maintaining a common horizontal base as the original membership function. From all contributing membership functions the centre of mass (centroid) is evaluated whose horizontal coordinate will give you the output. In this method all firing rules are catered for to provide a contiguous output.
3) Averaging method: The average membership value of the same logical outputs is calculated whose resultant becomes the new membership value of that logical output and the centroid can then be calculated. The main shortcoming of this method is its inability to increase the average value for an increase in the rules that give the same membership value.
4) Root-Sum-Square method: This method considers the influence of all the relevant rules and includes scaling of heights with sum of squares, after which the centroid is obtained from the resultant area. All firing rules are duly recognized.

The Max-Min method is used in this project as it is easier to calculate and it provides a continuous output without scaling of heights. The Max-Min (*which is associative*) method passes through the smaller value. Out of a number of possible outcomes, the smaller value is most likely to be stable, hence a better representation of the output. The actual value obtained represents the overall degree of membership of the linguistic term within acceptable tolerance.

2.3.3.3.1 Combined rule firing strength using Max-Min method

The maximum possible degree of membership value present for any rule is adopted as the valid degree of membership for the output linguistic term.

Output "Failed" is represented by the following rules:
Rule 1 degree of membership = 0, Rule 2 degree of membership = 0.2, Rule 3 degree of membership = 0, Rule 13 degree of membership = 0, Rule 14 degree of membership = 0, Rule 15 degree of membership = 0,
Hence **o**verall "Failed" degree of membership =0.2.

Output "Failing" is represented by the following rules:
Rule 6 degree of membership = 0.17, Rule 9 degree of membership = 0, Rule 12 degree of membership = 0,
Hence overall "Failing" degree of membership =0.17.

Output "Optimum" is represented by the following rules:
Rule 4 degree of membership = 0, Rule 5 degree of membership = 0.8, Rule 7 degree of membership = 0, Rule 8 degree of membership = 0, Rule 10 degree of membership = 0, Rule 11 degree of membership = 0,
Hence overall "Optimum" degree of membership =0.8.

2.3.3.3.2 Summation of Combined rule firing strength membership functions

The final overall fuzzy output membership function in Fig. 2.8 is obtained from the union of the resultant membership functions obtained in 2.3.3.3.1 above. In this case this would be:
Overall fuzzy output membership function = $Failed \cup Failing \cup Optimum$

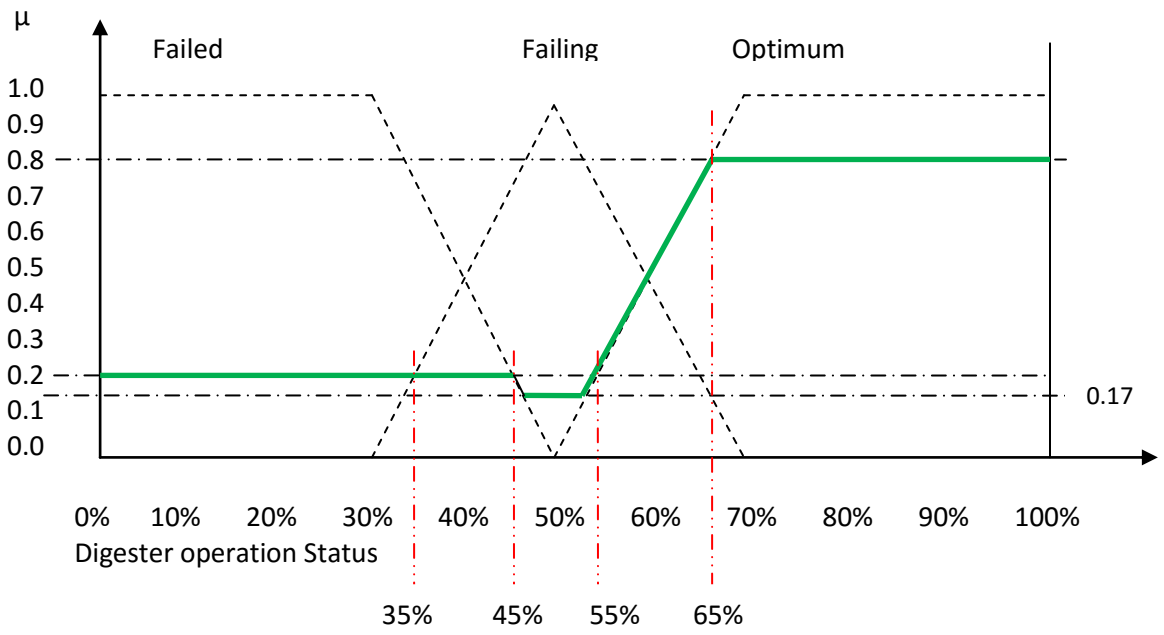

Fig. 2.8: Overall fuzzy output membership function

2.3.4 Defuzzification

Many defuzzification techniques abound and the use of a specific technique depends on the nature of the membership functions defining the system (including symmetrical nature). For this particular digester stability test, the output membership functions are symmetrical and the commonly used continuous centre of gravity (COG) also known as the centre of area (COA) or centroid method (Pappis & Siettos, 2005) is applied. For other algorithms for my project suitable techniques can be used. The equation for the COG method is given by Vas (1999) as:

$r_{out} = \frac{\int r\mu(r)dr}{\int \mu(r)dr}$ for continuous systems where μ(r) is resultant membership function from combination with r defining output member, and *(1)*

$r_{out} = \frac{\sum_{k=1}^{n} r_k \mu(rk)}{\sum_{k=1}^{n} \mu(rk)}$ for discrete systems where μ(rk) are the sampled resultant membership functions for k =1,2,3,….n.. *(2)*

2.3.4.1 Digester operation actual output

The output membership functions are normally modified after rule combination to give trapeziums as shown in Fig. 2.8. The COG defuzzification method then makes use of the area of each trapezium and the horizontal axis centroid points (Viot, 1993; Ross et al., 2002; Ross, 2004) to come up with the final output result. The resultant degree of membership from combination is taken as the height of the respect trapezium .With reference to Fig. 2.8 areas bounded by thick green lines:

1) $Failed\ area = \frac{0.2(50+45)}{2} = 9.5\ \%\ with\ centroid\ point\ of\ 30\ \%,$

2) $Failing\ area = \frac{0.17(40+29)}{2} = 5.87\ \%\ with\ centroid\ point\ of\ 50\ \%,$

3) $Optimum\ area = \frac{0.8(50+35)}{2} = 34\ \%\ with\ centroid\ point\ of\ 75\ \%.$

The crisp output is then given as:

$$r_{out} = \frac{Failed\ area*25\% + Failing\ area*50\% + Optimum\ area*75\%}{(Failed\ area + Failing\ area + Optimum\ area)\%}$$

$$= \frac{(9.5\%*25\%) + (5.87\%*50\%) + (34\%*75\%)}{(9.5 + 5.87 + 34)\%}$$

$$= \frac{3081}{49.37}$$

$$= 62.41\ \%$$

This result is interpreted from Fig. 2.8, to mean that the digester is operating approximately at $\mu = 0.52\ Optimum\ and\ \mu = 0.48\ Failing$. It is important to note that this makes sense since our input alkalinity (3900mg/L bicarbonate) is almost equal to that required of 4000mg/L bicarbonate for good buffering capacity (Eu-agrobiogas, 2009; Labatut & Gooch, 2015; Wisconsin, 1992). Furthermore our pH input of 5.9 will facilitate hydrolysis stage and falls 0.2 units shy of neutrality which is a required condition for methanogenesis (Eu-agrobiogas, 2009).

2.4 REVIEW OF THE RESEARCH

The measurement and control strategies investigated in this dissertation are shown in Figs. 2.9 & 2.10 for the biogas and photovoltaic systems respectively. Redox (ORP), conductivity (EC), composite gas pressure, feedstock level, oxygen (O_2), carbon dioxide (CO_2), methane gas concentration (CH_4), temperature (Temp.) and pH sensors monitored the biogas system.

The photovoltaic system, not incorporating maximum power point tracking (MPPT) algorithm was monitored by two current sensors (one for battery charging and the other for load overload protection), a voltage divider sensing circuit and two photocells attached to diagonal ends of the solar panels for prolonged shading detection. With typical array efficiencies that vary between 6% and 30% (Welch, 2010), the solar panels outputted reasonable power even without the

inclusion of MPPT as long as there was sunshine. The incorporation of photocells in the design sought to identify prolonged partial shading of the solar panels that could occur due to physical objects (leaves, cloth, paper, feathers, tree shadow etc). Photocells were used because current produced by a photocell is related to the sunlight available on it. This principle was used to detect partial shading of the solar panels and fuzzy algorithm would be most suitable as a significant number of shading levels could be quantified.

The fuzzy logic controller algorithm was to be embedded into an 8-bit enhanced mid-range or advanced architecture for microchip (Microchip, 2015b) microcontroller whilst simulation would be implemented in MPLABX IDE (Microchip, 2015a). Pre-amplification and signal scaling circuits were designed and incorporated into the measurements.

The expected outputs from the fuzzy logic controller included biogas digester stability status, emergency main gas pipe close valve, methane gas output amount, oxygen leak detection, feedstock low level detection and operating temperature status. Since the biogas digesters under consideration are naturally stirred and heated the main intervention was to be feedstock amount/composition loading rate and the addition of pH changing agent. The system did not have automatic stirring nor automatic loading of feedstock and acid/neutralizing agents. For the photovoltaic system the expected outputs included a sufficiently charged battery, detection of a break in the power flow, abnormal overload detection and prolonged partial or full shading of the solar panels during normal daylight.

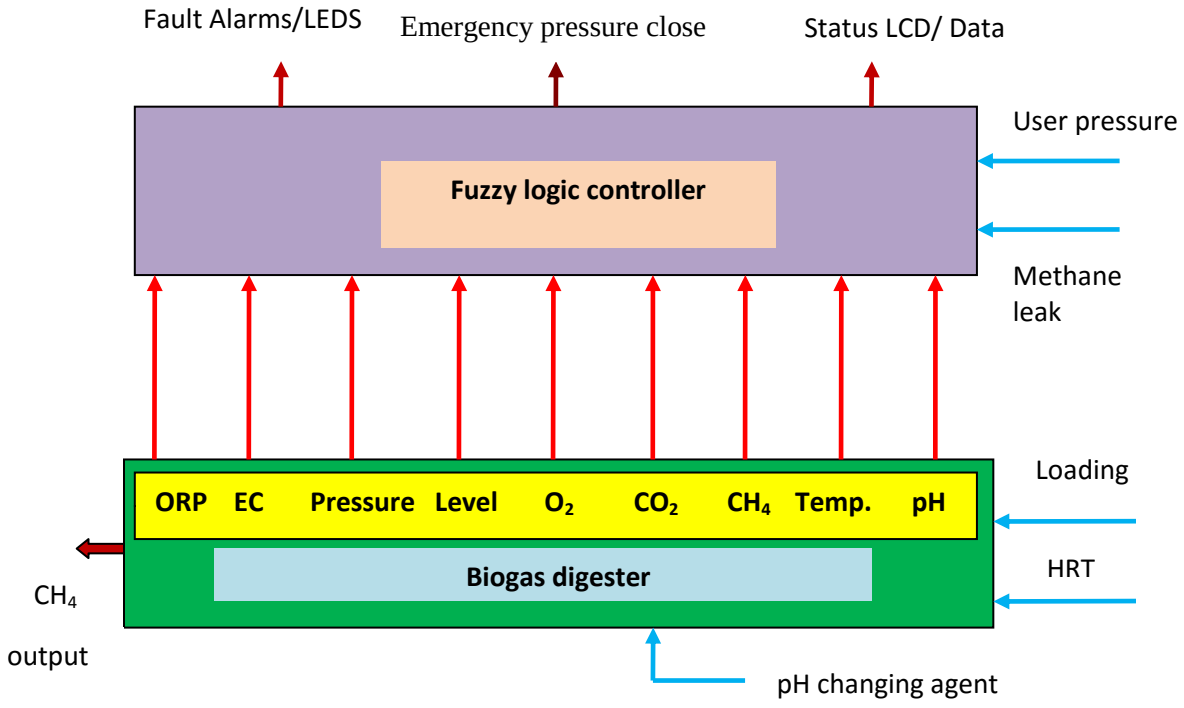

Fig. 2.9: Block diagram of proposed biogas system

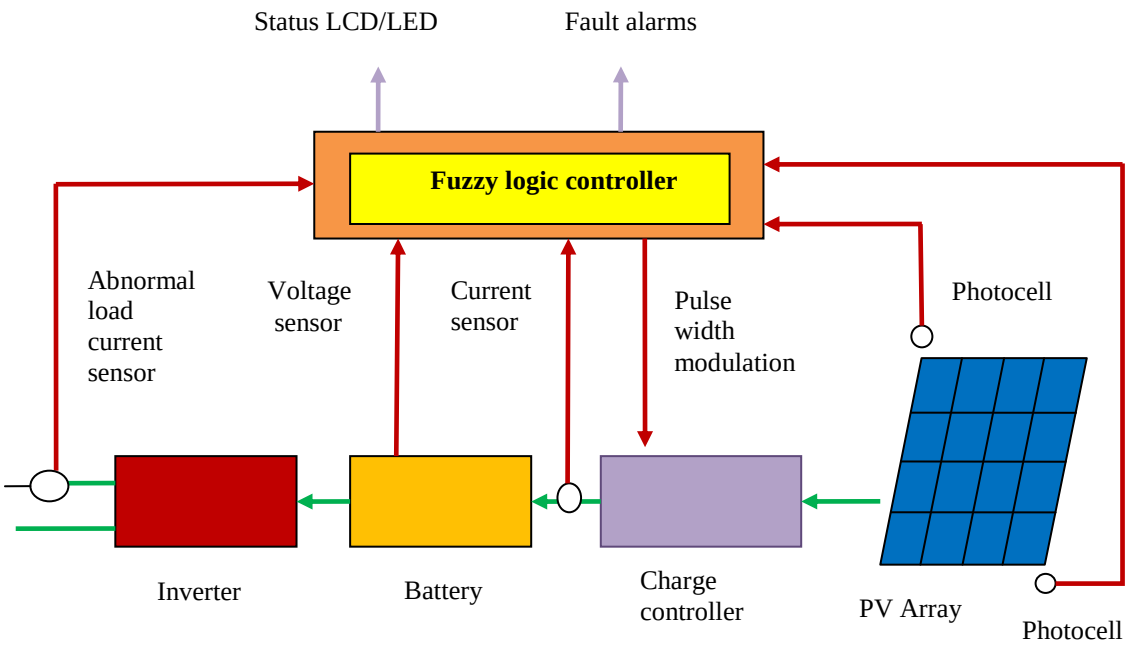

Fig. 2.10: Block diagram of proposed photovoltaic system

2.5 CONCLUSION

During the literature review process, it has been established that biogas and photovoltaic systems are not new technologies, having been in use for a long time now. Controlled biogas generation has taken place since time immemorial. Of recent, monitoring strategies have been developed and implemented on large stand alone installations. Information on mechanisms of energy generation and how system performance can be increased is readily available. However, an elaborate fault detection and control strategy, combined into a single unit for intermixed biogas and photovoltaic systems is not fully addressed in current installations (i.e. small, medium and large scale installations). Furthermore the use of fuzzy logic algorithms as has been done in this research addresses a gap in the use of intelligent methods in the monitoring of renewable energy systems.

CHAPTER 3

RESEARCH DESIGN AND METHODOLOGY

3.1 INTRODUCTION

This chapter gives a detailed discussion of the research design and methodology. Section 3.2 details the interview process, whilst, in section 3.3 the research paradigms and research methods used in this study are discussed. Section 3.4 is about the hypothesis and the translation (mapping) of research questions into their research methodology equivalents. The data collection process pertaining to the study is described in detail in section 3.5 which begins by giving a detailed discussion of data collection principle. The method of data analysis is described in section 3.6, whilst the research ethics and the conclusion to chapter 3 are given in section 3.7 and section 3.8 respectively.

3.2. INTERVIEW PROCESS

The results of the interviews carried out in rural establishments that have REF digesters and photovoltaic systems installed are given in Tables 3.1 and 3.2 respectively. A large percentage of the biogas and photovoltaic systems that where considered for the interview exist alone, as such interviews done on site were either only for biogas or only for the photovoltaic system. Furthermore it was observed that the number of biogas systems outweigh the number of photovoltaic installations of the said capacity, as even some rural establishments with grid electricity do also have biogas systems installed so as to reduce their electricity bill and to counteract on grid outages that are caused by faults and load shedding. The pie chart in Fig. 3.1 shows the relative nature of the biogas and photovoltaic installations at which interviews where done.

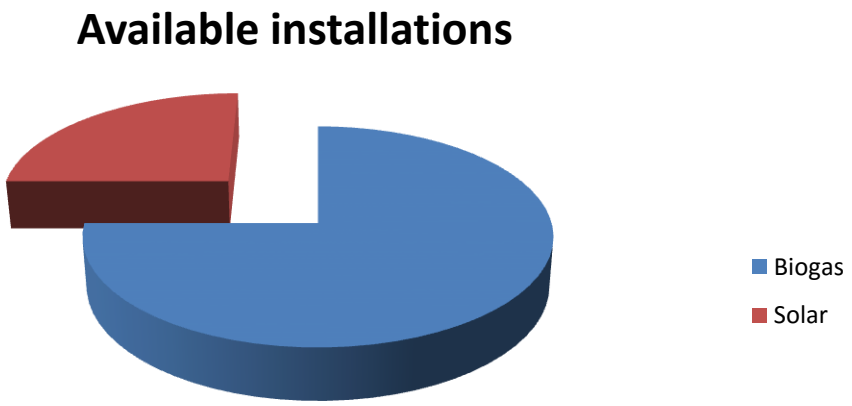

Fig. 3.1: Relative number of installations that where accessed

Table 3.1: Summarized interview results related to biogas generation

Main questions	Sub questions	Interviewee's response
1) is your bio digester for a single household or for a small community? OR -what size is your bio digester?	- how many people use this digester?	-small community, less than five hundred people
	- are there school going children among the users?	-many school children
	- is the gas output tap turned on continuously?	-mains always turned on
	- are there times when the gas supply is fully closed?	-no
2) does your bio digester supply enough biogas?	-for what purpose is the gas used?	-firewood also used - cooking and heating -just for functions at schools -continuous use for small foods
	-do you always obtain gas output as and when you need it?	-some always, others not enough gas sometimes
	-what are your gas storage facilities?	-high '' layman's response''
	-what can you say about the pressure of the gas coming out of the pipe?	-generally high
	-how far are the gas storage and digester from the house?	-250m to 400m
3) Do you troubleshoot gas related issues?	- How do you rectify continuous low biogas output from the digester?	-always refer faults to REF
	-What is the effect of gas leakage in the house?	-explosions occur with furniture burnt and injury to people usually at homesteads (few or no leakages at schools or clinics)
	-what biogas pressure irregularities are of concern?	-some times gas takes long to come
4) what type of waste is used in the bio digester?	-what are the daily solids (dry matter) to liquid (water) ratio input to the digester?	-difficult to say (REF knows better), only lots of water required
	- how do you know which solids to liquid ratio will give the best biogas output?	-1) human sewerage based 2) some piggery waste 3) some cow waste (also add hides, dead chickens, dead pigs in 2) and 3) above)
	- do you know the toxicity and pH of the feedstock?	-no way to tell

5) how do you monitor internal bio digester process?	-is feedstock level in the bio digester important? -what parameters are critical to bio digester sustained process operation?	-no internal monitoring -do not know
6) how is the used up waste from the bio digester removed?	-what is the typical retention time (i.e time between inputting waste and discharging it)? - how is the waste material used?	-minimum of about 21 days -(solids removed as fertilizer after 2 years) -waste water for garden pond - digester near vegetable garden
7) are there written down instructions on how to operate the biogas system?	-what are your observations and recommendations?	-not sure if they exist, never seen any instructions

Table 3.2: Summarized interview results related to photovoltaic generation

Main questions	**Sub questions**	**Interviewee's response**
1) is your photovoltaic system for a single household or for a small community? OR -what size is your photovoltaic system?	- how many people use this photovoltaic system? - are there users who need continuous electrical supply?	-small community (single household up to 500 people) -some important establishments also have stand-by generators
2) does your photovoltaic system supply enough electricity?	-for what purpose is the electricity used? -do you always obtain electricity when you need it? -how reliable is your battery bank? -what can you say about the power generated versas that taken by the users? -how far are the battery bank and inverter from the house?	-lighting, entertainment, computers, business equipment, small refrigerators -reliable -not enough for all user requirements -depends on intended installation
3) Do you troubleshoot electrical generation related issues?	- How do you rectify continuous low electrical output from the photovoltaic system? -How do you maintain the different components of the photovoltaic system from solar panel to inverter?	- we call REF - clean solar panels

	-what electrical generation irregularities are of concern? -what load conditions interfere with system operation?	-none, only low power during heavy clouds and rainy season -people trying to connect two plate stoves and electric irons
4) how do you monitor internal photovoltaic process?	-what aspects are critical to photovoltaic sustained process operation?	-do not know
5) are there written down instructions on how to operate the photovoltaic system?	-what are your observations and recommendations?	-some (including battery maintenance)

These interviews were done and concluded as per attached interview protocol in Appendix B and signed informed consent form in Appendix C. The interview results clearly consolidate the initial idea of designing a measurement and control system for intermixed biogas and photovoltaic systems. Existing systems also totally lack any forms of fault detection and control. The users of these renewable energies are heavily dependent on external expertise for solving serious issues that can arise during the operation of biogas and photovoltaic systems. The design of a fuzzy logic measurement and control system for intermixed biogas and photovoltaic systems will reduce or totally eliminate the external expert on a wide range of operational issues.

The study established that solar energy for most rural households is used for entertainment and lighting, while for public establishments that include clinics, hospitals and schools the use of solar power is more elaborate. In these establishments in addition to those uses similar to rural households the solar energy is required for equipment such as communication systems, refrigerators, computers and other critical electrical equipment. On the other hand biogas is heavily used for cooking and heating by both households and public establishments.

3.3 RESEARCH DESIGN

3.3.1 Research Paradigm

A paradigm[14] is defined by Chalmers 1982, p. 90 (cited in Jerry 2007) as being "made up of the general theoretical assumptions and laws, and techniques for their application that the members of a particular scientific community adopt". Chalmers 1982, p. 91 (cited in Jerry 2007) also states that a paradigm is made up of the following components:

1) "Explicitly stated laws and theoretical assumptions".
2) "Standard ways of applying the fundamental laws to a variety of situations".
3) "Instrumentation and instrumental techniques that bring the laws of the paradigm to bear on the real world".
4) "General metaphysical[15] principles that guide work within the paradigm".

[14] A paradigm can also be looked at as a world view or framework for that particular study.

[15] Metaphysics is a branch of philosophy that asks two questions and according to Jerry (2007) these are: 1. "What are the characteristics of existence?" and, 2. "How can we know the things that exist?"

5) "General methodological prescriptions about how to conduct work within the paradigm".

Research assumptions that are made by researchers include those known as ontological, epistemological, methodological and axiological. Ontological assumptions address the nature of reality of the system being studied while epistemological assumptions define the nature of the connection (knowledge) between the researcher and the system being studied. On the other hand methodological assumptions address the ways taken by the researcher to investigate and acquire knowledge on the system being studied. Finally, the axiological assumption seeks to identify any information that could be of importance to the study (Aliyu et al., 2014).

The research paradigms are mainly identified as positivism, post-positivism (interpretation) and constructivism and these are related to the research assumptions as shown in Table 3.3

Table 3.3: Research paradigms and associated assumptions (Aliyu et al., 2014)

Issue	**Positivism**	**Post positivism**	**Constructivism**
Ontology	naïve realism- "real" reality but apprehendable	critical realism- "real" reality but only imperfectly and probabilistically apprehendable	relativism- local and specific constructed realities
Epistemology	dualist/objectivist; findings true	modified dual/objectivist; critical tradition/ community ;findings probably true	Transactional/ subjectivist; created findings
Methodology	experimental/ manipulative; verification of hypothesis; chiefly quantitative methods	Modified experimental/ manipulative; critical multiplism; falsification of hypothesis; may include qualitative methods	Hermeneutic/ dialectical
Axiology	propositional knowing about the world is an end in itself, is intrinsically valuable	propositional knowing about the world is an end in itself, is intrinsically valuable	propositional, transactional knowing is instrumentally valuable as a means to social emancipation, which is an end itself, is intrinsically valuable

As far as positivism is concerned, knowledge is obtained by employing scientifically based measurements and observations on systems in the real world (O'Leary, 2007a; Payne, 2004). In the positivist attitude by considering the ontological, epistemological and methodological assumptions in Table 3.3, the system under research is definitely real, findings are objective/true, and the experimental based quantitative research can be done.

On the other hand the post-positivist believe in a complex, highly disordered world that is left to interpretation and cannot be measured directly (Aliyu et al., 2014; O'Leary, 2007b). In the ontological assumption, a number of realities exist and the epistemological findings that are observer based are probably true. The methodology in the interpretive paradigm can be qualitative with little reliance on the experimentation method.

Constructivism and participatory (not mentioned here) are both paradigms of inquiry (Howell, 2013) where knowledge is solely based on humans, either as individuals or as society. According to Howell (2013):

'*Constructivism understands reality as being locally constructed and based on shared experiences and, because groups/individuals are changeable, identifies it as 'relativist realism' or 'relative ontology'. Epistemologically, constructivism is similar to critical theory, however research results are created through consensus and individual constructions, including the constructions of the investigator. Theory in this paradigm is relative and changeable, reliability and prediction almost impossible and cause and effect difficult to identify.'*

In this scenario any research to be done cannot be separated from the human construct. The positivistic research paradigm (Jerry, 2007; O'Leary, 2007a) is adopted in this research since positivist attitude clearly accommodates the relevant assumptions that are required. In this study the energy generation processes in both the biogas and photovoltaic systems, though multi-parameter dependent do follow pre-defined steps. The state of each process which can be successfully assessed by the scientifically based measurement procedure lies within the positivistic research paradigm. This dissertation will include design and programming experiments, which indicates a high degree of empirical positivistic approach. Empiricism (O'Leary, 2007c) explains that valid results are only obtained from measuring, testing and making observations. However this study will also involve post-positivistic (interpretative) research approach in the form of qualitative literature and field study.

3.3.2 Research methods

Research methods are basically ways to get information that the researcher has to use. The type of method used is attributed to the source of information, how the information is acquired and the data collection instruments used. Research methods are globally indentified as either qualitative (Denzin, 2007) or quantitative (Salkind, 2010).

The qualitative research process involves the study of systems in their natural setup (Bloor & Wood, 2006) and attempts to provide relevant human based interpretation of the findings. The

methods used in qualitative research include case study, personal experience, interactional, historical, interview and observational (Denzin, 2007).

Quantitative research method is based on sound data investigation that has no bias. The results can be statistically or numerically used to describe the system population under study. The scientific research method (positivism), which is based on measurement (including experimentation) is the hallmark of the quantitative research method (Salkind, 2010). The descriptive form can also be used to represent the findings in quantitative research. Based on the nature of this study, the quantitative research method will be mainly used.

The overall research methodology strategy is to include both the qualitative and quantitative research methods in this research in what is termed the 'mixed method' research method. Mixed methods research according to Jupp (2006), is:

'*The combined use of both quantitative and qualitative methodologies within the same study in order to address a single research question.'*

However, this does not imply the use of multiple quantitative nor qualitative methods in any research question. One method can be used before the other, or both methods can be used at the same time between quantitative and qualitative research. In this research, established (historical) data from literature review is first used to test the accuracy of the algorithm and software development process with the aid of simulation software.

After this initial process of verification, the algorithms are then passed and implemented on the real system that measures and collects real time data. Immediately after development and verification of the algorithms, and before hardware implementation the results of the interviews/consultations that are qualitative in nature are considered. The interviews seek to establish the user's (experts and non-experts) perceptions on existing biogas and photovoltaic systems. Although the interviews are meant to be done earlier on in the study, their results are only considered after the initial measurement and control system simulation has passed since it becomes easy to make specific adjustments if any in the design. Hence the interviews can still be performed way into the study. The design of the sensor circuits, output circuits and embedded system is based on literature study and expert knowledge of the researcher.

The mixed research method is a triangulation[16] process that seeks to establish the functionality and accuracy of the designed algorithms from the simulation and implementation angles.

3.4 HYPOTHESIS AND RESEARCH QUESTIONS

The hypothesis for this dissertation is given as:

The measurement and control for intermixed biogas and photovoltaic systems is successfully implemented by the use of fuzzy logic algorithms.

[16] In triangulation a number of different approaches are taken to address a single research question issue.

The data used was obtained from an already installed and working biogas digester and photovoltaic system. Software and performance as given in Appendix E1 & E2, and Chapter 8, show that the hypothesis is true.

In this section, the research questions in this study are all translated (mapped) into their research methodology equivalents. For this study, Table 3.4 gives the relationship between a research question and the most suitable research method that can be used. An **X** indicates a correspondence between a research question and a data collection method that can be used. Table 3.4 shows a bias towards the quantitative research method as depicted by the pronounced measurement and experiment methods. High levels of the design and historical methods are also noted. The observation method is relatively significant, with the interview method contributing the least in this study. The positivism approach is hence consolidated within a mixed method situation. With this perspective in mind, the data collection methods are fully described in the following sections.

Table 3.4: Mapping of research questions into research methods

	Data			**Collection**		**Method**
Research Question Number *(See Page 4*)	Measurement	Experiment	Design	Historical/ Literature	Observation	Interview
1)	X			X		
2)	X	X		X		
3)				X	X	X
4)	X	X	X	X		
5)	X	X	X	X		
6)	X	X	X		X	

3.5 DATA COLLECTION

3.5.1 Historical/Literature Review

A detailed literature study was done to obtain existing information on the biogas and photovoltaic energy generation process with a view of determining the critical parameters required to improve system performance. A literature study on fuzzy logic concepts, relevant instrument sensors, output devices, suitable microcontroller and existing methods used to improve/optimize system performance was also been done. The literature was obtained from books, journals, conference papers, white papers, system design specifications and from the internet (mainly UNISA library).

3.5.2 Field Interviews

The interviews provided an opportunity for us to look at the biogas and photovoltaic systems from the ‘eyes ‘, of the day to day users of these energy establishments. The users were free to participate in the interviews and to provide any kind or amount of information they so wished pertaining to the operation of the biogas and photovoltaic systems. Depending on the interview outcomes, the information so provided by the interviewees was ether considered or not considered for modification of the designed program flowcharts.

3.5.3 Experiments

Initially the experiments took the form of simulations in this research. The writing of fuzzy logic algorithms was undertaken using various approaches. Flowcharts where developed followed by C language based source codes writing in the MPLABX IDE development software. The hardware simulation and development of circuit schematics were performed in the Labcenter’s Proteus (Labcenter, 2012) and National Instrument’s Multisim (National, 2013 software packages.

3.5.4 Field Measurements

Measurements were performed using the specified sensors and sensor circuits. Firstly, data was acquired from the real system using the sensors and sensor circuits not yet connected to program bearing microcontroller and the readings noted. Manual titration method was performed on a given sample of the digester substrate to determine the value of the buffering capacity. Secondly data was acquired by using the complete hardware and software based data acquisition system. The sensors were installed inside the digester, at the user end premises *(Figure 2.9 page 26)* and on the photovoltaic system points as per design *(Figure 2.10 page 27).*

3.5.5 Field Observations

The field observations entail observing the behavior and nature of the outputs that are the result of the implementation of the complete measurement and control system. The on-line outputs were observed to see if the system behaved as per design.

3.6 DATA ANALYSIS

3.6.1 Historical Data Analysis

From the literature review, we were able to provide a detailed breakdown of the energy process mechanism in biogas and photovoltaic systems. We were able to show how the different stages are linked together and how each stage affects the overall system output. With the knowledge of the role each stage, by product and/or parameter plays in achieving the desired output we could confidently design a monitoring system which was able to guide us to the successful production of biogas or photovoltaic energy. This review also assisted in showing that quite a number approaches of standalone system optimization have been developed and implemented, however the ‘gap’ that exists in the intelligent measurement and control of intermixed biogas and photovoltaic systems was further consolidated through the literature study. The initial stages of

the fuzzy logic algorithms development process and the embedded system hardware design were successfully done by incorporating the results of the literature review.

3.6.2 Interview Data Analysis

The interviews were performed using the interview protocol that was designed for this research. The numbers of the interviews were limited mainly due to the sparsely distributed nature of the energy installations in the rural areas. However, those who did participate provided invaluable information on the operation of the biogas and photovoltaic systems. The actual responses are given in the findings (Section 3.2), but it serves to mention here that no modification in the measurement and control system design was necessary as the initial design process had globally considered most aspects (from literature review and observation).

3.6.3 Experimental Based Data Analysis

The simulations were used to verify the proper functionality of the developed algorithms and whether the outputs generated are realistic when given specific input data, first from established literature sources and secondly from system measured data. The written software modules were continuously modified or fine tuned until they effectively addressed the flowchart with the least number of program lines. In summary, the outcome of the experimental data was to identify the best working fuzzy logic and control algorithms that addressed the problem at hand and to provide written code that was working without errors. Chapter 6 gives the complete simulation behavior of the programs to given input data, while chapter 7 gives the overall data acquisition and control system (designed and experimentally validated) ready to be directly installed in the field.

3.6.4 Field Based Measurement Data Analysis

The readings that were obtained by using the sensors and sensor circuits not yet connected to the microcontroller were used as data input for the simulation routines. The results of the simulation, so produced were used to cross-check the overall field measurement and control system response, since the same data range and type was used in each case. The results for the simulation are given in chapter 5, while the field based results/findings are given in chapter 8. The buffering capacity value obtained from manual titration was used in the multiple regression analysis formulation of the alkalinity prediction equation. The soft sensor routine and corresponding results are given in chapter 4, section 4.2.2.

3.7 RESEARCH ETHICS

According to Thomas & Hodges (2010) a research is supposed to be ethically undertaken. We were, required for our research to conform to a moral, transparent, original and above board way of dealing. In the strictest way possible we endeavored not to hurt or prejudice any individual as we carried out my research, nor where existing biogas and photovoltaic installations unduly negatively affected. Furthermore, due acknowledgement of all work and information which was not our own was made.

The requirements for research ethics guided by the UNISA revised policy on research ethics (2013) were duly met, and are tabulated below:

1) Ethical clearance (Appendix A) was obtained from the College of Science, Engineering and Technology's (CSET) Research and Ethics Committee at the University of South Africa (UNISA).
2) Human subjects were not directly used in this research.
3) Permission was sought and obtained from the administrators of the biogas and photovoltaic installations to conduct interviews where the interviewees were free to accept or decline to participate. To this end, a sample of a signed informed consent form is provided in Appendix B.
4) The research was implemented without interfering neither with the constructional designs nor the operation status of the existing biogas and photovoltaic systems.
5) Permission was sought and obtained from REF to implement the monitoring system on their installations provided the conditions in 3) above are observed.
6) Information from any other consultations done was treated in the strictest confidence and the anonymity of the participants maintained.

3.8 CONCLUSION

In chapter 3, we detailed the research paradigms and research methods used in this study. The translation (mapping) of the research questions into research methods was done and the relative contributions of each research method to the research questions was given *(Table 3.3 page 32).* The data collection methods, the data analysis procedure and the ethical considerations according to UNISA requirements are also fully explained in this chapter.

CHAPTER 4

FUZZY LOGIC ALGORITHMS AND SYSTEM FLOWCHART DESIGN

4.1 INTRODUCTION

In this chapter the fuzzy logic algorithms and module flowcharts are developed. The fuzzy logic algorithm and module flowchart for digester system stability test are developed in section 4.2. Section 4.3 looks at the development of the fuzzy logic algorithm and flowchart for biogas amount output. Section 4.4 develops the fuzzy logic algorithm and flowchart for biogas system fault detection and status, while the design of solar battery charging/discharging fuzzy logic algorithm and flowchart are detailed in section 4.5. Solar system fault detection and status fuzzy logic algorithm and flowchart are treated in section 4.6, with section 4.7 concluding this chapter.

4.2 DIGESTER SYSTEM STABILITY TEST

4.2.1 Fuzzy logic algorithm 1

The algorithm procedure given as an example in the literature review section *(Section* **2.3 FUZZY LOGIC ALGORITHMS***)*, was the adopted fuzzy logic algorithm for digester stability. This is made up of a two input and one output fuzzy logic controller with a total number of fifteen rules as shown. The inputs are pH and buffering capacity (Alkalinity), whilst the output is the stability status of the digester as a percentage. A high percentage value, of stability implies a greater confidence level in the digesters' capability to continually produce biogas. The pH parameter is directly measured by a pH sensor, whilst the alkalinity is inferred by the combined measurements of pH, redox and electrical conductivity of the digester substrate. The alkalinity prediction procedure and the overall stability test flowchart are given in the following sections.

4.2.2 Evaluation of alkalinity from soft sensors

The buffering capacity (Alkalinity) value that forms one of the inputs to the fuzzy logic routine was obtained by prediction from a soft sensor algorithm using multiple linear regression analysis (MLRA) of a number of independent bio digester parameters. This value of alkalinity could have been measured directly by using very expensive instruments which are however beyond the scope of this study. An alternative cheaper on-line method to measure alkalinity based on soft sensor method was considered.

A software sensor algorithm that uses pH, conductivity and redox (Eu-agrobiogas, 2009; Ward et al., 2008; Ward et al., 2011) was proposed and used. This method is supposed to produce a reasonable good prediction of alkalinity. However, as an alternative to the method just mentioned above, other software algorithms (Argyropoulos, 2013; Pham et al., 2014; Turkdogan, 2010) that may use only pH and gas production in its simplest form as the independent variables, as a way of reducing the number of probes and circuitry can be proposed.

The multiple linear regression method is based on making measurements of all the independent variables and the dependent variable (Bagos & Adams, 2015) over a suitable number of times, and then using this data in regression analysis to develop the following prediction equation:

$$Y = \alpha + \beta 1X1 + \beta 2X2 + \cdots \beta iXi + e \qquad (3)$$

Where : $Y = desired\ output$
$\alpha = Y\ axis\ intecept$
$\beta 1 = coefficient\ of\ X1\ input$
$\beta 2 = coefficient\ of\ X2\ input$
$\beta i = cofficient\ of\ Xi\ input$
$e = residual\ error$

A general (MLRA) model was developed using data (Table 4.1) which closely relates to the ranges for redox, conductivity and alkalinity in a typical digester as stated in the references (Bernhard, 2013 p.20; Franke, 2014; Labatut & Gooch, 2015). The ratio[17] $\frac{VFAs}{Alkalinty}$ is used to assess the stability (Feng, 2013; Lohri, 2008) of the digester in the offline mode. The titration (*See section* ***5.2.4.2 Titration procedure***) method was used to find this ratio. The alkalinity can also be obtained from titration by multiplying the millimoles per litre (mmol/l) value by the molar mass[18] of calcium carbornate in grammes per (g/mol) to give the units of alkalinity in mg/l. bicarbonate as used in this research. Field measurements of pH, electrical conductivity (EC) and oxygen reduction potential (ORP) or redox were made, after construction of the measuring circuits.

Table 4.1: Data for developing a general regression analysis model

Reading Number	**pH (X_1-*input*)**	**Redox in mV (X_3-*input*)**	**Electrical Conductivity (EC) in milli Siemens/cm (X_2-*input*)**	**Alkalinity in mg/L bicarbonate (*Y-output*)**
1	5.6	-250	8.7	3500
2	5.8	-300	9.6	3888
3	6.5	-330	9.8	4331
4	7.2	-350	10.9	4011
5	7.9	-375	20.1	4955

Using Excel regression in data analysis tools (Appendix D) the coefficients of $\alpha, \beta 1, \beta 2\ and\ \beta 3$ of Eqn.*(3)* were obtained and fitted as in Eqn.*(4)* for the readings of Table 4.1.

[17] 1) Ratio < 0.4 stable, 2) Ratio 0.4 – 0.8 some stability, and 3) Ratio >0.8 very unstable.
[18] Molar mass of calcium carbonate is 162.1146 g/mol.

$$Alkalinity = 2148.33 - 392.01pH + 86.39EC - 11.07Redox \quad (4)$$

Eqn.*(4)* gives the most likely output for alkalinity for specific values of pH, redox and electrical conductivity where the **Adjusted R Square** value of 0.696504 shows a reasonable good fit for the equation to predict the output alkalinity. Low values of ***P-value*** (P < 0.05) eliminate the possibility of any independent variable (pH, EC, Redox) having a value of zero ("*the null hypothesis*") in our prediction equation thereby consolidating its nature (Zaman & Alakus, 2005). Likewise $\boldsymbol{modulus\ t\ test}$ should be greater than the $\boldsymbol{critical\ t\ test}$ obtained in Excel for us to eliminate the "*null hypothesis*". However the data we have used says otherwise as $\boldsymbol{P} > 0.05$ and $\boldsymbol{all\ modulus\ t\ test} < 2.7764$ $the\ critical\ value,$ hence it is imperative for our measurements to be done accurately and the preceding tests done to establish a reliable prediction.

The software coding for Eqn. *(4)* was incorporated into **Listing one** (Appendix E1) which is the software code for the whole digester stability routine also known as the digester system imbalance early warning routine. The flowchart for the digester system imbalance early warning routine is shown in Fig. 4.1.

4.2.3 Digester System Imbalance Early Warning Flowchart Description

The digester system imbalance early warning routine starts by measuring the values of pH, redox and electrical conductivity (EC) of the digester substrate. These values are input to the soft sensor algorithm, whose output is the value of the buffering capacity (alkalinity). The value of the alkalinity so outputted is input together with the pH value read before into the fuzzy logic algorithm where the percentage level of the stability is evaluated.

Based on the fuzzy logic algorithm the digester system will either be stable or unstable. If the system is stable the program returns control back to the beginning to make a new sweep of the measurements. However, if the system is not stable, a failing or failed stability alarm will be activated. When this does occur, the program goes on to establish which between the pH and alkalinity is out of range and to give the remedial action to be taken by the user.

A liquid crystal display (LCD) is used to communicate instructions to the user on what remedial action has to be taken to return the pH or alkalinity value to an acceptable value. The pH can be increased by adding an acid reducing agent such as calcium carbonate (lime). Lime is good at suddenly increasing the value of the pH but unfortunately this does not translate to an equivalent increase in alkalinity. Hence, the addition of lime should be complemented by the addition of bicarbonate or carbonate salts such as sodium and potassium that will substantially increase alkalinity and fine tune the pH value to the required level. On the other hand the pH can be decreased by adding some form of pH reducing agent such as acetic acid or ferric chloride.
It should be noted that the addition of any chemical into the digester substrate should be gradual so as not to 'shock ' , the bacteria involved in the anaerobic process. Furthermore too often the addition of elevated chemical levels is not recommended as this can cause unwanted solids build-up inside the digester.

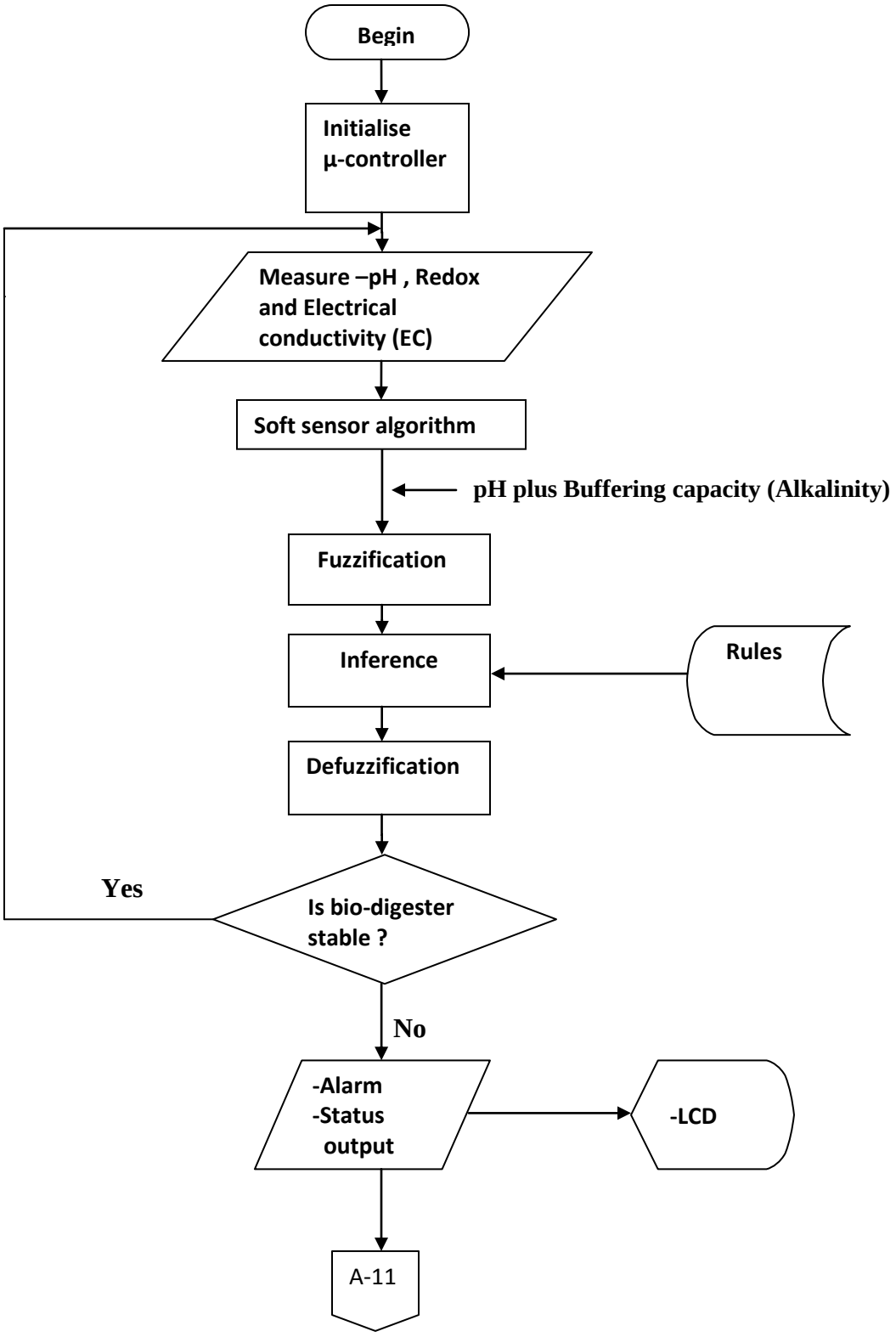

(continued on the next page)

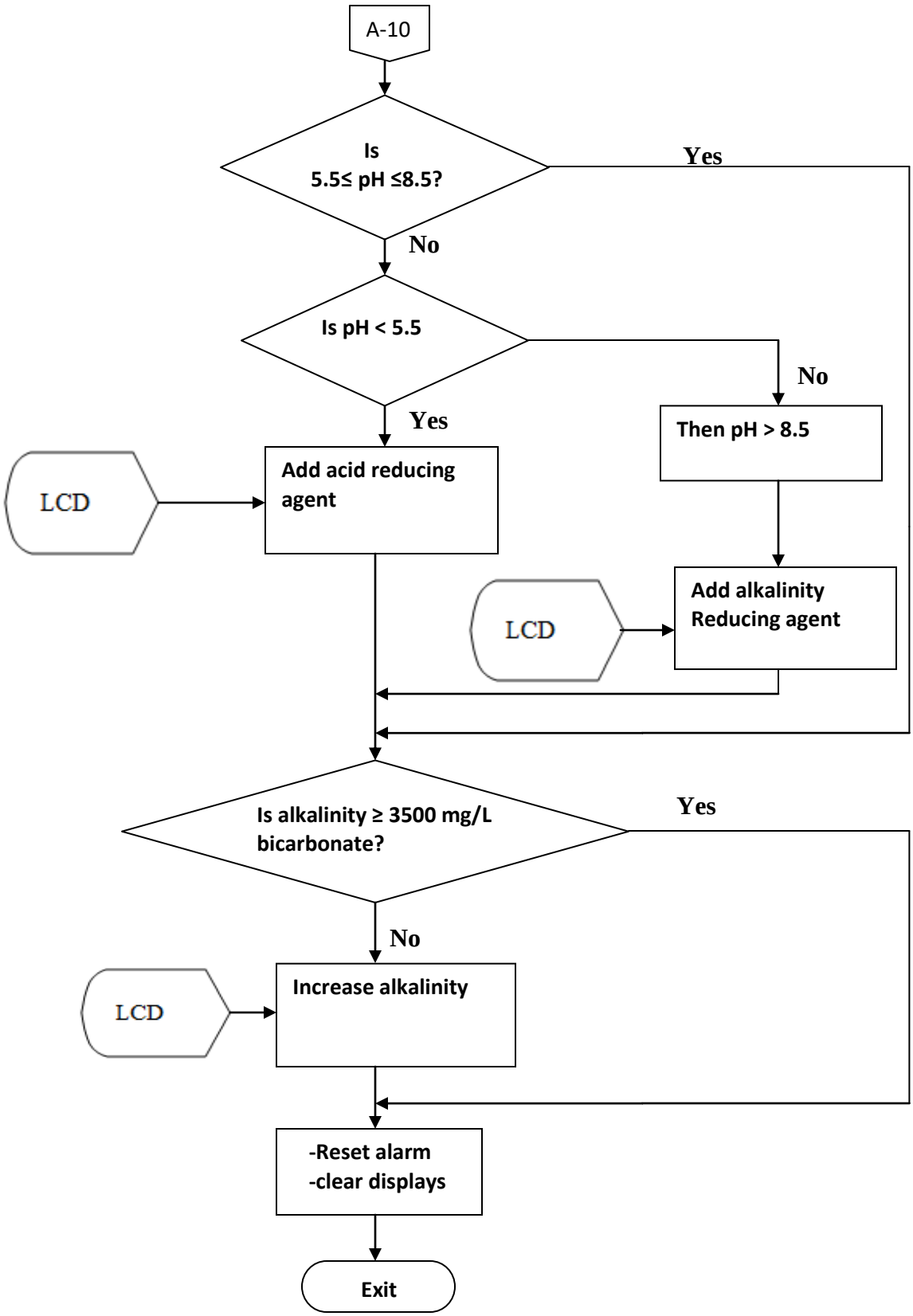

Fig. 4.1: Digester System Imbalance Early Warning Flowchart

4.3 BIOGAS AMOUNT (OUTPUT)

4.3.1 Fuzzy Logic Algorithm 2

The amount of biogas produced depends to a large extent on the organic loading rate (OLR) and digester temperature. Industrial bio digesters will operate at 43 to 55^{o}C (Thermophilic) as this gives minimum hydraulic retention time (HRT) of about 15 to 20 days for yield production, whilst domestic digesters will normally operate at 30 to 42^{o}C (Mesophilic) with HRT between 30 to 40 days (Teodarita et al., 2008). From this it is established that temperature affects the point at which biogas production starts and hence the amount of biogas produced in a given situation.

The fuzzy logic controller for biogas amount will be a two input controller of OLR and temperature. The biogas output amount consists of 58 to 65% methane by volume and 42 to 35% carbon dioxide by volume (Labatut & Gooch, 2015), hence a measurement of the ratio of methane/carbon dioxide from the sensors should be 1.38 to 1.86. For the REF 50m^3 biogas digesters under consideration the gas storage capacity is 7m^3 (7000 litres) and the exhausted slurry is 6m^3 per day.

The normally unheated and unmixed domestic digesters will have a loading rate (OLR) of 0.481 to 1.6kg of volatile solids (VS) per cubic meter per day whilst commercial digesters that are continuously fed normally have a loading rate (OLR) of 1.6 to 6.41 kg of volatile solids (VS) per cubic meter per day. However, too low an OLR will reduce biogas output potential while too high an OLR greater than 4.0kg.VS/m^3 day will result in too much feed for the bacteria to operate on thereby effectively reducing biogas output potential The daily intake of the volatile solids in kilograms over the usable biogas digester volume in m^3 will give the value of the organic loading rate in the units of kg.VS/m^3 day (Bioenergy, 2016; Winsconsin, 1992 pp.3).

4.3.1.1 Calculation of retention time and organic loading rate for REF 50m^3 Digesters

$$HRT(days) = (Effective\ digester\ volume)/(feedstock\ volume/day) \qquad (5)$$

Digester effective volume = 50 m^3

Feedstock(slurry) per day = 2.1875 m^3 /day of piggery and sewer waste

$HRT = \frac{50}{2.1875}$ = 22.85 days (A high level of bacteria already exists in the slurry)

$$Feedstock\ per\ day = 2.1875\ m^3[2187.5\ kg]$$

$$Total\ dry\ solids(TS) = Feedstock\ per\ day\ x\ 8\ \%$$

$$= 2187.5\ kgx8\ \%$$

$$= 175\ kg$$

$$Organic\ total\ dry\ solids = 85\ \%\ Total\ solids$$

$$= 85\ \%\ x175\ kg$$

$$= 148.75\ kg$$

$$Organic\ loading\ rate = (\frac{Organic\ total\ solids}{Digester\ \ effective\ volume})$$

$$= \frac{148.75}{50}$$

$$= 2.975\ \text{kgVS/m}^3\ \text{day}$$

Biogas output for these digesters ranges from 15 to 20 m^3 (1500 to 20000 litres), hence secondary gas storage facilities, input slurry regulation and continuous gas usage are required since the internal digester storage capacity is 7 m^3 (7000 litres).

4.3.1.2 Biogas amount organic loading rate based rules

From Fig. 4.2, the number of possible rules is 3 x 2 = 6 from the inputs. The linguistic variables are OLR ={ Low organic loading rate (OLRL), Good organic loading rate (OLRG), High organic loading rate (ORLH)} , Temperature ={Low temperature (TL), Optimum temperature (TO)} and Biogas output ={Gas low (GL), Gas average (GA), Gas high (GH)}.

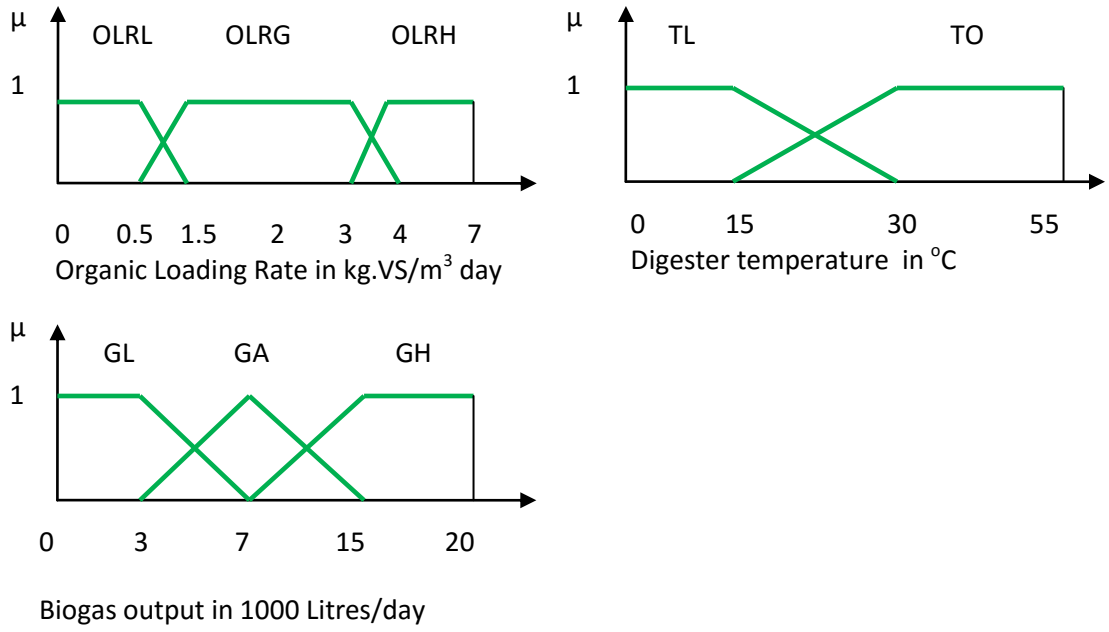

Fig. 4.2: Membership functions for biogas amount for REF 50m^3 digesters

(1) **IF** *Organic loading is OLRL* **AND** *Temperature is TL* **THEN** *Biogas Output is Gas low*

(2) **IF** *Organic loading is OLRL* **AND** *Temperature is TO* **THEN** *Biogas Output is Gas low*

(3) **IF** *Organic loading is OLRG* **AND** *Temperature is TL* **THEN** *Biogas Output is Gas average*

(4) **IF** *Organic loading is OLRG* **AND** *Temperature is TO* **THEN** *Biogas Output is Gas High*

(5) **IF** *Organic loading is OLRH* **AND** *Temperature is TL* **THEN** *Biogas Output is Gas Low*

(6) **IF** *Organic loading is OLRH* **AND** *Temperature is TO* **THEN** *Biogas Output is Average*

The rule base or rule matrix for the fuzzy logic control showing different biogas outputs in litres per day, for all possible combinations of organic loading rate and digester temperature inputs is given in Table 4.2

Table 4.2: Rule matrix for biogas output

OLR	**Temperature**	
	TL	TO
OLRL	GL	GL
OLRG	GA	GH
OLRH	GL	GA

4.3.2 Biogas amount Flowchart Description

Fig. 4.3 shows the overall flowchart used in the routine for the biogas output calculation. In this routine, we begin by inputting the total dry solids value in kilograms that is required per day. These can be weighed and mixed with water to fill up the digester. The organic loading rate (OLR) is hence specified. The weight of the total solids that are required also depends on whether the material is animal waste, vegetable waste or a mixture of the two. For human waste based systems the designed sewer system will provide a known estimate of the total solids per given volume of sewerage material. Automatic feedstock loading is a subject for latter research. The software coding for flowchart in Fig. 4.3 is part of **Listing one** (Appendix E1).

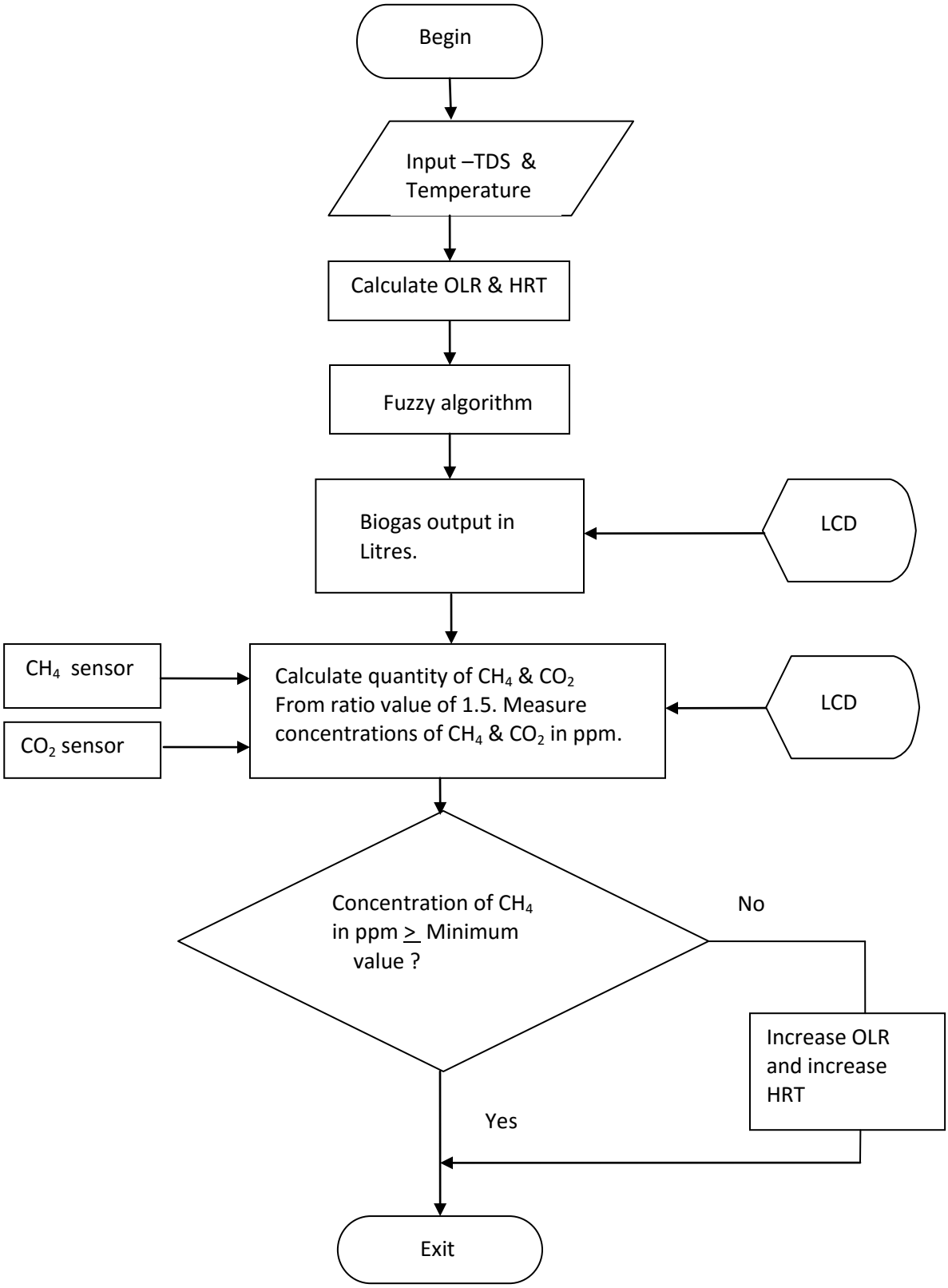

Fig. 4.3: Biogas output amount flowchart

The calculated OLR and measured digester temperature are input into the fuzzy logic algorithm to give the expected biogas output in litres. From literature study the ratio of methane gas to carbon dioxide gas has an average range of 1.5 *(See page 44)*, hence we can calculate the relative expected quantities of methane and carbon dioxide gases in our system. Methane and carbon dioxide sensors are also incorporated into the digester to make concentration measurements of the actual methane and carbon dioxide gases. Recommended[19] values of concentrations are compared with the measured values, and if the measured value of methane is less than the recommended value the system will either increase the organic load rate or the hydraulic retention times depending on which is most appropriate. If the measured methane value is equal to or greater than the recommended value the system will exit to go to the next routine.

4.4 BIOGAS SYSTEM FAULT DETECTION AND STATUS

4.4.1 Fuzzy Logic Algorithm 3

4.4.1.1 Biogas pressure and leaks considerations

The properties of methane are 1) non-poisonous to people, 2) colorless gas, 3) odorless gas (assuming hydrogen sulfide[20] has been filtered off), and 4) highly flammable. However, prolonged exposure to methane will lead to symptoms associated with lake of oxygen as the methane normally displaces oxygen bearing air due to its lower density. When biogas is mixed with air in certain proportions an explosive mixture is formed (Wisconsin, 1992; Zlochower & Green, 2016). Hence it is imperative that biogas is not unnecessarily exposed to air.

Situations that can contribute air mixing with biogas include gas leaks at user end confined space and gas storage facility, purging of gas from the gas reservoir for maintenance purposes or opening of the biogas digester for cleaning purposes. Another very important situation that deserves mention here is that of biogas storage compartment pressure. According to Marchaim (1992), in a well designed dome digester atmospheric pressure forces the total water body to occupy 95% of the total digester volume, leaving 5% as the dead volume. Dome type gas pressures are usually less than or equal to 120cm of water (11.77 KPa). Consequently the REF $50m^3$ digesters operate at around 15 KPa biogas pressure. The biogas digester should always be operated at a gas pressure greater than the external gas pressures above atmospheric value, since a lower pressure in the gas storage compartment would imply suction of air into it. If this where to happen the oxygen in the air would combine with the biogas to form either a combustible mixture or would incapacitate the anaerobic process, completely shutting down the gas production process. Hence gas usage should not be greater than that required to maintain a higher pressure in the gas storage compartment. Conversely too high a gas pressure will cause bubbles to appear at the outlet liberating methane to the ambient which can result an explosive mixture.

An emergency close valve is incorporated into the main gas outlet line to serve the dual purpose of mitigating against the possibility of air suction into the biogas digester (valve shuts off when pressure goes below a certain point and opens above this point) and also shuts off when there is a gas leak at user end.

[19] Carbon dioxide concentrations should be less than methane concentrations by a factor of 1.5 or more.
[20] Hydrogen sulphide smells like a typical rotten egg.

Signs of gas leakage include a rotten egg smell at end user side or an above normal gas pressure reduction rate from the gas storage compartment.

4.4.1.1.1 Methane leak at end user

According to Zlochower & Green (2016) methane has lower explosive limit (LEL) of 5.0% and an upper explosive limit (UEL) of 15.8%. This range defines the lowest and highest concentrations of the gas as a percentage by volume in air (oxygen) that will easily ignite and cause an explosion. However, this research will not carry out calculations for the exact concentration levels of methane in air but will design a system to sound an alarm while activating an emergency gas line solenoid close valve once methane is detected within the room far from the stove or lamp.

4.4.1.1.2 Oxygen ingress into the digester

Any increase in the concentration of oxygen within the gas storage compartment in the digester has both the potential of causing a explosion or killing the anaerobic process. Hence once there is any detectable oxygen in the digester an alarm will sound and the emergency close solenoid valve closed again activated to prevent dangerous gas mixture being transferred to the end user.

4.4.1.2 Slurry level considerations

The three components that make up the total volume of a fixed dome digester are the dead storage (V_d), the effective gas storage (V_g) and the effective slurry storage (V_s) as shown in Fig. 4.4

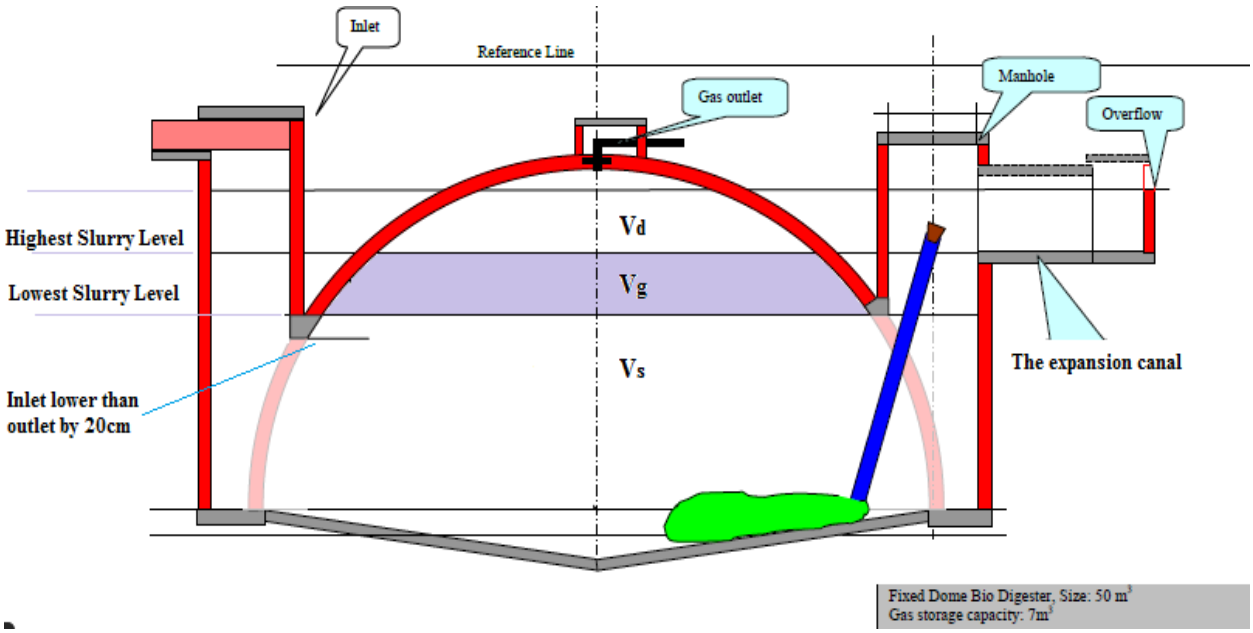

Fig. 4.4: Fixed dome biodigester volume components
(Rural Electrification Fund (REF), 2015)

In the fixed dome digester the level of the feedstock (slurry) decreases in direct relationship to the pressure or amount of biogas produced. The minimum recommended level of the feedstock in this case should just be above the digester outlet to prevent unnecessary loss of biogas through the outlet. According to Wafler (2008) it is established that the minimum feedstock level (P-line) represented by the lowest slurry level corresponds to the highest recommended gas pressure while the maximum feedstock level (zero line) represented by the highest slurry level corresponds to the minimum or no gas pressure. Hence it is necessary to monitor the feedstock level in the digester both as compliment to safe pressure operation and availability of adequate feedstock in the digester.

The fuzzy logic controller for Biogas System Fault/Status Detection is a two input controller of pressure and feedstock level. From Fig. 4.5 the number of possible rules is 3 x 3 = 9 from the inputs. The linguistic variables are pressure ={Low pressure (LP), Good pressure (GP), High pressure (HP)}, feedstock level ={Low level P-line (LL), Between P-line & Zero-line level (BPO), High level Zero line (HL)} and Digester Danger status output ={No danger (ND), Low danger (LD), High danger (HD)}. A few rules are shown below.

(1) **IF** *Gas pressure is LP* **AND** *Feedstock level is LL* **THEN** *Output is High danger*

(2) **IF** *Gas pressure is LP* **AND** *Feedstock level is BPO* **THEN** *Output is Low danger*

(3) **IF** *Gas pressure is LP* **AND** *Feedstock level is HL* **THEN** *Output is No danger*

(4) **IF** *Gas pressure is GP* **AND** *Feedstock level is LL* **THEN** *Output is Low danger*

(5) **IF** *Gas pressure is GP* **AND** *Feedstock level is BPO* **THEN** *Output is No danger*

(6) **IF** *Gas pressure is GP* **AND** *Feedstock level is HL* **THEN** *Output is Low danger*

The rule matrix for pressure and level status is given in Table 4.3.

Pressure	**Level**		
	LDIS	MDIS	HDIS
LP	ND	LD	HD
GP	LD	ND	LD
HP	HD	ND	ND

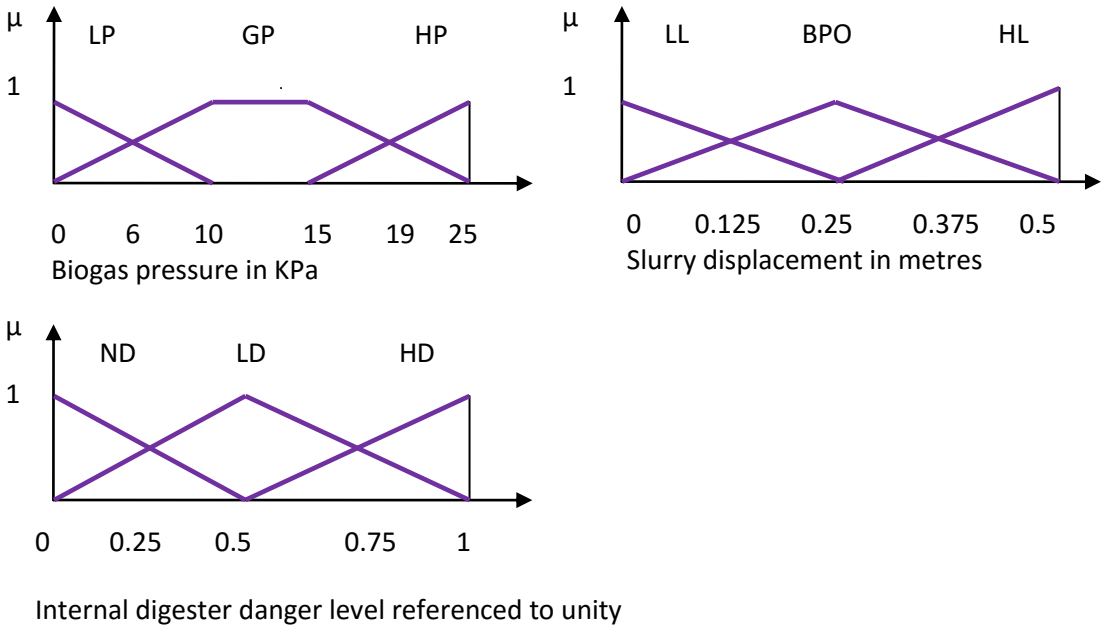

Fig. 4.5: Membership functions for pressure and level status of digester

4.4.2 Biogas system fault/status detection flowchart description

Fig. 4.6 gives the overall flowchart for the biogas system fault detection and control. In this routine the integrity of the system is evaluated by detection of unwanted methane or oxygen outside the digester or inside the digester respectively. If a methane leak occurs especially at the enclosed premises of the user an alarm comes on. If oxygen ingress into the digester occurs an alarm is also activated. In both cases a line valve is closed until the problem is rectified. If there are no leaks, the routine goes on to digester danger status level with respect to biogas pressure and slurry levels. The software coding for flowchart in Fig. 4.6 is incorporated in **Listing one** (Appendix E1).

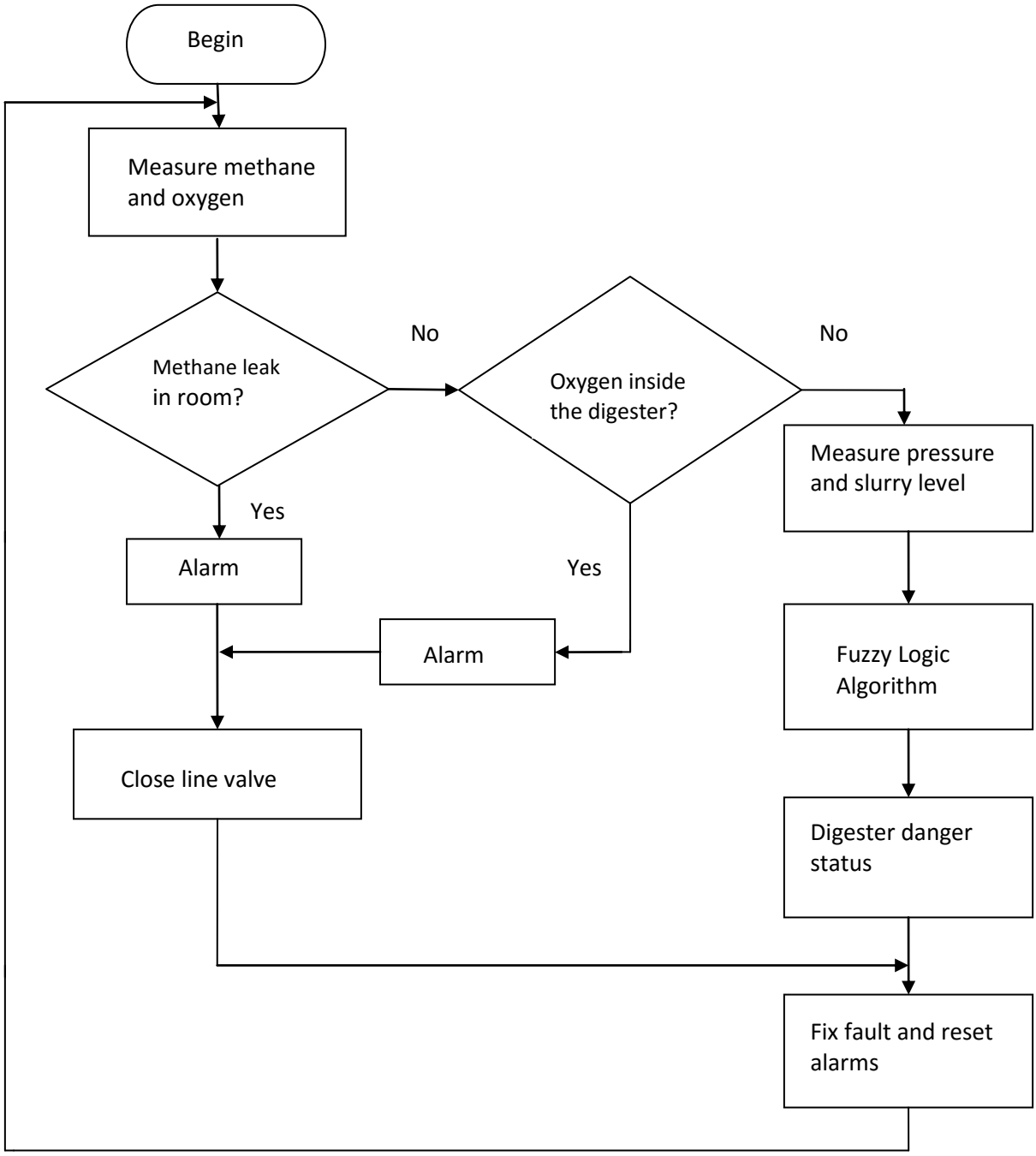

Fig. 4.6: Biogas system fault/status detection flowchart

4.5 SOLAR BATTERY CHARGING/DISCHARGING

4.5.1 Fuzzy Logic Algorithm 4

4.5.1.1 Battery state of charge

The simplest methods for SOC estimation are the open circuit voltage and the specific gravity (hydrometer) tests, the ranges of which are shown in Table 4.4, for the flooded batteries that are used by the Rural Electrification Fund (REF) formerly REA. Open circuit voltage measurement will give reasonable estimation whilst the specific gravity test will give a very good estimation of the SOC by following the procedures in the REF document, though both methods are not on-line implementable. An on-line SOC estimation method then, based on terminal voltage and charging/discharging current is most plausible (Saravanan et al., 2013) for this research. The static SOC methods are then used to verify the accuracy of the on-line SOC estimation method.

Table 4.4: State of charge as related to specific specific gravity and open circuit voltage (Rural Electrification Fund, 2015)

Percentage of Charge	Specific Gravity Corrected to 26.7^0C	Open-Circuit Voltage					
		6V	8V	12V	24V	36V	48V
100	**1.277**	**6.37**	**8.49**	**12.73**	**25.46**	**38.20**	**50.93**
90	**1.258**	**6.31**	**8.41**	**12.62**	**25.24**	**37.85**	**50.47**
80	**1.238**	**6.25**	**8.33**	**12.50**	**25.00**	**37.49**	**49.99**
70	**1.217**	**6.19**	**8.25**	**12.37**	**24.74**	**37.12**	**49.49**
60	**1.195**	**6.12**	**8.16**	**12.24**	**24.48**	**36.72**	**48.96**
50	**1.172**	**6.05**	**8.07**	**12.10**	**24.20**	**36.31**	**48.41**
40	**1.148**	**5.98**	**7.97**	**11.96**	**23.92**	**35.87**	**47.83**
30	**1.124**	**5.91**	**7.88**	**11.81**	**23.63**	**35.44**	**47.26**
20	**1.098**	**5.83**	**7.77**	**11.66**	**23.32**	**34.97**	**46.63**
10	**1.073**	**5.75**	**7.67**	**11.51**	**23.02**	**34.52**	**46.03**

4.5.1.2 Battery charging strategy

In this research the preferred method of battery charging as shown in Fig. 4.7, will be constant current at first followed by constant voltage later (Byrne, 2010).

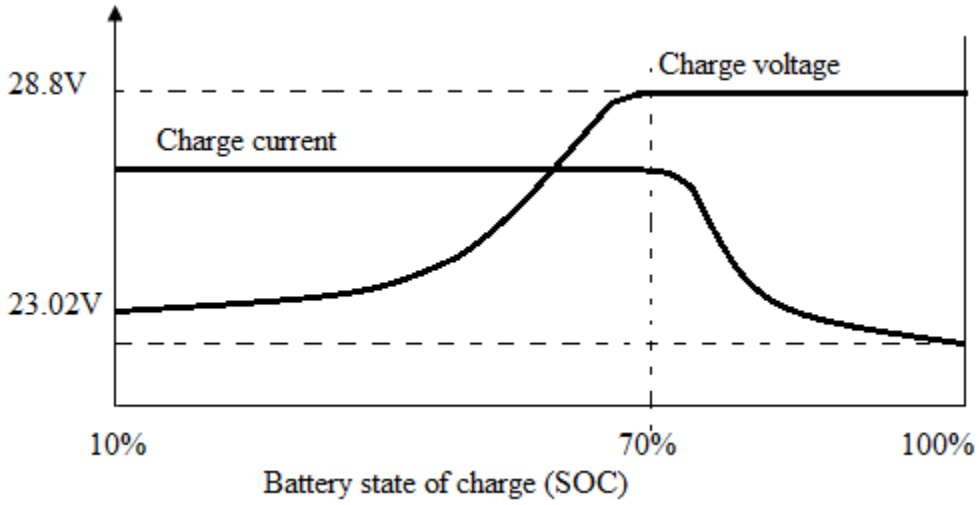

Fig. 4.7: Constant current and constant voltage battery charging profile

The buck regulator which steps down the supply (solar panel) voltage to a given load (the battery) of lower voltage is adopted in the formulation of the rules.
According to Rashid (2003), for the buck regulator with pulse-width modulation (PWM) duty cycle *D*, the output average voltage *Va* is related to the supply voltage *Vs* by the equation:

$$Va = DVs \qquad (6)$$

and the output average current *Ia* to the supply current *Is* by

$$Ia = \frac{Is}{D} \qquad (7)$$

Clearly applying equations *(6)* and *(7)* to the profile in Fig. 4.7, it is established that for high duty cycle *Va* approaches *Vs* whilst *Ia* approaches *Is* an overall condition for high SOC. On the other hand a low SOC condition is characterized by a low duty cycle where *Va* is far less than *Vs* and *Ia* is far higher than *Is*.

The fuzzy logic controller for Solar Charging/Discharging is a three input controller of SOC, charging voltage and charging current. From Fig. 4.8, the number of possible rules is 3 x 3 x 3 = 27 from the inputs. The linguistic variables are SOC ={Low SOC (LSOC), Medium SOC (MSOC), High SOC (HSOC)}, Charging voltage ={Low voltage (LV), Average voltage (AV), High voltage (HV)}, Charging current={Low current (LC), Average current (AC), High current (HC)}, and Charge controller PWM output ={Low duty cycle (LD), Medium duty cycle (MD, High duty cycle (HD)}. A few rules are shown below.

(1) **IF** *SOC is LSOC* **AND** *Charging voltage is LV* ***AND*** *Charging current is LC* **THEN** *Duty cycle is Low*
(2) **IF** *SOC is LSOC* **AND** *Charging voltage is AV* ***AND*** *Charging current is LC* **THEN** *Duty cycle is Medium*
(3) **IF** *SOC is LSOC* **AND** *Charging voltage is HV* ***AND*** *Charging current is LC* **THEN** *Duty cycle is Medium*
(4) **IF** *SOC is LSOC* **AND** *Charging voltage is LV* ***AND*** *Charging current is AC* **THEN** *Duty cycle is Medium*

The software coding for flowchart in Fig. 4.9 is shown in **Listing two** (Appendix E2).

It is important to note that normally the charging current in amperes, is not allowed to exceed 1/10 of the battery's rated capacity in ampere-hours (Ah). The 50 Ah battery used here should be charged at maximum of 5.0 amperes. However prior to electrolyte decomposition, this charging current can be momentarily higher. From this observation the UoD of the current membership function is defined.

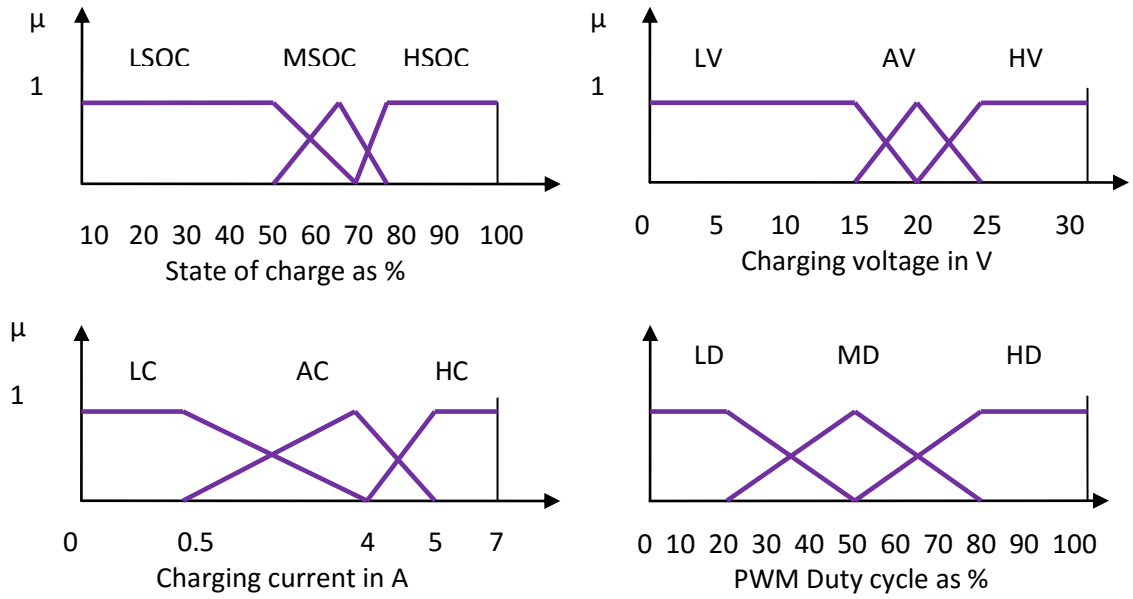

Fig. 4.8: Membership functions for solar battery charging/discharging

Table 4.5: Rule base table for solar battery charging/discharging

Rule number	**State of charge (%)**	**Charging voltage (V)**	**Charging current (A)**	**Duty cycle (%)**
1	LSOC	LV	LC	LD
2	LSOC	AV	LC	MD
3	LSOC	HV	LC	MD
4	LSOC	LV	AC	MD
5	LSOC	AV	AC	MD
6	LSOC	HV	AC	MD
7	LSOC	LV	HC	LD
8	LSOC	AV	HC	LD
9	LSOC	HV	HC	MD
10	MSOC	LV	LC	LD
11	MSOC	AV	LC	LD
12	MSOC	HV	LC	LD
13	MSOC	LV	AC	MD
14	MSOC	AV	AC	MD
15	MSOC	HV	AC	MD
16	MSOC	LV	HC	HD
17	MSOC	AV	HC	HD
18	MSOC	HV	HC	HD
19	HSOC	LV	LC	MD
20	HSOC	AV	LC	LD
21	HSOC	HV	LC	LD
22	HSOC	LV	AC	HD
23	HSOC	AV	AC	MD
24	HSOC	HV	AC	MD
25	HSOC	LV	HC	HD
26	HSOC	AV	HC	HD
27	HSOC	HV	HC	HD

4.5.2 Solar battery charging/discharging flowchart description

Fig. 4.9 gives the overall flowchart for solar battery control routine. This routine is characterized first by measuring the charging voltage and current and secondly by evaluating the state of charge (SOC) of the battery. The SOC is obtained either by a SOC on-line based algorithm or by keying in a value based on open circuit voltage test with the use of a look-up table such as Table 4.4. The SOC, charging voltage and charging current, form the inputs to the fuzzy logic controller (FLC) that outputs a PWM signal of required duty cycle to drive the buck type charge controller.

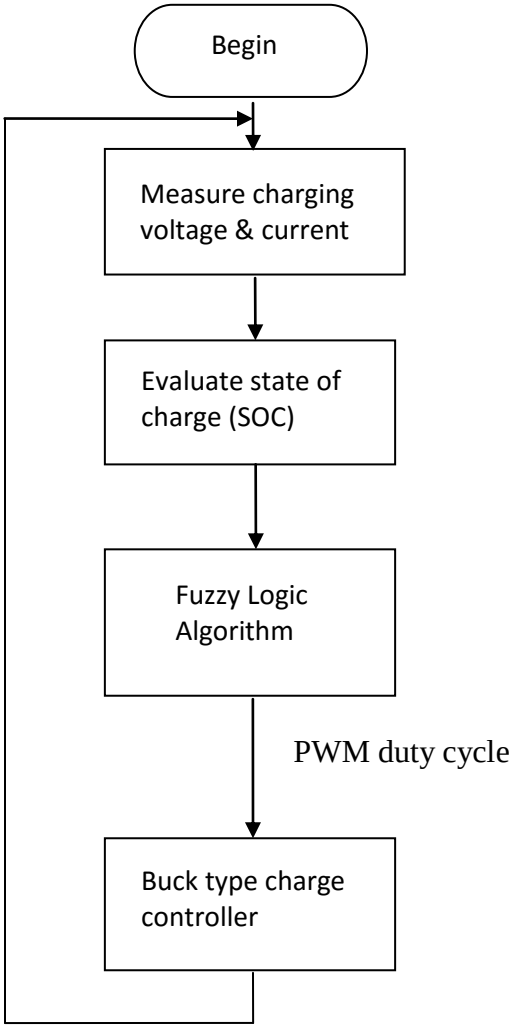

Fig. 4 9: Solar battery charging/discharging flowchart

4.6 SOLAR SYSTEM FAULT DETECTION AND STATUS

4.6.1 Fuzzy Logic Algorithm 5

4.6.1.1 Array shading

With respect to the solar panels reasonable output without the inclusion of maximum power point tracking algorithm can be obtained as long as there is sunshine even though typical solar panel array efficiencies vary between 6% and 30% (Welch, 2010). The incorporation of photocells in the design seeks to identify prolonged partial shading of the solar panels that can occur due to physical objects (leaves, cloth, paper, feathers, tree shadow etc). The resistance of the photocell is related to the sunlight available on it. This can be used to detect partial shading of the solar panels and fuzzy algorithm would be the most suitable as a significant number of shading levels can be quantified. The control output is in the form of status indication (LEDs) to inform the user on prolonged solar panel shading/obstruction.

Fig. 4.10, shows the reading of the light dependent resistor resistance of 143.9 Ω in direct sunlight, while Fig. 4.11 gives the circuit configuration for obtaining an analogue signal to the microcontroller from the photocell. The supply voltage is naturally 5V and the pull down resistance is chosen to be 4.7 KΩ so that we do not reach saturation of 5V early, getting a balanced tradeoff between the very dark and very bright light scales (*The resistance of the photocell used in this research varies from 4.0 MΩ to 144 Ω in complete darkness to direct sunlight respectively).*

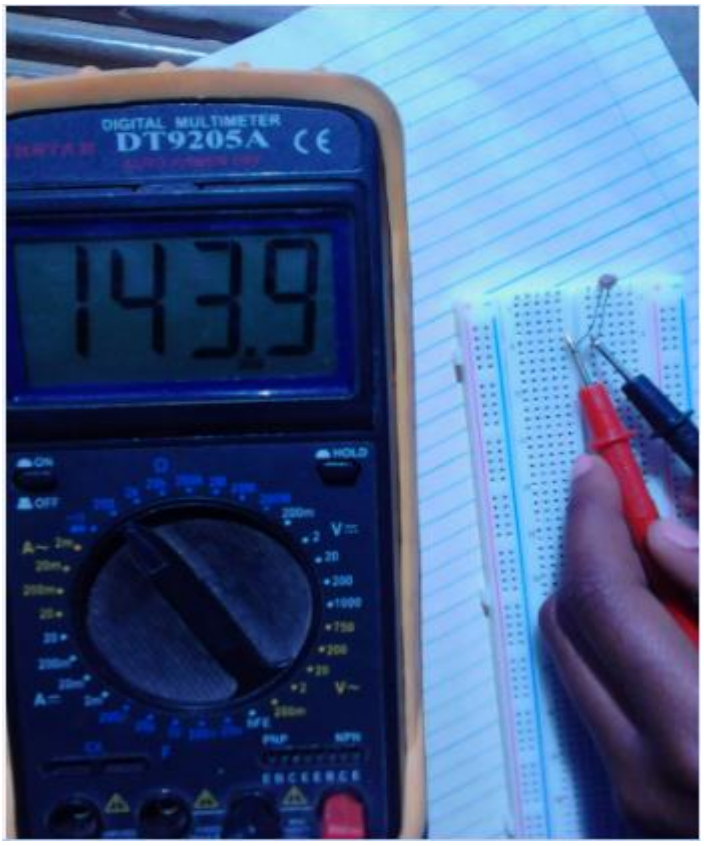

Fig. 4.10: Light dependent resistor resistance of 143.9 Ω reading in direct sunlight

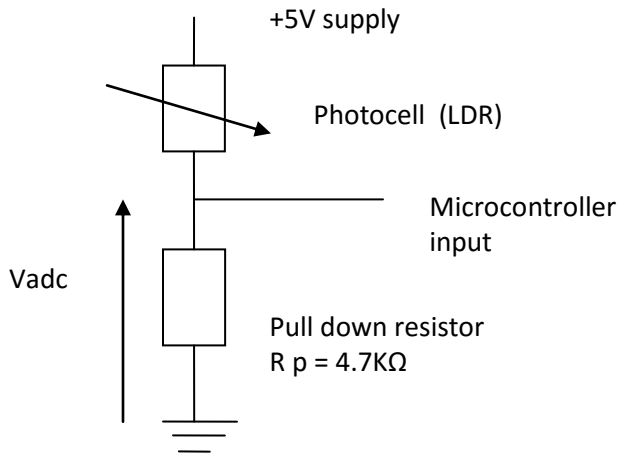

Fig. 4.11: Circuit configuration for photocell connection to microcontroller

$$\frac{Vadc}{5} = \frac{4.7K}{4.7K+4000K} \quad (8)$$

Hence $\text{Vadc} = 0.00585$ V for complete darkness.

$$\frac{Vadc}{5} = \frac{4.7K}{4.7K+0.144K} \quad (9)$$

Hence $\text{Vadc} = 4.85$ V for sunlight.

For the photocell type that is used in this research, Table 4.6 gives measured values of the photocell resistance, pull down resistor and the potential difference across the pull down resistor for various solar panel shading situations. The procedure involves measuring the photocell resistance and voltage across pull down resistor when photocell is completely covered in darkness, under a shadow in daylight, covered by slightly transparent paper and finally in broad daylight uncovered. **The fuzzy logic controller for panel shading is a single input controller of LDR voltage pull down resistor.** From Fig. 4.12 (a) & (b) the number of possible rules is 4 from the input. The linguistic variables are Potential difference across pull down resistor ={Low voltage (LVadc), Lower Medium voltage (LMVadc), Upper Medium voltage, High voltage (HVadc)}, and Panel shading level output ={Total shading (TS)[21], Heavy shading (HS), Partial shading (PS), No shading (NS)}. The rules are shown below.

(1) **IF** *Potential across pull down resistor is LVadc* **THEN** *Total shading of panels is TS*

(2) **IF** *Potential across pull down resistor is LMVadc* **THEN** *Total shading of panels is HS*

(3) **IF** *Potential across pull down resistor is UMVadc* **THEN** *Total shading of panels is PS*

(4) **IF** *Potential across pull down resistor is HVadc* **THEN** *Total shading of panels is NS*

[21] Total shading (TS) in photovoltaic systems is not to be confused with total solids (TS) in biogas systems.

Table 4.6: Sunlight shading levels versus photocell resistance

Panel shading situation	**Photocell resistance (KΩ)**	**Photocell plus Rp (KΩ)**	**Potential across Rp (V)**
Total darkness	4000	4004.7	0.00585
Room passageway	12.00	16.7	1.4072
Day light room average	5.09	9.79	2.4004
Outside leaf shadow	0.4	5.1	4.60785
Newsprint shadow	0.302	5.002	4.6981
Direct sunlight	0.144	4.844	4.85135

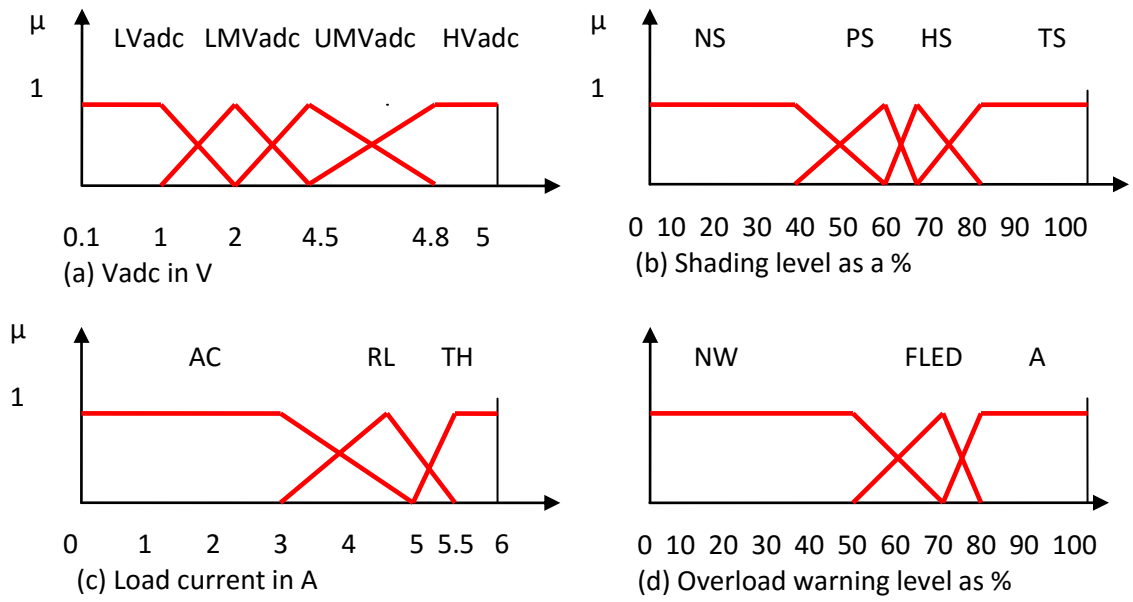

Fig. 4.12: Membership functions for (a) & (b) solar panel shading level and (c) & (d) user load control

4.6.1.2 User load control

The loads that are supplied by the photovoltaic stations include domestic and institutional users. For institutional users, some loads will need to be constantly connected requiring some form of priority load scheduling. Priority load scheduling fuzzy logic systems based on particle swarm optimization (Welch, 2010) algorithms have been studied. However, this research will develop a simpler algorithm to monitor the overall load current where its ceiling is limited to 5,43A for the

1250W, 230V, 50Hz inverter. The control output is in the form of alarms and status indicator to alert on increasing load condition.

The fuzzy logic controller for user load control is a single input controller of Load current. From Fig. 4.12 (c) & (d) the number of possible rules is 3 from the input. The linguistic variables are Load current ={Acceptable (AC), Reaching limit (RL), Too high (TH)}, and Overload warning level output ={No warning (NW), Approaching limit Flashing LED (FLED), Alarm (A)}. The rules are shown below.

(1) **IF** *Load current is acceptable (AC)* **THEN** *All overload indicators off (NW)*

(2) **IF** *Load current is reaching limit (RL)* **THEN** *Activate flashing LED (FLED)*

(3) **IF** *Load current is too high (TH)* **THEN** *Activate load overload alarm (A)*

4.6.1.3 PV panel, charge controller, battery and inverter fault detection

At first the battery and charge controller input currents are measured whose control output is to identify which between the solar panels and the charge controller is at fault. Secondly current into and out of the inverter is measured whose control output is to determine whether the battery or inverter is at fault.

4.6.2 Overall Flowchart for Solar Fault Detection and Status

The routine depicted by the flowchart in Fig. 4.13, begins by detecting the current from the photovoltaic (pv) array that goes into the charge controller, the output current of the charge controller which is the input to the battery, the output current from the battery which forms the input to the inverter and finally the inverter output current which is the load current. The output voltages at the photocells (LDRs), is also detected. The next stage in the flowchart, involves the pv array panel shading algorithm that determines the status of any shading that is available on the solar cells if any. The cases where total shading and prolonged shading of the solar panels occur are investigated and rectified. As the routine is further executed, the electrical functionality of the solar panels, charge controller, battery and inverter is also accessed. In the final stages, the routine addresses the situation where the current drawn from the inverter (load current) is greater than the permissible value.

The C-source codes software coding for the flowchart shown in Fig. 4.13 is included in **Listing two** (Appendix E2).

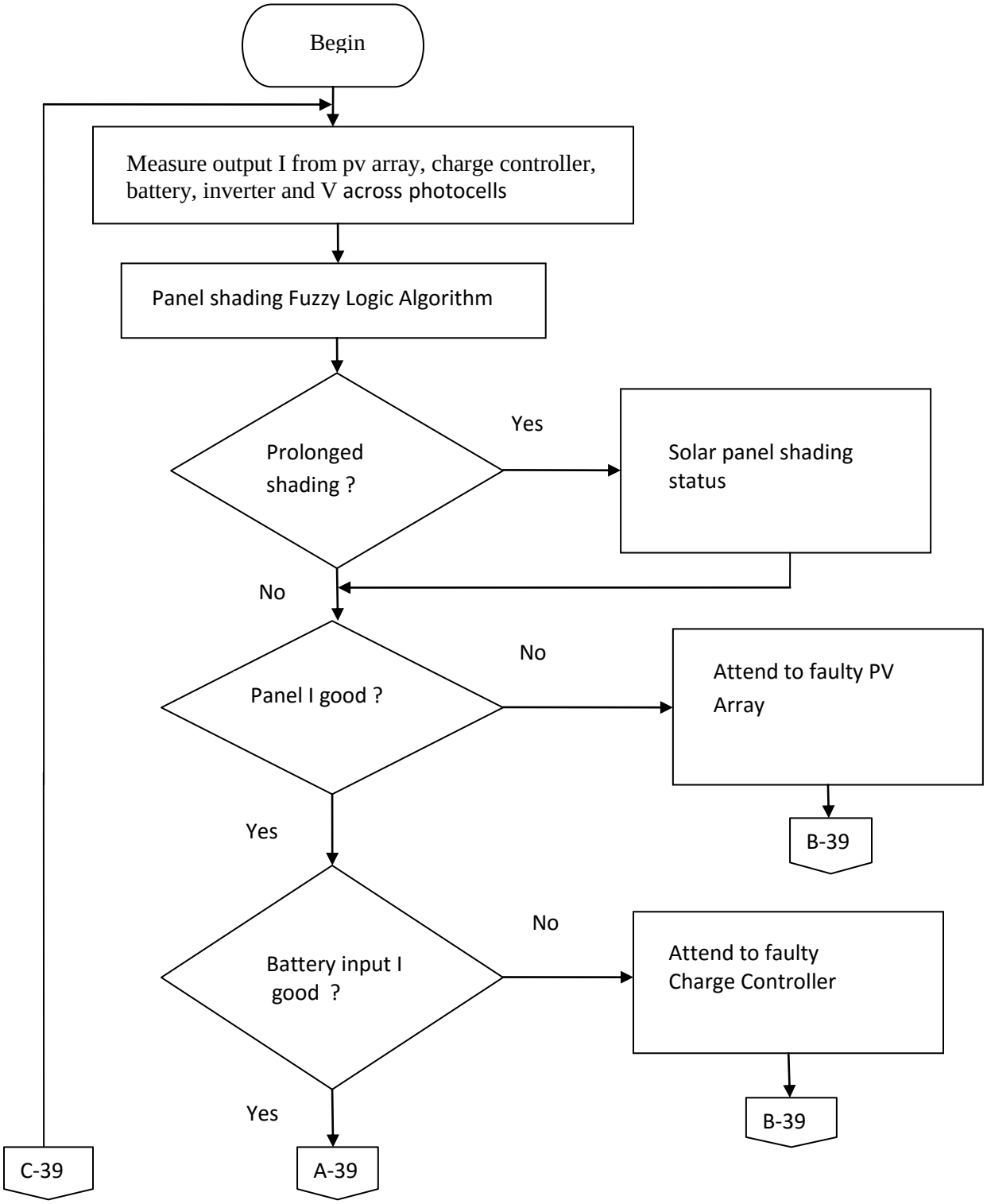

(continued on the next page)

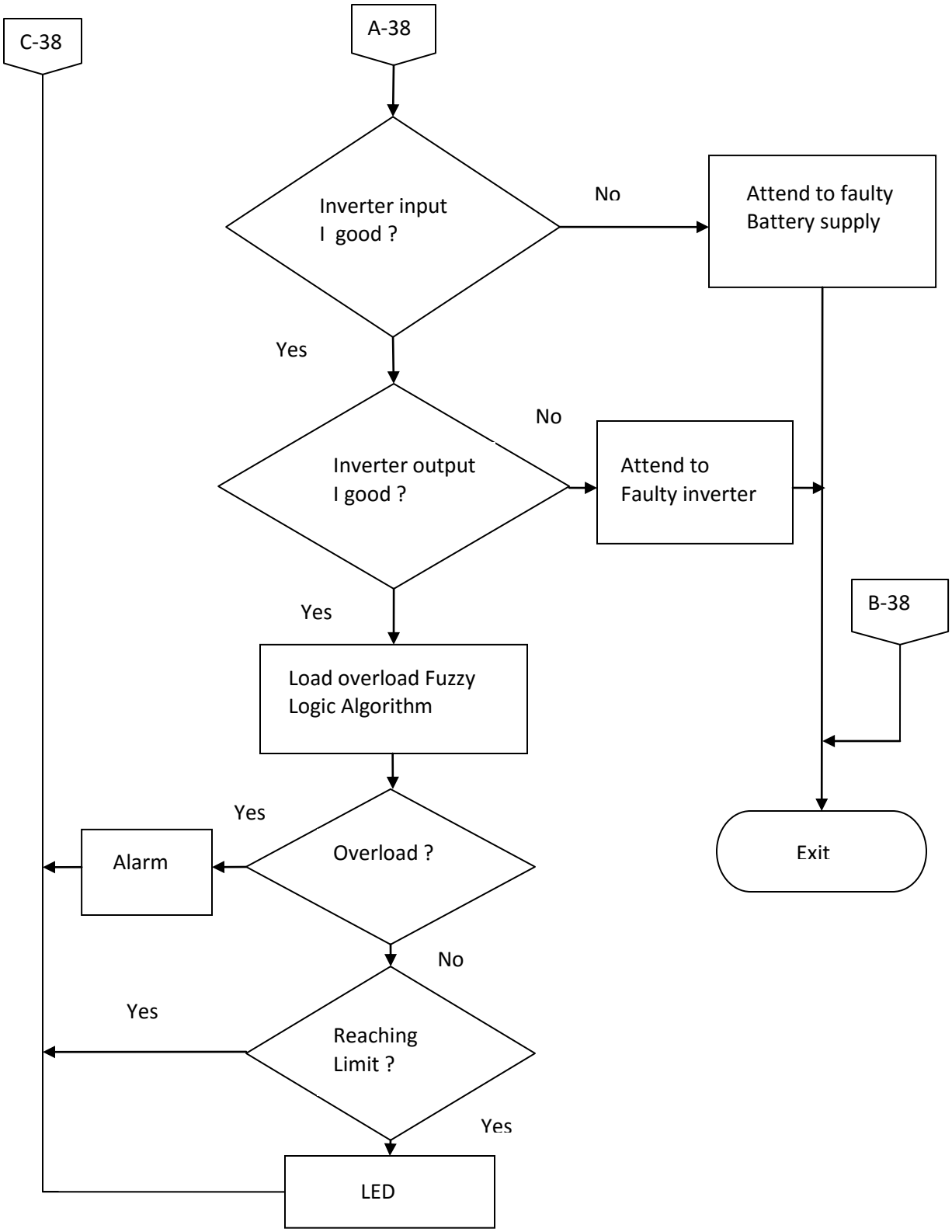

Fig. 4.13: Overall solar system fault detection and status flowchart

4.7 CONCLUSION

This chapter detailed the fuzzy logic algorithms and module flowcharts for 1) digester system imbalance early warning, 2) biogas output amount, 3) biogas system fault/status detection, 4) solar battery charging/discharging, and 5) solar fault/status detection which were successfully developed. The measurements for the inputs to the algorithms are achieved by the sensors specified in the next chapter, chapter 5.

CHAPTER 5

INPUT SENSOR, CONTROL SPECIFICATION AND CIRCUIT DESIGN

5.1 INTRODUCTION

In this chapter the input sensors and control output devices are specified and the respective circuits designed. Section 5.2 looks at the sensors and their circuits to include buffer capacity measurement by titration, while the outputs are treated in section 5.3 and finally the conclusion in section 5.4. These sensor and output device circuits are designed in such a way that they meet the input and output requirements[22] the PIC18F4550 microcontroller.

5.2 INPUT SENSORS AND CIRCUITS

5.2.1 pH

A pH value between 5 to 6.5, will facilitate the hydrolysis stage which is the first stage in anaerobic digestion, whilst in methanogenesis the pH is required to be neutral and in the range 6.5 to 7.6 (Eu-agrobiogas, 2009; Labatut & Gooch, 2015).

An ionized water solution contains a combination of hydrogen (H^+) and hydroxyl (OH^-) ions. On the basis of the relative concentrations of these ions we can either have an acidic or alkaline (base) solution where the hydrogen ions can be represented "*from a scale of 1(10^0) via 10^{-7} to 10^{-14} mole/litre*" (Springer, 2014) and the hydroxyl ions are represented on an inverted scale from the previous one. High concentrations of (H+) ions imply a strong acidic solution whilst those for (HO-) imply a strong alkaline solution. Conversely acids in aqueous solution form hydrogen ions whilst bases form hydroxyl ions as illustrated in the equations below.

$$HCl(hydochloric\ acid) = Cl^-(chlorine\ anion) + H^+(hydrogen\ ion) \quad \text{and} \qquad (10)$$

$$NaOH(sodium\ hydroxide\ base) = Na^+(sodium\ cation) + OH^-(hydroxyl\ ion) \qquad (11)$$

According to Springer (2014) the "*active*" hydrogen ion scale is more conveniently represented as a pH scale between 1 (most acidic), through 7 (neutral) to 14 (most alkaline) given by the following equation:

$$pH = \log \frac{1}{hydrogen\ ion\ concentration\left(\frac{mole}{litre}\right)} \qquad (12)$$

[22] The requirements include the microcontroller input and output voltages (analogue or digital), frequency consideration and the output sink currents.

An e.m.f (NERST's potential) is generated in the solution for every unit change in pH (Figure 5.1) where this e.m.f has a value of approximately 58.10 mV/pH at 20^{o}C (Rosemount, 2010; Springer, 2014).

The slope presented in Fig. 5.1, which is temperature dependent defines the sensitivity of the pH sensor and is given by:

$$Slope = \frac{Change\ in\ Voltage(mV)}{Change\ in\ pH} \qquad (13)$$

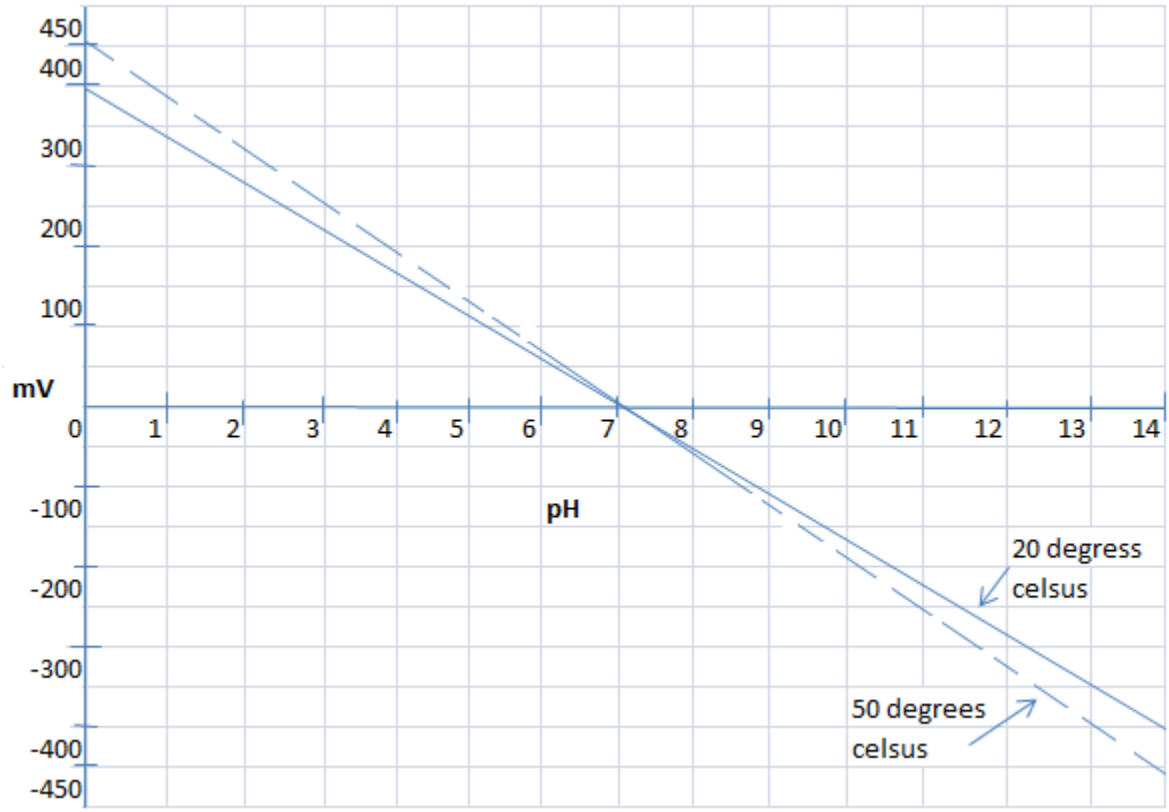

Fig. 5.1: Sensitivity of a pH sensor

5.2.1.1 pH sensor calibration

The initial pH measurement experiments where done using the DFRobot SEN0161 analogue pH sensor as shown in Fig. 5.3 (a), which was the replaced by the much robust **Lutron PE-21 industrial in line pH electrode** (Fig. 5.3 (b)), that lasts a longer time in the digester effluent. At least eight repeated measurements are made at each buffer solution as shown in Table 5.1, and the average value of the voltage calculated.

Table 5.1: Measured values of pH for sensor Lutron PE-21 cailbration

pH buffer solution	**1 (mV)**	**2 (mV)**	**3 (mV)**	**4 (mV)**	**5 (mV)**	**6 (mV)**	**7 (mV)**	**8 (mV)**	**Average (mV)**
4	150	140	147	144	153	158.3	151	152.1	149.4
7	7.1	9.5	3.0	6.1	9.2	8.7	1.5	14.5	7.45
10	-142	-153	-137	-149	-150	-138	-156.7	-144	-146.2

The time interval (5 minutes) between each measurement was determined when the reading from the sensor has stabilized within the specified tolerance value. The average readings are then used to provide the sensitivity plot (Fig. 5.2), of the Lutron PE-21 pH electrode so that:

$$y = ax + b \qquad (14)$$

where

(i) $y = voltage\ output\ in\ mV$
$(ii) a = negative\ slope\ in\ mV/pH$
$(iii) b = intercept\ on\ y\ axis\ in\ mV$, and
$(iv) x = pH\ value$.

Equation *(14)* which will be used in the software pH scaling process then simplifies for this sensor to, $y = -49.886x + 351.33$ .It is required to design a circuit to first amplify the small signal(y) to acceptable levels and then to scale the whole amplified signal range from negative to positive to between 0V and 5 V for microcontroller ADC input compatibility.

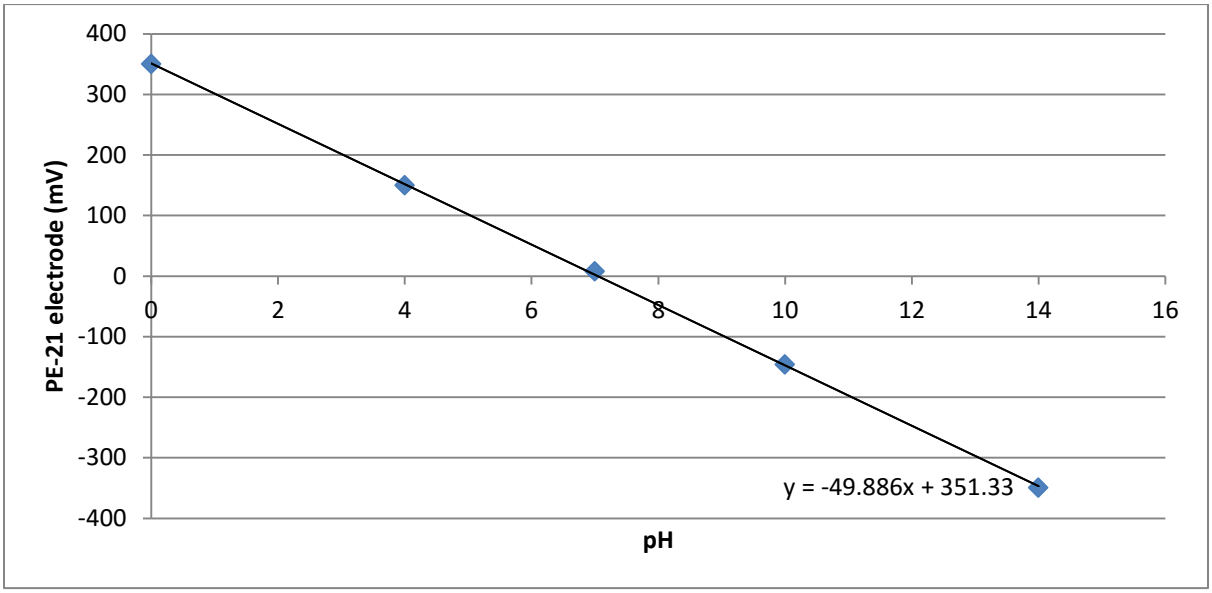

Fig. 5.2: Sensitivity plot for the Lutron PE-21 pH electrode

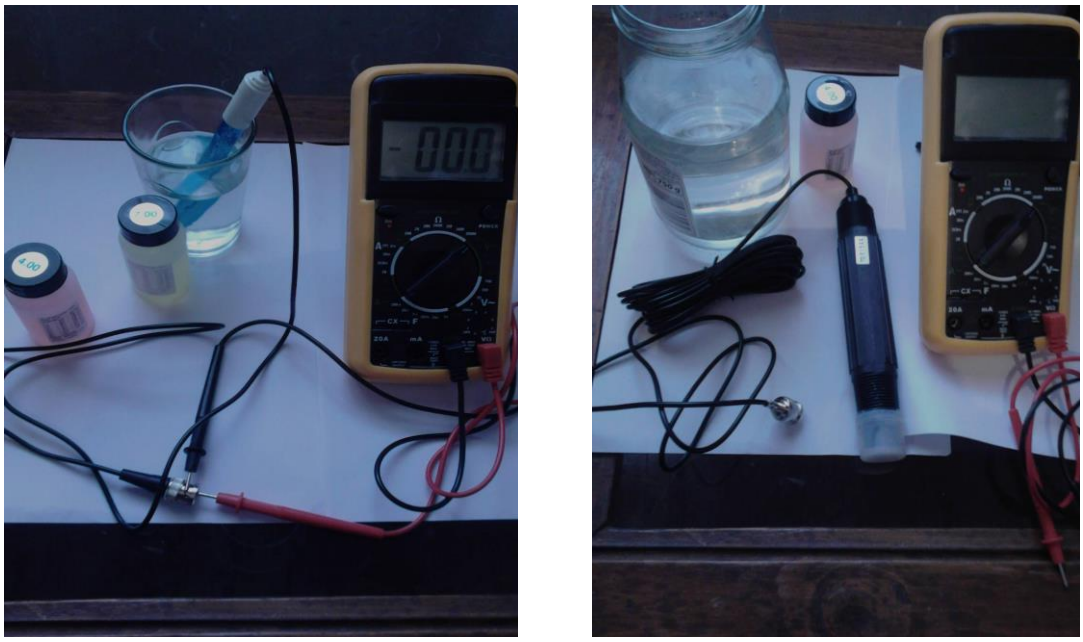

a. DFRobot SEN0161 pH electrode b. Lutron PE-21 pH electrode

Fig. 5.3: pH sensor calibration setup

5.2.1.2 pH amplifier

Practical pH sensors have a value of e.m.f/pH very close to the one given above (Fig. 5.1) and for the Lutron PE-21 pH electrode with slope of 50 mV/pH the range is +350 mV to -350 mV for 0 pH to 14 pH values.

The required amplifier shown in Fig. 5.4, should have an output slope of 1V/pH, that translates to an output voltage (V2) between the values of +7 V and -7 V as shown in Fig. 5.5. Hence the amplifier should have a gain of 20, from $\frac{+7V}{+350mV}$ or $\frac{-7V}{-350mV}$ such that,

$$V2 = \left(\frac{R2}{R1} + 1\right) Vin$$
$$= \left(\frac{19K}{1K} + 1\right) Vin$$
$$= Voltage\ gain \times Vin = 20 \times Vin\ . \qquad (15)$$

The voltage V2 is level shifted and scaled so that in varies between 0 to 5 V, compatible with microcontroller ADC input. pH sensors have very high output impedances (Hernandez, Medina & Hernander, 2012; Rosemount, 2010) and consequently for impedance matching to the amplifier stage it is recommended to use JFET operational amplifiers that have very high input

impedances such as the TL082CP Dual Bifet op-amp (TL082, 2000). Leakage current that would otherwise severely affect accuracy of the amplifier circuit is reduced by incorporation of a guard ring (Kumen, 2009) around the input signal paths of the amplifier on the printed circuit board as depicted in Fig. 5.6.

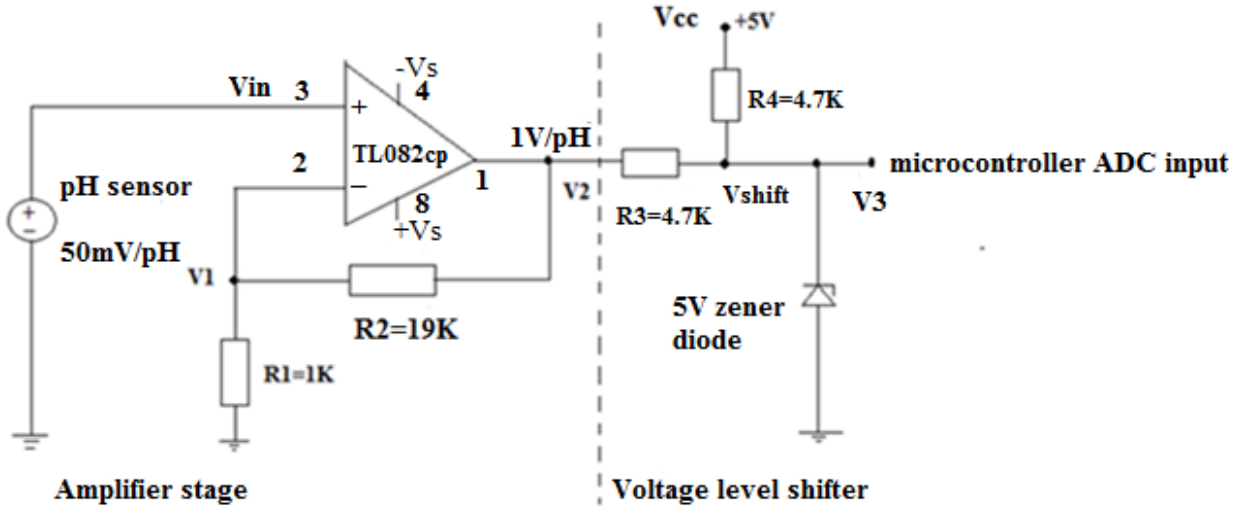

Fig. 5.4: pH amplifier and voltage level shifter section

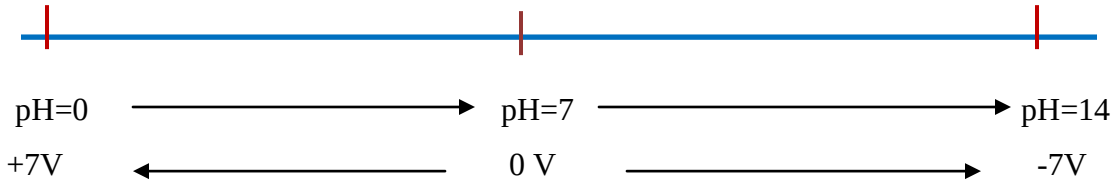

Fig. 5.5: pH probe voltage output for the range 0 pH to14 pH for a 1V/pH slope

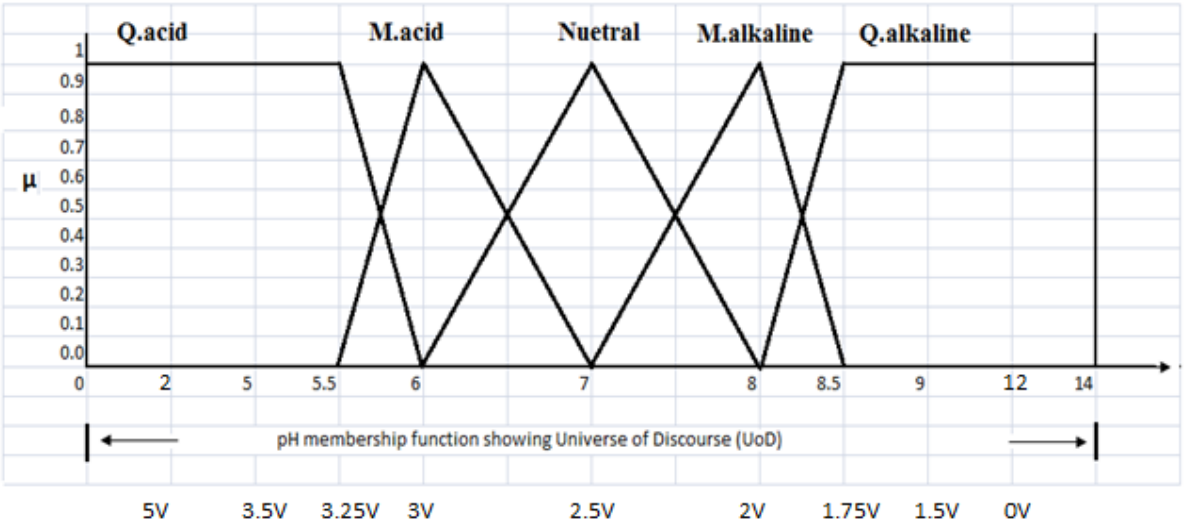

Fig. 5.6: Actual voltage allocation for pH membership function from pH12 to pH2

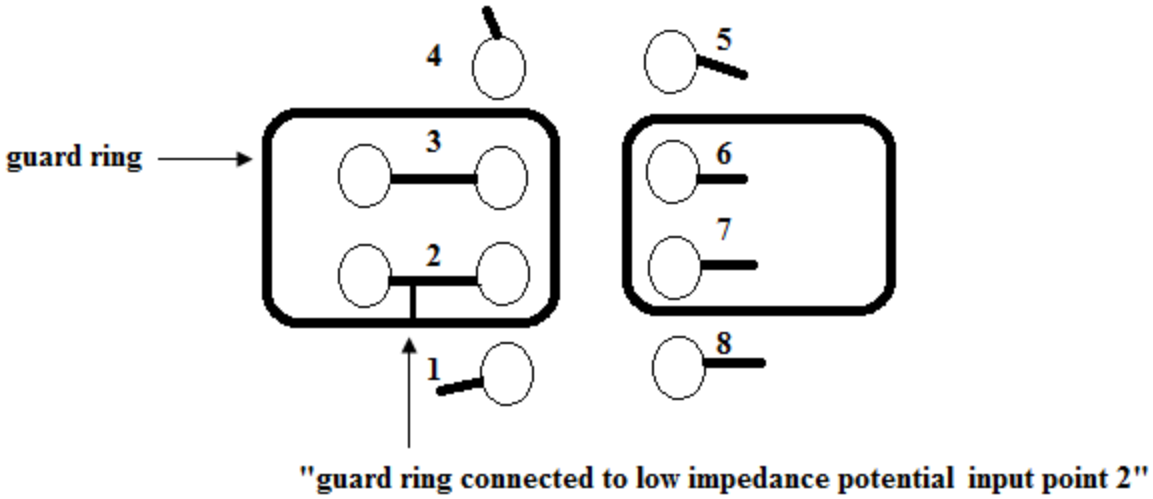

Fig. 5.7: BIFET OP-AMP printed circuit board incorporating a current leakage shield (guard) (https://www.qrz.ru/reference/micro/analog/ad712.pdf)

The voltage level shifter is designed for pH ranges between 2 and 12, corresponding to a V2 voltage range of +5V to-5V since digesters operating outside these ranges are not realistic. From this assertion it can be shown that:

(i) For pH12 and amplifier output V2 = -5 V,

$$\frac{Vshift-(-5)V}{4.7K} = \frac{Vcc-(-5)V}{4.7K+4.7K}$$

$$\frac{Vshift+5V}{4.7K} = \frac{(5+5)V}{4.7K+4.7K}$$

$$Vshift = 0\,V = ADC\ input. \qquad (16)$$

(ii) For pH7 and amplifier output V2 = 0 V,

$$\frac{Vshift-0V}{4.7K} = \frac{Vcc-0V}{4.7K+4.7K}$$

$$\frac{Vshift}{4.7K} = \frac{5V}{4.7K+4.7K}$$

$$Vshift = 2.5\,V = ADC\ input. \qquad (17)$$

(iii) For pH2 and amplifier output V2 = +5 V,

$$\frac{Vshift-5V}{4.7K} = \frac{Vcc-5V}{4.7K+4.7K}$$

$$\frac{Vshift-5V}{4.7K} = \frac{(5-5)V}{4.7K+4.7K}$$

$$Vshift = 5\,V = ADC\ input. \qquad (18)$$

5.2.2 Conductivity

This defines the ability of an aqueous solution to pass electricity, relative to the amount of ions in that solution. The more ions that are present in the solution the more conductive the solution is as depicted in Table 5.2. With reference to biogas digesters the concentration of dissolved salts in the total dissolved solids (TDS) will define how conductive that feedstock solution is, since salts readily form conducting ions. In addition to the total number of ions present the conductivity of the feedstock solution increases with temperature. The interpretation of high conductivity then, due to too much acidity or too much alkalinity is to indicate failing digester operation in-terms of the depletion of the micro-organisms that produce methane gas. This is related to a high organic loading rate and the presents of toxic soluble salts (Eu-agrobiogas, 2009; Kanokwan, 2006; McCarty & McKinney, 1961).The basic principle of conductivity measurements whose units are Siemens per cm (S/cm) is shown in Fig. 5.8.

Table 5.2: Conductivity values of common electrolytes at 25^{o}C
(http://www.analyticalchemistry.uoc.gr/files/items/6/618/agwgimometria_2.pdf)

Common electrolyte	**Conductivity value**
Pure water	0.055 µS/cm
Deionised water	1 µS/cm
Rainwater	50 µS/cm
Drinking water	500 µS/cm
Industrial wastewater	5 mS/cm
Seawater	50 mS/cm
1 mol/l NaCL	85 mS/cm
1 mol/l HCL	332 mS/cm

Let $reistance\ of\ electrolyte\ (R) = \frac{V}{I}\ \Omega$ and $its\ conductance(G) = \frac{1}{R}\ S\ , then$

$$Conductivity\ = Conductance\ x\ cell\ constant \qquad (19)$$

$$= \left(\frac{current}{voltage}\right) x\ \left(\frac{distance\ between\ electrodes}{electrode\ cross\ sectional\ area}\right)$$

$$= G\ x \frac{d}{a}\ S/cm$$

An ac voltage is used instead of a dc voltage to minimize the build-up of one specific polarity of ion that would otherwise accumulate on either electrode thereby affecting the current drawn from the supply and severely affecting the accuracy of measurement. The conductivity sensor will need to be calibrated against a solution of known conductivity. This calibration normally seeks to make correction for the cell constant.

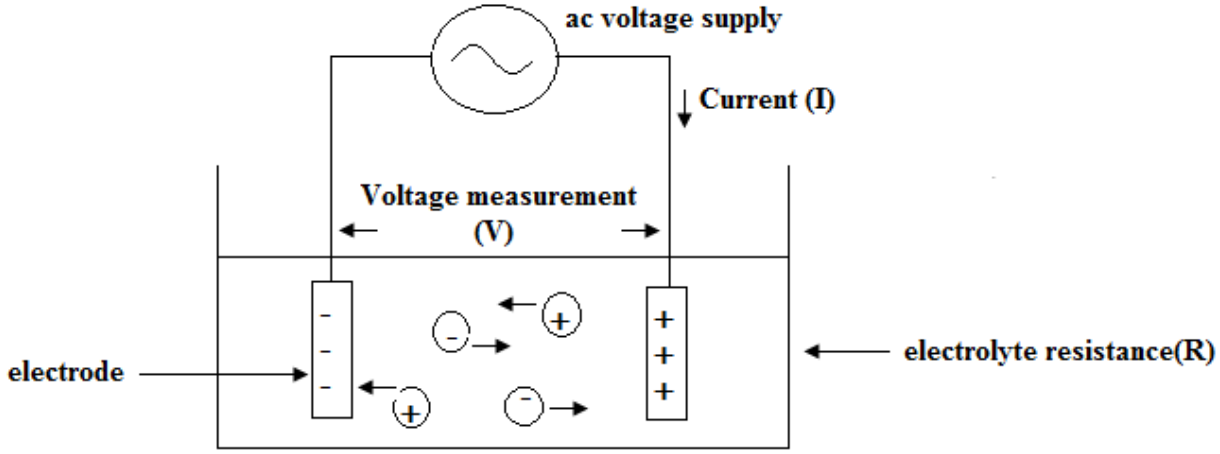

Fig. 5.8: Conductivity measurement principle
(http://www.analyticalchemistry.uoc.gr/files/items/6/618/agwgimometria_2.pdf)

Variations of the conductivity sensor include the two electrode, four electrode or the inductive type. The accuracy of measurement increases with adoption of the four electrode or the inductive types. The block diagram for the measurement circuit is shown in Fig. 5.9. The two electrode 208DH conductivity electrode with a measuring range of $0{\sim}199.9\ mS$ was used.

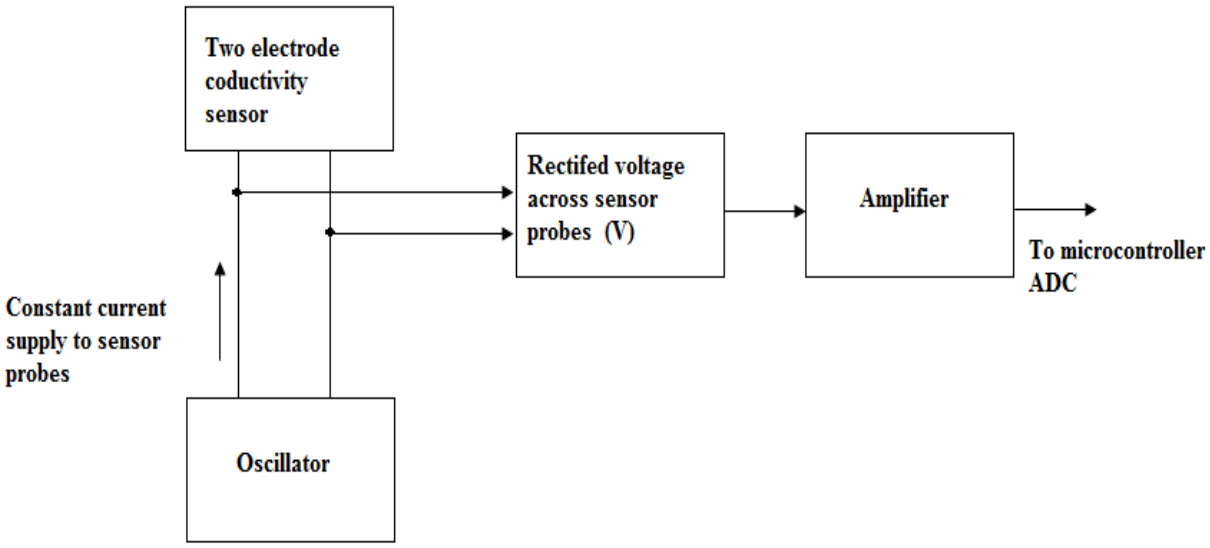

Fig. 5.9: Block diagram of conductivity measurement system

The oscillator was the typical Wein Bridge designed to give a 20 $V_{peak\text{-}peak}$ waveform of frequency 7.1 KHz as shown in Fig. 5.10. Fig. 5.11 shows the diagram for the conductance amplifier incorporating the range selector.

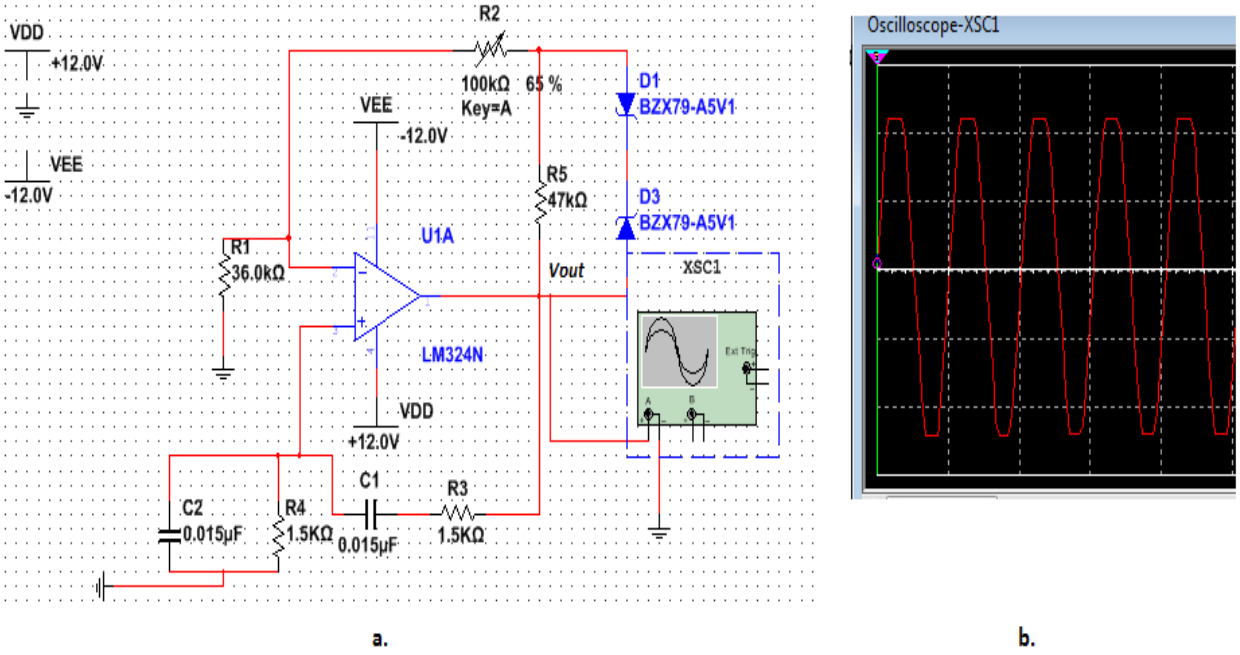

Fig. 5.10: a) Wein Bridge oscillator for the electrical conductivity sensor circuit, and b) output waveform

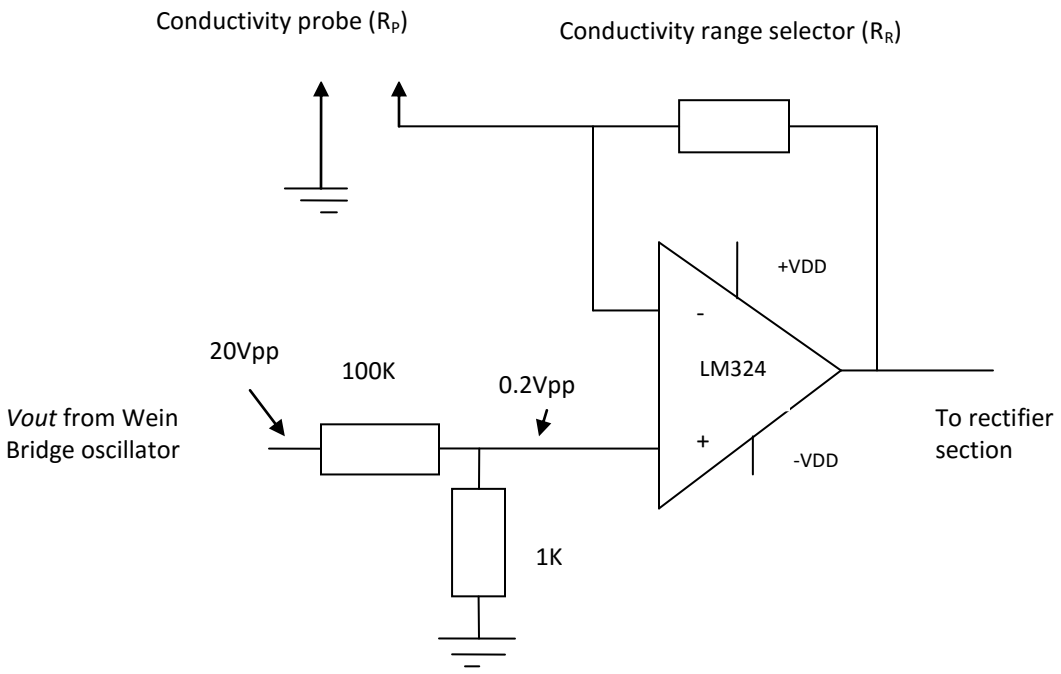

Fig. 5.11: Conductance amplifier

The complete circuit diagram is shown in Appendix F, where the conductivity probe was connected to pin 6 of the LM324N quad operational amplifier (LM 324, 2001). From Tables (4.1) & (5.2), a reasonable range of conductivity to select was 5 ~ 25 mS/cm. Now the electrolyte resistance expression is given as $Rp = 10^3/(Conductivity\ in \frac{mS}{cm})$, that translates to value range of 200 ~ 40 Ω. The output of this circuit varied from 0 to 5 V as the value of the electrolytes' electrical conductivity varied from very low to very high and a suitable range scaling resistor (R_R) was found to be 820 Ω.

Calibration was performed using two sodium chloride solutions pre-paired in-house at 25^{o}C to give conductivities of 10 mS/cm and 20 mS/cm respectively. The voltage output at each of these solutions was measured and recorded. A plot shown in Fig. 5.12, of conductivity against output voltage was done. From the plot the equation that relates electrical conductivity (EC) to final output voltage (Vecadc) is formulated and this equation is given as:

$$EC = 0.0049Vecadc - 0.3837 \qquad (20)$$

Equation *(20),* gives the actual value of electrical conductivity in mS/cm directly from the sensor immersed in the digester slurry. This equation is then incorporated into the software for use by the alkalinity prediction equation *(4).*

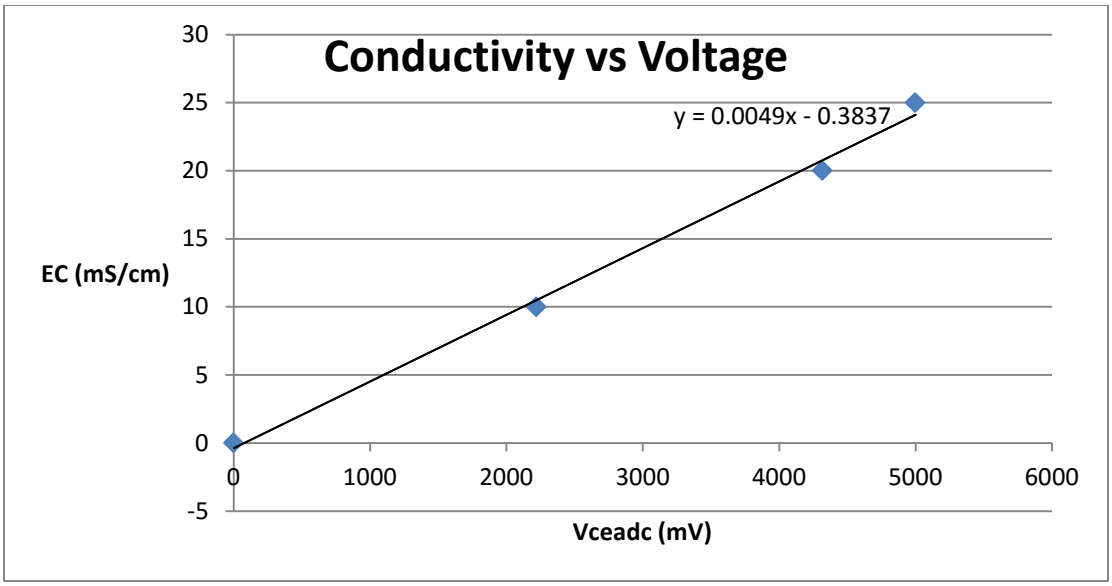

Fig. 5.12: Conductivity vs Voltage

5.2.3 Redox (Oxidation-reduction potential (ORP))

When an ion or atom releases an electron we term the process as oxidation of that ion or atom, whilst the acceptance of an electron by the same is termed reduction.
Consider the equation:

$$Fe^{2+} \leftrightarrow Fe^{3+} + e^{-} \quad (21)$$

Fe^{2+} is in a reduced state whilst Fe^{3+} is in an oxidized state.

Redox pontential(ORP) standardized against the hydrogen equation,

$$H_2 \leftrightarrow 2H^{+} + 2e^{-} \quad (22)$$

is a measure of the inclination of a substance(compound) to receive electrons. A high (positive) ORP then implies a gain in oxygen, whilst a low (negative) ORP implies a loss of oxygen. This is the voltage between the electron givers and the electron receivers that are present in the feedstock (Bernhard, 2013). By definition anaerobic bacteria operates when there is no oxygen, implying a low ORP. According to Bernhard (2013) an ORP of less than -300mV has been found to be ideal for anaerobic microbes to function optimally. The output voltage specification of the 201DH ORP probe to be used in this project is specified $0 \sim \pm 1999mV$. The same amplifier and level shifter configuration as for the pH probe *(See page 69)* will be used where the required amplifier should have an output voltage, corresponding to a V2 between the values of +5V and -5V compatible for level shifting for microcontroller ADC. Hence the amplifier should have a gain of 2½, from $\frac{+5V}{+1999mV}$ *or* $\frac{-5V}{-1999mV}$ such that,

$$V2 = \left(\frac{R2}{R1} + 1\right) Vin$$

$$= \left(\frac{15K}{10K} + 1\right) Vin$$

$$= Voltage\ gain \times Vin = 2½ \times Vin\ .$$ *(23)*

Fig. 5.13, gives the complete schematic incorporating both pH redox sensors.

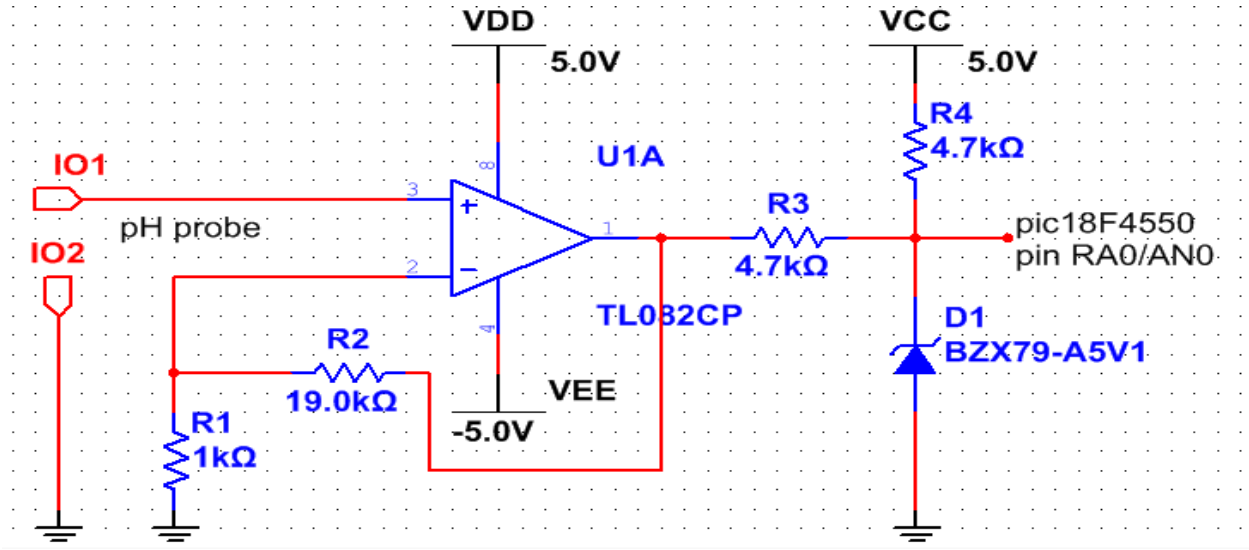

a.

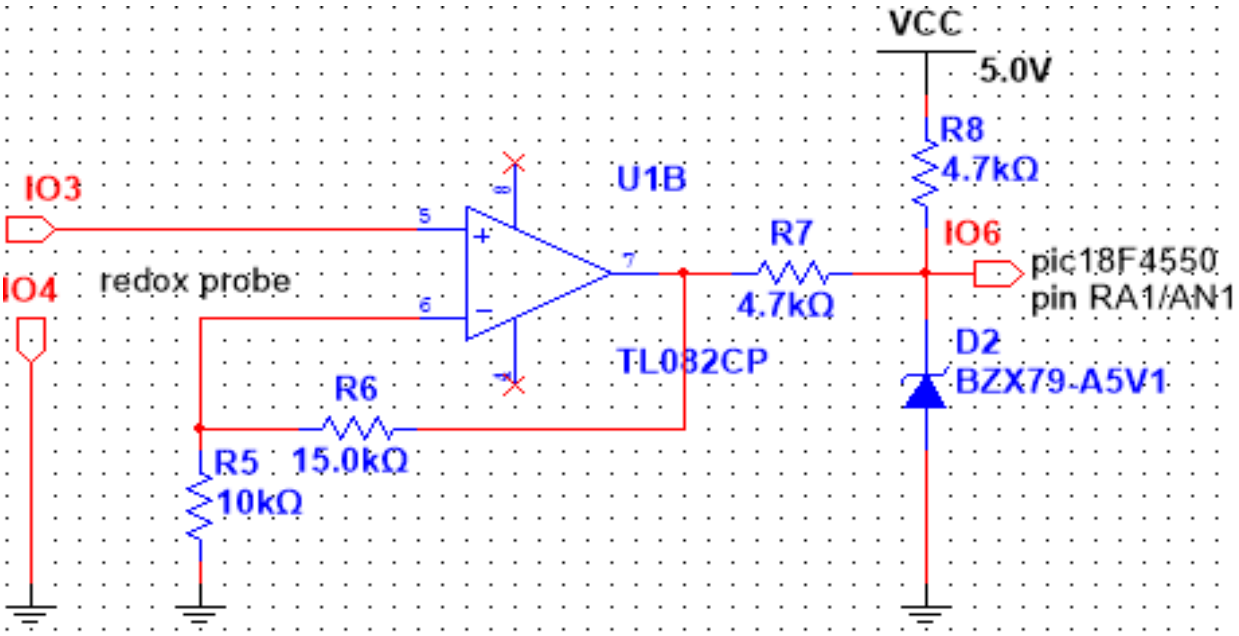

b.

Fig. 5.13: pH and redox TL082CP OP AMP based amplifier circuit

For an oxygen reduction potential (redox) $Vin = -250\,mV$, the value of *V2* from equation *(23)* is $-0.625V$ and substituting this value of *V2* into the expression $\frac{(\text{Vshift}-(V2))\text{V}}{4.7\text{K}} = \frac{(\text{Vcc}-(V2))\text{V}}{4.7\text{K}+4.7\text{K}}$, V_{shift} (V_{ADC}) is obtained as $+2.1875\,V$. Likewise with $Vin = -400\,mV$, V_{shift} is obtained as $+2\,V$. To supply the correct value of redox in the prediction equation c source code, software scaling of the analogue voltage at the input of the microcontroller is done. This is basically a reverse process to obtain the value of Vin from V_{shift}.

The constructed printed circuit board amplifier picture for pH and redox (ORP) is given in Appendix H.1.

.

5.2.4 Buffer capacity measurement by titration

5.2.4.1 Volatile fatty acids and Alkalinity

The carbon acids called volatile fatty acids (VFA) are a result of the acidogenesis process in the digester material. An increase in the concentration of the VFA between 1500 and 2000 mg/L will significantly suppress the biogas production process. Hence being able to monitor this parameter we can determine how stable the system is. Similarly alkalinity (buffer capacity) which is a measure of the tendency to avoid pH change can also be used to determine how stable the digestion process is. Typical alkalinity values in biodigesters range from 2000 – 5500 mg/L bicarbonate and above 4000 mg/L bicarbonate means a good buffering capacity (Eu-agrobiogas, 2009; Labatut & Gooch, 2015; Wisconsin, 1992).

For this research titration measurements to determine[23] the ratio of VFAs to Alkalinity (also known as TIC (Total Inorganic Carbon)) (Lohri, 2008) and to evaluate the actual value of alkalinity (can be used to formulate a much more accurate prediction equation) in mg/l.bicarbonate are performed.

5.2.4.2 Titration[24] procedure

(1) The sample is filtered through a fine membrane (order of 0.45μm) so as to remain with a solution with no solid particles.
(2) Capture between 20 to 50 ml of the filtered sample in a glass or transparent container.
(3) Titrate (add) carefully 0.1 N sulphuric acid until pH 5.0 is reached. Write down the added volume h1[ml] of titrant.
(4) Add more acid to get a pH 4.3 and write down the added volume h2[ml] of titrant.
(5) Add more acid to get a pH 4.0 and write down the added volume h3[ml] of titrant.
(6) During all these steps the resultant solution is constantly mixed as addition of acid is done.
(7) Calculate (Lohri, 2008) the values of alkalinity and volatile fatty acids as shown below.

[23] Assess digester stability in the off-line mode.
[24] Was done on-site and the results given in Chapter 8.

$$Alkalinity = \left[\frac{d1xNx1000}{sv}\right] mmo/l \quad (24)$$

d1 = Sulphuric acid (H_2SO_4, 0.1N) used to change from pH 5.0 to pH 4.3 in ml

$That\ is\ d1 = (h1 + h2)\ ml$

N= Normality[mmol/l]

Sv=Initial sample volume [ml]

$$VFA = \left[\frac{131340xNxd2}{sv} - 3.08xAlkalinity - 10.9\right] [\frac{mg}{l}\ acetic\ acid\ equivalents] \quad (25)$$

d2 = Sulphuric acid (H_2SO_4, 0.1N) used to change from pH 5.0 to pH 4.0 in ml due to HCO_3/CO_2 buffer

$That\ is\ d2 = (h2 + h3)\ ml$

N= Normality[mmol/l]

Sv=Initial sample volume [ml]

Alkalinity = Alkalinity [mmol/l]

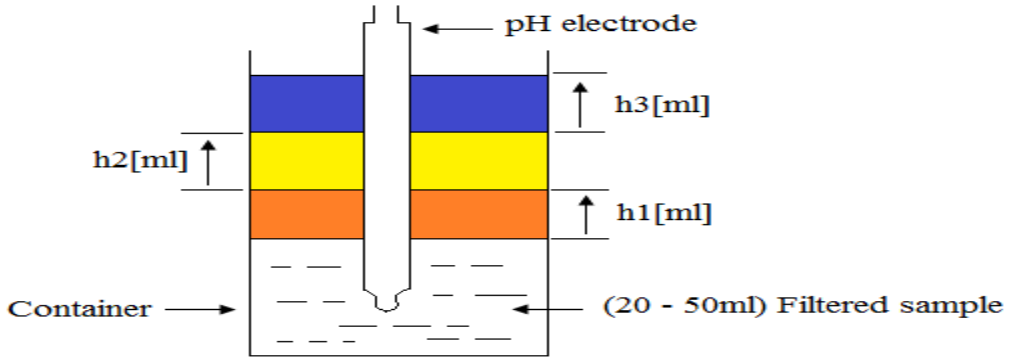

Fig. 5.14: The titration setup

5.2.5 Temperature

The temperature of the digester slurry is measured by using a PT100 platinum resistance temperature detector (RTD) that has the temperature resistance characteristics shown in Fig. 5.15. From the PT100 resistance table (Thermocouple, 1999), probe resistances at various temperatures are noted. However in this research the aspects considered when designing the circuit of Fig. 5.16 based on the TL061[25] operational amplifiers (TL061, 2004) are maximum permissible RTD current, maximum possible ground temperatures in the digester vicinity and the microcontroller voltage. A current of 1mA will cause some self-heating of 100 μW ($from\ P = I^2$R), however this current will cause a small measurable voltage change.

[25] The TL061CP operational amplifier is pin compatible with the 741 traditional operational amplifier.

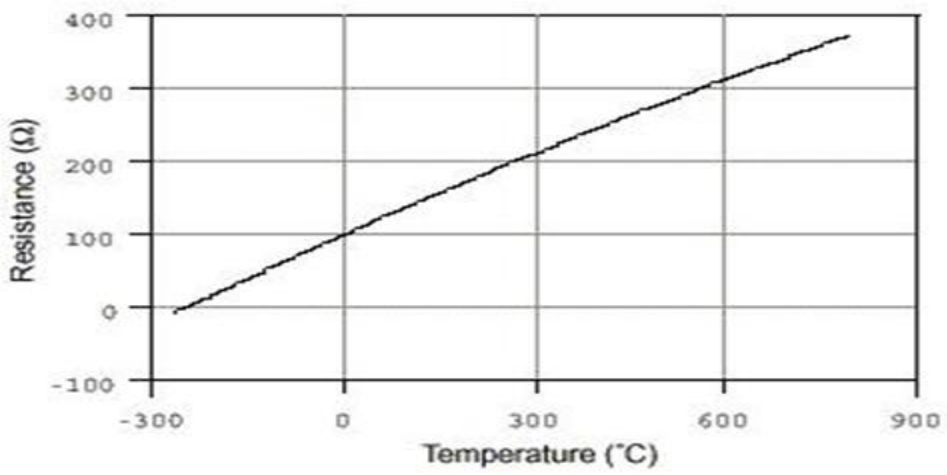

Fig. 5.15: Resistance-Temperature plot for a PT100 temperature probe
(http://www.ni.com/tutorial/7115/en/)

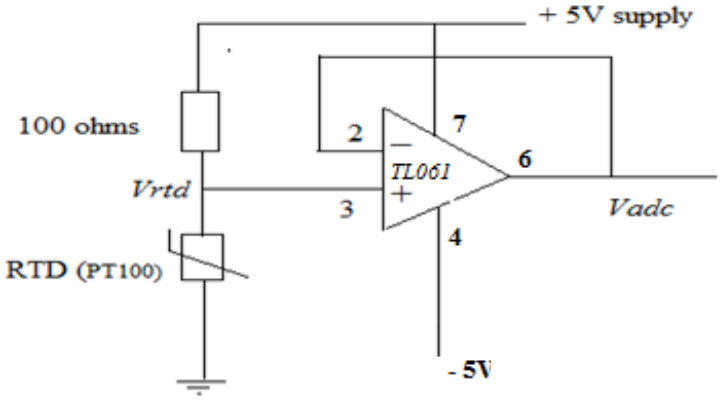

Fig. 5.16: PT100 temperature measurement circuit with photograph of printed circuit board amplifier shown in Appendix H.2

Fortunately the probe is operated completely immersed in liquid feedstock effectively counteracting the self heating effect. Hence higher currents than this as given in the calculation below can be used to give a larger measurable voltage (proper cable and printed circuit design screening was done). On the other hand ground temperatures will not go below 0℃ nor will digester temperature go above 60 ℃.
With reference to the designed circuit in Fig. 5.16 and taking a supply voltage of 5 V:

(1) $At\ 0℃\ RTD\ resistance = 100\ \Omega$

$$\frac{Vrtd}{5} = \frac{100\Omega}{100\Omega+100\Omega} \qquad (26)$$

$Vrtd = 2.5V\ and\ Vadc = 2.5\ V$

$$Maximmum\ RTD\ current = \frac{2.5V}{100\Omega} = 0.025\ A$$

$$(2)\ At\ 20℃\ RTD\ resistance = 107.79\ \Omega$$

$$\frac{Vrtd}{5} = \frac{107.79\Omega}{100\Omega+107.79\Omega} \quad (27)$$

$$Vrtd = 2.5937V$$

$$(3)\ At\ 60℃\ RTD\ resistance = 127.08\ \Omega$$

$$\frac{Vrtd}{5} = \frac{127.08\Omega}{100\Omega+127.08\Omega} \quad (28)$$

$$Vrtd = Vadc = 2.79815V$$

$$Current = \frac{2.79815V}{127.08\Omega} = 0.02202A$$

The voltage output was then calibrated to give temperature readings and the expression $temperature = 200.33Vrtd - 500.33$ (obtained from MS-Excel plot) used in the software development process.

5.2.6 Methane

In this research methane gas detection is made by use of the Flying Fish MH MQ2 gas sensor. The basic structure of this sensor as shown in Fig. 5.17, comprises of tin dioxide (SnO_2), the material of which decreases in conductivity as the air becomes cleaner. As the gas concentration increases the sensor's conductivity also increases. The sensor element (Rs) is heated to a specified temperature for it to operate, hence it gets uncomfortably hot when powered on.
The sensor used here (Fig. 5.18), incorporates an electronics (amplifier) circuit board with the following pins:

- GND
- +5 V
- Do (Digital out) and
- Ao (Analog out varying from 0 – 5 V)

The sensor module detects methane in the concentration ranges of 5000 ppm -20000 ppm.
Calibration of the sensor module is done by measuring a gas of known concentration (for example 1000 ppm liquefied petroleum gas) and making the necessary adjustment on the module potentiometer. However, the sensor module is factory calibrated. Fig. 5.19, gives a plot of the sensitivity characteristics of the MQ2 sensor for different gas measurements.

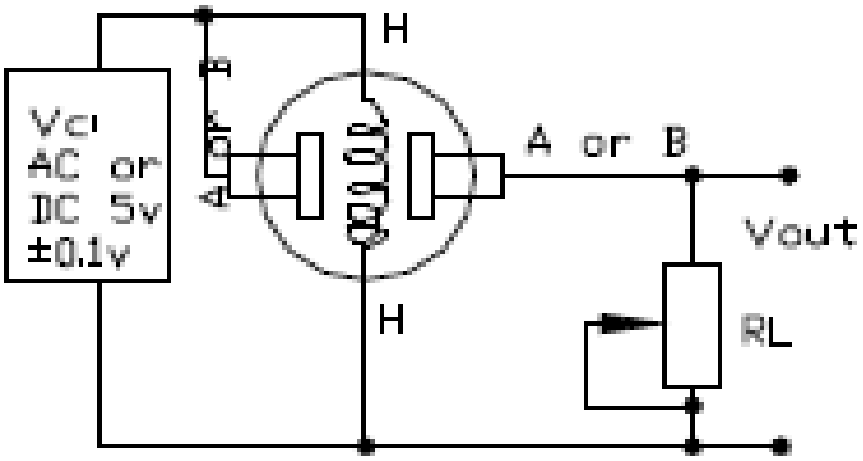

Fig. 5.17: MQ-2 basic measuring circuit
(*https://www.seeedstudio.com/depot/datasheet/MQ-2.pdf*)

Fig. 5.18: Flying Fish MH MQ2 gas sensor module

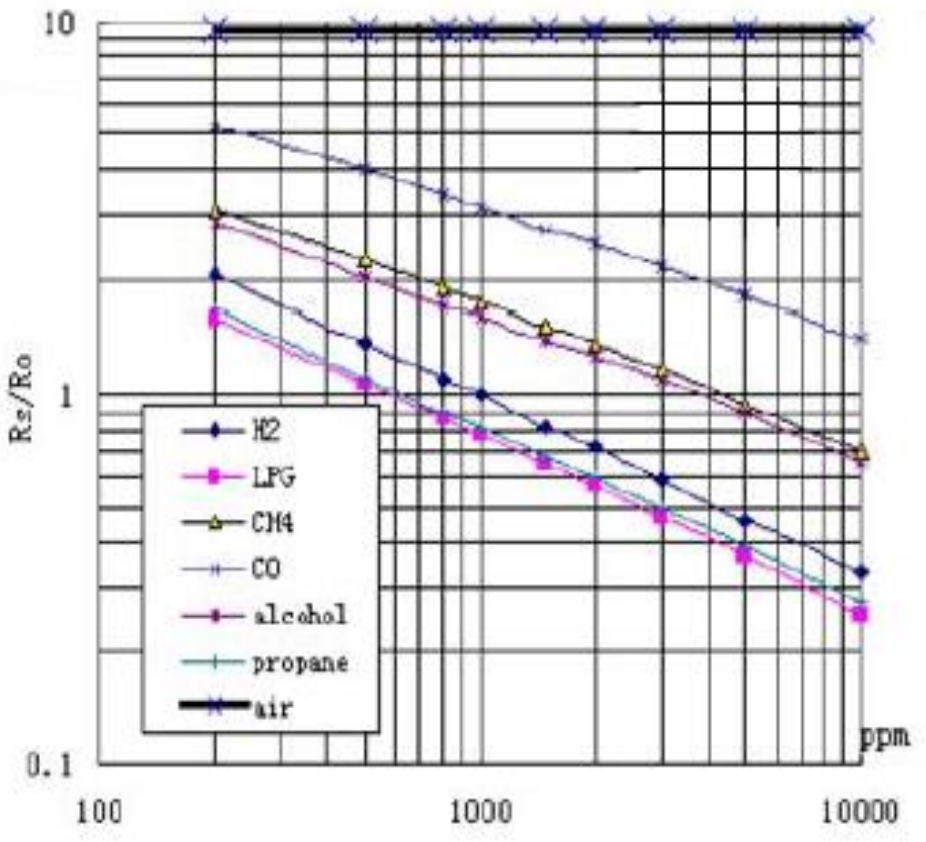

Fig. 5.19: Sensitivity characteristics of the MQ-2 gas sensor

(https://www.seeedstudio.com/depot/datasheet/MQ-2.pdf)

5.2.7 Carbon dioxide

For carbon dioxide measurement an MG811 carbon dioxide sensor module (Fig. 5.20) has the same constructional structure as for the methane module is used. The module has the following specifications:

- Four pins comprising +6 V supply, analog output (AO), digital output (DO) and GND
- LM393 and carbon dioxide sensor circuit board
- An output voltage range of $30 \sim 50\ mV$
- 0 to 10000ppm carbon dioxide detection concentration range.

Just like in the methane sensor the carbon dioxide sensor material is also heated to operating temperature. The carbon dioxide sensor material made up of polymer will produce an electromotive force (EMF) that is proportional to the carbon dioxide concentration as depicted in Fig. 5:22. The sensor module is factory calibrated.

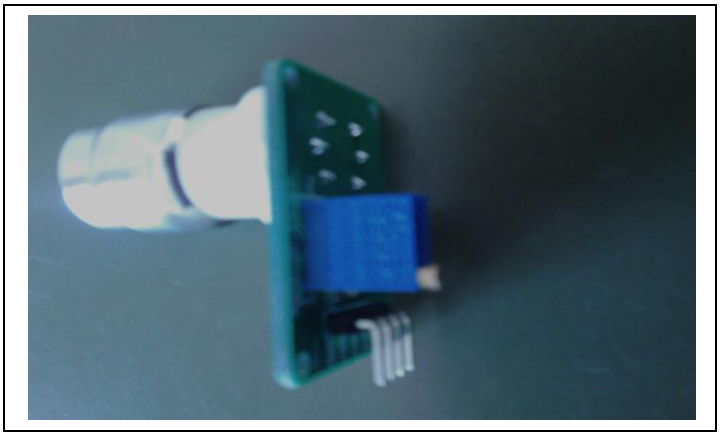

Fig. 5.20: MG811 carbon dioxide sensor module

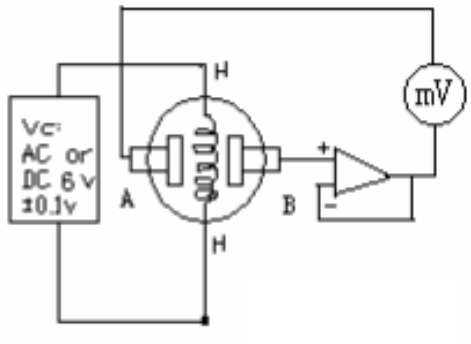

Fig. 5.21: MG811 basic measuring circuit
(http://sandboxelectronics.com/files/SEN-000007/MG811.pdf)

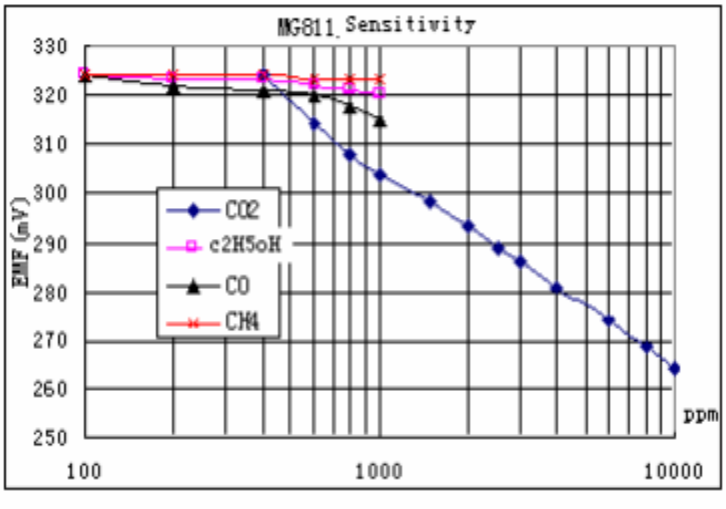

Fig. 5.22: Sensitivity characteristics of the MG811 gas sensor
(http://sandboxelectronics.com/files/SEN-000007/MG811.pdf)

5.2.8 Pressure

The gas pressure sensor specified here is of the type that is used on flammable gases. Since the normal accepted methane gas pressures in the digester are limited to 15 KPa (0.15 bar or 2.17557 psi), the pressure sensor used should measure at least 30 KPa (0.3 bar or 4.35113 psi). For this research use is made of the model RC 300 Liyuan Electronic 1MPa 4-20 mA 24 V gas pressure sensor. The pressure sensor supplied by the photovoltaic 24 V Dc supply directly provides an output between the limits of 4 to 20 mA as depicted in Fig. 5.23.

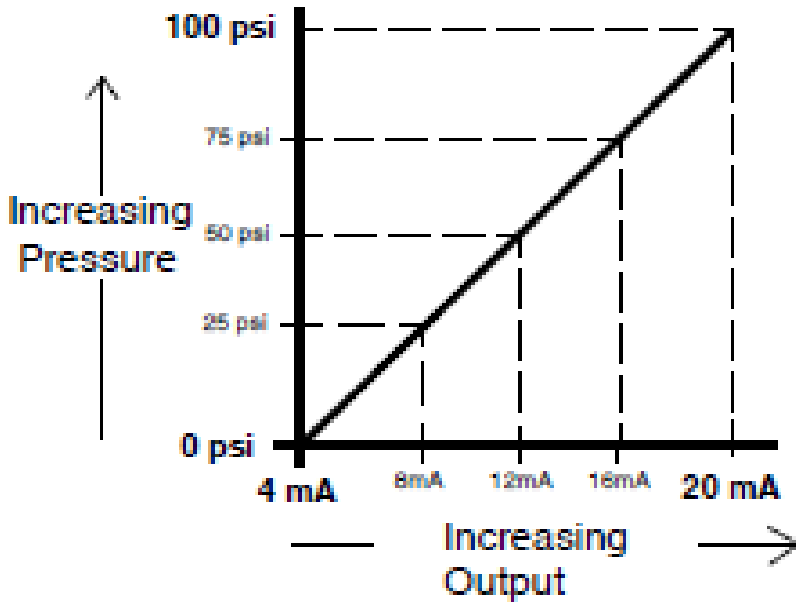

Fig. 5.23: Linear relationship between pressure and sensor output
(http://www.wika.us/upload/BR_CAT_Electronic_Pressure_en_us_17801.pdf)

Fig. 5.24 gives the circuit diagram of the 4-20mA to 1-5V converter for the analogue to digital converter (ADC) input to the microcontroller. From Fig. 5.24, it can be shown that:

(1) For 20 mA, $Vx = 0.02\ x\ 47 = 0.94\ V\ and\ from\ this$

$$Vadc = \frac{(Vx)x15K}{3K}$$

$$= 4.7\ V \text{ and} \qquad (29)$$

(2) For 4mA, $Vx = 0.004\ x\ 47 = 0.188\ V, hence$

$$Vadc = \frac{(Vx)x15K}{3K}$$

$$= 0.94\ V \qquad (30)$$

Calibration of the pressure transmitter module is done by using a bicycle pump that has a calibrated pressure gauge connected to it. The procedure involves the measurement of voltage output *(Vadc)* at different pressures up to 20 KPa and the resulting software equation (Fig. 5.25) of obtaining pressure at various voltage levels formulated. The constructed printed circuit board amplifier is shown in Appendix H.3.

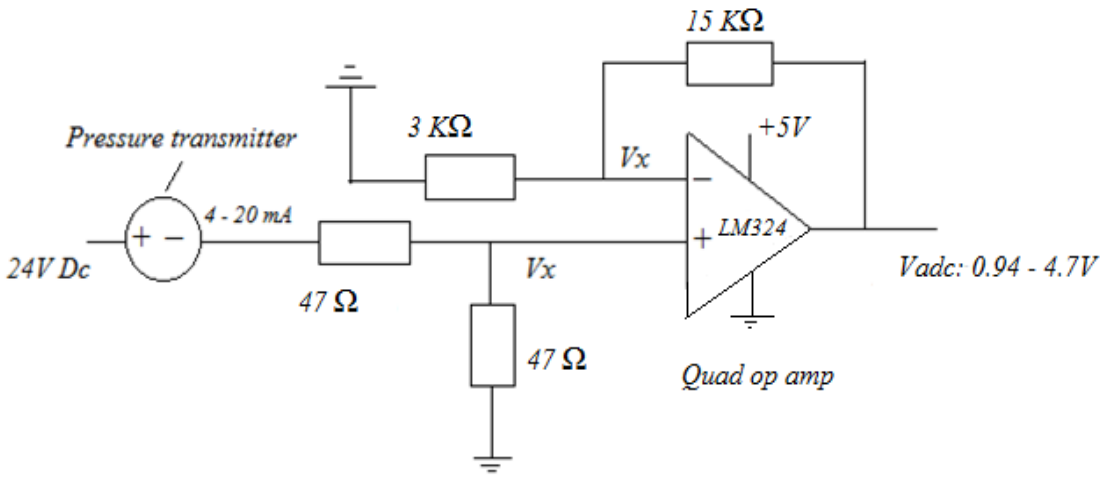

Fig. 5.24 Circuit diagram of the 4-20 mA to 1-5 V converter for the analogue to digital converter (ADC) input to the microcontroller

Table 5.3: Calibration of pressure sensor using bicycle pump

Pressure (KPa)	Voltage (V)
0	1.28
2	1.73
4	2.21
6	2.47
8	2.64
10	2.85
12	3.11
14	3.46
16	3.89
18	4.39

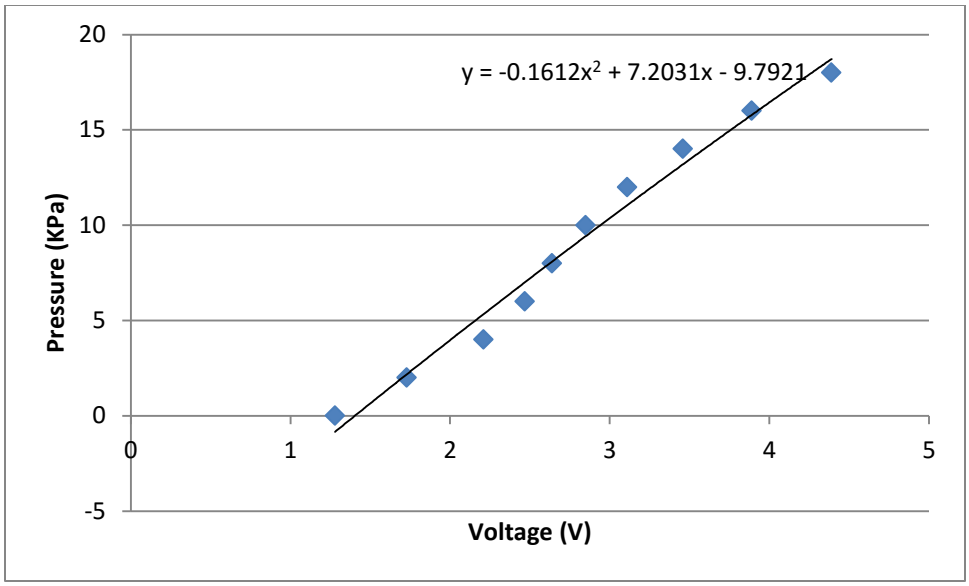

Fig. 5.25: Calibration of pressure sensor

The equation on Fig. 5.25, directly gives the value of biogas pressure (KPa) in the digester, and is used in the software coding of the pressure routine.

5.2.9 Level

Level is monitored by the use of two stainless steel sealed vertical float switches. One switch (SW1) is positioned to be at the highest slurry level point whilst the other switch (SW2) is positioned at the lowest slurry level point. The switching current of $\frac{5V}{10K\Omega} = 500\ \mu A$ is small enough not to cause any danger in the digester due to arcing. Fig. 5.26, shows how the switches are connected to the microcontroller.

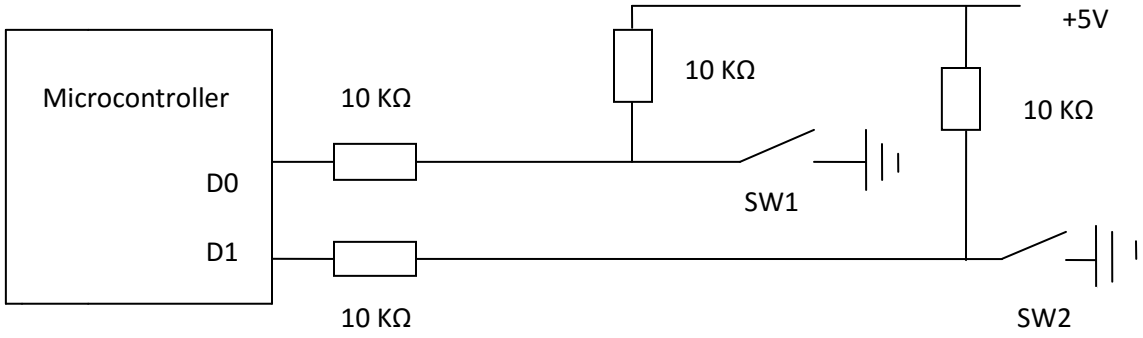

Fig. 5.26: Level float switches connected to microcontroller

5.2.10 Oxygen

The trace oxygen sensor module is made up of a *"galvanic fuel cell"* (electro-chemical in nature) and an electronics circuit board housing a resistive network that includes resistors and an NTC for current to voltage conversion and temperature compensation respectively. Initially no output is produced by the oxygen cell until it is placed in the presence of oxygen. Oxygen initiates a chemical reaction after which the oxygen cell produces an electrical current. This electrical current is converted to a voltage by placing a resistor across the cell terminals. The sensor voltage output that typically ranges from 8-13 mV in air to 175 mV in one hundred percent oxygen (Gurr, 2013) is directly proportional to the oxygen concentration. Calibration of the sensor is then easily done by measuring the voltage output of the known concentration of oxygen air which is 20.945 % (Lauer, 2016).

The oxygen cell is normally made up of a lead anode, a platinum cathode and a potassium electrolyte to give the following reaction breakdown:

$$O_2 + 2H_2 + 4e^- \rightarrow 4OH^- \; at \; the \; cathode \qquad (31)$$

$$2Pb + 4OH^- \rightarrow 2Pb^{2+} + 2H_2O + 4e^- \; at \; the \; anode \; and \qquad (32)$$

$$O_2 + 2Pb \rightarrow 2PbO \; overall \; reaction. \qquad (33)$$

Equation *(32)* clearly shows that electrons will flow from the anode to the cathode if an external path is provided, hence the current nature of the generated signal. Furthermore from the same equation it is noted that lead is depleted to form lead oxide which implies that the oxygen sensor will eventually run out of lead leading to its death. According to Gurr (2013) the average lifetime of this type of oxygen sensor is three years.

By the time the oxygen reaches 30 % the alarm system should have already come on. This corresponds to a voltage of $\frac{175mV}{3.333} = 52.5\ mV$, which is taken as the upper limit in the design.
To scale up the sensor signal to 0-5V the circuit of Fig. 5.27, with a gain of $\frac{5V}{0.0525V} = 95.23$ is used. A gain of 91 instead giving a voltage range of 0-4.78 V was used. The voltage output in air is 0.73-1.18 V.

The constructed printed circuit board amplifier is shown in Appendix H.3, where it shares the quad LM324 operational amplifier with the pressure sensor.

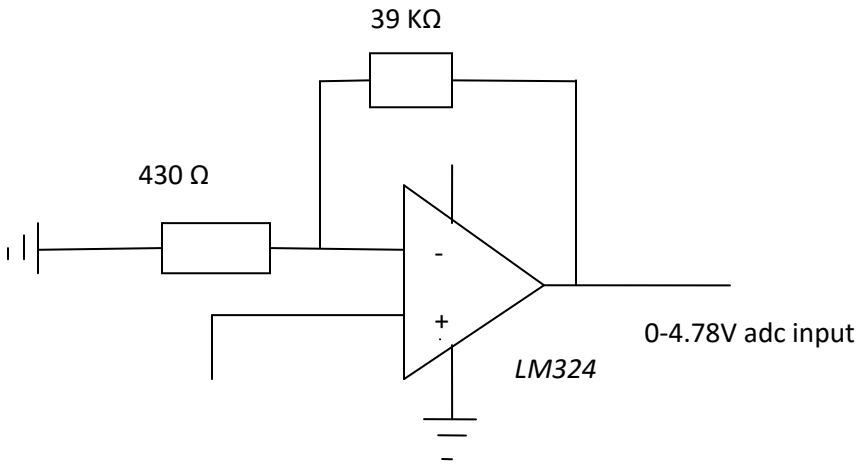

Fig. 5.27: Oxygen sensor signal amplifier

5.2.11 Voltage detection in PV system

In coming up with the voltage divider measurement circuit for converting the 24V photovoltaic battery value to 0-5V it was required to take into consideration the maximum allowable source impedance of the microchip microcontrollers. The recommended maximum source impedances for microchip 8/10 bits microcontrollers is 10KΩ and for 12bits its' 2.5 KΩ (Microchip, 2015b). With reference to Fig. 5.28, let:

$R1 + R2 = 56\,K$ and *(34)*

$5V = \frac{24V\ x\ R2}{56K}$, then

$R2 = 11.67K\Omega\ and\ R1 = 44.33\ K\Omega.$

The standard values of $R1\ and\ R2$ are taken as $47\ K\Omega\ and\ 11\ K\Omega$ respectively where the parallel combination (source impedance) of the resistors yields $\frac{11K\Omega\ x\ 47K\Omega}{58K\Omega} = 8.914\ K\Omega.$
The calculated source impedance is clearly less than the maximum allowable value. Furthermore the normal output of a 100 % SOC battery during charging about 26 V, implying that the current at this point through the resistors is $\frac{26V}{58K} = 0.44828\ A.$ Therefore the maximum output to the microcontroller is given as $Vadc = 0.44828\ A\ x\ 11\ K\Omega = 4.931\ V.$

The photocell output at the PV panel is measured by the sensing circuit as shown in Chapter 4, Fig. 4.11.

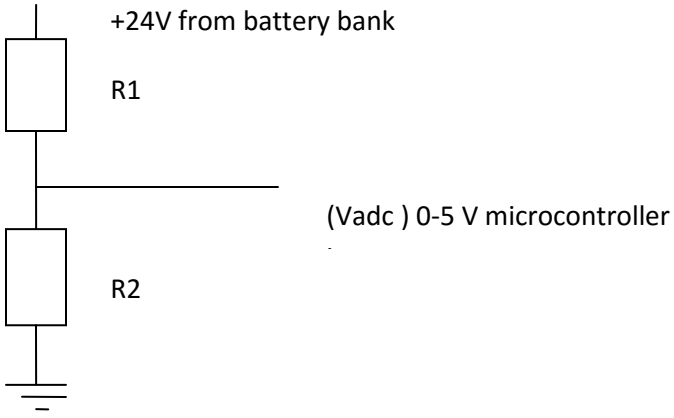

Fig. 5.28: Battery charging voltage measuring circuit for microcontroller input

5.2.12 Current detection in PV system

For the dc charging current which is limited to 5 A the current measurement system is as shown in Fig. 5.29, where the following observations are made:

A series resistance of 0.05 Ω is used to give a maximum power output of $5^2 x 0.05 = 1.25\ W$

- voltage drop across series resistor is *Vs* , where:

  $Vs = 0.05\ \Omega\ x\ 5\ A = 0.25\ V$

- $Gain = \frac{5V}{0.25V} = \frac{Rf}{Rin} = \frac{2.2K\Omega}{110\Omega}$
- $0.25\ V$ is scaled up to 5 V by multiplying by the gain factor. *(35)*
- Gain of op-amp circuit is 20.

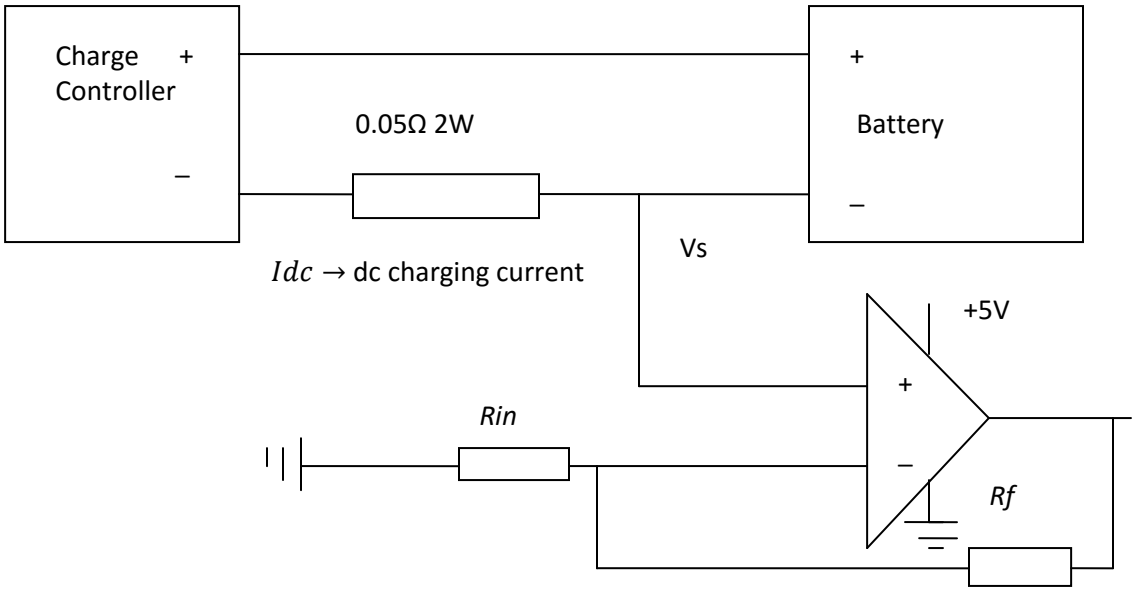

Fig. 5.29: LM324 Charging current sensing circuit for microcontroller

5.2.13 State of Charge (SOC) of PV battery

An offline state of charge evaluation based on open circuit voltage measurements is done when the load and charging source have been disconnected for some time and the open circuit voltage has attained a constant value. The value of the SOC read off from Table 4.4 *(See page 53)* according to the steady open circuit voltage measured is entered into the microcontroller program as a constant for the duration of time that the user decides. The SOC constant can be changed on a daily, weekly or monthly basis depending on the level of supply interruption that can be tolerated. A 4x4 Key pad is used to enter numeric values of the total dry solids (TDS) and state of charge (SOC) into the microcontroller.

5.2.14 PV fault detection currents

The current measurement system is made up of alternating current (ac) and direct current (dc) circuits. The ac circuits monitor the load current after the inverter whilst the dc circuits monitor all the currents prior to the inverter. The dc currents are the inverter, battery and charge controller input currents. The format for all dc current measurement circuits is as described in section 5.2.12 above, however with variations in the values of *Idc*, series resistor, *Vs*, *Rf* and *Rin*. The ac current is detected by a TA17-05 30 A/10 ma 1:1000 PCB mount current transformer (CT) with turns ratio (N) = 1:3000 (Fig. H.6). In the respective circuit shown in Fig. 5.30, the maximum primary (CT) current is 5.43 A. For the CT with the specifications given above the value of the burden resistor is calculated as follows:

$$i.\,Primary\ peak-peak\ current\ (Ipp) = 30x\sqrt{2}A = 42.42\ A \qquad (36)$$

$$ii.\,Secondary\ peak-peak\ current\ (Ispp) = \frac{Ipp}{N} = \frac{42.42A}{3000} = 0.01414\ A \qquad (37)$$

$$iii.\,Maximum\ resolution\ is\ achieved\ when\ the\ voltage\ is\ centred\ at +2.5\ V\ for \quad +5\ V\ supply\ (from\ R4\ and\ R5),\ hence\ burden\ resistance = \frac{2.5V}{Ispp} = \frac{2.5V}{0.01414A} = 176.80\ \Omega. \qquad (38)$$

The standard resistance values close to this calculated value are 180 Ω and 160 Ω. The smaller value of 160 Ω is taken to prevent a higher output than the supply to the adc input. Using the circuit of Fig. 5.30, the burden resistance value is increased two fold before being fed directly into the adc input. By developing a suitable software routine the peak value of the signal is calculated by the microcontroller.

The maximum secondary current transformer voltage $Vspp = 160\ \Omega\ x\ 10\ mAx\sqrt{2} = 2.2624\ V$ and after amplification this goes to $Vspp = 2.2624\ x\ 2\ V = 4.5248\ V$ (from R2 and R3 gain value) which is well within the $0-5\ V$ range for microcontroller. Any operational amplifier which is of the same type and with close parameter values as the OPA348 (OPA348, 2016) can be used.

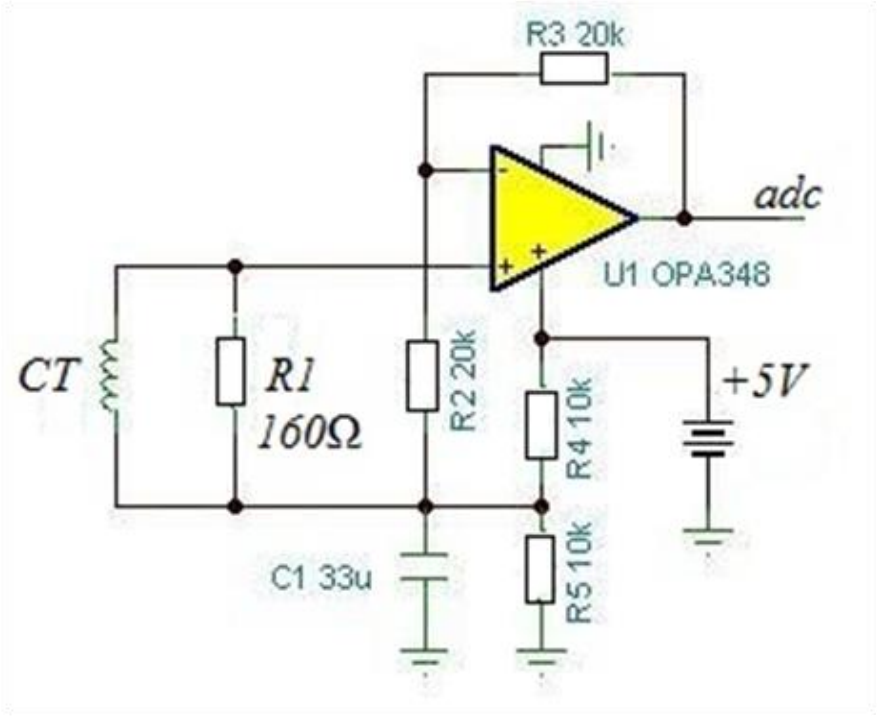

Fig. 5.30: Current transformer amplifier
(https://e2e.ti.com/support/amplifiers/precision_amplifiers/f/14/t/108187)

5.3 OUTPUT CIRCUITS

5.3.1 Standard output devices

For the audio alarms, status LEDs, solenoid close valve driver and LCD display, standard output interfacing circuits have been used. The following is the connection breakdown:

(1) An LED with a current limiting resistor in series is directly driven by one of the microcontroller output ports.

(2) A Piezo buzzer also driven directly at resonance by one the microcontroller output ports.

(3) A solenoid coil in parallel with a freewheeling diode connected to the collector of a transistor driven by one of the microcontroller output ports as shown in Appendix G.

(4) A 16x2 LCD display directly connected to six microcontroller output ports.

5.3.2 Pulse width modulation

The varying duty cycle which is the result of the charging/discharging fuzzy logic algorithm is used to control the output through the charge controller. The charge controller used in this study is the buck type. The design method and circuit diagram (Appendix G) for this charge controller is as detailed by Ejury (2013) and by Rashid (2003).

5.4 BASELINE MEASUREMENTS

Baseline measurements are those measurements made with the sensor circuits as standalone and not connected to the embedded system (offline measurements). These measurements assist in sensor calibration or in developing equations to be incorporated into the software development process prior to the simulations.

5.4.1 Titration baseline measurements

In addition to providing alkalinity value, titrations also allow for the calculation of volatile fatty acids (VFA) as a periodical offline compliment to access the stability of the digester in biogas generation. This includes the evaluation of the ratio of VFAs to Alkalinity given in equation *(39)* to complement the on line stability measurements. Using the titration procedure above *(See page 77)*, a sample of the results are shown in Table 5.4. At the same time, when the value of alkalinity was being calculated from titration, the other measurements of pH, redox and electrical conductivity where also done. The measurement results in this section are distributed over a number of days.

Table 5.4: Field titration results

Slurry pH	sv[ml]	h1[ml]	h2[ml]	h3[ml]	d1[ml]	d2[ml]	Alkalinity [mg/L bicarbonate]	VFAs [mg/L acetic acid equivalents]
6.9	20	4.5	0.8	0.13	5.3	0.93	2148.01845	518.211

$$\frac{A\left[\frac{mg}{l}\right]}{TIC\left[\frac{mg}{l}\right]} = \frac{VFA\left[\frac{mg}{l}\right]}{Alkalinity\left[\frac{mg}{l}\right]} \qquad (39)$$

Where A= Acids
TIC= Total Inorganic Carbon
VFA and Alkalinity are defined as before.

According to Lohri (2008), *'Alkalinity [mmol/l] needs to be converted to TIC [mg/l CaCO3] by multiplying it with half the molecular weight of CaCO3 (100.084/2=50.042), as each molecule of CaCO3 can take up* $2H^{+}(CaCO_3 + H_2O \rightarrow Ca^{2+} + HCO_3^{-} + OH^{-})$ '.

The soft sensor equation from measurement shows the accuracy of the initially formulated equation given by equation *(4).*

5.5 CONCLUSION

From chapter 5, all the sensors in this study were successfully specified and the amplifier sensor circuits **identified or designed** and fabricated. The circuits where tested, calibrated and found to be operational as required. Titration of the filtered digester sample was done on site to find the value of buffering capacity (alkalinity) and the volatile fatty acids (VFAs). The prediction equation to obtain alkalinity was firmly established for use in the digester stability routine source coding and the interpretation of the results of alkalinity and VFAs measurements at the end of this chapter is given in chapter 8. The output devices in this study were also successfully specified and all respective circuits **identified or designed**. The printed circuit boards of the output circuits were also fabricated, however they are not shown in this write-up. Finally the keypad and LCD are identified for interaction between the user and the controller.

CHAPTER 6

SOFTWARE DEVELOPMENT AND SIMULATION

6.1 INTRODUCTION

In this chapter, detailed software coding in C source codes is proposed to execute the fuzzy logic algorithms and module flowcharts. Simulation of the written programs that will be 'burnt' into the PIC18F4550 microcontroller is performed using both microchip's MPLABXIDE and Labcenter's Proteus software packages. Section 6.2 details the general procedure of calculating the degree of membership of the commonly used membership functions adopted in this study. Digester system stability test software coding development and simulation is done in section 6.3, while the development of the software code and simulation of the biogas output amount is performed in section 6.4. Section 6.5 details the biogas fault detection software development and simulation process. Software coding and simulation of the battery charging/discharging and solar system fault detection and status modules are detailed in section 6.6 and section 6.7 respectively, while section 6.8 covers the conclusion of this chapter.

6.2 UNIVERSAL DEGREE OF MEMBERSHIP CALCULATION METHOD

The common trapezoidal membership function shown in Fig. 6.1 (i) , can be reduced or modified either to a triangular function Fig. 6.1 (ii), a monotonically decreasing linear- function Fig. 6.1 (iii), or monotonically increasing linear- function Fig. 6.1 (iv) *(See page 18)* by appropriate shifting of the positions of b and c on the diagram.

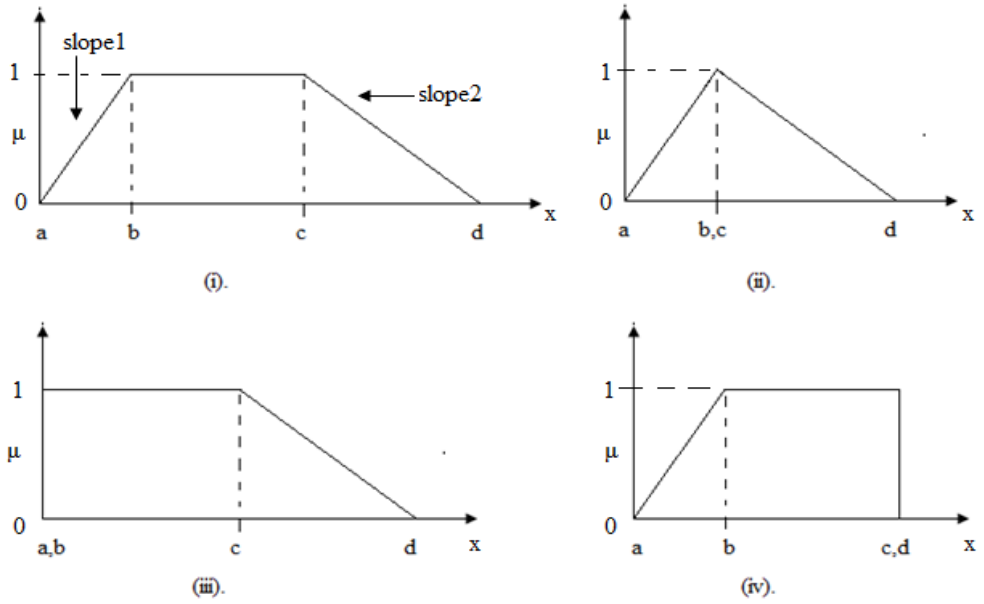

Fig. 6.1: (i).Trapezoidal function,(ii). Triangular function,(iii). Monotonically decreasing function and (iv). Monotonically increasing function

It is required to find the actual degree of membership for any value of input. This is done by establishing the slopes and lower/upper limits to be incorporated into the software development process for the particular membership function (Viot, 1993). In the Fig. 6.1, the lower limit is given by a, whilst the upper limit in given by d.

Universal degree of membership of the above membership functions subroutines whose expressions are given below are then easily developed (Nhivekar et al., 2011).

$$\mu(x) = \begin{cases} 0 & a > x \geq d \\ 1 & a \leq x \leq c \\ \frac{d-x}{d-c} & c < x < d \end{cases} \quad (40)$$

for monotonically decreasing linear-function membership function,

$$\mu(x) = \begin{cases} 0 & a \geq x \geq d \\ \frac{x-a}{b-a} & a < x \leq b \\ \frac{d-x}{d-c} & c < x < d \end{cases} \quad (41)$$

For triangular membership function, and

$$\mu(x) = \begin{cases} 0 & a \geq x > d \\ 1 & b \leq x \leq d \\ \frac{x-a}{b-a} & a < x < b \end{cases} \quad (42)$$

for monotonically increasing linear-function.

In the special case (which I have adopted in my project for simplicity of calculation) points 2 will directly be above points 1 as shown in Fig. 6.2. Discrimination between these special case, though not symmetrical membership functions is achieved by selecting the calculation of degree of membership (μ) between say points 1 and 2 for C as shown below (Vuong et al., 2006). The respective degree of membership for B between point 1 and point 2 as defined for C is then given as (1-μ).

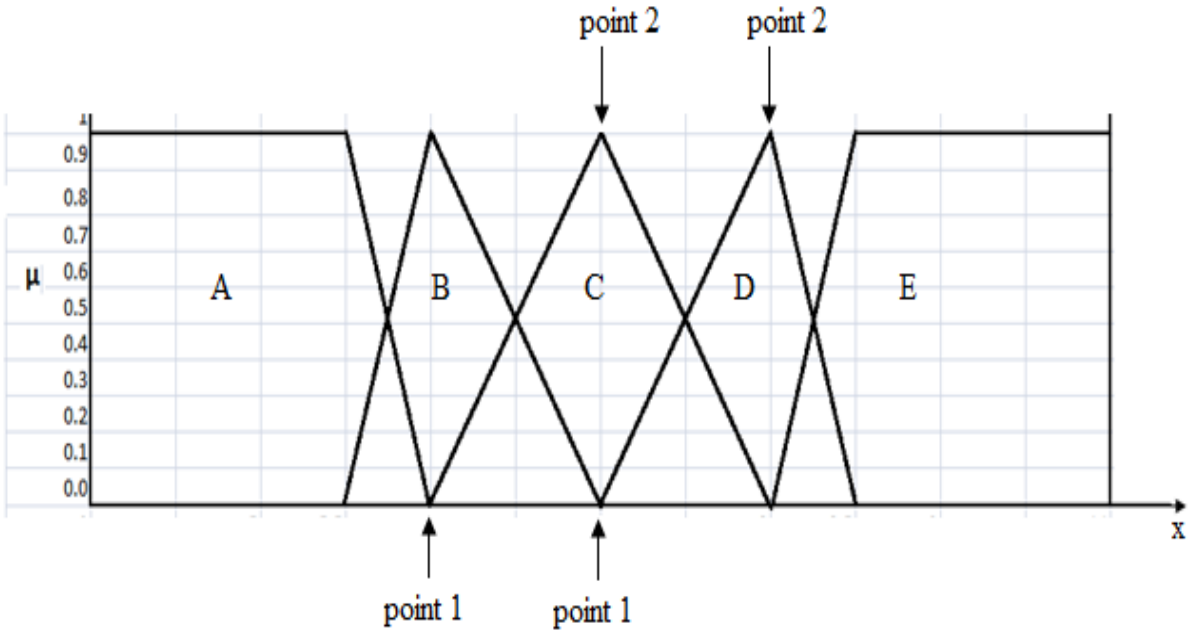

Fig. 6.2: Discrimination between overlapping membership functions

6.3 DIGESTER SYSTEM IMBALANCE EARLY WARNING SOFTWARE CODING AND SIMULATION

6.3.1 Stability routine software

The routine shown as **Listing one,** in Appendix E1, successfully calculates the degree of membership for both pH and Alkalinity membership functions for any given input and outputs these values onto a "2x4" $Array$ for latter retrieval (this is a dynamic system). The listing also shows the inference process that includes calculation of the firing strength of each rule by use of the data stored in the "$2x4$" $Array$ and simultaneous reference to the rule matrix for digester operation given in Table 6.1. The rule matrix is dynamically mapped onto a "$5x3$" $Array$ (digesterop[5][3] as shown in the listing.

The routine also calculates the output combination of the rules, defuzzification using the centre of gravity (COG) method, activates alarms and finds out whether the cause for poor digester stability is due to too low a pH value,too high a pH value or too low a buffering capacity.

Table 6.1: Structure of the "$2x4$" $Array$ used for pH and alkalinity degree of membership values

Q.acid degree of membership value *Array position [0][0]*
M.acid degree of membership value *Array position [0][1]*
Nuetral degree of membership value *Array position [0][2]*
M.alkaline degree of membership value *Array position [0][3]*
Q.alkaline degree of membership value *Array position [1][0]*
Low degree of membership value *Array position [1][1]*
Medium degree of membership value *Array position [1][2]*
High degree of membership value *Array position [1][3]*

6.3.2 Stability simulation results

Fig. 6.3 gives a representation of the analogue inputs of pH, redox and conductivity from the sensor circuits. The potentiometers given in the diagram vary the voltage from 0 to +5V in exactly the same way as the input sensor circuits would. The +2V shown, say for the potentiometer labeled pH corresponds to a pH value of 8, as read from the diagram in Fig. 5.6 *(See page 69)*. This is exactly the pH value given in Fig. 6.5.

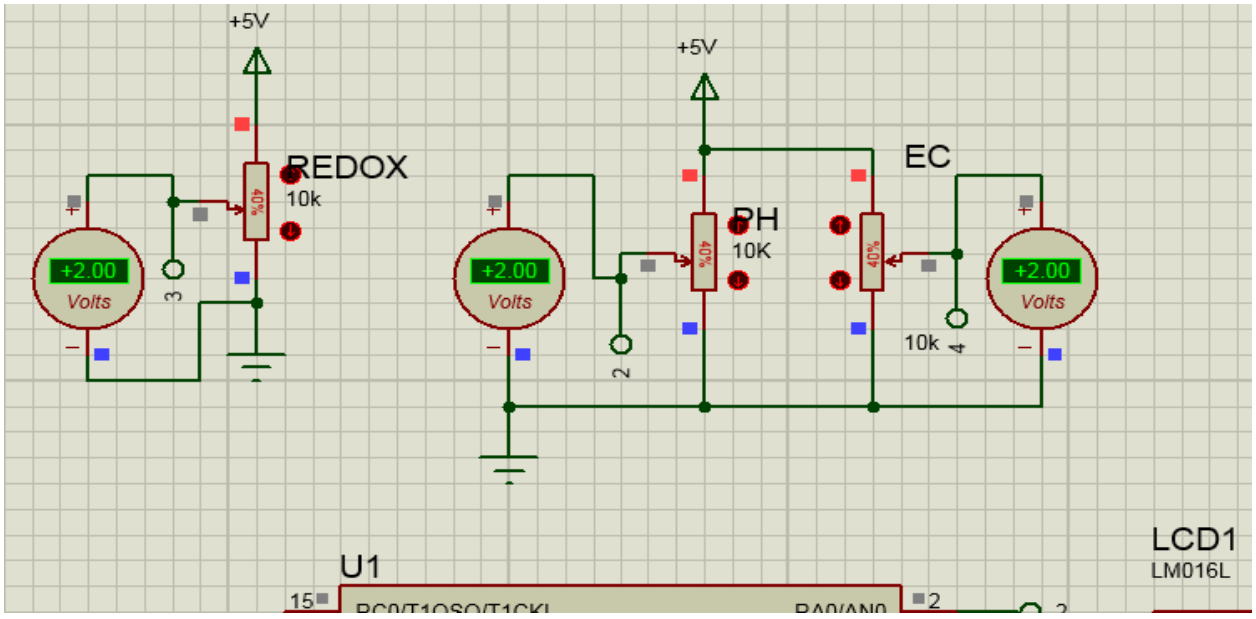

Fig. 6.3: pH, redox and electrical conductivity analogue voltage inputs

A sample reading of the percentage digester stability value reading is shown in Fig. 6.4. This value, including the values of pH and buffering capacity values given in Fig. 6.5 will momentarily appear on the LCD for the user, before the diagnostic information shown in Fig. 6.6 is given.

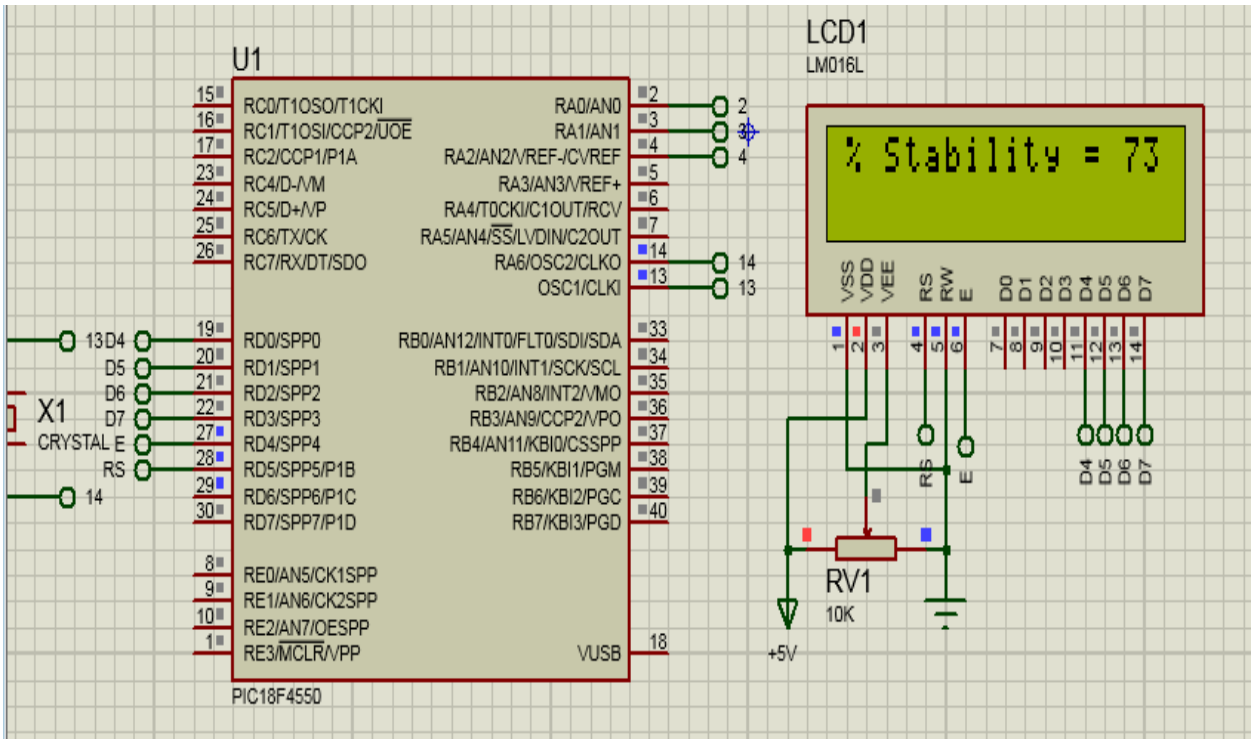

Fig. 6.4: Percent digester stability output on LCD

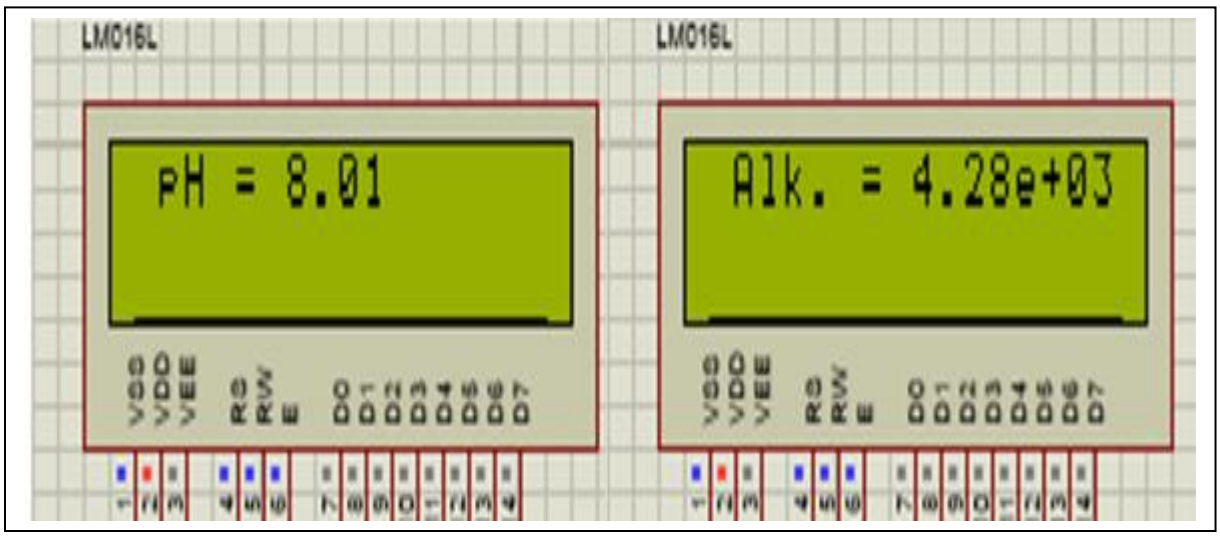

Fig. 6.5: Typical pH and alkalinity values from analogue inputs

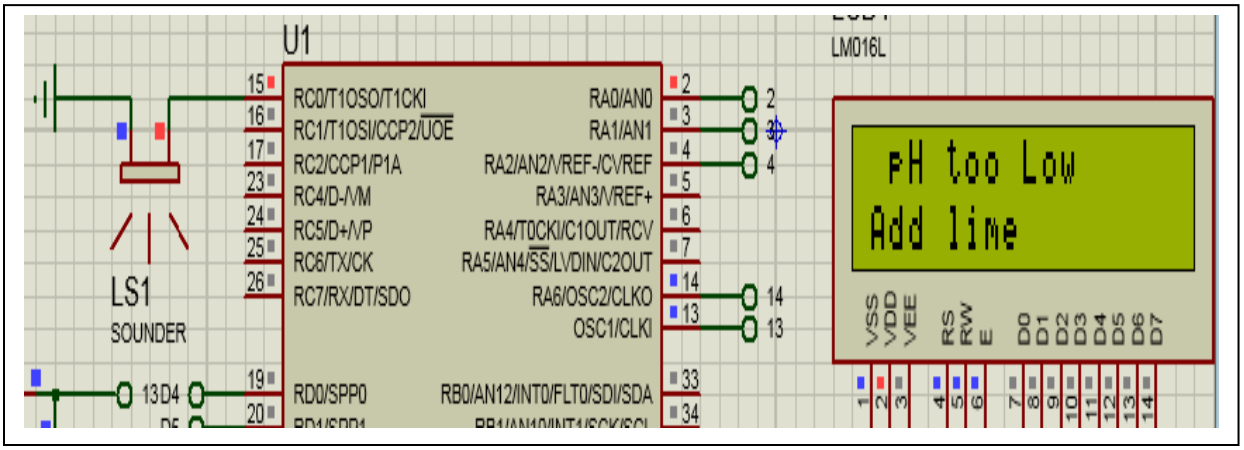

Fig. 6.6: Poor digester stability alarm sounder

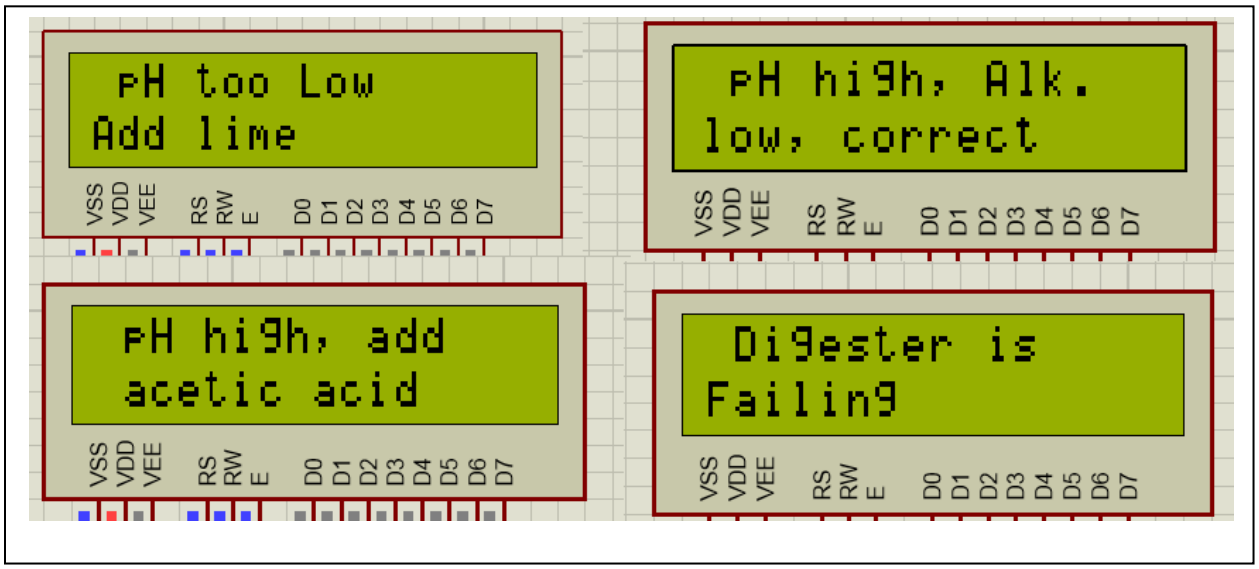

Fig. 6.7: Information on LCD about digester stability status

In the digester stability routine, the alarm takes the form of an audio sounder shown connected to the microcontroller in Fig. 6.6. These simulations provide successful activation of the digester failed alarm system. With respect to Fig. 6.7, the information given here is very important as in tells the user directly what the problem is, and what action he/she should take to address the problem at hand. From Table 6.2, the percentage stability status for various values of pH and alkalinity are observed. The defuzzified digester operation status is shown as a percentage for a specific pair of inputs of pH and alkalinity. From the output membership functions of Figure 2.8 *(See page 24)*, it is then established that any defuzzified output above 60 % is stable, between 40 % and 60 % is failing whilst that below 40 % is not stable.

As given by the MPLABXIDE clean and build option, the PIC18F4550 program memory used is 58.2 % and data memory used is 17.0% used by this routine which is part of **Listing one**.

Table 6.2: Digester stability output for the two inputs of pH and Alkalinity

Input 1 (pH)	Input 2 (Alkalinity in mg/L bicarbonate)					
	3499	3600	3800	4200	4400	4600
4.9	25%	25%	25%	25%	25%	25%
5.59	29%	49.1%	39.4%	37.4%	35.3%	35%
5.75	35%	50%	50%	50%	50%	50%
5.8	37%	50%	53.5%	54.5%	54.5%	54.5%
6	50%	58.3%	66.8%	75%	75%	75%
6.1	50%	58.3%	66.8%	75%	75%	75%
6.3	50%	58.6%	66.8%	75%	75%	75%
6.75	50%	58.5%	62%	75%	75%	75%
6.8	50%	58.3%	60.7%	75%	75%	75%
7	50%	58.3%	66.8%	75%	75%	75%
7.3	50%	58.6%	66.8%	75%	75%	75%
7.6	50%	60.7%	64.7%	75%	75%	75%
7.8	50%	64.3%	64.3%	75%	75%	755%
8.2	36.9%	50%	53.5%	50%	54.5%	54.5%
8.4	29.4%	50%	40.3%	42.1%	36.1%	36.1%
8.7	25%	25%	25%	25%	25%	25%

6.4 BIOGAS OUTPUT AMOUNT SOFTWARE CODING AND SIMULATION

6.4.1 Biogas amount routine software

The routine that is part of **Listing one** in Appendix E1, successfully measures digester temperature and calculates the OLR, HRT and the expected biogas quantity in litres. It also gives the actual quantities of methane and carbon dioxide in litres present in the biogas.

6.4.2 Biogas amount simulation results

The simulation results for this module are given in Figs. 6.8 & 6.9. The user of the digester reads real time temperature, hydraulic retention time, the organic loading rate and the actual amounts of methane and carbon dioxide produced.

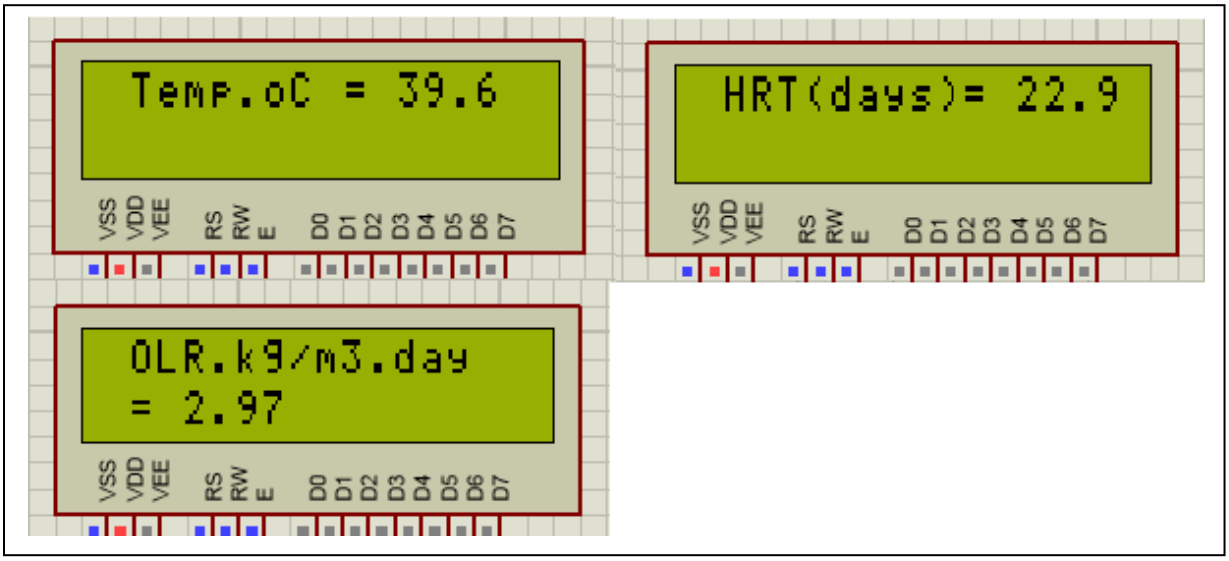

Fig. 6.8: Temperature, hydraulic retention time (HRT) and organic loading rate (OLR), LCD readings

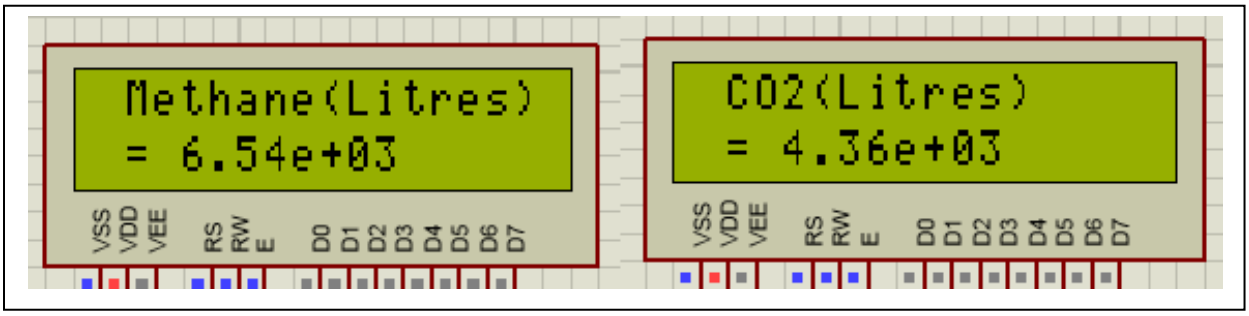

Fig. 6.9: Methane and carbon dioxide (CO2) outputs in thousands of litres

If the measured concentrations in parts per million (ppm) are less or greater for methane and carbon dioxide respectively than the recommended values , the measurement and control system advices the user to increase the organic loading rate and to extend the hydraulic retention time, provided the temperature is good or to take no action. The methane sensor module is calibrated using butane (cigarette lighter) and liquid petroleum (LPG) gases (Zlochower & Green, 2016).

From the MQ2 methane sensor datasheet *(See page 82)*, sensing resistance (Rs) varies from 2 KΩ (10000 ppm methane) to 20 KΩ (200 ppm methane). The equation relating Rs to load resistance (RL)[26], voltage across load or analogue output volatage (VRL) and supply voltage (Vc) is given as:

[26] Load resistance is adjustable through the potentiometer on the sensor module.

$$Rs = RL * \frac{(Vc - VRL)}{VRL}. , \quad (43)$$

Where the ratio value of $\frac{Rs}{RL}$ is used in the software coding.

From Fig. 5.20 *(See page 83),* with respect to the methane gas (CH4), corresponding values of ppm for different ratio values of Rs/Ro are obtained and shown in Table 6.3.

Table 6.3: Methane gas PPM readings[27] with respect to ratio Rs/Ro for the MQ2 sensor

PPM	**Rs/Ro**
200	3
500	2.25
800	2
1000	1.85
2000	1.6
3000	1.5
5000	1.1
10000	0.7

To obtain a linear equation for ppm calculation the natural logarithms of the values in Table 6.3 are used instead. These are tabulated in Table 6.4, and plotted as in Fig. 6.10. The resultant equation[28] is used in the software development process for ppm calculation. Fig. 6.11 shows typical ppm reading on the LCD.

Table 6.4: Natural logarithm methane gas PPM readings with respect to ratio Rs/Ro for the MQ2 sensor

lnPPM	**lnRs/Ro**
5.298317	1.098612
6.214608	0.81093
6.684612	0.693147
6.907755	0.615186
7.600902	0.470004
8.006368	0.405465
8.517193	0.09531
9.21034	-0.35667

[27] These values when plotted will result in an exponential equation for ppm calculation.
[28] It is necessary to convert the natural logarithms to common logarithms in the software process.

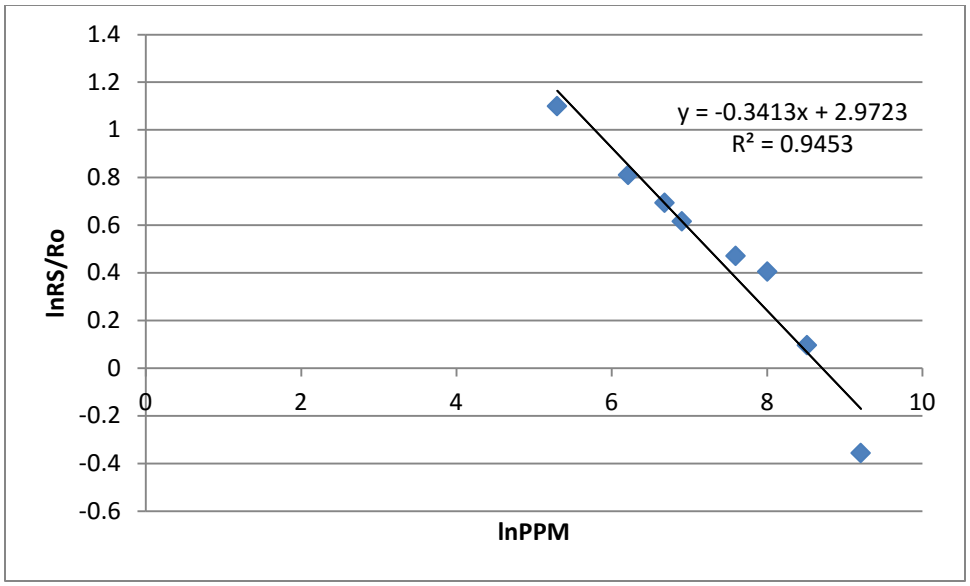

Fig. 6.10: Ratio lnRs/Ro against methane concentration in lnPPM

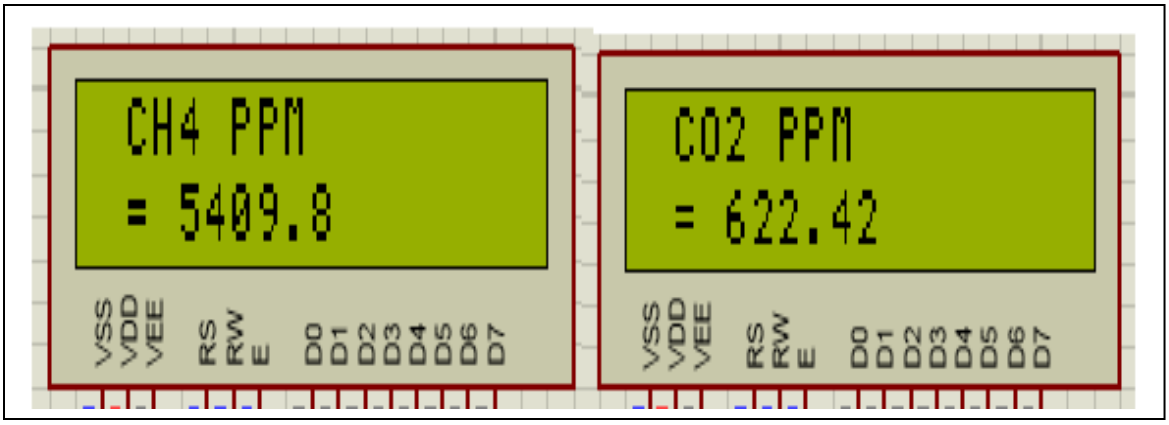

Fig. 6.11: Typical methane and carbon dioxide concentrations in ppm readings on LCD

In the same fashion as for the methane sensor, the ppm values for carbon dioxide are obtained by developing the software equation from the data in Fig. 5.22 *(See page 83).* The sensitivity of the carbon dioxide sensor module is adjusted for maximum sensitivity. Table 6.5, shows the electromotive force (EMF) values in millivolts (mV) for various common logarithm concentration values of carbon monoxide for the MG811 sensor module. The output voltage of the sensor falls as the concentration of carbon dioxide increases.

Table 6.5: Tabulated EMF values for the MG811 sensor against common logarithm carbon dioxide concentration in parts per million

EMF (mV)	PPM	Log_{10} PPM
324	400	2.60206
314	600	2.778151
308	800	2.90309
303	1000	3
298	1500	3.176091
293	2000	3.30103
290	2500	3.39794
286	3000	3.477121
281	4000	3.60206
275	6000	3.778151
269	8000	3.90309
265	10000	4

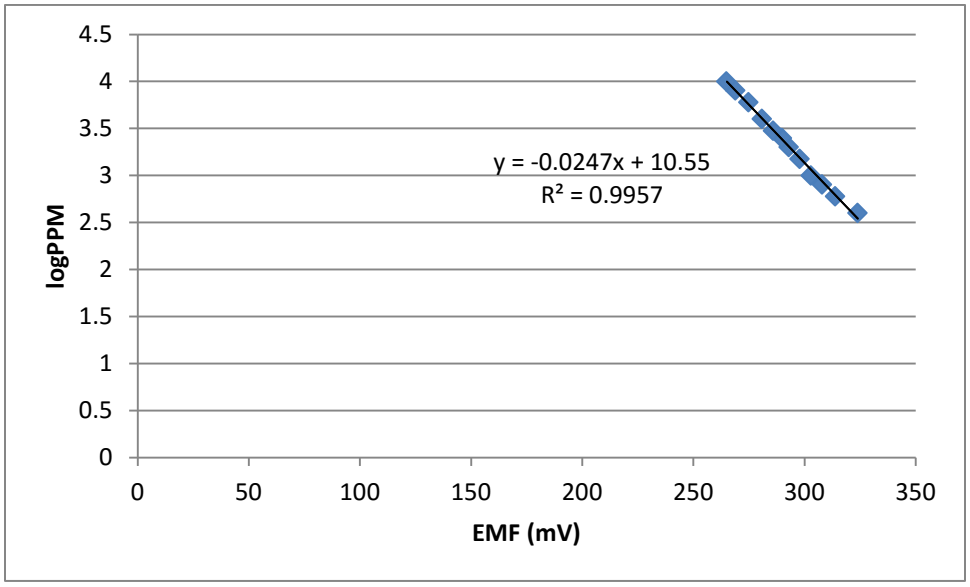

Fig. 6.12: Carbon dioxide concentration in logPPM against sensor EMF voltage

From Fig. 6.12, the equation used in the calculation[29] of the ppm for carbon dioxide is given by:

$$logPPM = -0.0247 * EMF(mV) + 10.55. \qquad (44)$$

[29] The anti-log of equation *(44)* gives the value of the ppm for carbon dioxide gas.

6.5 BIOGAS SYSTEM FAULT DETECTION AND STATUS SOFTWARE CODING AND SIMULATION

6.5.1 Biogas system fault detection and status routine software

The routine that is part of **Listing one** in Appendix E1, successfully performs biogas fault detection and informs about the safety status of the digester.

6.5.2 Biogas system fault detection and status simulation results

A methane leak (greater than 1000 ppm) in the room activates a leak alarm and switches on a yellow LED, while oxygen ingress (greater than 15%) into the digester is represented by a green LED coming on and activation of the same alarm which is common to both situations. Furthermore, in both cases of methane leak and oxygen ingress, an emergency solenoid valve is successfully activated to cut off the main line supplying the user until the problem is rectified[30]. The simulation also successfully monitors the biogas pressure and slurry level in the digester.
An additional float switch (SW12) to those in Fig. 5.26 *(See page 86*), is placed between SW1 and SW2 where:

1) SW1 is placed at P-line (will activate exactly at 0.13m above P-Line).
2) SW12 is placed between P-line and Zero-line (will activate at 0.25m above P-line).
3) SW2 is placed at Zero-line (will activate at 0.45m above P-line, just below Zero-line).
4) SW1 (OFF) - slurry too low (activate alarm).
5) SW1 (ON) – minimum slurry level (alarm off).
6) SW1 (ON) & SW12 (OFF) - take displacement as 0.13m (LL).
7) SW12 (ON) – take displacement as 0.25m (BPO).
8) SW2 (ON) – take displacement as 0.45m (HL).

It is important to note that, to obtain a finely tuned level measurement system for a large number of varying slurry displacement levels, a moving gauge needs to be used instead. This gauge will produce varying analogue voltages calibrated to give displacement values (not implemented in this study).
The equation from Fig. 5.25 *(See page 86),* gives the value of the pressure of the biogas in KPa, while the equation in Fig. 6.13, is used in the software coding to find the concentration of oxygen in the digester.

[30] When solenoid valve closes the program waits until reset button is pressed (MCLR pin 1 on PIC18F4550)

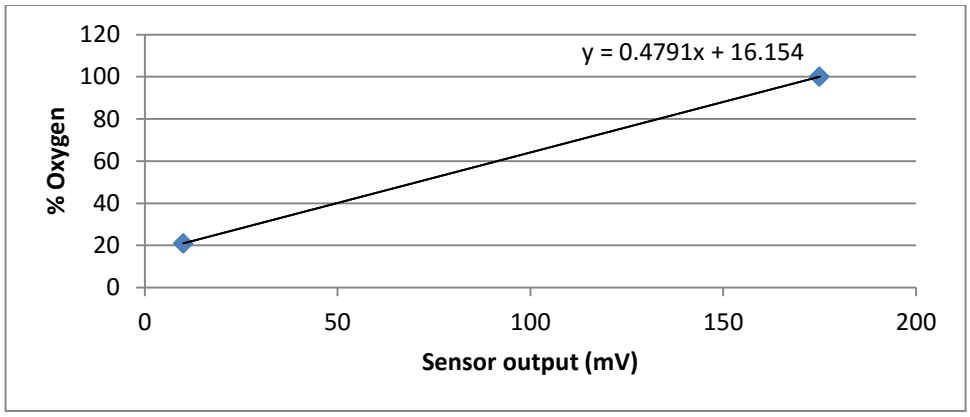

Fig. 6.13: Oxygen concentration as percentage against sensor output voltage

Fig. 6.14, shows a typical LCD output of the digester danger level as a percentage. The higher the percentage, the more compromised is the operation of the digester.

Fig. 6.14: Digester danger level LCD reading

6.6 SOALAR BATTERY CHARGING/DISCHARGING SOFTWARE CODING AND SIMULATION

6.6.1 Solar battery charging/discharging routine software

The routine given as **Listing two** in Appendix E2, successfully calculates the duty cycle that drives the buck charge controller. The duty cycle is based on the charging voltage, charging current and SOC of the battery.

The charging voltage is obtained from direct measurement as shown in Fig. 5.28 *(See page 89)*. The standard resistor values of R1 and R2 give a charging voltage of:

$$Vcharging = (Vadc * (11\ K\Omega + 47\ k\Omega)/11\ K\Omega\ , \qquad (45)$$

which this simplifies to $Vcharging = 5.27\, Vadc$.

With respect to charging current measurement, taking equation *(35)* and considering Fig. 5.29 *(See page 89)*, the voltage drop across the series resistor (0.05 Ω 2 W) is given by:

$$\frac{5}{Vdrop} = \frac{Rf}{Rin}. \qquad (46)$$

From equation *(46)*, the expression of the voltage drop simplifies to $Vdrop = Vadc/20$, and consequently the charging current is given by:

$$Icharging = \frac{Vdrop}{0.05} A \qquad (47)$$

The expressions of the charging voltage, charging current and SOC are used in the fuzzy logic controller software coding for battery charging/discharging.

6.6.2 Solar batter charging/discharging simulation results

The routine written for battery charging was successfully simulated. The routine sensed the charging voltage and charging current, adjusting the duty cycle accordingly in the process to obtain optimum battery charging. Fig. 6.15, shows typical values of duty cycle, charging voltage, charging current and battery's state of charge.

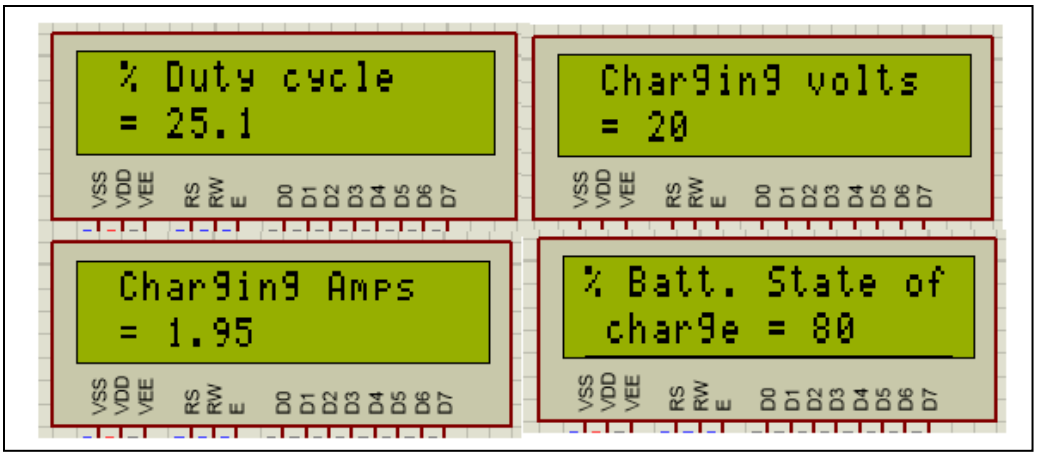

Fig. 6.15: Typical values of duty cycle, charging voltage, charging current and battery's state of charge

6.7 SOLAR SYSTEM FAULT DETECTION AND STATUS SOFTWARE CODING AND SIMULATION

6.7.1 Solar system fault detection and status routine software

The routine that is part of **Listing two** in Appendix E2, successfully identifies any faulty piece of equipment that makes up the photovoltaic system and performs overload protection of the inverter system from the users where an alarm is activated if the current limit is breached. The software also successfully notifies about the status of the solar panel shading levels to include partial, prolonged or very high[31] shading levels

6.7.2 Solar system fault detection and status simulation results

Fig. 6.16 (a), shows typical solar panel shading level. A high percentage reading as shown in Fig. 6.16 (a), implies a high shading level. Using the information given in section 5.2.14 *(See page 90)*, the analogue current transformer (CT) voltage from the CT amplifier in the microcontroller was converted to provide the value of the alternating load current being drawn from the inverter. Fig. 6.16 (b), shows the status of the load current being drawn by the user as percentage (%) of the maximum allowable value. With respect to user load current, the routine also successfully activates a flashing LED when this percentage becomes high and eventually activates an alarm when the current being drawn becomes too high.

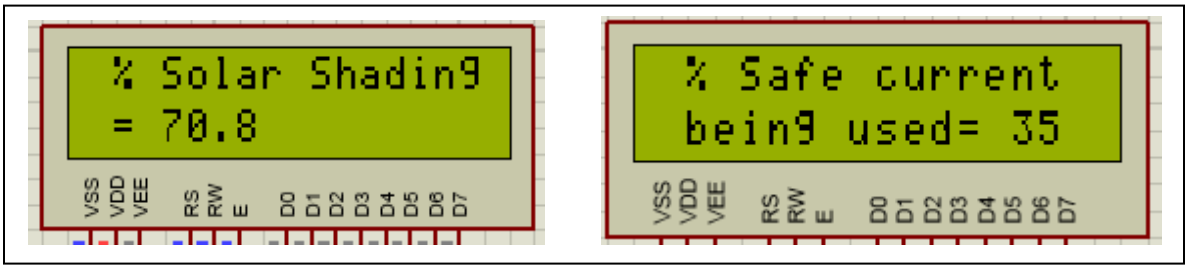

a. b.

Fig. 6.16: a) Shading level of solar panel, and b) load current as a percentage of allowed amperage

6.8 CONCLUSION

In chapter 6, all the software routines in this study were successfully coded in C source codes and all the simulations done. The simulations behaved as expected, however there was need to improve on the coding to make the programs smaller (consider coding in less memory occupying assemble language) so that they occupied less PIC18F4550 microcontroller memory. The PWM (duty cycle) output signal derived from the simulation software will be implemented in the CCP (compare capture pwm) registers and output through microcontroller pins RC1, RC2 or RB3 to switch on and off the charge controller. In Chapter 7, all the developed programs without further modification where uploaded ("burnt") into the microcontroller.

[31] These are shading levels higher than normal shadows in day light.

CHAPTER 7

EMBEDDED SYSTEM DESIGN

7.1 INTRODUCTION

In this chapter the complete hardware for the measurement and control system was realized. The hardware structure is dealt with in section 7.2, to include integrated circuit (i.c) pin designation and clock signal derivation. Section 7.3, details the procedure for programming PIC18F4550 microcontroller, while section 7.4 shows how the respective power supplies were obtained. Section 7.5, which is the conclusion, gives a description of how the different circuits of the embedded system were constructed.

7.2 HARDWARE STRUCTURE

7.2.1 Integrated circuit (i.c) pin designation

Fig. 7.1 shows the pin structures of the LM324N and TL082CP operational amplifiers (OP-AMP). From the analysis of these pin structures it is shown that one LM324N OP-AMP (LM 324, 2001) can accommodate up to four different inputs and the TL082CP (TL082CP, 2000) up to two different inputs. Specifically, the conductance amplifier used one complete LM324N OP-AMP, while one TL082CP was used for the pH and redox sensors.

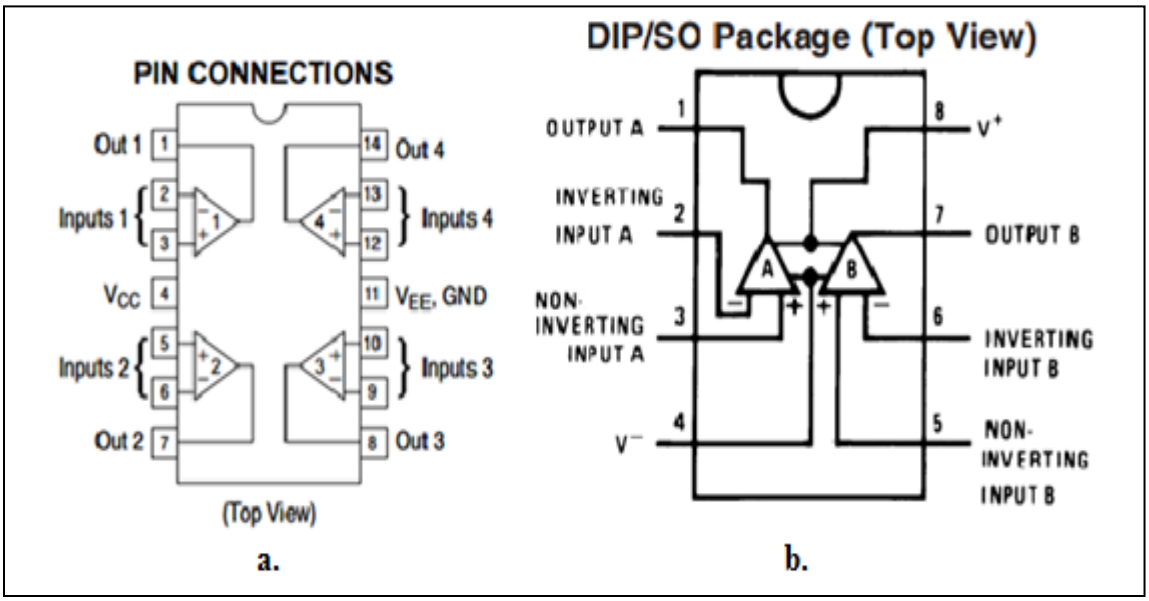

Fig. 7.1: Pin structures of the a) LM324N, and b) TL082CP operational amplifiers

The pressure, oxygen and photovoltaic current charging sensor amplifiers were accommodated in a second LM324N OP-AMP, while the temperature and CT sensors were incorporated in two TL061CP OP-AMPs whose pin structure is depicted in Fig. 7.2. The CT sensor used the TL061 OP AMP in single supply mode. The pin structure of the PIC18F4550 microcontroller which is

the heart of the embedded system is shown in Fig. 7.3. Table 7.1, shows how each pin on this microcontroller was used in this study.

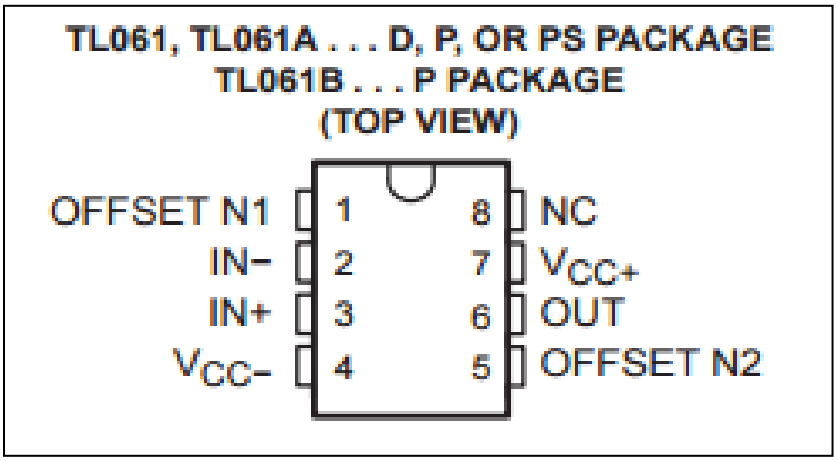

Fig. 7.2: Pin structure of the TL061CP operational amplifier
(http://datasheet.octopart.com/TL061CP-Texas-Instruments-datasheet-77091.pdf)

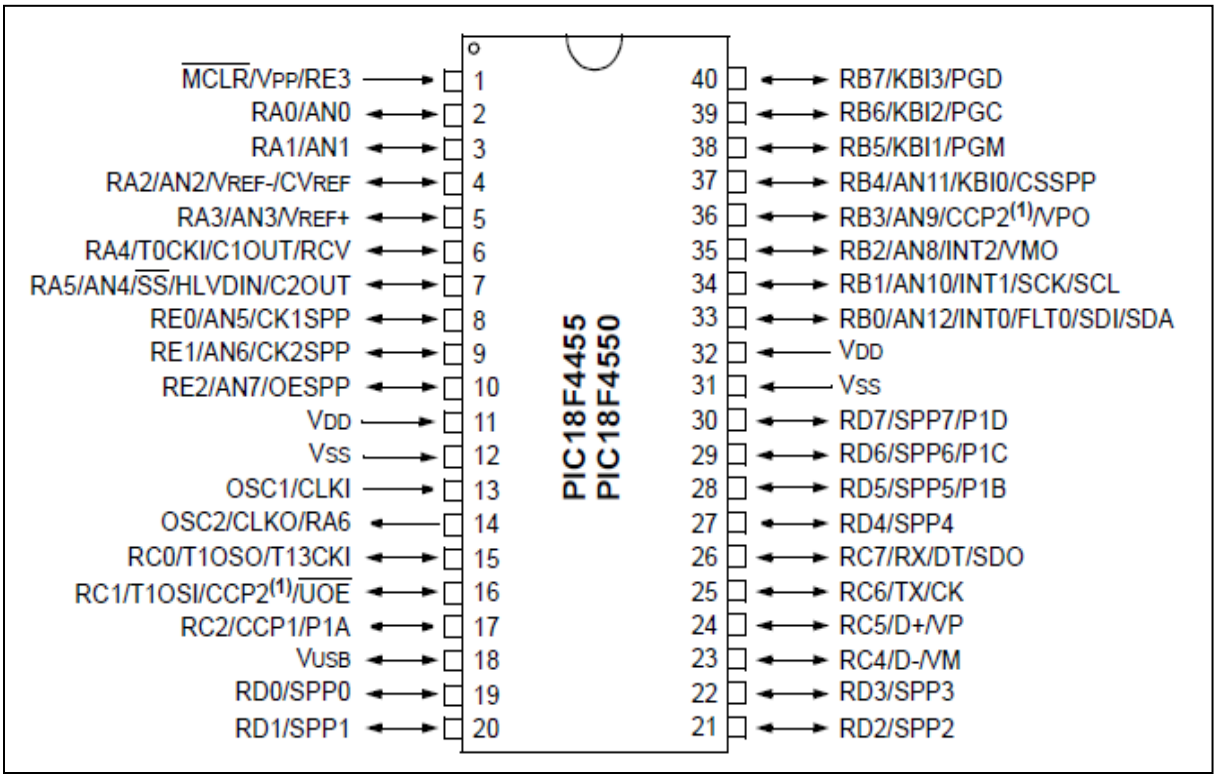

Fig. 7.3: Pin structure of the PIC18F4550 microcontroller
(http://ww1.microchip.com/downloads/en/devicedoc/39632c.pdf)

Table 7.1: Utilization of pins on the PIC18F4550 microcontroller

Pin number	Pin Designation & Type	Circuit/Device Name	Circuit/Device Type
1	MCLR/Vpp/RE3	Reset/ programming	Input
2	RA0/AN0	pH sensor	Input
3	RA1/AN1	Redox	Input
4	RA2/AN2	Electrical conductivity	Input
5	RA3/AN3	Temperature	Input
6	RA4	Flashing PV LED	Output
7	RA5/AN4	Methane inside digester	Input
8	RE0/AN5	Carbon dioxide	Input
9	RE1/AN6	Pressure	Input
10	RE2/AN7	LDR	Input
11	VDD	+5V	Supply
12	VSS	0V	Ground
13	OSC1/CLKI		
14	OSC2/CLK2/RA6		
15	RC0/T1OSO/T1CK1	Biogas and Solar systems shared alarm	Output
16	RC1	Level sensor low (SW1)	Input
17	RC2	PWM to solar regulator	Output
18	V_{USB}		
19	RD0/SPP0	LCD D4	Outpt
20	RD1/SPP1	LCD D5	Output
21	RD2/SPP2	LCD D6	Output
22	RD3/SPP3	LCD D7	Output
23	RC4		
24	RC5	Level sensor middle (SW12)	Input
25	RC6	Solenoid drive	Output
26	RC7	Level sensor high (SW2)	Input
27	RD4/SPP4	LCD E	Output
28	RD5/SPP5/PIB	LCD RS	Output
29	RD6	Green LED (CH_4 leak)	Output
30	RD7	Yellow LED (O_2 ingress)	Output
31	VSS	0V	Ground
32	VDD	+5V	Supply
33	RB0/AN12	CT amplifier voltage	Input
34	RB1/AN10	Charging current	Input
35	RB2/AN8	Methane leak in house	Input
36	RB3/AN9	Oxygen in digester	Input
37	RB4/AN11	Charging voltage	Input
38	RB5		
39	RB6/PGC	Pickit 3 programming	
40	RB7/PGD	Pickit 3 programming	

7.2.2 Clock signal

The PICF184550 microcontroller uses an external oscillator[32] comprising of a 20MHz crystal and two 22pF capacitors as shown in Fig. 7.4 connected to pin 13 (OSC1) and pin 14 (OSC2) of the microcontroller.

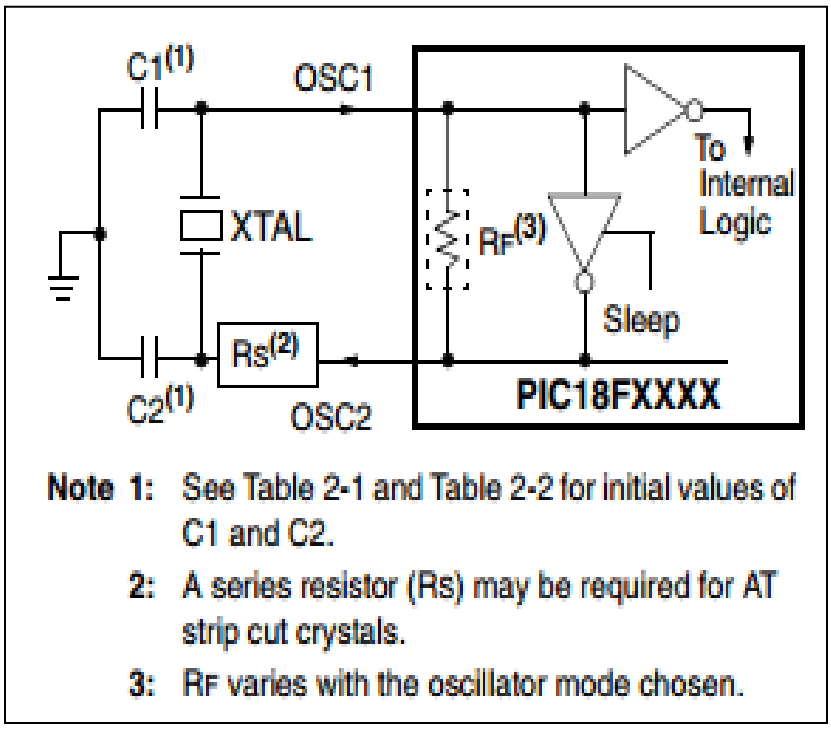

Fig. 7.4: PIC18F4550 external oscillator circuit
(http://ww1.microchip.com/downloads/en/devicedoc/39632c.pdf)

7.3 PIC18F4550 PROGRAMMING USING MPLABXIDE

The HEX file obtained from compilation of the overall routine in MPLABXIDE XC8 compiler was uploaded into the PIC18F4550 microcontroller through the use of the Pickit3 in-circuit debugger/programmer (PICkit™ 3, 2013). Fig. 7.5, shows how the pickit3 was connected to the microcontroller, while Fig. 7.6, shows a photograph of the pickit3 based PIC18F4550 programming setup. The pickit3 was connected between the personal computer and the microcontroller as shown.

[32] The oscillator setting in the header file is FOSC = HSPLL_HS // Oscillator Selection bits (HS oscillator, PLL enabled (HSPLL)) and #define _XTAL_FREQ 20000000

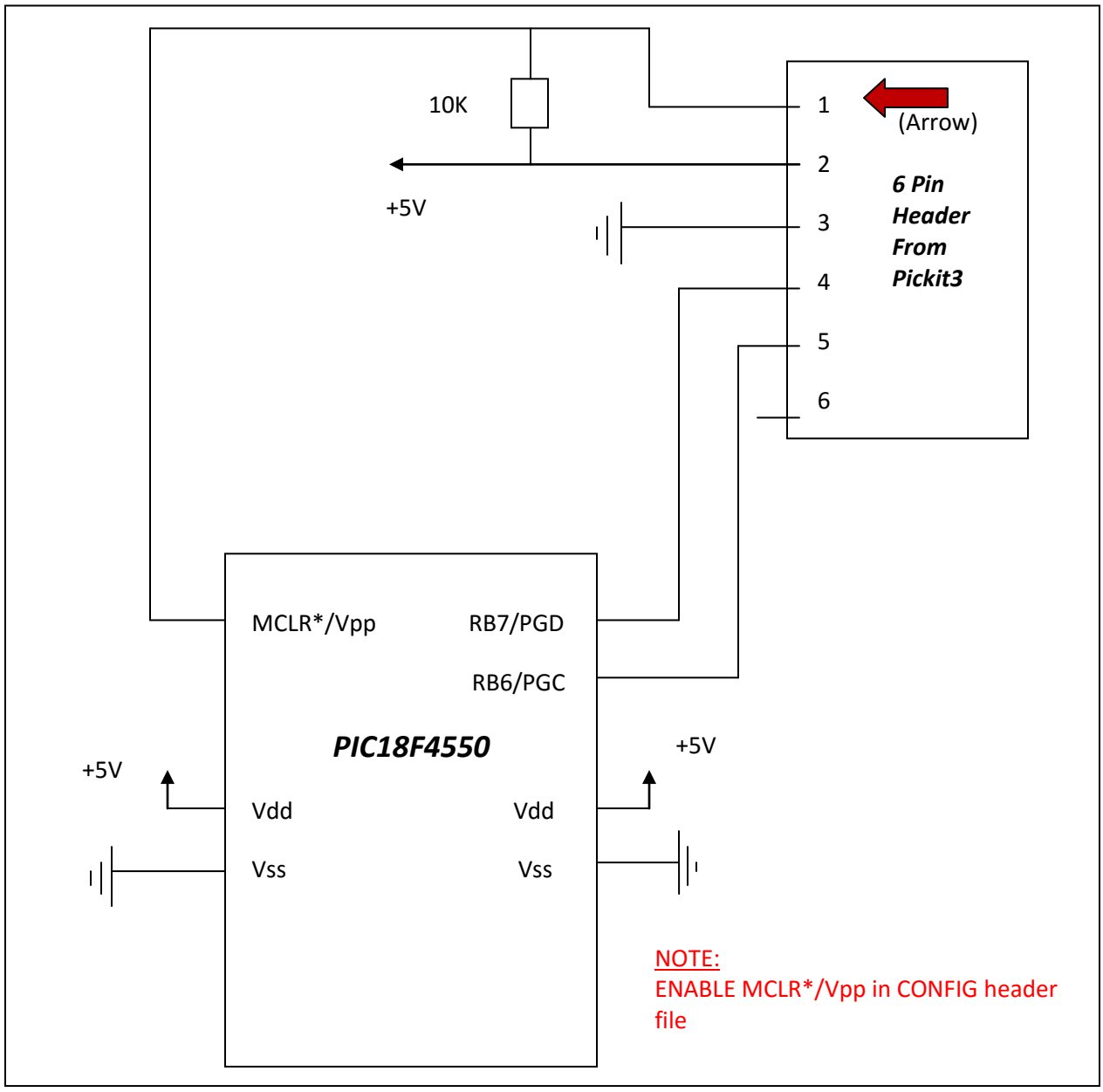

Fig. 7.5: Pickit3 programmer

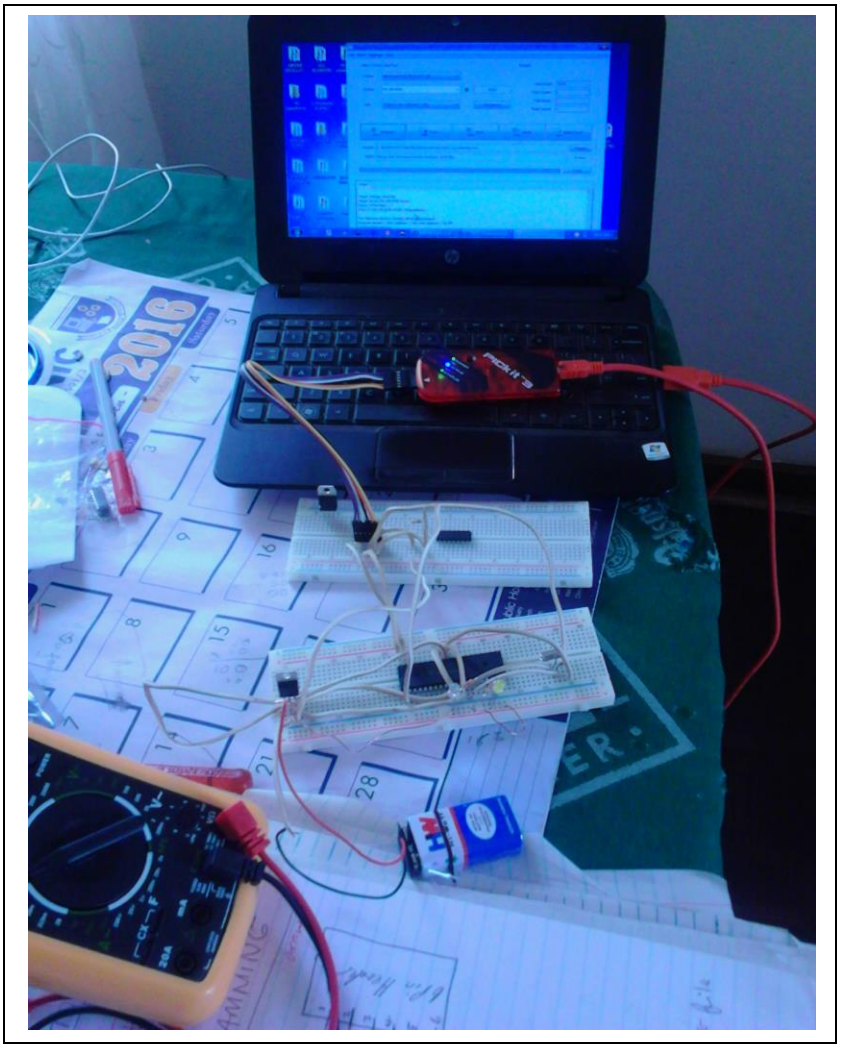

Fig. 7.6: Photograph of pickit3 programming

7.4 POWER SUPPLIES AND OVERALL EMBEDDED SYSTEM

The power supplies for the respective hardware modules were all derived from the solar battery bank. For the positive polarity levels, use was made of the LM78xx positive terminal voltage regulators whose xx value was selected based on the specifications of the device to be supplied. The negative polarity levels were obtained from the LM79xx negative terminal voltage regulators. The 24V dc supply for the pressure sensor was obtained from an LM7824 positive terminal voltage regulator supplied by the 24V solar battery bank. The methane and carbon dioxide sensors have heater elements that consume (drain) a large amount of heating power. However the power supply system was large enough to make this current drain insignificant. Basic equipment protection to excessive voltages and currents was based on module fuses, zener and power diodes.

7.5 CONCLUSION

The hardware was successfully designed and implemented. The sensor circuits, regulated power supply circuits, solenoid valve driver and buck regulator were constructed on printed circuit board[33], while the microcontroller and LCD connections was implemented on bread board due to the complexity of the printed circuit that would otherwise be required for the complete embedded system. Sample inputs and outputs connected to the PIC18F4550 microcontroller for the constructed embedded system designed for this study are given in Appendix I.

[33] The standard procedures for printed circuit board development where applied.

CHAPTER 8

RESEARCH FINDINGS

8.1 INTRODUCTION

This chapter gives a detailed presentation and analysis of the research findings of this study. The biogas field measurements were obtained from a REF digester of size 50 m^3 that used a combination of human and cow dung as feedstock. Due to ethical considerations the photovoltaic measurements were performed on a laboratory scale system with scaled down versions of the same specifications as that for the REF photovoltaic installations.

8.2 THREE MONTH PERIOD DIGESTER READINGS

Table 8.1, shows the readings over three months, of percent stability, methane quantity[34] in litres, carbon dioxide quantity in litres, methane ppm, carbon dioxide ppm and percent digester danger level. These are the derived outputs that provide information on the overall status of the digester and are indicated on the LCD. The pH, redox and electrical conductivity probes were submerged[35] into the digester slurry. The measurements were performed at around the same time in the afternoons where temperature was fairly constant. The organic loading rate was assumed to remain constant during the three month period under consideration.

Table 8.1: Three months digester status readings

Required output	**Date/ Period**						
	9/30/16	10/12/16	10/21/16	10/31/16	11/7/16	11/15/16	11/18/16
% Stability	67.9	67.1	67.4	66.1	70.1	50	58
Methane ($x10^3$ litres)	7.2	7.5	7.7	7.83	7.65	7.6	7.45
Methane (ppm)	3678	4501	4877	4999	3589	4770	4004
Carbon Dioxide ($x10^3$ litres)	3.7	3.75	3.89	3.9	3.86	3.85	3.82
Carbon Dioxide (ppm)	1200	1444	1905	2178	2033	1588	1334
% Digester danger level	25	25	27	25	33	26	25

[34] Quantities are based on the calculations from the actual measurements for an ORL of 2.975 Kg.VS/m^3.day which is the standard for this digester.

[35] The three probes were each secured by waterproof tape to the ends of long PVC electrical conduits and the probe cabling ran through the conduit to the outside control unit.

8.2.1 Graphs of digester outputs

In this section the graphs of all the outputs over a three month period as shown in Table 8.1 are given. The graph in Fig. 8.1, shows that the stability of the digester under observation is fairly constant over the three months in question. A dip in stability does occur on the sixth measurement and this was due to a massive increase in the amount of feedstock added prior to that and this upset the balance in the pH, redox and electrical conductivity. The stability started to rebound as seen after the seventh measurement.

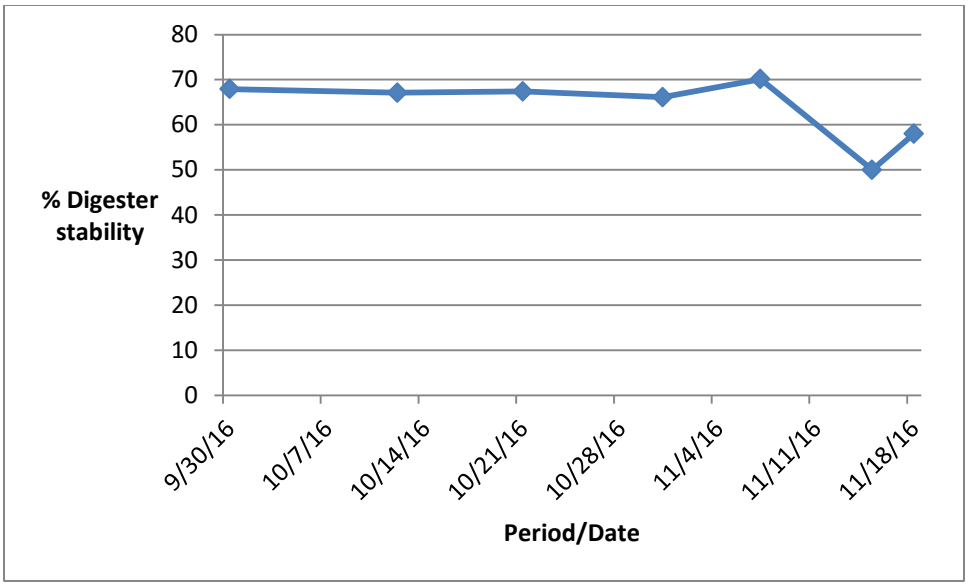

Fig. 8.1: Three month interval stability

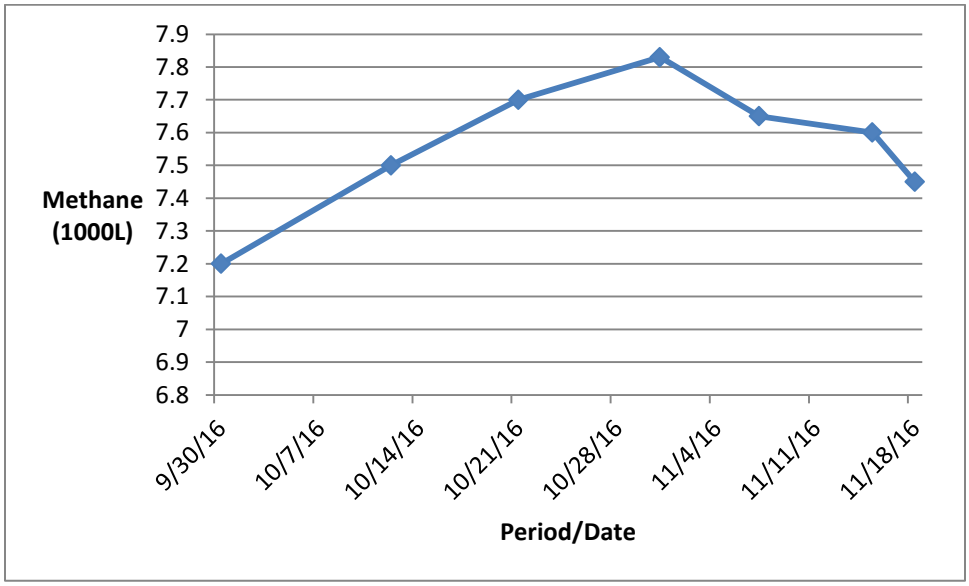

Fig. 8.2: Three months methane output

Fig. 8.2, shows how methane output is distributed over a three month period. The graph shows that biogas methane use peaked sometime towards the end of October 2016 with a dip on the sixth measurement. A dip in the methane level can be attributed to the instability issue at this point or increased user use. Fig. 8.3, gives the variation of methane concentration in the digester with time, giving an average concentration of about 4500 ppm.

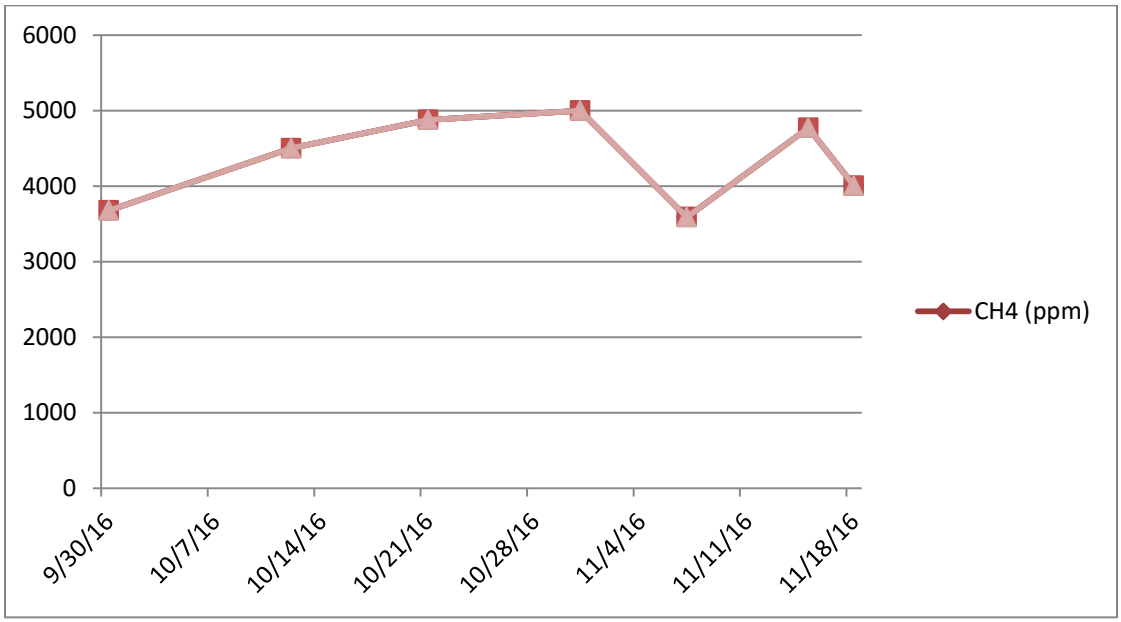

Fig. 8.3: Three months methane ppm concentration

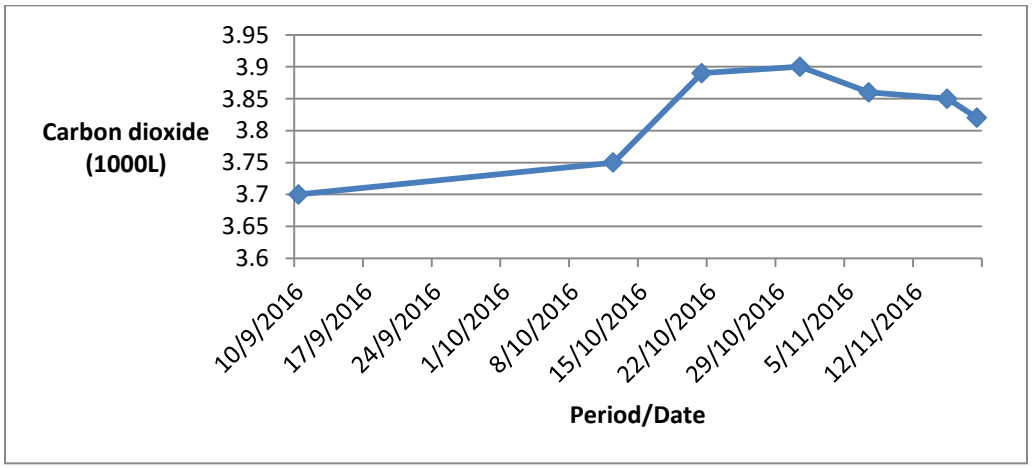

Fig. 8.4: Three months carbon dioxide output

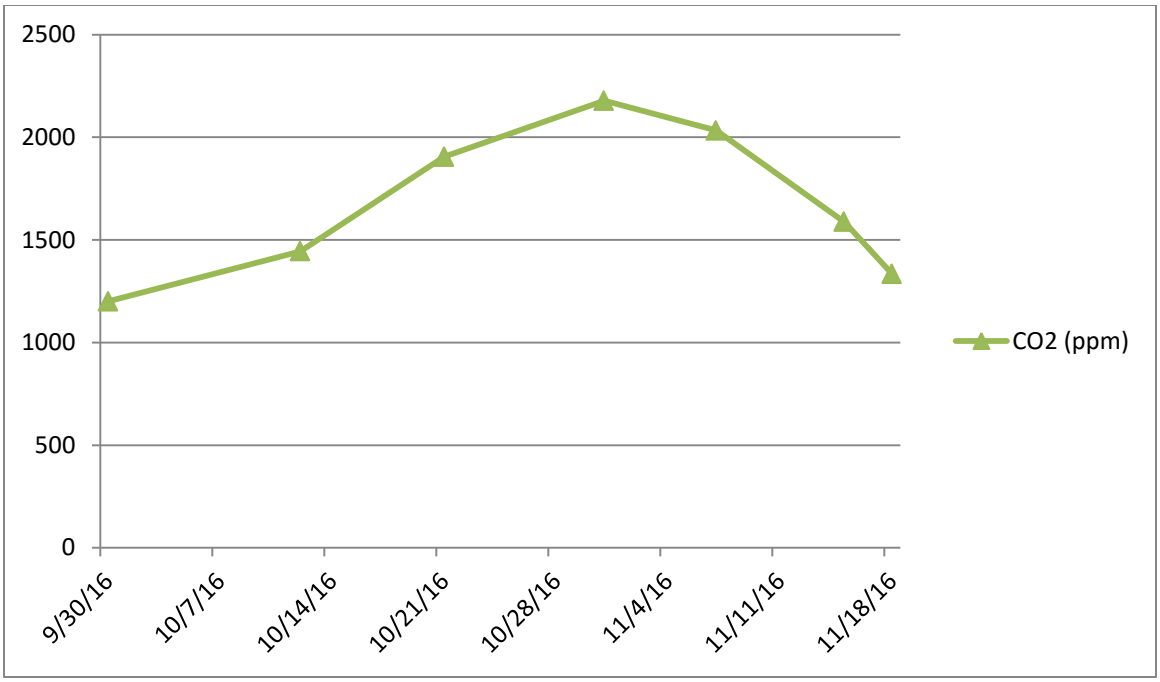

Fig. 8.5: Three months carbon dioxide ppm concentration

Figs. 8.4 & 8.5, give the variation of carbon dioxide in litres and ppm respectively. From the 10th of October 2016, an increase in the output of carbon dioxide is noted. This is to be expected since the amount of methane has also relatively increased, which implies an overall increase in the bulk biogas produced at this time. The concentration of carbon dioxide peaks between the 28th of October 2016 and the 4th of November 2016. It should be noted that the sensors for methane and carbon dioxide concentration were momentarily[36] exposed to the biogas just outside the digester through a conduit due to fear of explosion. From this observation, the concentration levels are only approximate, however, the readings do show the trend of concentrations involved with time.

Fig. 8.6 shows that the digester danger level due to abnormal pressures and slurry levels is very low during this period. Under normal[37] operating conditions, a dome type digester is self-regulating and will function with a relatively high level of safety as long as there is normal use of the output biogas as per design specification.

[36] These sensors contain heating elements, and a faulty sensor could cause serious accident. Industrial type sensors are recommended.

[37] These are operating conditions without gas blockages, leaks and continuous input and output flow of feedstock.

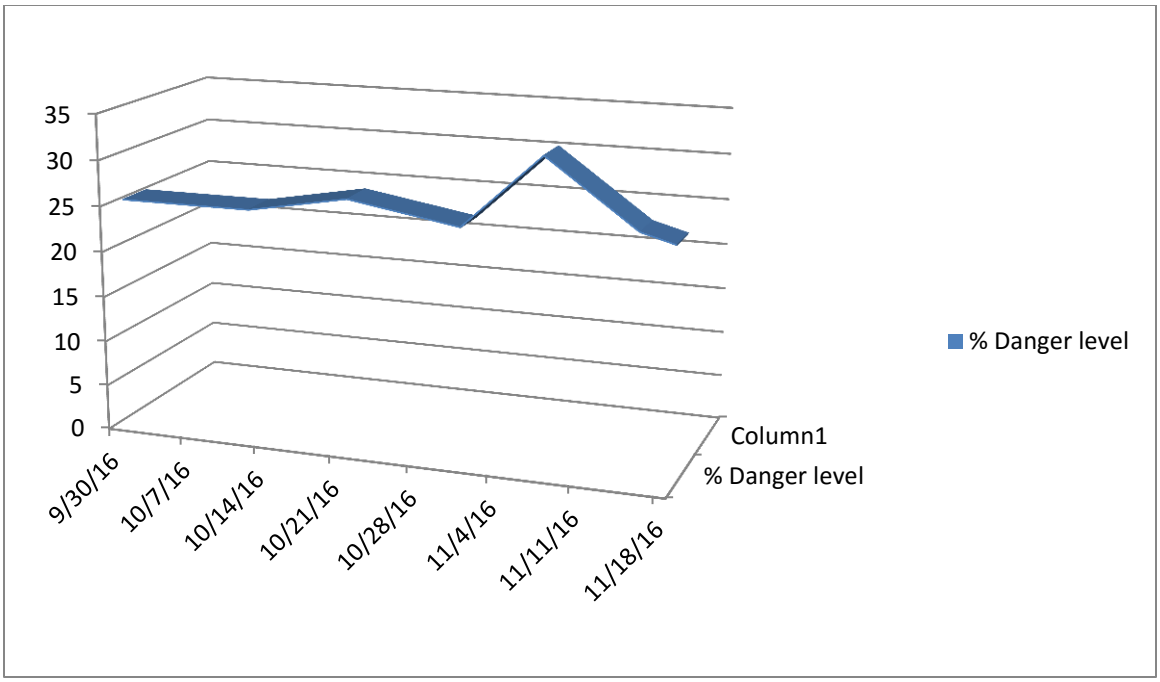

Fig. 8.6: Three months percent (%) digester danger level

To validate the digester danger status routine that was used online, there was need to record down specific values of biogas pressure, slurry level and percent danger status and to perform an analysis of these results. Table 8.2, shows these results of the internal digester danger status of the digester as a percentage based on measured inputs of biogas pressure and slurry displacement. A high percentage danger status value implied a high system breach. The results show that the danger status was elevated both at very low and very high pressures. At mid pressures the danger status was low as would be expected. However, the results failed to appreciably differentiate varying slurry displacements. The fuzzy algorithm and the direct proportional relationship concept between slurry displacement and pressure needed to be revised to take into consideration the varying densities of feedstock. However, the designed system shows a reasonable level of predicting the digester danger level as given in Fig. 8.6.

Table 8.2: Internal digester danger status

Biogas pressure (KPa)	**Slurry displacement (m)**		
	0.13	***0.25***	***0.45***
4	41.96%	43.10%	40.09%
9	33.26%	31.93%	37.84%
11	25%	25%	25%
12	25%	25%	25%
16	33.26%	31.93%	37.84%
19.5	41.11%	40.91%	41.67%

Table 8.3: Biogas system fault causes and correction

Type of fault	***Causes***	***Corrective action***	***Significance with respect to system danger***
Too low pressure	Biogas over use, leak, low hydraulic retention tme, little gas produced	Reduce usage rate, Check for leak at dome top, increase organic loading rate	Serious will cause negative pressure
Too High pressure	Low gas uasge, gas line blockage	Increase usage, purge system, reduce organic loading rate	Not very serious but gas loss through output
Too low slurry displacement	Too low gas pressure, high feeding, gas over use	Reduce usage rate, increase hydraulic retention time, reduce feeding	Not serious but little gas out
Too high slurry displacement	Too high gas pressure, low feeding	Increase gas usage, increase feeding	Serious can cause negative pressure
Methane leak	Broken pipe, taps left open	Check integrity of pipe work, close all valves and taps	Very serious
Oxygen ingress	Negative digester pressure, dome top not air tight	Increase digester pressure above low limit, check integrity of dome top, high slurry displacement from zero line	Very serious will kill process and cause explosion

Table 8.3 shows the possible causes and corrective actions that needed to be taken when a given fault condition or biogas system abnormality was observed. On the other hand, when tested the methane leak detector activated the sound alarm with the yellow light emitting diode (LED) coming on, simultaneously energizing the solenoid coil. The oxygen sensor responded to atmospheric oxygen levels. However, both sensors especially the oxygen sensor required detailed calibration to give accurate readings.

8.3 PHOTOVOLTAIC BASED MEASUREMENTS

The laboratory scale photovoltaic system was implemented by using two ten watt (2 x 10Watt) solar panels connected in series and two 12Volt 15Ah batteries also connected in series. This brings the test voltage to the level that is used in the full scale photovoltaic system, save for the current rating. To obtain valid current charging and voltage charging characteristics, the 24Volt

battery bank is first completely discharged through a 24Volt load, preferably a parallel combination of 24V vehicle indicator lamps and then connected to the 24V solar panel through the buck regulator. During the charging process, the charging voltage and charging currents are recorded at thirty minute time intervals from the beginning until full charge is obtained.
Each 10W solar panel has the following specifications:

- Peak Power (Pmax) of 10 Wp
- Maximum Power Current (Imp) of 0.58 A
- Maximum Power Voltage (Vmp) of 17.2 V
- Short-Circuit Current (Isc) of 0.65 A
- Open-Circuit Voltage (Voc) of 21.6 V
-

Hence two series connected solar panels have the following specifications:

- Peak Power (Pmax) of 20 Wp
- Maximum Power Current (Imp) of 0.58 A
- Maximum Power Voltage (Vmp) of 34.4 V
- Short-Circuit Current (Isc) of 0.65 A
- Open-Circuit Voltage (Voc) of 43.2 V

Table 8.4: Battery charging voltage and current measurements

Time (minutes)	**Charging voltage (V)**	**Charging current (I)**
0	21.2	0.942
30	21.3	0.937
60	21.8	0.915
90	22.6	0.883
120	23.8	0.838
150	24.7	0.808
180	25.81	0.773
210	25.87	0.771
240	25.9	0.770

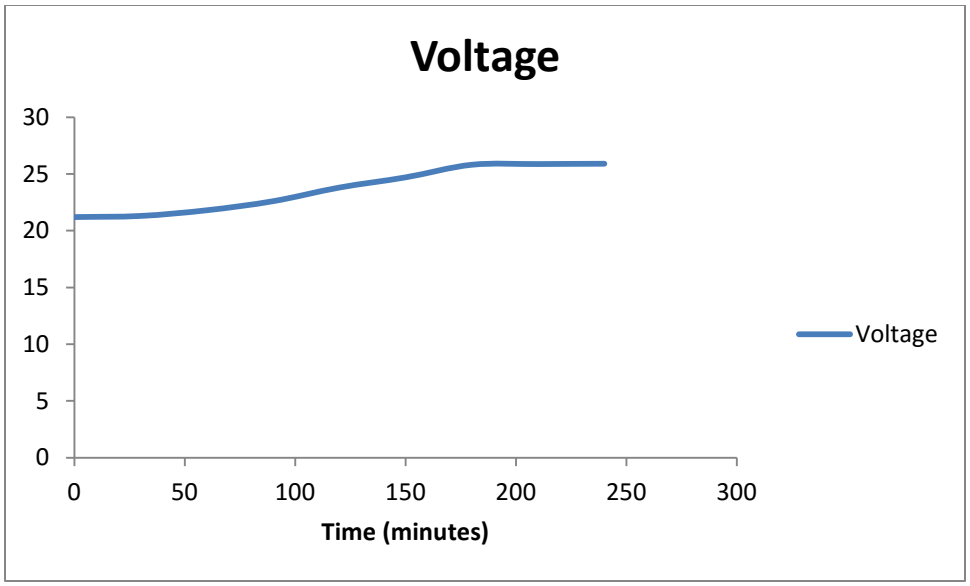

Fig. 8.7: Charging voltage characteristics

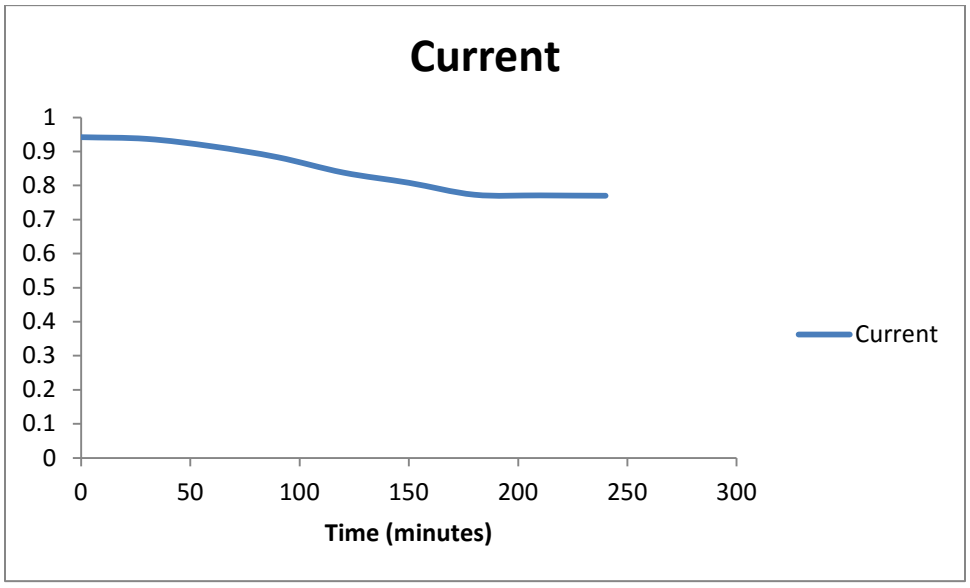

Fig. 8.8: Charging current characteristics

From Figs. 8.7 & 8.8, at the beginning of the charging process, the current is large, while the charging voltage is low. As the process progresses, after about one hundred and seventy minutes[38] the charging voltage becomes high, while the charging current becomes low.
With respect to solar panel shading, the designed system responds to various shading levels to inform the user through the LCD. An increased shading level significantly reduces the output of

[38] Which corresponds to about seventy percent state of charge the charging current decreases while the charging voltage increases.

the solar panels. However, most of the solar installations are in open space where trees will minimally impose any shading. The users are also encouraged to remove any litter in the form of paper or cloth near the solar panels and to occasionally clean the panels.

8.4 TITRATION RESULTS

The results obtained from titration of VFAs and alkalinity done on-site confirm that digester was stable during the period of observation from the 30th of October 2016 to the 18th of November 2016. Titrations are more accurate than the online measurement system and they do provide a reference point to improve the accuracy of the online measurements. The main disadvantage of titration method is its difficulty in direct online implementation and the fact that it is not advisable[39] for the average user to perform titration measurements without the presence of an expert. Hence titrations are to be used only by the designer or expert to validate the accuracy of the online system.

[39] The user is exposed to corrosive acid and danger of explosion if acid mixing method is wrongly followed.

CHAPTER 9

CONCLUSION AND RECOMMENDATIONS

The designed measurement and control system for intermixed biogas and photovoltaic systems functioned as intended. The system was able to successfully monitor the stability of the biogas system, to predict and measure the amount and concentrations of the main components of biogas in-terms of litres and parts per million (ppm) respectively. Biogas fault detection and status were also successfully performed. Due to ethical reasons pertaining to equipment modification (incorporation of pwm on solar charge controller) only the biogas system was fully implemented on the full scale installation, while the solar system was designed and tested on a laboratory scale version to carry out battery charging and solar fault detection and status. However the software routines where all incorporated into the same microcontroller and run as one program.

The success of the measurement and control system was considerably enhanced by the use of fuzzy logic algorithms as the basis for all the routines. The fuzzy logic algorithms are powerful at solving non-linear based problems, which constituted a great part of this research. The design and testing of the fuzzy logic algorithms including simulation took a considerable amount of time of this research. Measurements had to be done over and over again due sensor amplifier generated electrical noise. These sensor amplifiers are simple types prone to error, hence due care had to be taken (this is one major weakness of the system). Another weakness is due to the use of limited type of membership functions. For best results, a careful selection of the most suitable membership function for each measured parameter is required. The system also needs to be robust (existing systems outperform our design in this respect). However the overall monitoring ability is superior to existing systems.

The contributions of this paper include; 1) a new biogas system fault detection and control strategy which can used on any size of digester, 2) a comprehensive photovoltaic system fault detection and control strategy, and 2) a biogas and photovoltaic system easily and quickly fixed by persons with no expertise at all in the respective fields.

Based on this research, we recommend the use of the designed fuzzy logic based measurement and control system to be used on mixed biogas and photovoltaic systems. The system needs further development, especially on identifying cheaper hardware and improving on the accuracy of the fuzzy logic algorithms. The future plan involves the reduction in the number of sensors and parameters to be measured by developing better algorithms so as to obtain the same level or even better biogas fault detection and control. The development of an integrated system model (of whole system) with simulations done using type-2 fuzzy logic algorithms that address the uncertainty of the membership functions as a way of considerably improving the accuracy of the fuzzy logic controller is a possible future research area. Continued use of MPLABXIDE is recommended as this is a very powerful and authentic platform for developing software.

LIST OF PUBLICATIONS: PEER REVIEWED INTERNATIONAL CONFERENCE PROCEEDINGS

1. L. Matindife and Z. Wang, Biogas System Fault Detection and Control, THE SECOND IEEE INTERNATIONAL CONFERENCE ON ADVANCES IN COMPUTING, COMMUNICATION AND ENGINEERING, pp. 231-235, 28 – 29 NOVEMBER 2016, DURBAN, SOUTH AFRICA.

2. L. Matindife and Z. Wang, Fuzzy Logic Algorithms Based Measurement and Control System Design for Intermixed Biogas and Photovoltaic System, Accepted by THE FIRST INTERNATIONAL CONFERENCE ON SUSTAINABLE MATERIALS PROCESSING AND MANUFACTURING, 23 - 25 JANUARY 2017, KRUGER NATIONAL PARK, SOUTH AFRICA.

3. L. Matindife and Z. Wang, Fuzzy logic SOLAR Panel and Battery Control system design, submitted to 2017 IEEE FUTURE OF ELECTRONIC POWER PROCESSING AND CONVERSION (FEPPCON).

REFERENCES

ACHAIBOU, N., HADDADI, M. & MALEK, A. 2012, "Modeling of Lead Acid Batteries in PV Systems", *Energy Procedia*, vol. 18, no. 0, pp. 538-544. Available from: http://0-www.sciencedirect.com.oasis.unisa.ac.za/science/article/pii/S1876610212008351 Last access date: 24 June 2015

ALIYU, A.A., BELLO, M.U., KASIM, R., & MARTIN, D., 2014, "Positivist and Non-Positivist Paradigm in Social Science Research: Conflicting Paradigms or Perfect Partners?", Journal of Management and Sustainability; Vol. 4, No. 3, pp. 79-95, Canadian Centre for Science and Education. Available from: http://dx.doi.org/10.5539/jms.v4n3p79. Last access date: 13 October 2016

ARGYROPOULOS A. 2013, Soft sensor development and process control of anaerobic digestion, PhD Thesis, University of Exeter. Available from: https://ore.exeter.ac.uk/repository/bitstream/handle/10871/15068/ArgyropoulosA.pdf?sequence=1&isAllowed=y. Last access date: 5 April 2016

BAGOS P.G. AND ADAM M. 2015,On the Covariance of Regression Coefficients. *Open Journal of Statistics*, Vol.**5**,pp. 680-701. Available from: http://dx.doi.org/10.4236/ojs.2015.57069. Last access date: 6 April 2016

BERNHARD DROUSG 2013, Process monitoring in biogas plants, IEA Bioenergy. Available from: http://www.iea-biogas.net/technical-brochure-process_monitoring.pdf. Last access date: 26 January 2015

BHARATHIRAJA, B., SUDHARSANAA, T., BHARGHAVI, A., JAYAMUTHUNAGAI, J. & PRAVEENKUMAR, R. 2016, "Biohydrogen and Biogas – An overview on feedstocks and enhancement process", *Fuel*, vol. 185, pp. 810-828. Available from: http://0-www.sciencedirect.com.oasis.unisa.ac.za/science/article/pii/S0016236116307682 Last access date: 26 September 2016

BIOENERGY. 2016, How to calculate the retention time and the organic loading rate, Sunstainable Energy Authority of Ireland. Available from: http://www.seai.ie/Renewables/Bioenergy/Bioenergy_Technologies/Anaerobic_Digestion/The_Process_and_Techniques_of_Anaerobic_Digestion/How_to_calculate_the_retention_time_and_the_organic_loading_rate.pdf. Last access date: 4 June 2016

BIRÓ GYÖRGYI, LILI MÉZES, JÁNOS BORBÉLY, JÁNOS TAMÁS 2012, Automation and Control Developing Solutions of Anaerobic Fermentation Process, Institute of Water and Environmental Management, University of Debrecen, Hungary, pp. 307–315.

BLOOR, M & WOOD, F 2006, 'Naturalism', in *Keywords in qualitative methods*, SAGE Publications Ltd, pp. 123-125. Available from: http://0-methods.sagepub.com.oasis.unisa.ac.za/book/keywords-in-qualitative-methods/n60.xml. Last access date: 16 October 2016

BURGOS, C., SÁEZ, D., ORCHARD, M.E. & CÁRDENAS, R. 2015, "Fuzzy modelling for the state-of-charge estimation of lead-acid batteries", *Journal of Power Sources*, vol. 274, no. 0, pp. 355-366. Available from: http://0-www.sciencedirect.com.oasis.unisa.ac.za/science/article/pii/S0378775314016450 Last access date: 24 June 2015

BUSINESS REPORTER 2013,'REA to roll out 64 biogas digesters', NewsDay, 24 July. Available from: https://www.newsday.co.zw/2013/07/24/rea-to-roll-out-64-biogas-digesters/. Last access date: 17 February 2015

CARR DAVE & SHEARER JEFF. 2007,'Nonlinear control and decision making using fuzzy logic in Logix', Rockwell Automation. Available from: https://www.isa.org/WorkArea/DownloadAsset.aspx?id=123309. Last access date: 15 July 2015

CHANG WEN-YEAU. 2013, "The State of Charge Estimating Methods for Battery: A Review," Applied Mathematics, vol. 2013. Available from: http://www.hindawi.com/journals/isrn/2013/953792/. Last access date: 25 July 2016

ÇINAR,S.M.& AKARSLAN,E. 2012,' Research Article On the Design of an Intelligent Battery Charge Controller for PV Panels', Journal of Engineering Science and Technology Review5(4),pp. 30 -34. Available on: http://www.jestr.org. Last access date: 5 October 2014

CIRSTEA, M.N., DINU, A., KHOR, J.G. & McCORMICK, M. 2002, "6 - Fuzzy logic fundamentals" in *Neural and Fuzzy Logic Control of Drives and Power Systems*, eds. M.N. CIRSTEA, A. DINU, J.G. KHOR & M. McCORMICK, Newnes, Oxford, pp. 113-122. Available from: http://ac.els-cdn.com/B9780750655583500064/3-s2.0-B9780750655583500064-main.pdf?_tid=a7270e50-c4c3-11e4-90df-00000aab0f27&acdnat=1425730713_4722050b561e0b05f7676aa5bfebbbd7. Last access date: 7 March 2015

CORRO, G., PANIAGUA, L., PAL, U., BAÑUELOS, F. & ROSAS, M. 2013, "Generation of biogas from coffee-pulp and cow-dung co-digestion: Infrared studies of postcombustion emissions", *Energy Conversion and Management*, vol. 74, pp. 471-481. Available http://0-www.sciencedirect.com.oasis.unisa.ac.za/science/article/pii/S0196890413003889 Last access date: 26 September 2016

DAOUD,A., MIDOUN, A. 2005, 'Fuzzy Control of a Lead Acid Battery Charger', J. Electrical Systems 1-1, pp. 52-59.

DENZIN,N, & RYAN,K 2007,'Qualitative Methodology (Including Focus Groups)', in W Outhwaite, & Stephen P. Turner (eds), SAGE Publications Ltd, London, England, pp. 578-95. Available from: http://0-dx.doi.org.oasis.unisa.ac.za/10.4135/9781848607958.n32. Last access date: 15 March 2015

DEUBLEIN, D. & STEINHAUSER, A., (EDS). 2008, '*Biogas from Waste and Renewable Resources',* John Wiley & Sons Inc., Germany.

EJURY JENS. 2013, '*Buck converter design'*, Design Note, V1.0, Infineon Technologies. Available on: http://www.mouser.com/pdfdocs/BuckConverterDesignNote.pdf. Last access date: 03 December 2016

EU-AGRO-BIOGAS 2009, European Biogas Initiative to improve the yield of agricultural biogas plants, Partner N° 2, North Wyke Research, (Rothamsted Research). Available on: http://rtd-services.com/euagrobiogas/images/d18.pdf. Last access date: 5 April 2016

FALK HARRY MICHAEL 2011, Monitoring the anaerobic digestion process, PhD Thesis, Jacobs University. Available from: http://www.jacobs-university.de/phd/files/phd20111213_falk-harry.pdf. Last access date: 5 February 2015

FENG LU. 2013, Biochemical Methane Potential (BMP) of Vinegar Residue and the Influence of Feed to Inoculum Ratios on Biogas Production. Available from: https://www.researchgate.net/publication/273221251. Last access date: 12 November 2016

FRANKE-WHITTLE I.H., WALTER A., EBNER, C. & INSAM, H. 2014, "Investigation into the effect of high concentrations of volatile fatty acids in anaerobic digestion on methanogenic communities", *Waste Management,* vol. 34, no. 11, pp. 2080-2089. Available from: http://www.sciencedirect.com/science/article/pii/S0956053X14003250. Last access date: 6 April 2016

GIOVANNINI, G., DONOSO-BRAVO, A., JEISON, D., CHAMY, R., RUÍZ-FILIPPI, G. & VANDE WOUWER, A. 2016, "A review of the role of hydrogen in past and current modelling approaches to anaerobic digestion processes", *International Journal of Hydrogen Energy,* vol. 41, no. 39, pp. 17713-17722. Available from: http://0-www.sciencedirect.com.oasis.unisa.ac.za/science/article/pii/S0360319916320201 Last access date: 26 September 2016

GOPAL A.K, RAOL J.R. 2012, 'Mobile Intelligent Autonomous Systems', Technology & Engineering, CRC Press, pp. 16. Available from: https://books.google.co.zw/books?id=HaS91phGuRQC&pg=PA106&dq=gopal+and+Raol&hl=en&sa=X&ved=0ahUKEwjpysXOu_PLAhWJYZoKHbhLD9YQuwUIHTAA#v=onepage&q=gopal%20and%20Raol&f=false. Last access date: 2 April 2016

GURR KEVIN. 2013, Oxygen sensors and their use within Rebreathers. Available from: http://rebreatherpro.typepad.com/Oxygen%20Sensors%20for%20use%20in%20rebreathers%20-%20release%20V1.pdf. Last access date: 08 August 2016

HASAN, M.A. & PARIDA, S.K. 2016, "An overview of solar photovoltaic panel modeling based on analytical and experimental viewpoint", *Renewable and Sustainable Energy Reviews*, vol. 60, pp. 75-83. Available from: http://0-www.sciencedirect.com.oasis.unisa.ac.za/science/article/pii/S1364032116001179 Last access date: 26 September 2016

HERNANDEZ, J, MEDINA ,R, HERNANDER ,M 2012, 'Instrumentation and Design of a Supervisory System for an Anaerobic Biodigestor', IEEE Conference, International Symposium on Alternative Energies and Energy Quality(SIFAE) IEEE, pp. 1- 6. Available from: http://0-ieeexplore.ieee.org.oasis.unisa.ac.za/stamp/stamp.jsp?tp=&arnumber=6478900. Last access date: 13 February 2015

HOWELL, KE 2013, 'Constructivist and participatory paradigms of inquiry: introducing action research', in *An introduction to the philosophy of methodology*, SAGE Publications Ltd, London, , pp. 88-100. Available from: http://0-methods.sagepub.com.oasis.unisa.ac.za/book/an-introduction-to-the-philosophy-of-methodology/n6.xml. Last access date: 15 October 2016

HIVOS & SNV 2012,' Feasibility on a national domestic biogas programme in Zimbabwe'. Available from: https://www.academia.edu/9075196/Feasibility_on_a_national_domestic_biogas_programme_in_Zimbabwe. Last access date: 18 February 2015

IANCU ION ,ELMER DADIOS (Ed.). 2012, A Mamdani Type Fuzzy Logic Controller, Fuzzy Logic - Controls, Concepts, Theories and Applications, InTech, Available from: http://www.intechopen.com/books/fuzzy-logic-controls-concepts-theories-and-applications/a-mamdani-typefuzzy-logic-controller. Last access date: 19 July 2015

IANCU ION & GABROVEANU MIHAI.2010,' Fuzzy Logic Controller Based on Association Rules', Mathematics and Computer Science Series, Vol. 37 no.3, 2010, pp. 12-21 http://www.researchgate.net/publication/265201384_Fuzzy_Logic_Controller_Based_on_Association_Rules. Last access date: 19 July 2015

JERRY, W. WILLIS 2007,'Chapter 1.World Views, Paradigms, and the Practice of Social Science Research', SAGE Publications, Inc., Thousand Oaks, CA, pp. 1-27. Available from: http://0-dx.doi.org.oasis.unisa.ac.za/10.4135/9781452230108.n1. Last access date: 15 March 2015

JUPP, V. 2006. *The SAGE dictionary of social research methods* : SAGE Publications Ltd. Available from: http://0-methods.sagepub.com.oasis.unisa.ac.za/base/download/ReferenceEntry/the-sage-dictionary-of-social-research-methods/n120.xml. Last access date: 16 October 2016

KANOKWAN, BOE 2006, Online monitoring and control of the biogas process**.** Ph.D. Thesis Institute of Environment & Resources Technical University of Denmark. Available from: http://www2.er.dtu.dk/./MR2006-055.pdf. Last access date: 5 October 2014

KARIMOV, Kh.S., MUHAMMAD ABID, UMAROV,S.U.2012, 'Designs of Some Low Power Renewable Energies Installations', Proceedings of the 2012 International Conference on Industrial Engineering and Operations Management Istanbul, Turkey, pp. 317-325. Available from: http://iieom.org/ieom2012/pdfs/85.pdf. Last access date: 26 September 2016

KLIR, G.J. 2003, "Chapter 2 Fuzzy logic", *Developments in Petroleum Science*, vol. 51, no. 0, pp. 33-49. Available from: http://ac.els-cdn.com/S0376736103800067/1-s2.0-S0376736103800067-main.pdf?_tid=fddaebbe-c4c2-11e4-b0cc-00000aab0f6b&acdnat=1425730429_7990aad4d4760c232437b58b1b5c4c5f. Last access date: 27 June 2015

KUMEN BLAKE. 2009, Op Amp Precision Design: PCB Layout Techniques,Microchip Technology Inc. Available from: http://ww1.microchip.com/downloads/cn/AppNotes/cn540604.pdf. Last access date: 2 May 2016

LABCENTER ELECTRONICS. 2012, PROTEUS DESIGN SUITE 8.0 [Software package].

LABATUT R. A. and GOOCH C. A. 2015, MONITORING OF ANAEROBIC DIGESTION PROCESS TO OPTIMIZE PERFORMANCE AND PREVENT SYSTEM FAILURE, Department of Biological and Environmental Engineering Cornell University, Ithaca, NY. Available from: https://dspace.library.cornell.edu/bitstream/1813/36531/1/21.Rodrigo.Labatut.pdf. Last access date: 13 June 2015

LM 324. 2001, Low power quad operational amplifiers. Available from: http://pdf.datasheetcatalog.com/datasheet/stmicroelectronics/2156.pdf. Last access date: 27 October 2016

LOHRI CHRISTIA. 2008, TITRATION METHODOLOGY ACCORDING TO KAPP FOR MONITORING OF ANAEROBIC DIGESTION: VFA, alkalinity and A/TIC-ratio, Zurich University of Applied Sciences (ZHAW), Switzerland. Available from: https://www.eawag.ch/fileadmin/Domain1/Abteilungen/sandec/publikationen/SWM/Anaerobic_Digestion/Lohri_2009_Appendix.pdf. Last access date: 30 July 2016

McCARTY, P.L. & McKINNEY, R.E. 1961, "Salt Toxicity in Anaerobic Digestion", *Journal (Water Pollution Control Federation)*, vol. 33, no. 4, pp. 399-415. Available from: http://www.jstor.org/stable/25034396?seq=1#page_scan_tab_contents. Last access date: 14 May 2016

MARCHAIM, U., 1992, *Biogas processes for sustainable development*, Rome. Available from: https://books.google.co.zw/books?id=NLDRTXyp0IcC&pg=PA63&lpg=PA63&dq=total+pressure+in+a+fixed+dome+digester&source=bl&ots=jEVqdulBXO&sig=W8Kc8I3s6j4sMOZGqUNPAqO_ESQ&hl=en&sa=X&ved=0ahUKEwiRuu6vqozOAhVFCMAKHaS_DAAQ6AEILTAD#v=onepage&q=total%20pressure%20in%20a%20fixed%20dome%20digester&f=false. Last access date: 24 July 2016

MICROCHIP 2015a, MPLAB XDE (Version: 3.00) [Computer program]. Available from:

http://www.microchip.com/pagehandler/en-us/family/mplabx/. Last access date: 20 May 2015

MICROCHIP 2015b,'Products-PIC microcontrollers 8 bit'. Available from: http://www.microchip.com/. Last access date: 29 March 2015

NATIONAL INSTRUMENTS. 2013, NI CIRCUIT DESIGN SUITE 13.0 PROFESSIONAL EDITION [Software package].

NHIVEKAR G.S., NIRMALE S.S, MUDHOLKER R.R. 2011, *Implementation of fuzzy logic control algorithm in embedded microcomputers for dedicated application*, International Journal of Engineering, Science and Technology Vol. 3, No. 4, pp. 276-283, MultiCraft. Available from: http://www.ijest-ng.com/vol3_no4/ijest-ng-vol3-no4-pp276-283.pdf. Last access date: 24 February 2015

O'LEARY, Z 2007a,'Positivism', SAGE Publications Ltd, London, England, pp. 197-9. Available from: http://0-dx.doi.org.oasis.unisa.ac.za/10.4135/9780857020147.n98. Last access date: 15 March 2015

O'LEARY ,Z 2007b,'Post-positivism', SAGE Publications Ltd, London, England, pp. 203-5. Available from: http://0-dx.doi.org.oasis.unisa.ac.za/10.4135/9780857020147.n101. Last access date: 15 March 2015

O'LEARY, Z 2007c,'Empiricism', SAGE Publications Ltd, London, England, pp. 75-6. Available from: http://0-dx.doi.org.oasis.unisa.ac.za/10.4135/9780857020147.n37. Last access date: 15 March 2015

OPA348. 2016, Operational Amplifier, Texas Instruments. Available from: http://www.ti.com/lit/ds/symlink/opa348-q1.pdf. Last access date: 27 October 2016

PAPPIS COSTAS P. & SIETTOS CONSTANTINOS I .2005,''Fuzzy reasoning'', *in Search Methodologies Introductory Tutorials in Optimization and Decision Support Techniques*, eds. E. K. Burke, G. Kendall , Springer US, pp. 437 – 474. Available from: http://0-link.springer.com.oasis.unisa.ac.za/chapter/10.1007/0-387-28356-0_15. Last access date: 25 March 2016

PAYNE, G, & PAYNE, J 2004, 'Positivism and realism', in *Key concepts in social research*, The SAGE key concepts series, SAGE Publications, Ltd, London, England, pp. 171-5. Available from: http://0-dx.doi.org.oasis.unisa.ac.za/10.4135/9781849209397.n36 Last access date: 15 March 2015

PICkit™ 3. 2013, In-Circuit Debugger/Programmer User's Guide For MPLAB® X IDE, Microchip Technology Inc. Available from: http://ww1.microchip.com/downloads/en/DeviceDoc/52116A.pdf Last access date: 16 November 2016

RASHID M.H. 2003, Power Electronics Circuits and Devices, 3rd edition, Prentice Hall

REDDY THOMAS B. 2011, Linden's Handbook of Batteries, 4th edition, McGraw-Hill Education. Available from:

http://0-accessengineeringlibrary.com.oasis.unisa.ac.za/browse/lindens-handbook-of-batteries-fourth-edition/p2001c2f299716_1001?subject=%23DISCIPLINE%23Energy+%26+petroleum+engineering%23Batteries+%2F+Fuel+Cells&q=lead+acid+battery+charging+methods.
Last access date: 18 June 2015

REKHA, B. R. & KAVITHA, D.,2014, 'Simulation and Digital Implementation of Fuzzy Logic Controller for Solar Maximum Power Tracker Application', International Journal of Digital & Contemporary research Application , Volume 2, Issue 9, April 2014. Available from: http://www.ijdar.com . Last access date: 07 August 2014

ROSEMOUNT ANALYTICAL INC. 2010, *The theory of pH measurement*, Application Data Sheet, Emerson Process Management. Available from: http://www2.emersonprocess.com/siteadmincenter/PM%20Rosemount%20Analytical%20Documents/Liq_ADS_43-002.pdf.
Last access date: 24 April 2016

ROSS TIMOTHY.J., BOOKER JANE.M, PARKINSON W.JERRY (Eds). 2002, Fuzzy Logic and Probability Applications: Bridging the Gap, ASA SIAM.

ROSS T.J. 2004, *Fuzzy Logic with Engineering Applications*, USA, Second edition: John Wiley & Sons Ltd.

RURAL ELECTRIFICATION AGENCY. 2015, "Solar Mini grid System Project", Design, Installation and Maintenance Manual.

SALKIND, NJ 2010, *Encyclopedia of research design*, SAGE Publications, Inc., Thousand Oaks, CA. Available from: http://0-methods.sagepub.com.oasis.unisa.ac.za/base/download/ReferenceEntry/encyc-of-research-design/n352.xml. Last access date: 16 October 2016

SAMOLADAS, V. & PETROU, L. 1994, "Special-purpose architectures for fuzzy logic controllers", *Microprocessing and Microprogramming*, vol. 40, no. 4, pp. 275-289. Available on: http://ac.els-cdn.com/016560749490135X/1-s2.0-016560749490135X-main.pdf?_tid=4e67cf2c-c4bc-11e4-a7fa-00000aacb360&acdnat=1425727557_2920ed7efcff9d5b44a9627bf92468ff.
Last access date: 7 March 2015

SARAVANAN S., VIDYHA R., THANGAVEL S. 2013, "Online SOC estimation and Intelligent Battery Charger for Solar PV System", International Journal of Engineering and Advanced Technology (IJEAT), Volume. 2, Issue-4, pp. 2249 – 8958.
Available from:
http://citeseerx.ist.psu.edu/viewdoc/download?doi=10.1.1.681.2551&rep=rep1&type=pdf
Last access date: 26 July 2016

SHAH, F.A., MAHMOOD, Q., RASHID, N., PERVEZ, A., RAJA, I.A. & SHAH, M.M. 2015,

"Co-digestion, pretreatment and digester design for enhanced methanogenesis", *Renewable and Sustainable Energy Reviews*, vol. 42, pp. 627-642. Available from: http://www.sciencedirect.com/science/article/pii/S1364032114008788. Last access date: 19 October 2016

SINGH HARPREET, GUPTA MADAN M. , MEITZLER THOMAS, HOU ZENG-GUANG, GARG KUM KUM, SOLO ASHU M. G. AND, ZADEH LOTFI A, (Eds) 2013, '*Real-Life Applications of Fuzzy Logic',* Advances in Fuzzy Systems Vol. 2013, 3 pages. Available from: http://www.hindawi.com/journals/afs/2013/581879/. Last access date: 8 March 2015

SOUTHERN BIOPOWER LTD 2015, 'National Biogas Programme Zimbabwe', Zambia. Available from :http://www.southernbiopower.com/?page_id=34. Last access date: 1 February 2015

SPRINGER ERICH K. 2014,pH Measurement Guide, Hamilton Bonduz AG. Available from: www.hamiltoncompany.com/~/.../pH%20**Measurement**%20Guide.ashx Last access date: 24 April 2016

TEODORITA AL SEADI, DOMINIK RUTZ, HEINZ PRASSL, MICHAEL KÖTTNER, TOBIAS FINSTERWALDER, SILKE VOLK, RAINER JANSSENBIOGAS 2008, biogas HANDBOOK, University of Southern Denmark. Available from: http://www.lemvigbiogas.com/ . Last access date: 1 July 2014

THERMOCOUPLE 1999, Temperature measurement: PT100 resistance table. Available from: http://www.micropik.com/PDF/pt100.pdf. Last access date: 24 October 2016

THOMAS, DR, & HODGES, ID 2010, 'Research ethics and ethics reviews', in *Designing and managing your research project: Core skills for social and health research*, SAGE Publications Ltd, London, pp. 83-105. Available from: http://0-dx.doi.org.oasis.unisa.ac.za/10.4135/9781446289044.n6. Last access date: 10 May 2015

TL061. 2004. *Low-Power JFET-Input Operational Amplifiers*, Texas Instruments. Available from: http://datasheet.octopart.com/TL061CP-Texas-Instruments-datasheet-77091.pdf. Last access date: 16 November 2016

TL082. 2000, *Wide Bandwidth Dual JFET Input Operational Amplifier*, National Semiconductor. Available from: www.mantech.co.za/Datasheets/Products/TL082.pdf. Last access date: 2 May 2016

TSENG CHYUAN-YOW , LIN CHIU-FENG 2005, "Estimation of the state-of-charge of lead–acid batteries used in electric scooters", *Journal of Power Sources, Vol. 147, no. 1–2, pp.282-287.* Available from: http://0-www.sciencedirect.com.oasis.unisa.ac.za/science/article/pii/S0378775305001485?np=y Last access date: 24 June 2015

VAS PETER. 1999, **Artificial-Intelligence-based Electrical Machines and Drives:** Application of Fuzzy, Neural, Fuzzy-neural, and Genetic-algorithm-based Techniques, OUP Oxford. Available from: https://books.google.co.zw/books?id=16Ai4r7qjuIC&pg=PA207&lpg=PA207&dq=max-dot++fuzzy+rule++inference+example&source=bl&ots=sfbcp2l6am&sig=pR5WMjZICiSNHuLd5penODGa0wM&hl=en&sa=X&ved=0ahUKEwj248ej-KvJAhXM7xQKHQVuA-wQ6AEIMzAE#v=onepage&q=maxdot%20%20fuzzy%20rule%20%20inference%20example&f=false. Last access date: 25 November 2015

VIOT GREGORY. 1993, *Fuzzy Logic in C, Dr Dobb's Journa*l Vol.18, No. 2, pp. 40-49, CMP Media, Inc., USA. Available from: http://www.drdobbs.com/cpp/fuzzy-logic-in-c/184408940. Last access date: 24 February 2016

WAFLER MARTIN. 2008, "Capacity Building for Ecological Sanitation in Bhutan", Training Material on Anaerobic Wastewater Treatment, *Ecosan ecological sanitation*, seecon gmbh. Availble from: http://www.sswm.info/sites/default/files/reference_attachments/WAFLER%202008%20Training%20Material%20on%20Anaerobic%20Wastewater%20Treatment.pdf. Last access date: 23 July 2016

WARD A, HOBBS P,HOLLIMAN P , RAVELLA S.R,1 , PARDO G, WILLIAMS J AND RETTER A . 2008.' Software sensor monitoring and expert control of biogas production. Available from: http://www.ramiran.net/doc08/RAMIRAN_2008/Ward.pdf. Last access date: 5 April 2016

WARD A.J, HOBBS P.J, Peter J. HOLLIMAN P.J , JONES D.L. 2011, "Evaluation of near infrared spectroscopy and software sensor methods for determination of total alkalinity in anaerobic digesters", *Bioresource Technology, Elsevie*r, pp. 4083 – 4090. Available from: https://www.researchgate.net/publication/49748387_Evaluation_of_near_infrared_spectroscopy_and_software_sensor_methods_for_determination_of_total_alkalinity_in_anaerobic_digesters. Last access date: 5 April 2016

WELCH RICHARD L.,VENAYAGAMOORTHY GANESH KUMAR 2010,' Energy dispatch fuzzy controller for a grid-independent photovoltaic system', Energy Conversion and Management, Vol.51,Issue 5, pp. 928 – 937. Available from: http://0-www.sciencedirect.com.oasis.unisa.ac.za/science/article/pii/S0196890409004816 Last access date: 23 June 2015

WISCONSIN DEPARTMENT OF NATURAL RESOURCES 1992,' Advanced Anaerobic Digestion Study Guide', Madison. Available from: http://dnr.wi.gov/regulations/opcert/documents/wwsganaerobdigadv.pdf. Last access date: 17 July 2015

YONG YIN, XING LUO, SHEN GUO, ZUDE ZHOU AND JIHONG WANG 2008, 'A Battery Charging Control Strategy for Renewable Energy Generation Systems', Proceedings of the World Congress on Engineering Vol. 1, July 2 - 4 , London, U.K. Available from: ww.iaeng.org/publication/WCE2008/WCE2008_pp356-361.pdf. Last access date: 19 October 2016

ZADEH, L.A.1965, ' *Fuzzy Sets*.', Information and Control, vol.8, no.3, pp. 338-353. Available from: http://www.cs.berkeley.edu/~zadeh/papers/Fuzzy%20Sets-Information%20and%20Control-1965.pdf. Last access date: 8 March 2015

ZAMAN T. and ALAKUS K. 2015, Analysis of the Invariance and Generalizability of Multiple Linear Regression Model Results Obtained from Maslach Burnout Scale through Jackknife Method. *Open Journal of Statistics*, Vol.5, pp. 645-651.Available from: http://dx.doi.org/10.4236/ojs.2015.57065. Last access date: 6 April 2016

ZLOCHOWER ISAAC A. & GREEN GREGORY M. 2016, "The limiting oxygen concentration and flammability limits of gases and gas mixtures", Pittsburgh Research Laboratory, National Institute for Occupational Safety and Health, Pittsburgh, USA. Available from: https://www.cdc.gov/niosh/mining/UserFiles/works/pdfs/tloca.pdf. Last access date: 24 July 2016

Appendix A: UNISA ethical clearance approval

UNISA | college of science, engineering and technology

Dear Mr. Lieton Matindile (57476295)

Date: 2015-08-26

Application number:
013/LM/2015/CSET SOE

REQUEST FOR ETHICAL CLEARANCE: (Fuzzy logic algorithms based measurement and control system design for intermixed biogas and photovoltaic systems)

The College of Science, Engineering and Technology's (CSET) Research and Ethics Committee has considered the relevant parts of the studies relating to the abovementioned research project and research methodology and is pleased to inform you that ethical clearance is granted for your research study as set out in your proposal and application for ethical clearance.

Therefore, involved parties may also consider ethics approval as granted. However, the permission granted must not be misconstrued as constituting an instruction from the CSET Executive or the CSET CREC that sampled interviewees (if applicable) are compelled to take part in the research project. All interviewees retain their individual right to decide whether to participate or not.

We trust that the research will be undertaken in a manner that is respectful of the rights and integrity of those who volunteer to participate, as stipulated in the UNISA Research Ethics policy. The policy can be found at the following URL:
http://cm.unisa.ac.za/contents/departments/res_policies/docs/ResearchEthicsPolicy_apprvCouncil_21Sept07.pdf

Please note that the ethical clearance is granted for the duration of this project and if you subsequently do a follow-up study that requires the use of a different research instrument, you will have to submit an addendum to this application, explaining the purpose of the follow-up study and attach the new instrument along with a comprehensive information document and consent form.

Yours sincerely

Prof Ernest Mnkandla
Chair: College of Science, Engineering and Technology Ethics Sub-Committee

Prof IDG Macha
Executive Dean: College of Science, Engineering and Technology

RECEIVED
2015 -08- 27
OFFICE OF THE EXECUTIVE DEAN
College of Science, Engineering and Technology

University of South Africa
College of Science, Engineering and Technology
The Science Campus
Cnr Christiaan de Wet Road and Pioneer Avenue
Florida Park, Roodepoort
Private Bag X6, Florida, 1710

UNISA | college of science, engineering and technology

Appendix B: Sample interview protocol

Interview number:……

Date:……

INTERVIEW PROTOCOL

(Semi-structured)

A. How you operate the bio digester

Main questions	Sub questions	Sub-sub questions
-is your bio digester for a single household or for a small community? OR -what size is your bio digester?	- how many people use this digester? - are there school going children among the users? - is the gas output tap turned on continuously? - are there times when the gas supply is fully closed?	- can you elaborate? - can you explain?
-Do you troubleshoot gas related issues?	- How do you rectify continuous low biogas output from the digester? -What is the effect of gas leakage in the house? -what biogas pressure irregularities are of concern?	- can you explain how this is done? -can you expand on the biogas' undesirable properties and whether any measures if any are taken to counter this? -would you recommend an automatic system of troubleshooting?
-what type of waste is used in the bio digester?	-what are the daily solids(dry matter) to liquid(water) ratio input to the digester? - how do you know which solids to liquid ratio will give the best biogas output? - do you know the toxicity and pH of the feedstock?	- can you give figures of actual quantities (kgs, buckets etc)? -can you elaborate?
-how do you monitor internal bio digester process?	-is feedstock level in the bio digester important? -what parameters are critical to bio digester sustained process operation?	-can you elaborate? -can you explain how tracking of these may be important? -how best can you implement a tracking system?
-how is the used up waste from the bio digester removed?	-what is the typical retention time (i.e time between inputting waste and discharging it)? - how is the waste material used?	-can you explain further?

-are there written down instructions on how to operate the biogas system?	-what are your observations and recommendations?	-can you explain further?

B. How you operate your photovoltaic system

Main questions	Sub questions	Sub-sub questions
-is your photovoltaic system for a single household or for a small community? OR -what size is your photovoltaic system?	- how many people use this photovoltaic system? - are there users who need continuous electrical supply?	-can you elaborate? -can you explain?
-does your photovoltaic system supply enough electricity?	-for what purpose is the electricity used? -do you always obtain electricity when you need it? -how reliable is your battery bank? -what can you say about the power generated versas that taken by the users? -how far are the battery bank and inverter from the house?	-can you elaborate to include cloudy conditions and night time?
-Do you troubleshoot electrical generation related issues?	- How do you rectify continuous low electrical output from the photovoltaic system? -How do you maintain the different components of the photovoltaic system from solar panel to inverter? -what electrical generation irregularities are of concern? -what load conditions interfere with system operation?	-can you explain how this is done? -can you elaborate? -how do you rectify them? -would you recommend an automatic system of troubleshooting? -how can these be rectified?
-how do you monitor internal photovoltaic process?	-what aspects are critical to photovoltaic sustained process operation?	-can you elaborate? -can you explain how tracking of these may be important? -how best can you implement a tracking system?
-are there written down instructions on how to operate the photovoltaic system?	-what are your observations and recommendations?	-can you explain further?

C. Conclusion of Interview

1. Do you feel we have exhausted the most important aspects on how to operate a bio digester and photovoltaic system in which case you may want to make additions?

OR

Have we left anything else on how to operate a bio digester and photovoltaic system?

2. I would like to express my profound appreciation of the time you took for this interview.

Once again thank you.

Appendix C: Sample of signed informed consent form

INFORMED CONSENT FORM

Interviewer:

Good morning/afternoon sir/madam, my name is *Liston Matindife* and I am undertaking a master of technology (MTech) degree in electrical engineering research project with the University of South Africa (UNISA). My research area is on designing a measurement and control system for both biogas and photovoltaic systems with a view of increasing output efficiency.

I would like to interview you on the following topics: how you operate your bio digester from waste material feeding, process monitoring, methane gas collection (including low output troubleshooting) up to effluent discharge and how you operate, monitor and troubleshoot your photovoltaic set up from solar panels up to the inverter and load.

With these topics in mind and my assurance of your anonymity in the interview as I will assign numbers to the interviews may I take about thirty to forty minutes of your precious time for you to answer the following few questions if you are available. Your responses will only be used in assisting to improve the monitoring system I am developing and will in no way be taken as final. You may withdraw from participation at any time if you so wish.

Interviewee:

I acknowledge that I have sufficiently understood the nature of the intended research and I freely give my consent to be interviewed. Furthermore I am free now and I have sole authority or have sought permission from my superiors to be interviewed for no remuneration.

place of interview: ……

name of interviewee: ……

signature of interviewee:……. **Date:**……...

name of interviewer: ……

signature of interviewer:……. **Date:**……

Appendix D: Excel based multiple linear regression coefficients for alkalinity soft sensor

SUMMARY OUTPUT

Regression Statistics	
Multiple R	0.961315
R Square	0.924126
Adjusted R Square	0.696504
Standard Error	300.5343
Observations	5

ANOVA

	df	*SS*	*MS*	*F*	*Significance F*
Regression	3	1100085	366695	4.059914	0.34623
Residual	1	90320.89	90320.89		
Total	4	1190406			

	Coefficients	*Standard Error*	*t Stat*	*P-value*	*Lower 95%*	*Upper 95%*	*Lower 95.0%*	*Upper 95.0%*
Intercept	2148.33	1414.918	1.518343	0.370771	-15829.9	20126.57	-15829.9	20126.57
pH	-392.01	610.5598	-0.64205	0.636639	-8149.91	7365.887	-8149.91	7365.887
EC	-11.0743	9.587449	-1.15508	0.454267	-132.894	110.7458	-132.894	110.7458
Redox	86.38605	63.56982	1.358916	0.403874	-721.345	894.1172	-721.345	894.1172

prob	5%	
	0.116117	EqualsTDIST(x,degree_freedom,tails)
t -critical	2.776445	equalsTINV(prob.,degree_freedom)
		equalsTINV(0.05,N-1)

Appendix E: Sample MPLABXIDE XC8 complier based C- source codes

E1: Listing one

```
/*File:  BIOGAS SYSTEM.c
 * Author: L.Matindife: University of south Africa (UNISA)
 */
/*Listing one*/
/* THIS LISTING COVERS 1)DIGESTER STABILITY, 2) BIOGAG OUTPUT AMOUNT , AND
 3}BIOGAS SYSTEM FAULT DETECTION AND STATUS*/
#include "Old3_1.h"
#include <math.h>
#include <stdio.h>
#include <stdlib.h>
#include <plib/delays.h>
#include <plib/xlcd.h>
#include <plib/adc.h>


void init_ADC1(void);               //Initialize ADC
void init_XLCD(void);               //Initialize LCD display
void DelayFor18TCY( void );         //18 cycles delay
void DelayPORXLCD (void);           // Delay of 15ms
void DelayXLCD (void);              // Delay of 5ms
float d_membershipmd(float k,float a,float b,float c,float d);/*Subroutine to
calculate
degree of membership of any monotonically decreasing function.In this case
this is the Q.acid membership function*/
float d_membershiptr(float k,float a,float b,float c,float d);/*Subroutine to
calculate
degree of membership of any triangular function.In this case these are the
M.acid,Nuetral
and M.alkaline membership functions*/
float d_membershipmi(float k,float a,float b,float c,float d);/*Subroutine to
calculate
degree of membership of any monotonically increasing function.In this case
this is the Q.alkaline membership function*/
float d_membershipmda(float xa,float a,float b,float c,float d);/*Subroutine
to calculate
degree of membership of the Low buffering capacity membership function*/
float d_membershiptra(float xa,float a,float b,float c,float d);/*Subroutine
to calculate
degree of membership of High buffering capacity membership function*/
float d_membershipmia(float xa,float a,float b,float c,float d);/*Subroutine
to calculate
degree of membership of the High buffering capacity membership function*/

//**************Declare Global
Varaibles************************************
unsigned int ADCResult[9]=0;
unsigned char ResultStr[10];
unsigned char Buffer[20];
//int i;//integer value for screen display
```

```
          float
voltage1,voltage2,voltage3,voltage4,voltage5,voltage6,voltage7,voltage8;
              float
voltage9,Vrll,k,ec,orp,xa,dmf,a,b,c,d,V21,V22,V23,V24,pHs;
              float degreestore[2][4]={{0},{0}};/*Array to store all degrees
of membership
              at specific memory locations for latter retrieval*/
              float digesterop[5][3]={{0},{0}};/*Rule matrix of digester
operation*/
              float firingcomb[3]={0};/*Array to store values of overall
combined firing
                                                    strengths of the rules*/
              float a1,a2,a3,b1,b2,b3,area1,area2,area3;
              float top1,top2,top3,crispout;

         float ts,fsd,hrt,ots,CH4,CO2,Vrl,Vrl2,V7,V8,Pressure,Oxygen;//..
         double lgPPM,logPPM,PPMCO2,PPM,Ratio,Ratio1,lgPPM1,PPM1;

void main(void)
{
    TRISCbits.RC0=0;//Stability alarm out
    TRISDbits.RD6=0;//Green methane leak LED output
    TRISDbits.RD7=0;//Yellow oxygen ingress LED output
    TRISCbits.RC1=1;//Level sensor SW1
    TRISCbits.RC2=1;//Level sensor SW12
    TRISCbits.RC6=0;//Soleniod valve drive
    TRISCbits.RC7=1;//Level sensor SW2
   //OSCCON=0x70;                   //Configure to use 8MHz internal
oscillator.
   init_XLCD();                    //Call the Initialize LCD display function
   init_ADC1();                   //Call the Initialize ADC function

    putrsXLCD(" DIGESTER ");              //Display "DIGESTER"
    SetDDRamAddr(0x40);             //shift cursor to beginning of second line
    putrsXLCD("STABILITY");       //Display "STABILITY"
    for (int i=0; i<=100;i++) __delay_ms(10); // 1 second delay
    WriteCmdXLCD(0x01);         //Clear Screen

    while(1)
    {

    //---sample and convert----
        for (unsigned char m=0; m<=8; m++)
        {

            ADCON0bits.CHS = m;
            DelayFor18TCY();
    ConvertADC();                    //Start conversion
    while(BusyADC());               //Wait here until conversion is finished
    ADCResult[m] = (unsigned int)ReadADC();          //Read the converted
data
    // convert the converted data into voltage
    //we divide by 1024 because its a 10-bit converted data

    voltage1 = (ADCResult[0]*5.0)/1024;//From pH sensor
       voltage2 = (ADCResult[1]*5.0)/1024;//From Redox sensor
```

```
       voltage3 = (ADCResult[2]*5.0)/1024;// From Electrical conductivity
sensor
       voltage4 = (ADCResult[3]*5.0)/1024;//Temperature sensor
       voltage5 = (ADCResult[4]*5.0)/1024;//Methane sensor
       voltage6 = (ADCResult[5]*5.0)/1024;//Carbon dioxide sensor
       voltage7 = (ADCResult[6]*5.0)/1024;//Pressure sensor
       voltage8 = (ADCResult[7]*5.0)/1024;//Oxygen sensor
       voltage9 = (ADCResult[8]*5.0)/1024;//Methane leak sensor

        }


            V21=2*voltage1 - 5;//Scale back pH value
           pHs = V21*1000/20;
               k = (350.0 - pHs)/50.0;//pH


           V22=2*voltage2 - 5;//Scale back Redox reading
           orp = (2*V22/5)*1000;//Redox


           V23= (4.9*voltage3)- 0.3837;//Scale conductivity input multiply
eqn. (25) *1000
           ec=V23;//Electrical conductivity mS/cm

           V24=(200.33*voltage4)-500.33;//.. Temperature
           ts=175;//..Total solids

           xa = (2148.33 - 392.01*k + 86.39*ec - 11.07*orp); // Alkalinity
prediction equation

           Vrl = voltage5;//Methane analogue voltage
           Ratio = (5-Vrl)/Vrl;//Ratio = Rs/Ro
           lgPPM = (log10(Ratio)*-2.6) + 2.7;//MQ2 sensor equation
           PPM =  pow(10,lgPPM);//Methane ppm

           Vrl2=voltage6;//Carbon dioxide analogue voltage
           logPPM= (-0.0247*Vrl2*1000)+10.55;//MG811 sensor equation
           PPMCO2=pow(10,logPPM);//Carbon dioxide ppm

              if (k>=0 && k<=5.5){//Select Q.acid membership function
              a=0;//Limits for the Q.acid membership function
            b=0;
            c=5.5f;
            d=6;
              dmf=d_membershipmd( k, a, b, c, d);//Degree of membership from
subroutine
              degreestore[0][0]=dmf;//Q.acid degree of membership for this
input
              degreestore[0][1]=(1-dmf);}//M.acid degree of membership for
this input
              else if(k>5.5 && k<=6)//Select M.acid membership function
              {a=5.5f;//Limits for the M.acid membership function
            b=6;
            c=6;
            d=7;
```

```
              dmf=d_membershiptr( k, a, b, c, d);//Degree of membership from
subroutine
              degreestore[0][1]=dmf;//M.acid degree of membership
              degreestore[0][0]=(1-dmf);}//Q.acid degree of membership
              else if(k>6 && k<=7)//Select Nuetral membership function
              {a=6;//Limits for the Nuetral membership function
            b=7;
            c=7;
            d=8;
              dmf=d_membershiptr( k, a, b, c, d);//Degree of membership from
subroutine
              degreestore[0][2]=dmf;//Nuetral degree of membership
              degreestore[0][1]=(1-dmf);}//M.acid degree of membership
          else if(k>7 && k<=8)//Select M.alkaline membership function
              {a=7;//Limits for the M.alkaline membership function
            b=8;
            c=8;
            d=8.5f;
              dmf=d_membershiptr( k, a, b, c, d);//Degree of membership from
subroutine
            degreestore[0][3]=dmf;//M.alkaline degree of membership
              degreestore[0][2]=(1-dmf);}//Nuetral degree of membership
              else {//Select Q.alkaline membership function
              a=8;//Limits for the Q.alkaline membership function
            b=8.5f;
            c=14;
            d=14;
              dmf=d_membershipmi( k, a, b, c, d);//Degree of membership from
subroutine
            degreestore[1][0]=dmf;//Q.alkaline degree of membership
              degreestore[0][3]=(1-dmf);}//M.alkaline degree of membership
       if (xa>=1500 && xa<=3500){//Select LOW buffer capacity membership
function
              a=1500;//Limits for LOW buffer capacity membership function
            b=1500;
            c=3500;
            d=4000;
              dmf=d_membershipmda( xa, a, b, c, d);//Degree of membership
from subroutine
              degreestore[1][1]=dmf;//LOW degree of membership
              degreestore[1][2]=(1-dmf);}//MEDIUM degree of membership
              else if(xa>3500 && xa<=4000)//Select MEDIUM buffer capacity
membership function
              {a=3500;//Limits for the MEDIUM alkalinity membership function
            b=4000;
            c=4000;
            d=4500;
              dmf=d_membershiptra( xa, a, b, c, d);//Degree of membership
from subroutine
              degreestore[1][2]=dmf;//MEDIUM degree of membership
              degreestore[1][1]=(1-dmf);}//LOW degree of membership
              else {//Select HIGH buffer capacity membership function
              a=4000;//Limits for HIGH buffer capacity membership function
            b=4500;
            c=5500;
            d=5500;
```

```
              dmf=d_membershipmia( xa, a, b, c, d);//Degree of membership
from subroutine*/
              degreestore[1][3]=dmf;//HIGH degree of membership
              degreestore[1][2]=(1-dmf);}//MEDIUM degree of membership


  /*Evaluate the firing strengths of the fifteen (15) rules for the required
digester operation status*/
  /*The results according to the Max-Min method are stored in an array
digesterop*/
              if((degreestore[0][0])>(degreestore[1][3])){//Rule 1 (Failed
output)
                    digesterop[0][0]=degreestore[1][3];}
              else
              {digesterop[0][0]=degreestore[0][0];}
              if((degreestore[0][0])>(degreestore[1][2])){//Rule 2 (Failed
ouput)
                    digesterop[0][1]=degreestore[1][2];}
              else
              {digesterop[0][1]=degreestore[0][0];}
          if((degreestore[0][0])>(degreestore[1][1])){//Rule 3 (Failed ouput)
                    digesterop[0][2]=degreestore[1][1];}
              else
              {digesterop[0][2]=degreestore[0][0];}
          if((degreestore[0][1])>(degreestore[1][3])){//Rule 4 (Optimum
ouput)
                    digesterop[1][0]=degreestore[1][3];}
              else
              {digesterop[1][0]=degreestore[0][1];}
              if((degreestore[0][1])>(degreestore[1][2])){//Rule 5 (Optimum
ouput)
                    digesterop[1][1]=degreestore[1][2];}
              else
              {digesterop[1][1]=degreestore[0][1];}
          if((degreestore[0][1])>(degreestore[1][1])){//Rule 6 (Failing
ouput)
                    digesterop[1][2]=degreestore[1][1];}
              else
              {digesterop[1][2]=degreestore[0][1];}
              if((degreestore[0][2])>(degreestore[1][3])){//Rule 7 (Optimum
ouput)
                    digesterop[2][0]=degreestore[1][3];}
              else
              {digesterop[2][0]=degreestore[0][2];}
              if((degreestore[0][2])>(degreestore[1][2])){//Rule 8 (Optimum
ouput)
                    digesterop[2][1]=degreestore[1][2];}
              else
              {digesterop[2][1]=degreestore[0][2];}
              if((degreestore[0][2])>(degreestore[1][1])){//Rule 9 (Failing
ouput)
                    digesterop[2][2]=degreestore[1][1];}
              else
              {digesterop[2][2]=degreestore[0][2];}
              if((degreestore[0][3])>(degreestore[1][3])){//Rule 10 (Optimum
ouput)
                    digesterop[3][0]=degreestore[1][3];}
```

```
              else
              {digesterop[3][0]=degreestore[0][3];}
              if((degreestore[0][3])>(degreestore[1][2])){//Rule 11 (Optimum
ouput)
                    digesterop[3][1]=degreestore[1][2];}
              else
              {digesterop[3][1]=degreestore[0][3];}
              if((degreestore[0][3])>(degreestore[1][1])){//Rule 12 (Failing
ouput)
                    digesterop[3][2]=degreestore[1][1];}
              else
              {digesterop[3][2]=degreestore[0][3];}
            if((degreestore[1][0])>(degreestore[1][3])){//Rule 13 (Failed
ouput)
                    digesterop[4][0]=degreestore[1][3];}
              else
              {digesterop[4][0]=degreestore[1][0];}
              if((degreestore[1][0])>(degreestore[1][2])){//Rule 14 (Failed
ouput)
                    digesterop[4][1]=degreestore[1][2];}
              else
              {digesterop[4][1]=degreestore[1][0];}
              if((degreestore[1][0])>(degreestore[1][1])){//Rule 15 (Failed
ouput)
                    digesterop[4][2]=degreestore[1][1];}
              else
              {digesterop[4][2]=degreestore[1][0];}


             /*Max-Min method for output combination of the rules, by
measuring relative
               magnitudes of the respective firing strengths of the rules and
taking note
               of the most significant one*/

              if ((digesterop[0][0])<(digesterop[0][1])){      /* Degree of
membership*/
                    firingcomb[0]=digesterop[0][1];}             /* of Failed
status of */
              else if ((digesterop[0][1])<(digesterop[0][2])){ /* digester
operation  */
                    firingcomb[0]=digesterop[0][2];}
              else if ((digesterop[0][2])<(digesterop[4][0])){
                    firingcomb[0]=digesterop[4][0];}
              else if ((digesterop[4][0])<(digesterop[4][1])){
                    firingcomb[0]=digesterop[4][1];}
              else if ((digesterop[4][1])<(digesterop[4][2])){
                    firingcomb[0]=digesterop[4][2];}
              else {
                    firingcomb[0]=digesterop[0][0];}

              if ((digesterop[1][2])<(digesterop[2][2])){      /* Degree of
membership*/
                    firingcomb[1]=digesterop[2][2];}             /* of
Failing status of */
              else if ((digesterop[2][2])<(digesterop[3][2])){ /* digester
operation  */
```

```
                  firingcomb[1]=digesterop[3][2];}
            else {
                  firingcomb[1]=digesterop[1][2];}

            if ((digesterop[1][0])<(digesterop[1][1])){      /* Degree of
membership*/
                  firingcomb[2]=digesterop[1][1];}             /* of
Optimum status of */
            else if ((digesterop[1][1])<(digesterop[2][0])){ /* digester
operation  */
                  firingcomb[2]=digesterop[2][0];}
            else if ((digesterop[2][0])<(digesterop[2][1])){
                  firingcomb[2]=digesterop[2][1];}
            else if ((digesterop[2][1])<(digesterop[3][0])){
                  firingcomb[2]=digesterop[3][0];}
            else if ((digesterop[3][0])<(digesterop[3][1])){
                  firingcomb[2]=digesterop[3][1];}
            else {
                  firingcomb[2]=digesterop[1][0];}


            /*DEFUZZIFICATION using CENTER OF GRAVITY(COG) method*/

            a1=0;       //slope1 of Failed =0
            a2=firingcomb[1]*20;//height x slope1 of Failing trapezium
            a3=firingcomb[2]*20;//height x slope1(slope2=0) of optimum
trapezium
            b1=firingcomb[0]*20;//height x slope2 of Failed
            b2=firingcomb[1]*20;//height x slope 2 of Failing
            b3=0;
            top1=50-a1-b1;
            top2=40-a2-b2;
            top3=50-a3-b3;
            area1=firingcomb[0]*((50+top1)/2);//Area of Failed
            area2=firingcomb[1]*((40+top2)/2);//Area of Failing
            area3=firingcomb[2]*((50+top3)/2);//Area of Optimum
          crispout=((area1*25)+(area2*50)+(area3*75))/(area1+area2+area3);


    WriteCmdXLCD(0x01);
    putrsXLCD("% Stability = ");         //Display "Stability" on the screen
    sprintf(Buffer, "%.3g", crispout );    // Convert stability to string
    putsXLCD(Buffer);              //Display the Stability on the screen
    putrsXLCD("   ");           // Clear after comma
    WriteCmdXLCD(0x02);             //Home position on LCD
    for (int i=0; i<=100;i++) __delay_ms(10); //// 1 second delay
    WriteCmdXLCD(0x01);       ///Clear Screen
    putrsXLCD(" pH = ");          ////Display "pH" on the screen
    sprintf(Buffer, "%.3g", k );    //// Convert pH to string
    putsXLCD(Buffer);              ////Display the pH on the screen
    putrsXLCD("   ");           //// Clear after comma
    WriteCmdXLCD(0x02);             ////Home position on LCD
    for (int i=0; i<=100;i++) __delay_ms(10); //// 1 second delay
    WriteCmdXLCD(0x01);       ///Clear Screen
    putrsXLCD(" Alk. = ");          ////Display "Alkalinity" on the screen
    sprintf(Buffer, "%.3g", xa );    //// Convert Alkalinity to string
    putsXLCD(Buffer);              ////Display the Alkalinity on the screen
```

```
    putrsXLCD("   ");           //// Clear after comma
    WriteCmdXLCD(0x02);             ////Home position on LCD
    for (int i=0; i<=100;i++) __delay_ms(10); //// 1 second delay
    ////////////////////////////////////////////////
    /*Find out whether the cause for poor digester stability is due to too
low a pH value,
      too high a pH value or too low a buffering capacity*/
    // RESTORE SYSTEM TO STABILITY and Reset Alarms and Clear displays\n");

    if((k>=5.5) && (k<=8.5) && (xa<3500)){
        WriteCmdXLCD(0x01);
        LATCbits.LATC0=1;//Activate Stability Alarm

     putrsXLCD(" pH Good,Low Alk.");             //Display "pH Good, Low
Alk."
    SetDDRamAddr(0x40);            //shift cursor to beginning of second line
    putrsXLCD("Increase Alk. ");      //Display "Increase Alk."
    WriteCmdXLCD(0x02);
     for (int i=0; i<=100;i++) __delay_ms(10); // 1 second delay
    LATCbits.LATC0=0;//Clear Alarm

    }
      else if(k<5.5 && xa>=3500){
        WriteCmdXLCD(0x01);
        LATCbits.LATC0=1;//Activate Stability Alarm
        putrsXLCD(" pH too Low");             //Activate failed alarm
    SetDDRamAddr(0x40);            //shift cursor to beginning of second line
    putrsXLCD("Add lime ");      //Display "Add lime"
    WriteCmdXLCD(0x02);
     for (int i=0; i<=100;i++) __delay_ms(10); // 1 second delay
    LATCbits.LATC0=0;//Clear Alarm

    }
    else if(k<5.5 && xa<3500){
        WriteCmdXLCD(0x01);
        putrsXLCD(" pH low, Alk.");             //Display "pH low, Alk."
    SetDDRamAddr(0x40);            //shift cursor to beginning of second line
    putrsXLCD(" low, correct ");      //Display " low correct"
    WriteCmdXLCD(0x02);
     for (int i=0; i<=100;i++) __delay_ms(10); // 1 second delay

    }

      else if(k>8.5 && xa>=3500){
        WriteCmdXLCD(0x01);
        putrsXLCD(" pH high, add");             //Display "pH high, add"
    SetDDRamAddr(0x40);            //shift cursor to beginning of second line
    putrsXLCD(" acetic acid");      //Display "acetic acid"
    WriteCmdXLCD(0x02);
     for (int i=0; i<=100;i++) __delay_ms(10); // 1 second delay

    }

      else if(k>8.5 && xa<3500){
        WriteCmdXLCD(0x01);
        putrsXLCD(" pH high, Alk.");             //Display "pH high, Alk."
    SetDDRamAddr(0x40);            //shift cursor to beginning of second line
```

```
    putrsXLCD("low, correct ");      //Display " low correct"
    WriteCmdXLCD(0x02);
     for (int i=0; i<=100;i++) __delay_ms(10); // 1 second delay


    }
      else {
        WriteCmdXLCD(0x01);
        putrsXLCD(" Digester is");             //Display " Digester is"
    SetDDRamAddr(0x40);            //shift cursor to beginning of second line
    putrsXLCD("Failing");      //Display "Failing"
    WriteCmdXLCD(0x02);
     for (int i=0; i<=100;i++) __delay_ms(10); // 1 second delay

    }
////////////////////////////////////////////////////////////////////////////
//////////////////
    // BIOGAS AMOUNT
CALCULATION.....................................................
    //degreestore[2][4]={{0},{0}};//..
    //digesterop[5][3]={{0},{0}};//..
    //firingcomb[3]={0};//..
    k=0;
    xa=0;
    crispout=0;
    fsd=(ts/80);//..Feedstock(slurry) per day
    hrt=50/fsd;//..Hyraulic retention time
    ots=ts*0.85f;//Organic total solids

              k=ots/50;//Organic loading rate
          xa=V24;

          if (k>=0 && k<=0.5){//Select OLRL membership function
              a=0;//Limits for the OLRL membership function
            b=0;
            c=0.5f;
            d=1.5f;
              dmf=d_membershipmd( k, a, b, c, d);//Degree of membership from
subroutine
              degreestore[0][0]=dmf;//OLRL degree of membership for this
input
              degreestore[0][1]=(1-dmf);}//OLRG degree of membership for this
input
              else if(k>0.5 && k<=4)//Select OLRG membership function
              {a=0.5f;//Limits for the OLRG membership function
            b=1.5f;
            c=3;
            d=4;
              dmf=d_membershiptr( k, a, b, c, d);//Degree of membership from
subroutine
              degreestore[0][1]=dmf;//OLRG degree of membership
              degreestore[0][0]=(1-dmf);}//OLRL degree of membership

              else {//Select OLRH membership function
              a=3;//Limits for the OLRH membership function
            b=4;
            c=7;
```

```
            d=7;
              dmf=d_membershipmi( k, a, b, c, d);//Degree of membership from
subroutine
            degreestore[1][0]=dmf;//OLRH degree of membership
              degreestore[0][1]=(1-dmf);}//OLRG degree of membership
       if (xa>=0 && xa<=15){//Select LOW Temperature membership function
              a=0;//Limits for LOW Temperature membership function
            b=0;
            c=15;
            d=30;
              dmf=d_membershipmda( xa, a, b, c, d);//Degree of membership
from subroutine
              degreestore[1][1]=dmf;//LOW Temperature degree of membership
              degreestore[1][2]=(1-dmf);}//Optimum Temperature degree of
membership

              else {//Select Optimum Temperature membership function
              a=15;//Limits for HIGH buffer capacity membership function
            b=30;
            c=55;
            d=55;
              dmf=d_membershipmia( xa, a, b, c, d);//Degree of membership
from subroutine*/
              degreestore[1][2]=dmf;//Optimum Temperature degree of
membership
              degreestore[1][1]=(1-dmf);}//Low Temperature degree of
membership

  /*Evaluate the firing strengths of the fifteen (15) rules for the required
digester operation status*/
  /*The results according to the Max-Min method are stored in an array
digesterop*/
              if((degreestore[0][0])>(degreestore[1][1])){//Rule 1 (Biogas
Low output)
                    digesterop[0][0]=degreestore[1][1];}
              else
              {digesterop[0][0]=degreestore[0][0];}
              if((degreestore[0][0])>(degreestore[1][2])){//Rule 2 (Biogas
Low ouput)
                    digesterop[0][1]=degreestore[1][2];}
              else
              {digesterop[0][1]=degreestore[0][0];}
          if((degreestore[0][1])>(degreestore[1][1])){//Rule 3 (Biogas
Average ouput)
                    digesterop[0][2]=degreestore[1][1];}
              else
              {digesterop[0][2]=degreestore[0][1];}
          if((degreestore[0][1])>(degreestore[1][2])){//Rule 4 (Biogas High
ouput)
                    digesterop[1][0]=degreestore[1][2];}
              else
              {digesterop[1][0]=degreestore[0][1];}
              if((degreestore[1][0])>(degreestore[1][1])){//Rule 5 (Biogas
Low ouput)
                    digesterop[1][1]=degreestore[1][1];}
              else
              {digesterop[1][1]=degreestore[1][0];}
```

```
          if((degreestore[1][0])>(degreestore[1][2])){//Rule 6 (Biogas
Average ouput)
                digesterop[1][2]=degreestore[1][2];}
              else
              {digesterop[1][2]=degreestore[1][0];}


             /*Max-Min method for output combination of the rules, by
measuring relative
              magnitudes of the respective firing strengths of the rules and
taking note
              of the most significant one*/

              if ((digesterop[0][0])<(digesterop[0][1])){      /* Degree of
membership*/
                    firingcomb[0]=digesterop[0][1];}             /* of Gas
low of */
              else if ((digesterop[0][1])<(digesterop[1][1])){ /* biogas
output  */
                    firingcomb[0]=digesterop[1][1];}
              else {
                    firingcomb[0]=digesterop[0][0];}

              if ((digesterop[0][2])<(digesterop[1][2])){      /* Degree of
membership*/
                    firingcomb[1]=digesterop[1][2];}             /* of Gas
Average of */
              else if ((digesterop[1][2])<(digesterop[1][0])){ /* biogas
output  */
                    firingcomb[1]=digesterop[1][0];}
              else {
                    firingcomb[1]=digesterop[0][2];}                    /*
Degree of membership*/
                        firingcomb[2]=digesterop[1][0];
      /* of Gas High of */

            /* biogas output*/

              /*DEFUZZIFICATION using CENTER OF GRAVITY(COG) method*/

              a1=0;       //slope1 of Failed =0
              a2=firingcomb[1]*4;//height x slope1 of Failing trapezium
              a3=firingcomb[2]*8;//height x slope1(slope2=0) of optimum
trapezium
              b1=firingcomb[0]*4;//height x slope2 of Failed
              b2=firingcomb[1]*8;//height x slope 2 of Failing
              b3=0;
              top1=7-a1-b1;
              top2=12-a2-b2;
              top3=13-a3-b3;
              area1=firingcomb[0]*((7+top1)/2);//Area of Failed
              area2=firingcomb[1]*((12+top2)/2);//Area of Failing
              area3=firingcomb[2]*((13+top3)/2);//Area of Optimum
          crispout=((area1*3.5)+(area2*7)+(area3*13.5))/(area1+area2+area3);
```

```
                          //printf("Biogas output in 1000litres/day = %.2f\n
",crispout);//Print Array
      //while(crispout>=60)/*If digester stability is greater or equal to 60%
then system is
                                  //stable , go back to start of program else
flag alarm*/
            //goto label;

              CH4=crispout*0.6*1000;
              CO2=crispout*0.4*1000;

              WriteCmdXLCD(0x01);
    putrsXLCD(" Temp.oC = ");         //Display "Temp.oC" on the screen
    sprintf(Buffer, "%.3g", xa );    // Convert Temperature to string
    putsXLCD(Buffer);              //Display the Temperature on the screen
    putrsXLCD("   ");           // Clear after comma
    WriteCmdXLCD(0x02);             //Home position on LCD
    for (int i=0; i<=100;i++) __delay_ms(10); //// 1 second delay
    WriteCmdXLCD(0x01);       ///Clear Screen
    putrsXLCD(" HRT(days)= ");         ////Display "HRT" on the screen
    sprintf(Buffer, "%.3g", hrt );    //// Convert HRT to string
    putsXLCD(Buffer);              ////Display the HRT on the screen
    putrsXLCD("   ");           //// Clear after comma
    WriteCmdXLCD(0x02);             ////Home position on LCD
    for (int i=0; i<=100;i++) __delay_ms(10); //// 1 second delay

          WriteCmdXLCD(0x01);
    putrsXLCD(" OLR.kg/m3.day ");         //Display "OLR" on the screen
   SetDDRamAddr(0x40);
   putrsXLCD(" = ");
    sprintf(Buffer, "%.3g", k );    // Convert OLR to string
    putsXLCD(Buffer);              //Display the OLR on the screen
    putrsXLCD("   ");           // Clear after comma
    WriteCmdXLCD(0x02);             //Home position on LCD
    for (int i=0; i<=100;i++) __delay_ms(10); //// 1 second delay
          WriteCmdXLCD(0x01);
    putrsXLCD(" Methane(Litres)");         //Display "Stability" on the
screen
   SetDDRamAddr(0x40);
   putrsXLCD(" = ");
    sprintf(Buffer, "%.3g", CH4 );    // Convert stability to string
    putsXLCD(Buffer);              //Display the Stability on the screen
    putrsXLCD("   ");           // Clear after comma
    WriteCmdXLCD(0x02);             //Home position on LCD
    for (int i=0; i<=100;i++) __delay_ms(10); //// 1 second delay
    WriteCmdXLCD(0x01);       ///Clear Screen
    putrsXLCD(" CO2(Litres)"); ////Display "CO2 (Litres)" on the screen
   SetDDRamAddr(0x40);
   putrsXLCD(" = ");
    sprintf(Buffer, "%.3g", CO2 );    //// Convert CO2 to string
    putsXLCD(Buffer);              ////Display the CO2 on the screen
    putrsXLCD("   ");           //// Clear after comma
    WriteCmdXLCD(0x02);             ////Home position on LCD
    for (int i=0; i<=100;i++) __delay_ms(10); //// 1 second delay
    WriteCmdXLCD(0x01);       ///Clear Screen
     putrsXLCD(" CH4 PPM");    ////Display "CH4 PPM" on the screen
   SetDDRamAddr(0x40);
```

```
   putrsXLCD(" = ");
    sprintf(Buffer, "%.5g", PPM );     //// Convert PPM to string
    putsXLCD(Buffer);               ////Display the PPM on the screen
    putrsXLCD("   ");            //// Clear after comma
    WriteCmdXLCD(0x02);              ////Home position on LCD
    for (int i=0; i<=100;i++) __delay_ms(10); //// 1 second delay
    // degreestore[2][4]={{0},{0}};//..
    //digesterop[5][3]={{0},{0}};//..
    //firingcomb[3]={0};//..

    k=0;
    xa=0;
    crispout=0;


//.....................................................................
.......

//xxxxxxxxxxxxxxxxxxxxxxxxxxxxxxxxxxxxxxxxxxxxxxxxxxxxxxxxxxxxxxxxxxxxxxxxxxxxxxxxxx
xxxxxxxxxxx
    //DIGESTER FAULT DETECTION AND STATUS INDICATION
    V7=voltage7;//Analogue pressure voltage
    V8=voltage8;//Analogue oxygen voltage
    Pressure = (-0.1612*V7*V7)+ 7.203*V7-9.7921;//Pressure equation
    k=Pressure;
    //k=9;
    Vrll = voltage9;//Methane leak analogue voltage
           Ratio1 = (5-Vrll)/Vrll;//Ratio = Rs/Ro
           lgPPM1 = (log10(Ratio1)*-2.6) + 2.7;//MQ2 sensor equation
           PPM1 =  pow(10,lgPPM1);//Methane leak ppm

    Oxygen=(0.479*V8/91)*1000+16.54;
    if (Oxygen>=15){
        LATDbits.LATD7=1;//Yellow LED On
        LATCbits.LATC0=1;//Activate Oxygen Alarm
        LATCbits.LATC6=1;//Solenoid ON until MCLR reset
       for (int i=0; i<=100;i++) __delay_ms(10); // 1 second delay
       LATCbits.LATC0=0;//Switch off Low level Alarm
       LATDbits.LATD7=0;//Yellow LED Off
    }

    if (PPM1>=1000){
        LATDbits.LATD6=1;//Green LED On
        LATCbits.LATC0=1;//Activate methane leak Alarm
        LATCbits.LATC6=1;//Solenoid ON until MCLR reset
       for (int i=0; i<=100;i++) __delay_ms(10); // 1 second delay
       LATCbits.LATC0=0;//Switch off Low level Alarm
       LATDbits.LATD6=0;//Green LED Off
    }


    if (k>=0 && k<=10){//Select LP biogas pressure membership function
              a=0;//Limits for the LP membership function
            b=0;
            c=0;
            d=10;
```

```
              dmf=d_membershipmd( k, a, b, c, d);//Degree of membership from
subroutine
              degreestore[0][0]=dmf;//LP degree of membership for this input
              degreestore[0][1]=(1-dmf);}//GP degree of membership for this
input
              else if(k>10 && k<=15)//Select GP biogas pressure membership
function
              {a=0;//Limits for the GP membership function
            b=10;
            c=15;
            d=25;
              dmf=d_membershiptr( k, a, b, c, d);//Degree of membership from
subroutine
              degreestore[0][1]=dmf;//GP biogas pressure degree of membership
              degreestore[0][0]=(1-dmf);}//LP degree of membership

              else {//Select HP biogas pressure membership function
              a=15;//Limits for the HP membership function
            b=25;
            c=25;
            d=25;
              dmf=d_membershipmi( k, a, b, c, d);//Degree of membership from
subroutine
            degreestore[1][0]=dmf;//HP biogas pressure degree of membership
              degreestore[0][1]=(1-dmf);}//GP degree of membership
    if((PORTCbits.RC1==0) && (PORTCbits.RC2==0)&& (PORTCbits.RC7==0)){
       LATCbits.LATC0=1;//Activate Low level Alarm
       for (int i=0; i<=100;i++) __delay_ms(10); // 1 second delay
       LATCbits.LATC0=0;//Switch off Low level Alarm
    }
       //if (xa>=0 && xa<=0.25){//Select LL displacement membership function
    if((PORTCbits.RC1==1) && (PORTCbits.RC2==0)){
          xa=0.13;
          a=0;//Limits for LOW Temperature membership function
            b=0;
            c=0;
            d=0.25f;
              dmf=d_membershipmda( xa, a, b, c, d);//Degree of membership
from subroutine
              degreestore[1][1]=dmf;//LL slurry displacement degree of
membership
              degreestore[1][2]=(1-dmf);}//BPO slurry displacement degree of
membership
             // else if(xa>0 && xa<0.5)//Select BPO slurry displacement
membership function
    else if ((PORTCbits.RC2==1) && (PORTCbits.RC7==0)){
        xa=0.25;
              a=0;//Limits for BPO membership function
            b=0.25f;
            c=0.25f;
            d=0.5f;
              dmf=d_membershiptra( xa, a, b, c, d);//Degree of membership
from subroutine
              degreestore[1][2]=dmf;//BPO degree of membership
              degreestore[1][1]=(1-dmf);}//LL degree of membership*/
              else {//Select HL slurry displacement membership function
        xa=0.45;
```

```
              a=0.25f;//Limits for HL slurry displacement membership function
            b=0.5f;
            c=0.5f;
            d=0.5f;
              dmf=d_membershipmia( xa, a, b, c, d);//Degree of membership
from subroutine*/
              degreestore[1][3]=dmf;//HL slurry displacement degree of
membership
              degreestore[1][2]=(1-dmf);}//BPO degree of membership

  /*Evaluate the firing strengths of the nine (9) rules for the required
digester danger status*/
  /*The results according to the Max-Min method are stored in an array
digesterop*/
              if((degreestore[0][0])>(degreestore[1][1])){//Rule 1 (No danger
output)
                    digesterop[0][0]=degreestore[1][1];}
              else
              {digesterop[0][0]=degreestore[0][0];}
              if((degreestore[0][0])>(degreestore[1][2])){//Rule 2 (Low
danger ouput)
                    digesterop[0][1]=degreestore[1][2];}
              else
              {digesterop[0][1]=degreestore[0][0];}
          if((degreestore[0][0])>(degreestore[1][3])){//Rule 3 (High danger
output)
                    digesterop[0][2]=degreestore[1][3];}
              else
              {digesterop[0][2]=degreestore[0][0];}
          if((degreestore[0][1])>(degreestore[0][0])){//Rule 4 (Low danger
ouput)
                    digesterop[1][0]=degreestore[0][0];}
              else
              {digesterop[1][0]=degreestore[0][1];}
              if((degreestore[0][1])>(degreestore[1][2])){//Rule 5 (No danger
ouput)
                    digesterop[1][1]=degreestore[1][2];}
              else
              {digesterop[1][1]=degreestore[0][1];}
          if((degreestore[0][1])>(degreestore[1][3])){//Rule 6 (Low danger
ouput)
                    digesterop[1][2]=degreestore[1][3];}
              else
              {digesterop[1][2]=degreestore[0][1];}
              if((degreestore[1][0])>(degreestore[0][0])){//Rule 7 (High
danger ouput)
                    digesterop[2][0]=degreestore[0][0];}
              else
              {digesterop[2][0]=degreestore[1][0];}
              if((degreestore[1][0])>(degreestore[1][2])){//Rule 8 (Low
danger ouput)
                    digesterop[2][1]=degreestore[1][2];}
              else
              {digesterop[2][1]=degreestore[1][0];}
              if((degreestore[1][0])>(degreestore[1][3])){//Rule 9 (No danger
ouput)
                    digesterop[2][2]=degreestore[1][3];}
```

```
              else
              {digesterop[2][2]=degreestore[1][0];}

             /*Max-Min method for output combination of the rules, by
measuring relative
               magnitudes of the respective firing strengths of the rules and
taking note
               of the most significant one*/

              if ((digesterop[0][0])<(digesterop[1][1])){      /* Degree of
membership*/
                    firingcomb[0]=digesterop[1][1];}             /* of No
danger */
              else if ((digesterop[1][1])<(digesterop[2][2])){ /* digester
output  */
                    firingcomb[0]=digesterop[2][2];}

              else {
                    firingcomb[0]=digesterop[0][0];}

              if ((digesterop[0][1])<(digesterop[1][0])){      /* Degree of
membership*/
                    firingcomb[1]=digesterop[1][0];}             /* of Low
danger */
              else if ((digesterop[1][0])<(digesterop[1][2])){ /* digester
output  */
                    firingcomb[1]=digesterop[1][2];}
                  else if ((digesterop[1][2])<(digesterop[2][1])){
                    firingcomb[1]=digesterop[2][1];}
              else {
                    firingcomb[1]=digesterop[0][1];}

              if ((digesterop[0][2])<(digesterop[2][0])){      /* Degree of
membership*/
                     firingcomb[2]=digesterop[2][0];}             /* of High
danger */

              else {
                    firingcomb[2]=digesterop[0][0];}


              /*DEFUZZIFICATION using CENTER OF GRAVITY(COG) method*/

              a1=0;       // +ve slope1 of No danger =0
              a2=firingcomb[1]*50;//height x +ve slope1 of Low danger
trapezium
              a3=firingcomb[2]*50;//height x +ve slope1(slope2=0) of high
danger trapezium
              b1=firingcomb[0]*50;//height x -ve slope2 of No danger
              b2=firingcomb[1]*50;//height x -ve slope 2 of Low danger
              b3=0;// -ve slope of No danger
              top1=50-a1-b1;//varying top1 width from maximum to minimum
              top2=100-a2-b2;
              top3=50-a3-b3;
              area1=firingcomb[0]*((50+top1)/2);//Area of No danger
              area2=firingcomb[1]*((100+top2)/2);//Area of Low danger
              area3=firingcomb[2]*((50+top3)/2);//Area of High danger
```

```
          crispout=((area1*25)+(area2*50)+(area3*75))/(area1+area2+area3);
          WriteCmdXLCD(0x01);       ///Clear Screen
     putrsXLCD(" %Digest.Danger ");////Display "%Digest.Danger" on the screen
   SetDDRamAddr(0x40);
   putrsXLCD(" Level = ");
    sprintf(Buffer, "%.3g", crispout ); //// Convert %Digest.Danger to string
    putsXLCD(Buffer);     ////Display the %Digest.Danger on the screen
    putrsXLCD("   ");           //// Clear after comma
    WriteCmdXLCD(0x02);             ////Home position on LCD
    for (int i=0; i<=100;i++) __delay_ms(10); //// 1 second delay

          k=0;
          xa=0;
          crispout=0;
//XXXXXXXXXXXXXXXXXXXXXXXXXXXXXXXXXXXXXXXXXXXXXXXXXXXXXXXXXXXXXXXXXXXXXXXXXXXXx
xXXXXXXXXXXXXXXXXXXXX


    }
    }

void init_XLCD(void)                 //Initialize LCD display
{
    OpenXLCD(FOUR_BIT&LINES_5X7);  //configure LCD in 4-bit Data Interface
mode
                                     //and 5x7 characters, multiple line
display
    while(BusyXLCD());              //Check if the LCD controller is not busy
                                     //before writing some commands?
    WriteCmdXLCD(0x06);             // move cursor right, don?t shift display
    WriteCmdXLCD(0x0C);             //turn display on without cursor

 }

void init_ADC1(void)               //Initialize ADC
{
  /**** ADC configured for:
    * FOSC/2 as conversion clock
    * Result is right justified
    * Aquisition time of 2 AD
    * Channel 1 for sampling
    * ADC interrupt off
    * ADC reference voltage from VDD & VSS
*/
    OpenADC(ADC_FOSC_2 & ADC_RIGHT_JUST & ADC_2_TAD,
            ADC_CH0 & ADC_INT_OFF & ADC_REF_VDD_VSS,
            ADC_9ANA);
}

void DelayFor18TCY( void )          //18 cycles delay
{
  Delay10TCYx(2);
return;
}

void DelayPORXLCD (void)   // Delay of 15ms
{
```

```
    Delay1KTCYx(60);        // Cycles=(Time Delay*Fosc)/4
   //__delay_ms(15);        // Cycles =(15ms*16MHz)/4
                            // Cycles =60000
}

void DelayXLCD (void)        // Delay of 5ms
{
   Delay1KTCYx(20);          // Cycles = 20000
    //__delay_ms(5);

}

float d_membershipmd(float k,float a,float b,float c,float d) /*x is input
value
     from sensor into subroutine*/
            {
      //float dmf;
    if (k>c && k<d)
      { dmf=(d-k)/(d-c); }
      else if (k>=b && k<=c)
      {dmf=1.0; }
      else
      { dmf=0; }
      return dmf;//Return value from subroutine into main program
      }
      float d_membershiptr(float k,float a,float b,float c,float d) /*k is
input value
     from sensor into subroutine*/
            {
      //float dmf;
      if (k >a && k <b)
      { dmf=(k-a)/(b-a);}
      else if (k>c && k<d)
      { dmf=(d-k)/(d-c); }
      else if (k>=b && k<=c)
      {dmf=1.0; }
      else
      { dmf=0; }
      return dmf;//Return value from subroutine into main program
      }
      float d_membershipmi(float k,float a,float b,float c,float d) /*x is
input value
     from sensor into subroutine*/
            {
      //float dmf;
      if (k >a && k <b)
      { dmf=(k-a)/(b-a);}
      else if (k>=b && k<=c)
      {dmf=1.0; }
      else
      { dmf=0; }
      return dmf;//Return value from subroutine into main program
      }
    float d_membershipmda(float xa,float a,float b,float c,float d) /*xa is
input value
     from sensor into subroutine*/
            {
```

```
      //float dmf;
    if (xa>c && xa<d)
      { dmf=(d-xa)/(d-c); }
      else if (xa>=b && xa<=c)
      {dmf=1.0; }
      else
      { dmf=0; }
      return dmf;//Return value from subroutine into main program
      }
      float d_membershiptra(float xa,float a,float b,float c,float d) /*xa is
input value
     from sensor into subroutine*/
            {
      //float dmf;
      if (xa >a && xa <b)
      { dmf=(xa-a)/(b-a);}
      else if (xa>c && xa<d)
      { dmf=(d-xa)/(d-c); }
      else if (xa>=b && xa<=c)
      {dmf=1.0; }
      else
      { dmf=0; }
      return dmf;//Return value from subroutine into main program
      }
      float d_membershipmia(float xa,float a,float b,float c,float d) /*xa is
input value
     from sensor into subroutine*/
            {
      //float dmf;
      if (xa >a && xa <b)
      { dmf=(xa-a)/(b-a);}
      else if (xa>=b && xa<=c)
      {dmf=1.0; }
      else
      { dmf=0; }
      return dmf;//Return value from subroutine into main program
      }
```

E2: Listing two

```
/*File:  PHOTOVOLTAIC SYSTEM.c
 * Author: L.Matindife: University of south Africa (UNISA)
 */
/*Listing two*/
//THIS LISTING COVERS 1) SOLAR BATTERY CHARGING/DISCHARGING, AND 2) SOLAR
FAULT DETECTION AND STATUS
#include "Old3_1.h"
#include <stdio.h>
#include <stdlib.h>
#include <plib/delays.h>
#include <plib/xlcd.h>
#include <plib/adc.h>


void init_ADC1(void);               //Initialize ADC
void init_XLCD(void);               //Initialize LCD display
void DelayFor18TCY( void );         //18 cycles delay
void DelayPORXLCD (void);           // Delay of 15ms
void DelayXLCD (void);              // Delay of 5ms
float d_membershipmd(float k,float a,float b,float c,float d);/*Subroutine to
calculate
degree of membership of any monotonically decreasing function.In this case
this is charging voltage membership function*/
float d_membershiptr(float k,float a,float b,float c,float d);/*Subroutine to
calculate degree of membership of charging voltage triangular function*/
float d_membershipmi(float k,float a,float b,float c,float d);/*Subroutine to
calculate
degree of membership of monotonically increasing charging voltage function*/.
float d_membershipmda(float xa,float a,float b,float c,float d);/*Subroutine
to calculate degree of membership of the Charging current membership
function*/
float d_membershiptra(float xa,float a,float b,float c,float d);/*Subroutine
to calculate degree of membership of charging current membership function*/
float d_membershipmia(float xa,float a,float b,float c,float d);/*Subroutine
to calculate degree of membership of charging current membership function*/
float d_membershipmdSOC(float SOC,float a,float b,float c,float d);
/*Subroutine to calculate degree of membership of the SOC membership
function*/
float d_membershiptrSOC(float SOC,float a,float b,float c,float d);
/*Subroutine to calculate
degree of membership of SOC membership function*/
float d_membershipmiSOC(float SOC,float a,float b,float c,float d);
/*Subroutine to calculate
degree of membership of the SOC membership function*/


//**************Declare Global
Varaibles************************************
unsigned int ADCResult[4]=0;
unsigned char ResultStr[10];
unsigned char Buffer[20];
```

```
          float voltage10,voltage11,voltage12,voltage13;
              float k,ec,orp,xa,dmf,a,b,c,d,V21,V22,V23,pHs,Ich,Irms;
              float degreestore[4][4]={{0},{0}};/*Array to store all degrees
of membership
              at specific memory locations for latter retrieval*/
              float digesterop[27][1]={{0},{0}};/*Rule matrix of digester
operation*/
              float firingcomb[3]={0};/*Array to store values of overall
combined firing
                                                  strengths of the rules*/
          float firing[7]={0};
              float a1,a2,a3,a4,b1,b2,b3,b4,area1,area2,area3,area4;
              float SOC,top1,top2,top3,top4,crispout;

void main(void)
{
    TRISCbits.RC0=0;//Combined Photovoltaic and Biogas Alarm
    TRISAbits.RA4=0;//User PV current Flashing LED (FLED)
   //OSCCON=0x70;                    //Configure to use 8MHz internal
oscillator.
   init_XLCD();                     //Call the Initialize LCD display function
   init_ADC1();                    //Call the Initialize ADC function

    putrsXLCD(" SOLAR  ");              //Display "SOLAR"
    SetDDRamAddr(0x40);             //shift cursor to beginning of second line
    putrsXLCD(" SYSTEM ");       //Display "SYSTEM"
    for (int i=0; i<=100;i++) __delay_ms(10); // 1 second delay
    WriteCmdXLCD(0x01);         //Clear Screen

    while(1)
    {

    //---sample and convert----
        for (unsigned char m=0; m<=2; m++)
        {

            ADCON0bits.CHS = m;
            DelayFor18TCY();
    ConvertADC();                    //Start conversion
    while(BusyADC());               //Wait here until conversion is finished
    ADCResult[m] = (unsigned int)ReadADC();          //Read the converted
data
    // convert the converted data into voltage
    //we divide by 1024 because its a 10-bit converted data

    voltage10 = (ADCResult[0]*5.0)/1024;//From voltage charging sensor
       voltage11 = (ADCResult[1]*5.0)/1024;//From current charging  sensor
       voltage12 = (ADCResult[2]*5.0)/1024;//Solar  photocell voltage
       voltage13 = (ADCResult[3]*5.0)/1024;//Load voltage sensor

        }


             V21=5.27*voltage10;//Charging voltage

               k = V21;
```

```
            V22=voltage11/20;//Vdrop in series current sensing circuit
            Ich=V22/0.05f;//Charging current

            xa = Ich;

            SOC= 80;


               if (k>=0 && k<=15){//Select Low Voltage membership function
               a=0;//Limits for the LV membership function
             b=0;
             c=15;
             d=20;
               dmf=d_membershipmd( k, a, b, c, d);//Degree of membership from
subroutine
               degreestore[0][0]=dmf;//LV degree of membership for this input
               degreestore[0][1]=(1-dmf);}//AV degree of membership for this
input
               else if(k>15 && k<=20)//Select AV membership function
               {a=15;//Limits for the AV membership function
             b=20;
             c=20;
             d=25;
               dmf=d_membershiptr( k, a, b, c, d);//Degree of membership from
subroutine
               degreestore[0][1]=dmf;//AV degree of membership
               degreestore[0][0]=(1-dmf);}//LV degree of membership
           else {
               a=20;
               b=25;
               c=30;
               d=30;
              dmf=d_membershipmi( k, a, b, c, d);//Degree of membership from
subroutine
             degreestore[0][2]=dmf;//HV degree of membership
               degreestore[0][1]=(1-dmf);//AVdegree of membership
          }
       if (xa>0 && xa<=0.5){//Select LOW CURRENT membership function
               a=0;//Limits for LOW current membership function
             b=0;
             c=0.5f;
             d=4;
               dmf=d_membershipmda( xa, a, b, c, d);//Degree of membership
from subroutine
               degreestore[0][3]=dmf;//LOW Voltage degree of membership
               degreestore[1][0]=(1-dmf);}//AV degree of membership
               else if(xa>0.5 && xa<=4)//Select AC membership function
               {a=0.5f;//Limits for the AC membership function
             b=4;
             c=4;
             d=5;
               dmf=d_membershiptra( xa, a, b, c, d);//Degree of membership
from subroutine
               degreestore[1][0]=dmf;//AC degree of membership
               degreestore[0][3]=(1-dmf);}//LC degree of membership
               else {//Select HIGH current membership function
               a=4;//Limits for HIGH current membership function
```

```
            b=5;
            c=7;
            d=7;
             dmf=d_membershipmia( xa, a, b, c, d);//Degree of membership from
subroutine*/
              degreestore[1][1]=dmf;//HC degree of membership
              degreestore[1][0]=(1-dmf);}//AC degree of membership

   if(SOC>10 && SOC<=50)//Select LSOC membership function
              {a=10;//Limits for the LSOC membership function
            b=10;
            c=50;
            d=70;
              dmf=d_membershiptrSOC( SOC, a, b, c, d);//Degree of membership
from subroutine
              degreestore[1][2]=dmf;//LSOC degree of membership
              degreestore[1][3]=(1-dmf);}//MSOC degree of membership
          else if(SOC>50 && SOC<=70)//Select MSOC membership function
              {a=50;//Limits for the M.alkaline membership function
            b=70;
            c=70;
            d=80;
              dmf=d_membershiptrSOC( SOC, a, b, c, d);//Degree of membership
from subroutine
            degreestore[1][3]=dmf;//MSOC degree of membership
              degreestore[1][2]=(1-dmf);}//LSOC degree of membership
              else {//Select HSOC membership function
              a=70;//Limits for the HSOC membership function
            b=80;
            c=100;
            d=100;
       dmf=d_membershipmiSOC( SOC, a, b, c, d);//Degree of membership from
subroutine
            degreestore[2][0]=dmf;// HSOCdegree of membership
              degreestore[1][3]=(1-dmf);}//MSOC degree of membership
  /*Evaluate the firing strengths of the fifteen (15) rules for the required
digester operation status*/
  /*The results according to the Max-Min method are stored in an array
digesterop*/
              if((degreestore[1][2])>(degreestore[0][0])){//Rule 1 LD
                    digesterop[0][0]=degreestore[0][0];}
              else if((degreestore[1][2])>(degreestore[0][3]))
              {digesterop[0][0]=degreestore[0][3];}
              else
              {digesterop[0][0]=degreestore[1][2];}

    if((degreestore[1][2])>(degreestore[0][1])){//Rule 2 MD
                    digesterop[1][0]=degreestore[0][1];}
              else if((degreestore[1][2])>(degreestore[0][3]))
              {digesterop[1][0]=degreestore[0][3];}
              else
              {digesterop[1][0]=degreestore[1][2];}
    if((degreestore[1][2])>(degreestore[0][2])){//Rule 3 MD
                    digesterop[2][0]=degreestore[0][2];}
              else if((degreestore[1][2])>(degreestore[0][3]))
              {digesterop[2][0]=degreestore[0][3];}
              else
```

```
            {digesterop[2][0]=degreestore[1][2];}


   if((degreestore[1][2])>(degreestore[0][0])){//Rule 4 MD
                  digesterop[3][0]=degreestore[0][0];}
            else if((degreestore[1][2])>(degreestore[1][0]))
            {digesterop[3][0]=degreestore[1][0];}
            else
            {digesterop[3][0]=degreestore[1][2];}

   if((degreestore[1][2])>(degreestore[0][1])){//Rule 5 MD
                  digesterop[4][0]=degreestore[0][1];}
            else if((degreestore[1][2])>(degreestore[1][0]))
            {digesterop[4][0]=degreestore[1][0];}
            else
            {digesterop[4][0]=degreestore[1][2];}
   if((degreestore[1][2])>(degreestore[0][2])){//Rule 6 MD
                  digesterop[5][0]=degreestore[0][2];}
            else if((degreestore[1][2])>(degreestore[1][0]))
            {digesterop[5][0]=degreestore[1][0];}
            else
            {digesterop[5][0]=degreestore[1][2];}


   if((degreestore[1][2])>(degreestore[0][0])){//Rule 7 LD
                  digesterop[6][0]=degreestore[0][0];}
            else if((degreestore[1][2])>(degreestore[1][1]))
            {digesterop[6][0]=degreestore[1][1];}
            else
            {digesterop[6][0]=degreestore[1][2];}

   if((degreestore[1][2])>(degreestore[0][1])){//Rule 8 LD
                  digesterop[7][0]=degreestore[0][1];}
            else if((degreestore[1][2])>(degreestore[1][1]))
            {digesterop[7][0]=degreestore[1][1];}
            else
            {digesterop[7][0]=degreestore[1][2];}
   if((degreestore[1][2])>(degreestore[0][2])){//Rule 9 MD
                  digesterop[8][0]=degreestore[0][2];}
            else if((degreestore[1][2])>(degreestore[1][1]))
            {digesterop[8][0]=degreestore[1][1];}
            else
            {digesterop[8][0]=degreestore[1][2];}
//zzzzzzzzzzzzzzzzzzzzzzzzzzzzzzzzzzzzzzzzzzzzzzzzzzzzzzzzz

   if((degreestore[1][3])>(degreestore[0][0])){//Rule 10 LD
                  digesterop[9][0]=degreestore[0][0];}
            else if((degreestore[1][3])>(degreestore[0][3]))
            {digesterop[9][0]=degreestore[0][3];}
            else
            {digesterop[9][0]=degreestore[1][3];}

   if((degreestore[1][3])>(degreestore[0][1])){//Rule 11 LD
                  digesterop[10][0]=degreestore[0][1];}
            else if((degreestore[1][3])>(degreestore[0][3]))
            {digesterop[10][0]=degreestore[0][3];}
            else
```

```
            {digesterop[10][0]=degreestore[1][3];}
    if((degreestore[1][3])>(degreestore[0][2])){//Rule 12 LD
                  digesterop[11][0]=degreestore[0][2];}
            else if((degreestore[1][3])>(degreestore[0][3]))
            {digesterop[11][0]=degreestore[0][3];}
            else
            {digesterop[11][0]=degreestore[1][3];}


    if((degreestore[1][3])>(degreestore[0][0])){//Rule 13 MD
                  digesterop[12][0]=degreestore[0][0];}
            else if((degreestore[1][3])>(degreestore[1][0]))
            {digesterop[12][0]=degreestore[1][0];}
            else
            {digesterop[12][0]=degreestore[1][3];}

    if((degreestore[1][3])>(degreestore[0][1])){//Rule 14 MD
                  digesterop[13][0]=degreestore[0][1];}
            else if((degreestore[1][3])>(degreestore[1][0]))
            {digesterop[13][0]=degreestore[1][0];}
            else
            {digesterop[13][0]=degreestore[1][3];}
    if((degreestore[1][3])>(degreestore[0][2])){//Rule 15 MD
                  digesterop[14][0]=degreestore[0][2];}
            else if((degreestore[1][3])>(degreestore[1][0]))
            {digesterop[14][0]=degreestore[1][0];}
            else
            {digesterop[14][0]=degreestore[1][3];}


    if((degreestore[1][3])>(degreestore[0][0])){//Rule 16 HD
                  digesterop[15][0]=degreestore[0][0];}
            else if((degreestore[1][3])>(degreestore[1][1]))
            {digesterop[15][0]=degreestore[1][1];}
            else
            {digesterop[15][0]=degreestore[1][3];}

    if((degreestore[1][3])>(degreestore[0][1])){//Rule 17 HD
                  digesterop[16][0]=degreestore[0][1];}
            else if((degreestore[1][3])>(degreestore[1][1]))
            {digesterop[16][0]=degreestore[1][1];}
            else
            {digesterop[16][0]=degreestore[1][3];}
    if((degreestore[1][3])>(degreestore[0][2])){//Rule 18 HD
                  digesterop[17][0]=degreestore[0][2];}
            else if((degreestore[1][3])>(degreestore[1][1]))
            {digesterop[17][0]=degreestore[1][1];}
            else
            {digesterop[17][0]=degreestore[1][3];}

//yyyyyyyyyyyyyyyyyyyyyyyyyyyyyyyyyyyyyyyyyyyyyyyyyyyyyyyyyyyyyyyyyyyyyyyyyyyyy
yy

    if((degreestore[2][0])>(degreestore[0][0])){//Rule 19 MD
                  digesterop[18][0]=degreestore[0][0];}
            else if((degreestore[2][0])>(degreestore[0][3]))
            {digesterop[18][0]=degreestore[0][3];}
```

```
          else
          {digesterop[18][0]=degreestore[2][0];}

if((degreestore[2][0])>(degreestore[0][1])){//Rule 20 LD
                digesterop[19][0]=degreestore[0][1];}
          else if((degreestore[2][0])>(degreestore[0][3]))
          {digesterop[19][0]=degreestore[0][3];}
          else
          {digesterop[19][0]=degreestore[2][0];}
if((degreestore[2][0])>(degreestore[0][2])){//Rule 21 LD
                digesterop[20][0]=degreestore[0][2];}
          else if((degreestore[2][0])>(degreestore[0][3]))
          {digesterop[20][0]=degreestore[0][3];}
          else
          {digesterop[20][0]=degreestore[2][0];}


if((degreestore[2][0])>(degreestore[0][0])){//Rule 22 HD
                digesterop[21][0]=degreestore[0][0];}
          else if((degreestore[2][0])>(degreestore[1][0]))
          {digesterop[21][0]=degreestore[1][0];}
          else
          {digesterop[21][0]=degreestore[2][0];}

if((degreestore[2][0])>(degreestore[0][1])){//Rule 23 MD
                digesterop[22][0]=degreestore[0][1];}
          else if((degreestore[2][0])>(degreestore[1][0]))
          {digesterop[22][0]=degreestore[1][0];}
          else
          {digesterop[22][0]=degreestore[1][3];}
if((degreestore[2][0])>(degreestore[0][2])){//Rule 24 MD
                digesterop[23][0]=degreestore[0][2];}
          else if((degreestore[2][0])>(degreestore[1][0]))
          {digesterop[23][0]=degreestore[1][0];}
          else
          {digesterop[23][0]=degreestore[2][0];}


if((degreestore[2][0])>(degreestore[0][0])){//Rule 25 HD
                digesterop[24][0]=degreestore[0][0];}
          else if((degreestore[2][0])>(degreestore[1][1]))
          {digesterop[24][0]=degreestore[1][1];}
          else
          {digesterop[24][0]=degreestore[2][0];}

if((degreestore[2][0])>(degreestore[0][1])){//Rule 26 HD
                digesterop[25][0]=degreestore[0][1];}
          else if((degreestore[2][0])>(degreestore[1][1]))
          {digesterop[25][0]=degreestore[1][1];}
          else
          {digesterop[25][0]=degreestore[2][0];}
if((degreestore[2][0])>(degreestore[0][2])){//Rule 27 HD
                digesterop[26][0]=degreestore[0][2];}
          else if((degreestore[2][0])>(degreestore[1][1]))
          {digesterop[26][0]=degreestore[1][1];}
          else
          {digesterop[26][0]=degreestore[2][0];}
```

```
/*Max-Min method for output combination of the rules, by measuring relative
magnitudes of the respective firing strengths of the rules and taking note
              of the most significant one*/

      if ((digesterop[0][0])<(digesterop[6][0])) /* Degree of membership*/
                  firingcomb[0]=digesterop[6][0];}        /* of Low DUTY */
            else if ((digesterop[6][0])<(digesterop[7][0])){ /* CYCLE LD  */
                  firingcomb[0]=digesterop[7][0];}
             else if ((digesterop[7][0])<(digesterop[9][0])){
                  firingcomb[0]=digesterop[9][0];}
             else if ((digesterop[9][0])<(digesterop[10][0])){
                  firingcomb[0]=digesterop[10][0];}
             else if ((digesterop[10][0])<(digesterop[11][0])){
                  firingcomb[0]=digesterop[11][0];}
             else if ((digesterop[11][0])<(digesterop[19][0])){
                  firingcomb[0]=digesterop[19][0];}
             else if ((digesterop[19][0])<(digesterop[20][0])){
                  firingcomb[0]=digesterop[20][0];}

          else {
                  firingcomb[0]=digesterop[0][0];}

    if ((digesterop[1][0])<(digesterop[2][0])){ /* Degree of membership*/
                  firingcomb[1]=digesterop[2][0];}   /* of MEDIUM DUTY */
            else if ((digesterop[2][0])<(digesterop[3][0])){ /* CYCLE MD  */
                  firingcomb[1]=digesterop[3][0];}
             else if ((digesterop[3][0])<(digesterop[4][0])){
                  firingcomb[1]=digesterop[4][0];}
             else if ((digesterop[4][0])<(digesterop[5][0])){
                  firingcomb[1]=digesterop[5][0];}
             else if ((digesterop[5][0])<(digesterop[8][0])){
                  firingcomb[1]=digesterop[8][0];}
             else if ((digesterop[8][0])<(digesterop[12][0])){
                  firingcomb[1]=digesterop[12][0];}
             else if ((digesterop[12][0])<(digesterop[13][0])){
                  firingcomb[1]=digesterop[13][0];}
             else if ((digesterop[13][0])<(digesterop[14][0])){
                  firingcomb[1]=digesterop[14][0];}
             else if ((digesterop[14][0])<(digesterop[18][0])){
                  firingcomb[1]=digesterop[18][0];}
             else if ((digesterop[18][0])<(digesterop[22][0])){
                  firingcomb[1]=digesterop[22][0];}
          else if ((digesterop[22][0])<(digesterop[23][0])){
                  firingcomb[1]=digesterop[23][0];}
          else {
                  firingcomb[1]=digesterop[1][0];}
    if ((digesterop[15][0])<(digesterop[16][0])){/* Degree of membership*/
                  firingcomb[2]=digesterop[16][0];}    /* of HIGH DUTY */
      else if ((digesterop[16][0])<(digesterop[17][0])){ /* CYCLE HD  */
                  firingcomb[2]=digesterop[17][0];}
             else if ((digesterop[17][0])<(digesterop[21][0])){
                  firingcomb[2]=digesterop[21][0];}
             else if ((digesterop[21][0])<(digesterop[24][0])){
                  firingcomb[2]=digesterop[24][0];}
             else if ((digesterop[24][0])<(digesterop[25][0])){
                  firingcomb[2]=digesterop[25][0];}
             else if ((digesterop[25][0])<(digesterop[26][0])){
```

```
                firingcomb[2]=digesterop[26][0];}

        else {
                firingcomb[2]=digesterop[15][0];}


 //?????????????????????????????????????????/////////


            /*DEFUZZIFICATION using CENTER OF GRAVITY(COG) method*/

            a1=0;       //slope1 of Low duty cycle =0
            a2=firingcomb[1]*30;//height x slope1 of MD trapezium
            a3=firingcomb[2]*30;//height x slope1(slope2=0) of HD trapezium
            b1=firingcomb[0]*30;//height x slope2 of LD
            b2=firingcomb[1]*30;//height x slope 2 of MD
            b3=0;
            top1=50-a1-b1;
            top2=60-a2-b2;
            top3=50-a3-b3;
            area1=firingcomb[0]*((50+top1)/2);//Area of LD
            area2=firingcomb[1]*((60+top2)/2);//Area of MD
            area3=firingcomb[2]*((50+top3)/2);//Area of HD
        crispout=((area1*25)+(area2*50)+(area3*75))/(area1+area2+area3);


    WriteCmdXLCD(0x01);       ///Clear Screen
 putrsXLCD(" % Duty cycle ");     ////Display "% Duty cycle" on the screen
SetDDRamAddr(0x40);
putrsXLCD(" = ");
 sprintf(Buffer, "%.3g", crispout );    //// Convert Duty cycle to string
 putsXLCD(Buffer);              ////Display the Duty cycle on the screen
 putrsXLCD("   ");           //// Clear after comma
 WriteCmdXLCD(0x02);             ////Home position on LCD
 for (int i=0; i<=100;i++) __delay_ms(10); //// 1 second delay
   WriteCmdXLCD(0x01);       ///Clear Screen
 putrsXLCD(" Charging volts "); ////Display "Charging volts" on the screen
SetDDRamAddr(0x40);
putrsXLCD(" = ");
 sprintf(Buffer, "%.3g", k ); //// Convert Charging volts to string
 putsXLCD(Buffer);             ////Display the Charging volts on the screen
 putrsXLCD("   ");           //// Clear after comma
 WriteCmdXLCD(0x02);             ////Home position on LCD
 for (int i=0; i<=100;i++) __delay_ms(10); //// 1 second delay
 WriteCmdXLCD(0x01);
 putrsXLCD(" Charging Amps ");     //Display "Charging Amps" on the screen
 SetDDRamAddr(0x40);
 putrsXLCD(" = ");
 sprintf(Buffer, "%.3g", xa ); // Convert Charging Amps to string
 putsXLCD(Buffer);              //Display the Charging Amps on the screen
 putrsXLCD("   ");           // Clear after comma
 WriteCmdXLCD(0x02);             //Home position on LCD
 for (int i=0; i<=100;i++) __delay_ms(10); //// 1 second delay
 putrsXLCD("% Batt. State of ");//Display "% Batt. State of" on the screen
 SetDDRamAddr(0x40);
 putrsXLCD(" charge = ");
 sprintf(Buffer, "%.3g", SOC );    // Convert SOC to string
```

```
    putsXLCD(Buffer);              //Display the SOC on the screen
    putrsXLCD("   ");           // Clear after comma
    WriteCmdXLCD(0x02);             //Home position on LCD
    for (int i=0; i<=100;i++) __delay_ms(10); //// 1 second delay
    //0000000000000000000000000000000000000000000000000000000000000000
    //SOLAR PANEL SHADING ROUTINE

    k=0;
    crispout=0;
    k=voltage12;

    if (k>=0.1f && k<=1){//Select LVadc membership function
              a=0,1f;//Limits for the LV membership function
            b=0.1f;
            c=1;
            d=2;
              dmf=d_membershipmd( k, a, b, c, d);//Degree of membership from
subroutine
              degreestore[0][0]=dmf;//LVadc degree of membership for this
input
              degreestore[0][1]=(1-dmf);}//LMVadc degree of membership for
this input
              else if(k>1 && k<=2)//Select AV membership function
              {a=1;//Limits for the AV membership function
            b=2;
            c=2;
            d=4.5f;
              dmf=d_membershiptr( k, a, b, c, d);//Degree of membership from
subroutine
              degreestore[0][2]=dmf;//LMVadc degree of membership
              degreestore[0][3]=(1-dmf);}//LVadc degree of membership
          else if(k>2 && k<=4.5f)//Select AV membership function
              {a=2;//Limits for the AV membership function
            b=4.5f;
            c=4.5f;
            d=4.8f;
              dmf=d_membershiptr( k, a, b, c, d);//Degree of membership from
subroutine
              degreestore[1][0]=dmf;//UMVadc degree of membership
              degreestore[1][1]=(1-dmf);}//LMVadc degree of membership

          else {
              a=4;
              b=4.8f;
              c=5;
              d=5;
             dmf=d_membershipmi( k, a, b, c, d);//Degree of membership from
subroutine
            degreestore[1][2]=dmf;//HVadc degree of membership
              degreestore[1][3]=(1-dmf);//UMVdegree of membership
          }

    if((degreestore[0][0])<(degreestore[0][3])){//Rule 1 LVadc (TS)
                    firing[0]=degreestore[0][3];}
              else
              {firing[0]=degreestore[0][0];}
```

```
    if((degreestore[0][1])<(degreestore[0][2])){//Rule 2 LMVadc (HS))
                    firing[1]=degreestore[0][2];}
              else if((degreestore[0][2])<(degreestore[1][1]))
              {firing[1]=degreestore[1][1];}
              else
              {firing[1]=degreestore[0][1];}
    if((degreestore[1][0])<(degreestore[1][3])){//Rule 3 UMVadc (PS)
                    firing[2]=degreestore[1][3];}

              else
         { firing[2]=degreestore[1][0];}

    {firing[3]=degreestore[1][2];}


     /*DEFUZZIFICATION using CENTER OF GRAVITY(COG) method*/

              a1=0;       //slope1 of NS =0
              a2=firing[2]*20;//height x slope1 of PS trapezium
              a3=firing[1]*10;//height x slope1(slope2=0) of HS trapezium
              a4=firing[0]*15;//TS
         b1=firing[3]*20;//height x slope2 of NS
              b2=firing[2]*10;//height x slope 2 of PS
              b3=firing[1]*15;//HS
         b4=0;
              top1=60-a1-b1;
              top2=30-a2-b2;
              top3=25-a3-b3;
         top4=30-a4-b4;
              area1=firing[3]*((60+top1)/2);//Area of NS
              area2=firing[2]*((30+top2)/2);//Area of PS
              area3=firing[1]*((25+top3)/2);//Area of HS
         area4=firing[0]*((30+top4)/2);//Area of TS

crispout=((area1*30)+(area2*55)+(area3*72.5)+(area4*85))/(area1+area2+area3+a
rea4);

           WriteCmdXLCD(0x01);       ///Clear Screen
   putrsXLCD(" % Solar Shading ");////Display "% Solar Shading" on the screen
   SetDDRamAddr(0x40);
   putrsXLCD(" = ");
    sprintf(Buffer, "%.3g", crispout ); //// Convert Solar shading to string
    putsXLCD(Buffer);             ////Display the Solar shading on the screen
    putrsXLCD("   ");           //// Clear after comma
    WriteCmdXLCD(0x02);             ////Home position on LCD
    for (int i=0; i<=100;i++) __delay_ms(10); //// 1 second delay

    k=0;// Reset values for next routine
    crispout=0;

    //SOLAR USER LOAD CONTROL

    //Vspp=Vadc/2 (secondar peak to peak voltage)
    //Ispp(secondary peak to peak current)=Vspp/(160*1.414)
    //Ippp (primary peak to peak current)=N*Ispp =3000*Ispp

    Irms = 1.172*voltage13;
```

```
    k = Irms;
    if (k>=0 && k<=3){//Select Acceptable current membership function
              a=0;//Limits for the AC membership function
            b=0;
            c=3;
            d=4;
              dmf=d_membershipmd( k, a, b, c, d);//Degree of membership from
subroutine
              degreestore[2][1]=dmf;//AC degree of membership for this input
              degreestore[2][2]=(1-dmf);}//RL degree of membership for this
input
    else if(k>3 && k<=5)//Select Reaching limit membership function
              {a=3;//Limits for the AV membership function
            b=5;
            c=5;
            d=5.5f;
              dmf=d_membershiptr( k, a, b, c, d);//Degree of membership from
subroutine
              degreestore[2][3]=dmf;//RL degree of membership
              degreestore[3][0]=(1-dmf);}//AC degree of membership
          else {
              a=5;
              b=5.5f;
              c=6;
              d=56;
             dmf=d_membershipmi( k, a, b, c, d);//Degree of membership from
subroutine
            degreestore[3][1]=dmf;//HVadc degree of membership
              degreestore[3][2]=(1-dmf);//UMVdegree of membership
         }

    if((degreestore[2][1])<(degreestore[3][0])){//Rule 1 AC(No warning-NW)
                    firing[4]=degreestore[3][0];}
              else
              {firing[4]=degreestore[2][1];}

    if((degreestore[2][2])<(degreestore[2][3])){//Rule 2 RL(Flashing LED-
FLED))
                   firing[5]=degreestore[2][3];}
              else if((degreestore[2][3])<(degreestore[3][2]))
              {firing[5]=degreestore[3][2];}
              else
              {firing[5]=degreestore[2][2];}

    {firing[6]=degreestore[3][1];}//Rule 3 TH(Alarm- A)


     /*DEFUZZIFICATION using CENTER OF GRAVITY(COG) method*/

              a1=0;       //slope1 of NW =0
              a2=firing[5]*20;//height x slope1 of FLED trapezium
              a3=firing[6]*10;//height x slope1(slope2=0) of A trapezium
          b1=firing[4]*20;//height x slope2 of NW
              b2=firing[5]*10;//height x slope 2 of FLED
              b3=0;//A
              top1=70-a1-b1;
              top2=30-a2-b2;
```

```
            top3=30-a3-b3;
            area1=firing[4]*((70+top1)/2);//Area of NW
            area2=firing[5]*((30+top2)/2);//Area of FLED
            area3=firing[6]*((30+top3)/2);//Area of A
         crispout=((area1*35)+(area2*65)+(area3*85))/(area1+area2+area3);

        if(Irms>3 && Irms<5.5){//Flashing load current LED
            LATAbits.LATA4=1;//Put a high on RA4
            for (int i=0; i<=100;i++) __delay_ms(10); //// 1 second delay
            LATAbits.LATA4=0;//Put a low on RA4
            LATAbits.LATA4=1;//Put a high on RA4
            for (int i=0; i<=100;i++) __delay_ms(10); //// 1 second delay
            LATAbits.LATA4=0;//Put a low on RA4
            LATAbits.LATA4=1;//Put a high on RA4
            for (int i=0; i<=100;i++) __delay_ms(10); //// 1 second delay
            LATAbits.LATA4=0;//Put a low on RA4
        }

         if(Irms>=5.5){
             LATCbits.LATC0=1;//Put pv current breach alarm ON
            for (int i=0; i<=100;i++) __delay_ms(10); //// 1 second delay
            LATCbits.LATC0=0;//Switch off alarm
         }

    WriteCmdXLCD(0x01);       ///Clear Screen
    putrsXLCD(" % Safe current ");////Display "% Safe current" on the screen
   SetDDRamAddr(0x40);
   putrsXLCD(" being used = ");
    sprintf(Buffer, "%.3g", crispout ); //// Convert % Safe current to string
    putsXLCD(Buffer);      ////Display the % Safe current on the screen
    putrsXLCD("   ");           //// Clear after comma
    WriteCmdXLCD(0x02);             ////Home position on LCD
    for (int i=0; i<=100;i++) __delay_ms(10); //// 1 second delay

          k=0;
          crispout=0;

    }
////////////////////////////////////////////////////////////////////////////
//////////////////
}
  //  }

void init_XLCD(void)                //Initialize LCD display
{
    OpenXLCD(FOUR_BIT&LINES_5X7);  //configure LCD in 4-bit Data Interface
mode
                                    //and 5x7 characters, multiple line
display
    while(BusyXLCD());             //Check if the LCD controller is not busy
                                    //before writing some commands?
    WriteCmdXLCD(0x06);            // move cursor right, don?t shift display
    WriteCmdXLCD(0x0C);            //turn display on without cursor

 }

void init_ADC1(void)              //Initialize ADC
```

```
{
  /**** ADC configured for:
    * FOSC/2 as conversion clock
    * Result is right justified
    * Aquisition time of 2 AD
    * Channel 1 for sampling
    * ADC interrupt off
    * ADC reference voltage from VDD & VSS
*/
    OpenADC(ADC_FOSC_2 & ADC_RIGHT_JUST & ADC_2_TAD,
            ADC_CH0 & ADC_INT_OFF & ADC_REF_VDD_VSS,
            ADC_4ANA);
}

void DelayFor18TCY( void )         //18 cycles delay
{
  Delay10TCYx(2);
return;
}

void DelayPORXLCD (void)    // Delay of 15ms
{
    Delay1KTCYx(60);        // Cycles=(Time Delay*Fosc)/4
   //__delay_ms(15);        // Cycles =(15ms*16MHz)/4
                            // Cycles =60000
}

void DelayXLCD (void)        // Delay of 5ms
{
   Delay1KTCYx(20);          // Cycles = 20000
    //__delay_ms(5);

}

float d_membershipmd(float k,float a,float b,float c,float d) /*x is input
value
     from sensor into subroutine*/
            {
      //float dmf;
    if (k>c && k<d)
      { dmf=(d-k)/(d-c); }
      else if (k>=b && k<=c)
      {dmf=1.0; }
      else
      { dmf=0; }
      return dmf;//Return value from subroutine into main program
      }
      float d_membershiptr(float k,float a,float b,float c,float d) /*k is
input value
     from sensor into subroutine*/
            {
      //float dmf;
      if (k >a && k <b)
      { dmf=(k-a)/(b-a);}
      else if (k>c && k<d)
      { dmf=(d-k)/(d-c); }
      else if (k>=b && k<=c)
```

```
      {dmf=1.0; }
      else
      { dmf=0; }
      return dmf;//Return value from subroutine into main program
      }
      float d_membershipmi(float k,float a,float b,float c,float d) /*x is
input value
     from sensor into subroutine*/
            {
      //float dmf;
      if (k >a && k <b)
      { dmf=(k-a)/(b-a);}
      else if (k>=b && k<=c)
      {dmf=1.0; }
      else
      { dmf=0; }
      return dmf;//Return value from subroutine into main program
      }
    float d_membershipmda(float xa,float a,float b,float c,float d) /*xa is
input value
     from sensor into subroutine*/
            {
      //float dmf;
    if (xa>c && xa<d)
      { dmf=(d-xa)/(d-c); }
      else if (xa>=b && xa<=c)
      {dmf=1.0; }
      else
      { dmf=0; }
      return dmf;//Return value from subroutine into main program
      }
      float d_membershiptra(float xa,float a,float b,float c,float d) /*xa is
input value
     from sensor into subroutine*/
            {
      //float dmf;
      if (xa >a && xa <b)
      { dmf=(xa-a)/(b-a);}
      else if (xa>c && xa<d)
      { dmf=(d-xa)/(d-c); }
      else if (xa>=b && xa<=c)
      {dmf=1.0; }
      else
      { dmf=0; }
      return dmf;//Return value from subroutine into main program
      }
      float d_membershipmia(float xa,float a,float b,float c,float d) /*xa is
input value
     from sensor into subroutine*/
            {
      //float dmf;
      if (xa >a && xa <b)
      { dmf=(xa-a)/(b-a);}
      else if (xa>=b && xa<=c)
      {dmf=1.0; }
      else
      { dmf=0; }
```

```
      return dmf;//Return value from subroutine into main program
      }
float d_membershipmdSOC(float SOC,float a,float b,float c,float d) /*x is
input value
     from sensor into subroutine*/
            {
      //float dmf;
    if (SOC>c && SOC<d)
      { dmf=(d-SOC)/(d-c); }
      else if (SOC>=b && SOC<=c)
      {dmf=1.0; }
      else
      { dmf=0; }
      return dmf;//Return value from subroutine into main program
      }
      float d_membershiptrSOC(float SOC,float a,float b,float c,float d) /*k
is input value
     from sensor into subroutine*/
            {
      //float dmf;
      if (SOC >a && SOC <b)
      { dmf=(SOC-a)/(b-a);}
      else if (SOC>c && SOC<d)
      { dmf=(d-k)/(d-c); }
      else if (SOC>=b && SOC<=c)
      {dmf=1.0; }
      else
      { dmf=0; }
      return dmf;//Return value from subroutine into main program
      }
      float d_membershipmiSOC(float SOC,float a,float b,float c,float d) /*x
is input value
     from sensor into subroutine*/
            {
      //float dmf;
      if (SOC >a && SOC <b)
      { dmf=(SOC-a)/(b-a);}
      else if (SOC>=b && SOC<=c)
      {dmf=1.0; }
      else
      { dmf=0; }
      return dmf;//Return value from subroutine into main program
                                          }
```

Appendix F: Conductivity sensor circuit

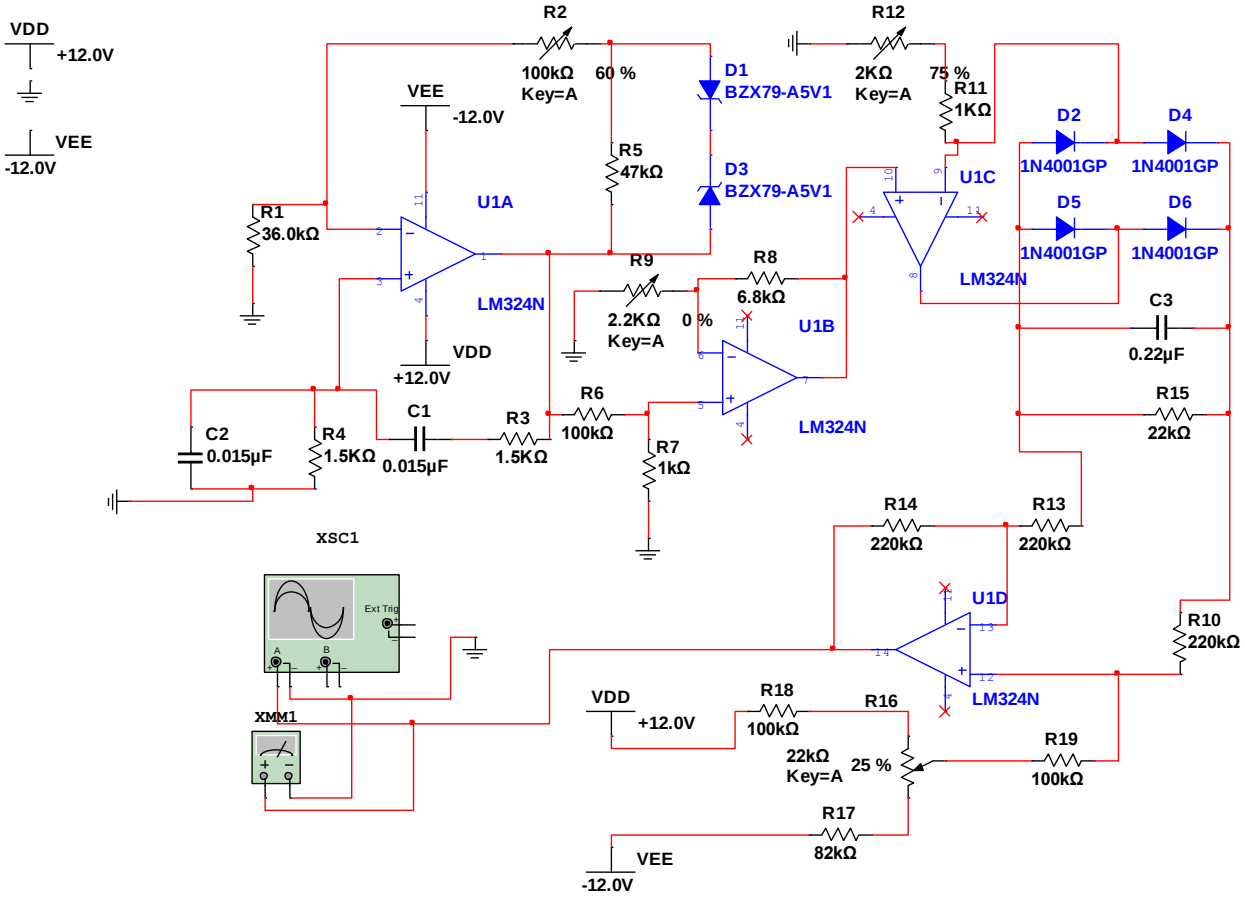

Fig. F.1: Conductivity sensor circuit

Appendix G: Output circuits

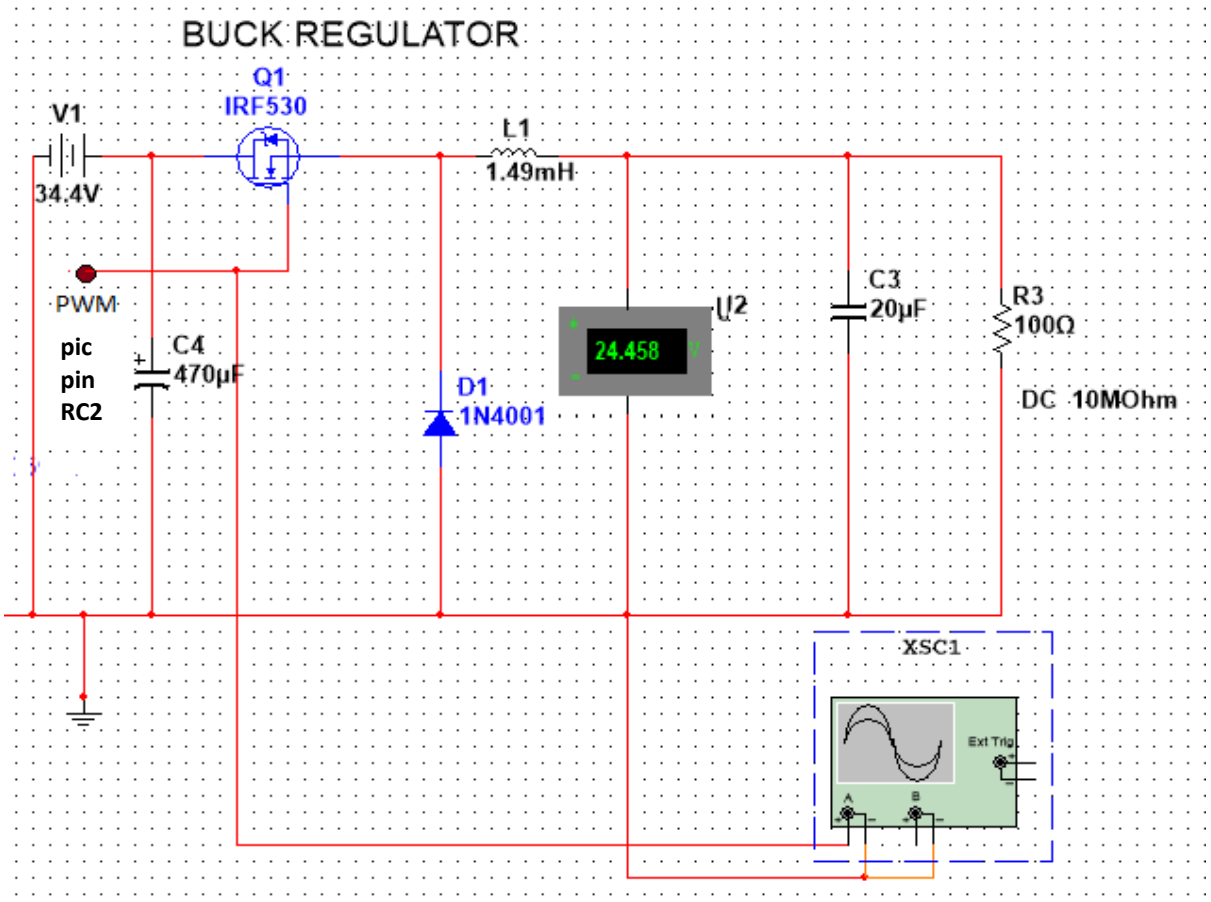

Fig. G.1: Buck regulator

With reference to Figure H.1:

- V_{in} = 34.4V (series connected solar panels)
- V_{out} = 26.2V (Maximum charging voltage)
- I_{load} = 0.56A (Maximum current rating of single 10W solar panel)
- F = 25KHz (fixed frequency of converter operation)
- $D = \frac{Vout}{Vin} = \frac{26.2V}{34.4V} = 0.76163$
- $Iripple = 0.3xIload = 0.3x0.56 = 0.168A$ (ripple current< 30% of I_{load} maximum)
- Vripple = 50mV (Maximum ripple voltage).

From Rashid (2003), the following expressions of L1 and C3 are obtained:

$L1 = ((Vin - Vout)D/f))/Iripple = 1.49mH$, and

$C3 = \frac{(Vin-Vout)D}{8Vripplexf^2xL1}$ =20µF

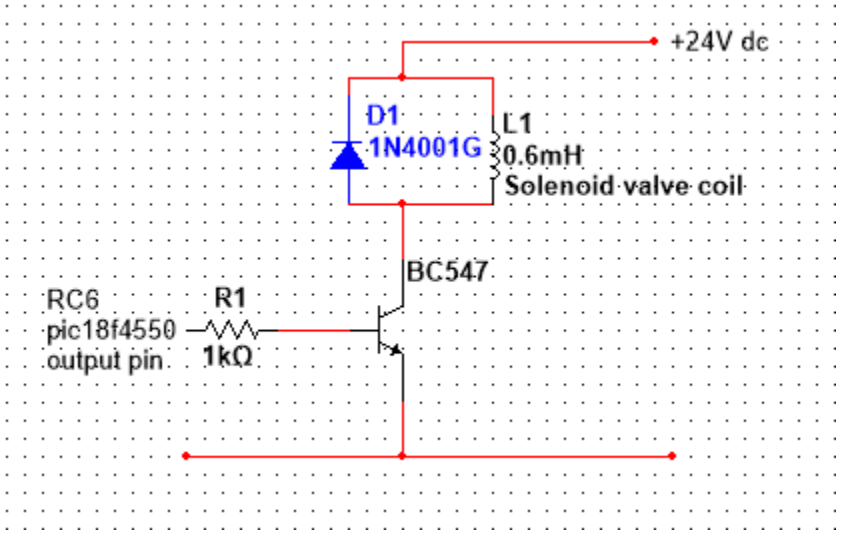

Fig. G.2: Solenoid valve driver

Appendix H: Sample research photographs

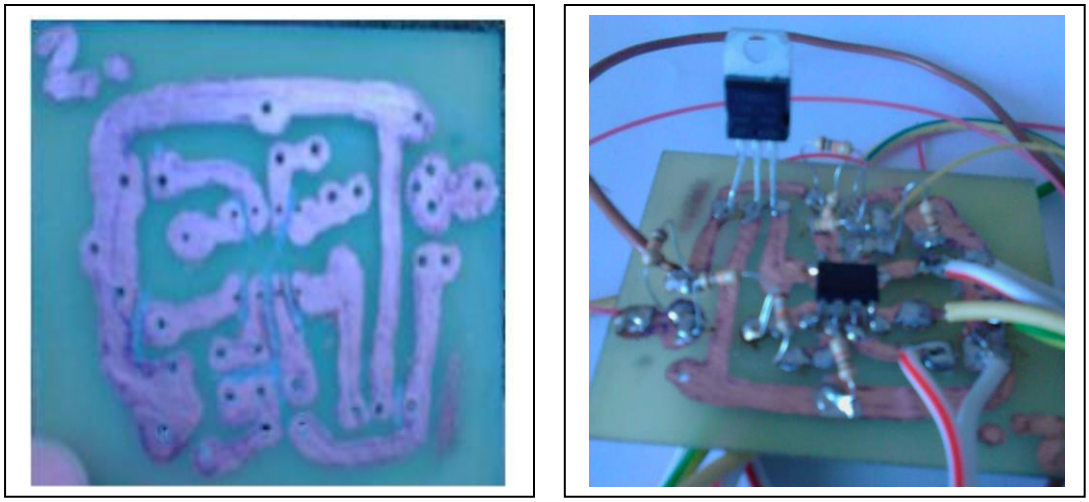

a. PCB track layout b. Constructed board

Fig. H.1: pH and redox sensor amplifiers

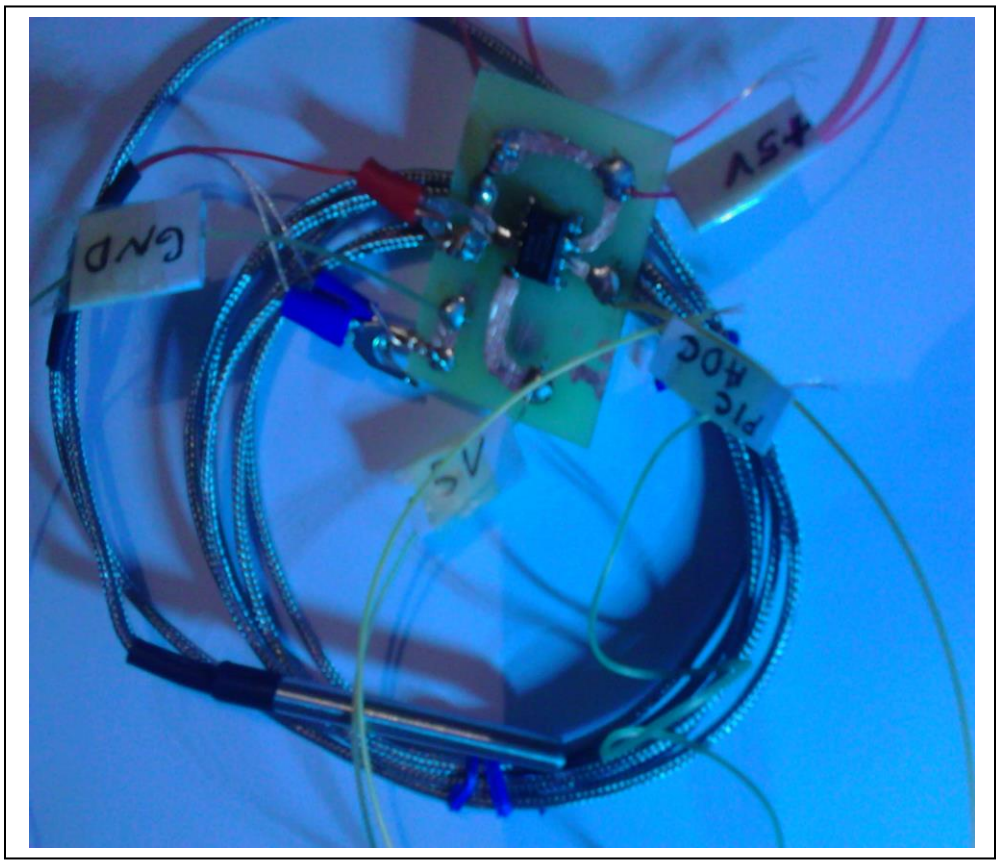

Fig. H.2: Three (3) wire PT100 temperature measurement constructed board amplifier

a. PCB track layout

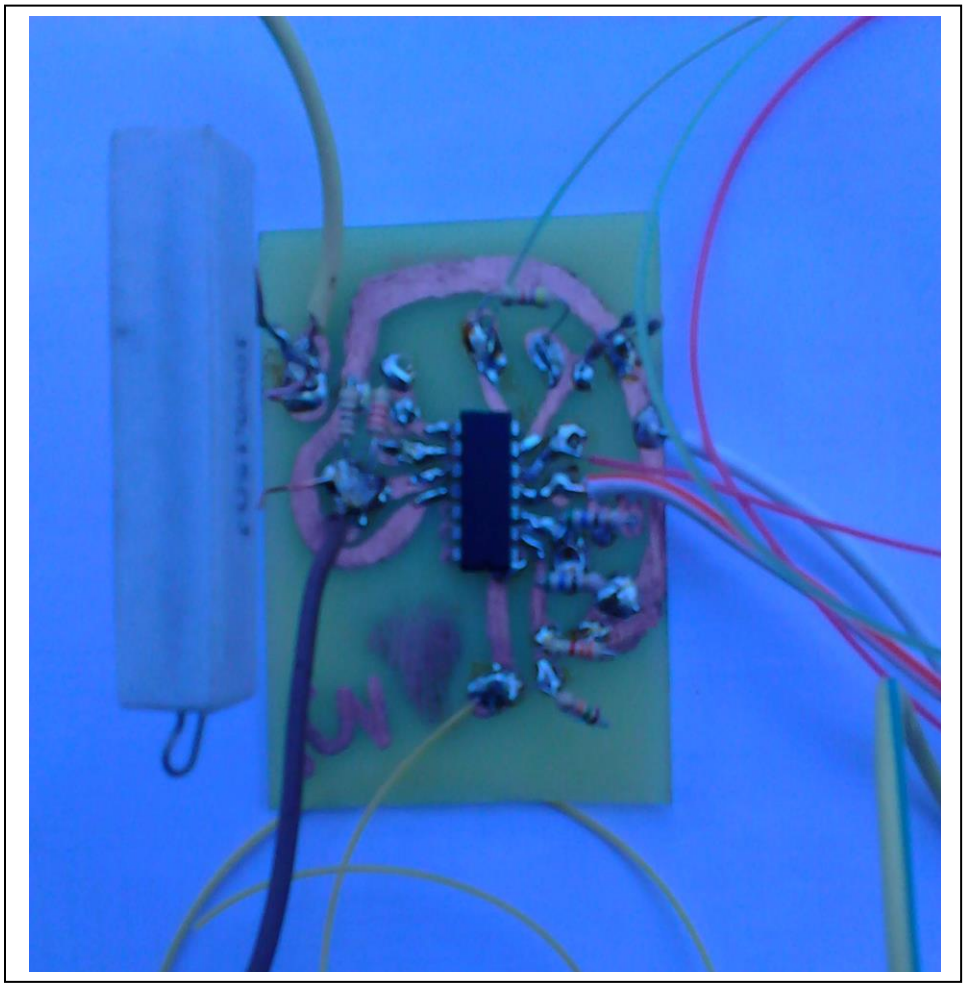

b. Constructed board

Fig. H.3: Board incorporating pressure, oxygen and charging current on a single supply quad LM324 OP-AMP

Fig. H.4: pH, redox and electrical conductivity sensors mounted on 6m 19mm PVC conduits

Fig. H.5: 24V 30VA battery bank with 10W and 20W series connected panels for the experiment

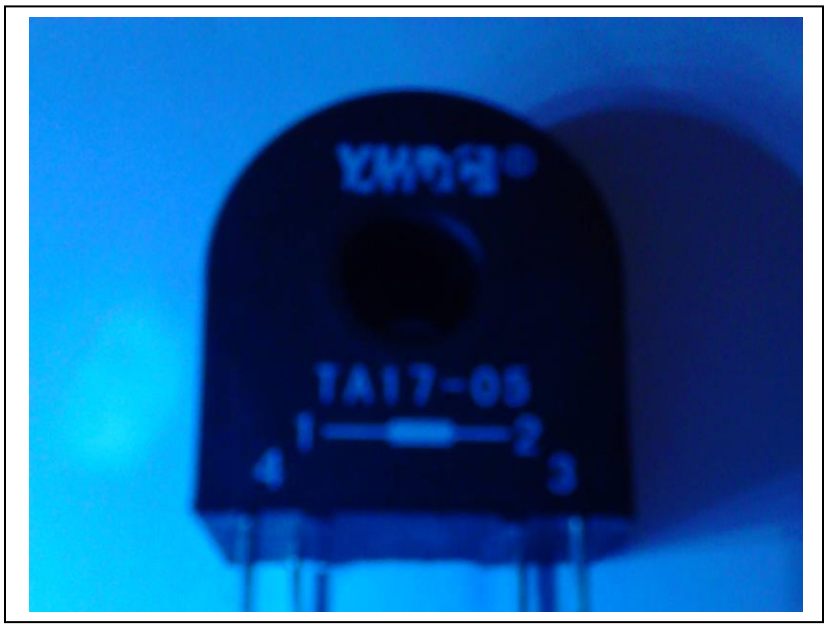

Fig. H.6: 30 A printed circuit-board transformer

Appendix I: PIC18F4550 embedded system layout

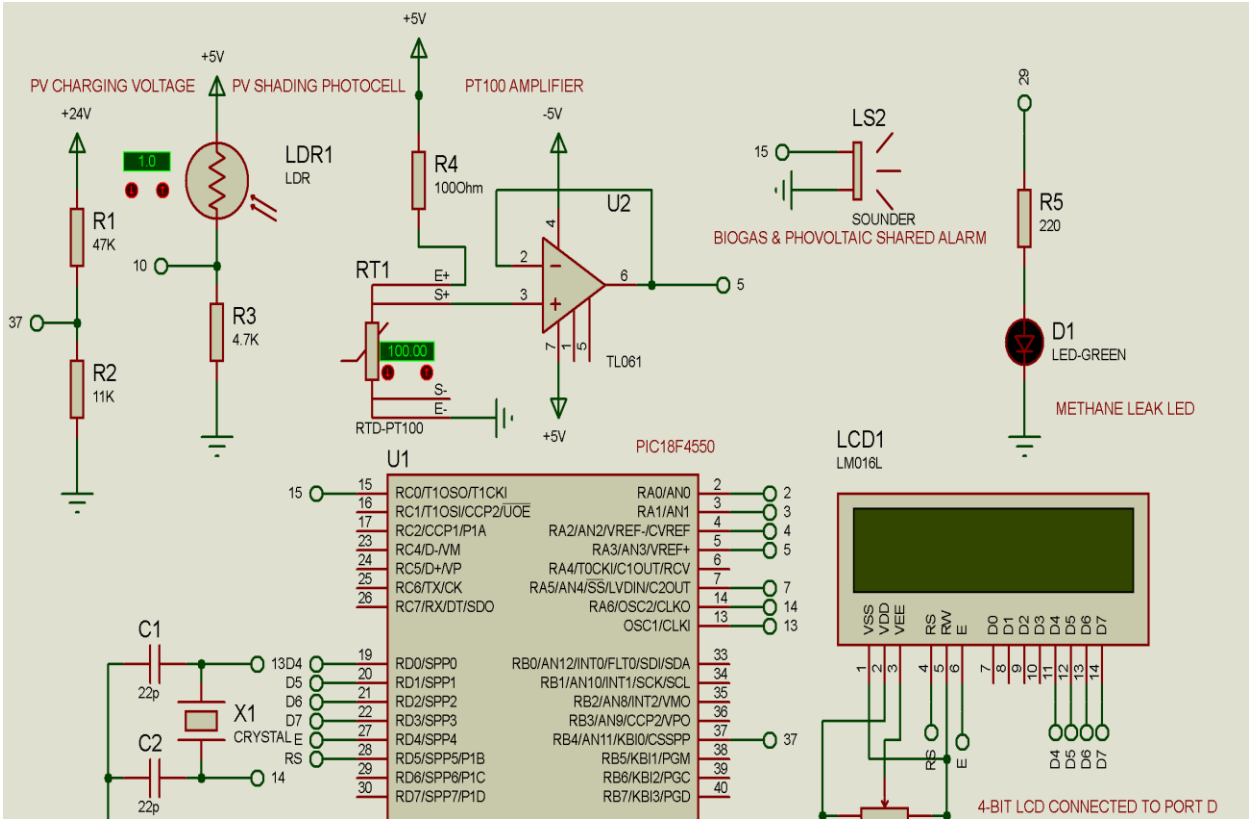

Fig. I1: Sample PIC18F4550 microcontroller inputs & outputs